An Investigation of the Chemistry Involved in the Mixing of an Industrial Effluent with Fine Ash

by

Emma W. Koch

Thesis submitted in partial fulfilment of the requirements for the Degree

Master of Science in Engineering

(Chemical Engineering)

in the Department of Chemical Engineering,

University of Stellenbosch

Supervised by

Prof. L. Lorenzen and B. Schutte

STELLENBOSCH

DECEMEBER 2002

Declaration

I, the undersigned, hereby declare that the work presented in this thesis is my own original work except where acknowledged in the text. Furthermore, neither this entire thesis, nor part thereof, has been submitted previously for a degree at any university.

Emma W. Koch Date

Abstract

Can salts present in an aqueous industrial effluent be retained by the fine ash that is produced as a by-product of gasification or by power stations utilising coal as the raw material? In order to answer this question, the actual chemistry that occurs during the mixing and settling process, needs to be understood.

At the Sasol Secunda petrochemical plants in South Africa, ash is produced as a by-product from the gasification of coal, and by the coal-fired power stations (steam plants). The fine portion of the ash (± 50μm in diameter) is disposed of through the use of a closed loop wet ash disposal system. The ash is transported as a slurry to the disposal sites (ash dams). The industrial effluent used to transport the ash consists mainly of the recycled ash effluent, known as clear ash effluent (CAE), as well as a variety of process waste streams containing high concentrations of salts. This mixture of ash and water is pumped to ash dams, where the ash is allowed to settle and is therefore separated from the effluent. From the ash dams the effluent flows into evaporation dams, and finally into CAE dams before being returned to the ash plant in Sasol 2 and 3 to be mixed once again with the ash. During this contact time of the ash with the water certain chemical reactions may occur. If one understands what chemical reactions occur during this process, and under what conditions they occur, then it will be possible to utilise the ash disposal system to its full potential, possibly enhancing the salt retention ability. An investigation was thus conducted into what processes actually occurs during the entire ash water contact period. The overall aim of the project was to obtain an understanding of the functioning of the fine ash disposal system so that its efficiency can be improved upon, and furthermore, so that the ash dams can be utilised more effectively in retaining salts.

This investigation focussed on the chemical reactions that occur when an industrial effluent is mixed with fine ash, and consisted of four main aspects:

- A literature survey on related issues.
- An analysis and evaluation of the changes that occur in the actual disposal system.
- Laboratory column experiments to investigate, in more detail, the different chemical reactions, which occur during the different stages of the disposal process.
- The drilling of boreholes into the ash dams to obtain core material at a variety of depths and locations for analysis purposes.

From this investigation it was concluded that salts are retained in the ash dams; based on the results obtained from the laboratory column experiments and the production rate of the fine ash from Sasol 2 and Sasol 3, the potential amount of salts that can be removed from the system (either due to precipitation or water retention in the ash dams) is approximately 95 tons/day. The salts that were found to be most pertinent to the wet ash disposal system utilised at Sasol, Secunda, are Ca, SO_4, Na, and Cl. Of these, Ca, SO_4 and Na were identified in literature to be the components most commonly associated with fly ash leachate. The Ca chemistry, which occurs in the ash disposal system, was explored extensively. Is was found that Ca, which is initially present in the fresh fine ash as lime, is leached from the ash into the effluent, where it reacts with carbon dioxide in the atmosphere, and is therefore removed from the system due to the precipitation of calcite. Sodium, SO_4, and Cl were all found to be retained in the ash; the SO_4 appears to be retained in a stable form within the ash, not merely due to hydraulic retention, which suggests that the ash system has the potential to act as a salt sink for SO_4 ions.

The mechanism of salt retention in the ash dams was found to be predominantly by means of hydraulic retention, and therefore the salts have the potential to be flushed out of the ash dams into the underlying soil material. However, results from the core drilling exercise revealed that there doesn't appear to be a significant seepage of elements from the ash fill material into the underlying vertisol material. Some components (Al, Fe, Na, K, Mg, Cr, P, Ti and V) from the older, and inactive ash dam, do appear to have percolated into the underlying material. However, a significant amount of water, and therefore salts, are still retained in the ash dam.

In terms of the mineralogical composition of the ash dams, a significant difference was observed between the mineral phases present in the ash fill material of an active and an inactive ash dam. Ettringite was detected throughout the borehole drilled into the inactive ash dam, and was not evident at all in the core material from the two boreholes drilled into the active dam, which suggests that this mineral is formed in the ash dams over a long time period. The minerals quartz and mullite were found in the fresh fine ash as well as in most of the core material obtained from the drilling exercise. The mineralogical composition of the ash fill samples, from the boreholes drilled into the centre of the active and inactive ash dams, was found to be very consistent with depth. This finding, combined with the fact that the chemical composition of the core samples varied more significantly in the borehole located near the edge of the active fine ash dam, indicated that the lateral position of the ash in the ash dam influences the chemical reactions that occur.

Overall, from this investigation it was concluded that although the chemistry, involved in the mixing of an industrial effluent with fine ash, is extremely complex and site-specific, it is possible to determine the most significant changes which occur within a wet ash disposal system. Besides providing one with a better understanding of the working of the Secunda ash disposal system, the results of this investigation have also provided the framework for future research on this topic and related issues, i.e. the construction of a pilot scale ash dam set-up; further column experiments to investigate the extent to which SO_4 ions can be removed from the system; the influence of the addition of CO_2 to the system; and more extensive core drilling in the vicinity of the ash dams.

Sinopsis

Kan soute teenwoordig in 'n industriële uitvloeisel teruggehou word in fynas geproduseer as neweproduk van steenkoolkragsentrales? Om 'n antwoord op hierdie vraag te kry, moet die chemiese reaksies wat gebeur tydens die meng en wegdoening van die as en aswater verstaan word.

By die Sasol petrochemiese aanlegte in Secunda, Suid Afrika, word fynas geproduseer as 'n neweproduk in die vergassing en die stoomopwekkingprosesse. Die fynas (50µm diameter) word weggedoen deur 'n geslote nat asstelsel. Die industriële uitvloeisel wat gebruik word vir die vervoer van die as bestaan hoofsaaklik uit hergebruikte aswater (genoem CAE – clear ash effluent), asook 'n verskeidenheid ander prosesafvalstrome wat hoë konsentrasies soute bevat. Die mengsel van as en aswater word in 'n asflodder gepomp na die asdamme, waar die as besink en sodoende geskei word van die waterfase (aswater). Vanaf die asdamme vloei die aswater na verdampingsdamme, en daarna na die CAE damme, vanwaar die CAE weer na die Sasol aanleg teruggepomp word om weer met as gemeng te word.

Gedurende die kontak tussen die CAE en as gebeur sekere chemiese reaksies. Indien hierdie reaksies verstaan word, en onder watter toestande dit plaasvind, kan die asdamstelsel tot volle kapasiteit benut word deur moontlik die soutretensie binne die asdam te verhoog. 'n Ondersoek is gedoen om te bepaal watter prosesse plaasvind gedurende kontak tussen die as en water. Die doel van die ondersoek was om 'n beter begrip te kry oor die funksionering van die fynas-wegdoeningstelsel en om te bepaal of die asdamme meer effektief bedryf kan word om moontlik meer soute te akkommodeer.

Die ondersoek het uit vier hoofaspekte bestaan:

- Literatuuroorsig,
- 'n Analise en evaluering van die veranderinge wat plaasvind oor die asdamstelsel,

- Laboratoriumskaal kolomeksperimente om in meer besonderhede die chemiese reaksies wat 'n rol in die aswaterstelsel speel, te bepaal, en
- Die boor van toetsgate op die bestaande asdamme om boorkerne te ontleed by bepaalde dieptes en liggings.

Uit die ondersoek is bevind dat soute wel in die asdamme behou word. As die kolomtoetse as basis gebruik word, en die produksietempo van fynas vanaf Sasol 2 en 3, dan kan daar 'n potensiële 95 ton soute per dag deur die asstelsel verwyder word (deur hoofsaaklik waterretensie en presipitasie van soute). Die mees prominente soute wat in die Sasol asstelsel voorkom is Ca, SO_4, Na, en Cl. Van hierdie soute, is Ca, SO_4, en Na deur die literatuur geïdentifiseer as komponente wat met vliegas loog geassosieer word. Die Ca chemie, wat in die asstelsel plaasvind, is in besonderhede ontleed. Dit is bevind dat Ca, teenwoordig in die vars fynas as kalk, vanuit die as in die aswater geloog word, waar dit dan met atmosferiese CO_2 reageer en dan vanuit die stelsel verwyder word deur die presipitasie van kalsiet. Natrium, SO_4 en Cl word in die as teruggehou. Dit wil voorkom asof die SO_4 in 'n stabiele vorm in die as teruugehou word, nie net deur die hidrouliese retensie nie en dat die asstelsel dalk as 'n potensiële sink vir SO_4 kan optree.

Die meganisme van soutretensie in die asdamme is hoofsaaklik deur hidrouliese retensie, met die gevolg dat die soute potensieel in die onderliggende grond uitgewas kan word. Die resultate van die boorkernondersoek wys egter dat daar nie beduidende uitwassing van hierdie soute in die grond is nie. Dit wil voorkom of sekere komponente (Al, Fe, Na, K, Mg, Cr, P, Ti en V) van die ou en onaktiewe asdam in die grond geloog is.

'n Beduidende verskil was gevind tussen die minerale fases in die asmateriaal van die aktiewe en onaktiewe asdamme. Ettringiet was teenwoordig deur die hele diepte van die boorkern van die onaktiewe dam, maar was nie teenwoordig in beide boorkerns van die gate op die aktiewe asdam nie. Dit impliseer dat hierdie mineraal oor 'n langer tyd gevorm word. Kwarts en mulliet was deurentyd in al die boorkerne teenwoordig. Die mineralogie van die boorkern van die middel van die aktiewe asdam was baie konstant met diepte (in teenstelling met dié van die boorkern op die kant van die asdam) wat

daarop dui dat die laterale posisie van die as in die asdam die chemiese reaksies wat mag plaasvind kan beïnvloed.

Die ondersoek bevestig dat alhoewel die chemiese reaksies betrokke in die aswaterstelsel baie kompleks en liggingspesifiek is, die mees beduidende veranderinge wat in die asstelsel plaasvind, wel bepaal kan word. Die ondersoek het benewens 'n beter begrip van hoe die asdamme reageer, ook 'n raamwerk gegee vir verdere navorsing in hierdie veld, bv. die bou van 'n loodsskaal-asdam, verdere kolomtoetse om die vermoë van die asstelsel om SO_4 ione te verwyder te bepaal en die invloed van gemanipuleerde kalsiet presipitasie deur die byvoeging van CO_2.

Acknowledgements

I would like to express my most sincere gratitude to the following people and institutions for their assistance during the course of my thesis:

SASOL, for their financial backing, interest and support throughout the duration of this project. In particular I would like to extend my most sincere appreciation to all those people at the Water Research Division of SASTECH R&D in Secunda, for their constant support and guidance: Mr G.H. du Plessis, Mr P.C. Pretorius and Mr J.G. Nieuwenhuis to mention but a few. Furthermore I would like to thank Ms N. Kruger for all her time and patience in helping me to gather the available plant data pertaining to the ash water system. Last, but not least, I would like to express my appreciation to Mr M. Ginster for his keen interest and enthusiasm in the project as well as for his assistance with the XRD analyses.

My supervisors, Professor L. Lorenzen and Mr B. Schutte, for their valuable guidance, discussion and advice, and support during the course of this project. I would also like to extend my most sincere thanks to Mr B. Schutte for his assistance during the site visits. (Thank you in particular for sacrificing your good shoes and pants in order to retrieve a sample of the precipitate from one of the CAE dams!).

The staff at the Department of Chemical Engineering (University of Stellenbosch) for their invaluable assistance with different aspects of this project: The workshop personnel for the construction of the laboratory column set-up, Mrs J.E. Botha for her assistance with the operation of the AA and Dionex machines, and Mr F.E Greeff for his enthusiasm and willingness to always provide assistance in all aspects of my experiments.

The staff at the Department of Geology (University of Stellenbosch) for their invaluable advice and assistance pertaining to the analyses of my ash samples: Professor R.

Scheepers and Ms E. Spicer for their assistance with the XRF analyses, and Prof G. Stevens for his assistance with the XRD analyses.

Contents

CHAPTER 5

CORE DRILLING INTO AN ACTIVE AND INACTIVE ASH DAM 207

APPENDIX B

ACTUAL PLANT DATA

APPENDIX C

COLUMN EXPERIMENTS

APPENDIX D

CORE DRILLING DATA

APPENDIX E

PRINCIPAL COMPONENT ANALYSIS

List of Tables

List of Figures

Nomenclature

COD	Chemical Oxygen Demand	mg/L
D	dielectric constant for water	-
e	void ratio	-
I	ionic strength	moles/l
IQR	interquartile range	-
T	temperature	K
$K_s^{'}$	solubility equilibrium constant for calcite	$(moles/l)^2$
LI	Langelier Saturation Index	-
LL	liquid limit	mass % H_2O
LIF	lower inner fence	-
M	M-Alkalinity	mg/l as $CaCO_3$
n	porosity	-
NMC	natural moisture content	mass % H_2O
P	P-Alkalinity	mg/l as $CaCO_3$
pH	measured pH of the water	-
pH_s	calculated saturation pH of the water	-
PI	plasticity index	mass % H_2O
PL	plastic limit	mass % H_2O
TDS	Total Dissolved Solids	mg/L
SS	Suspended Solids	mg/L
Q_1	first quartile	-
Q_2	middle quartile	-
Q_3	third quartile	-
UIF	upper inner fence	-
w	moisture content	mass % H_2O
Z	oxidation number of the chemical species of interest	-

Greek Symbols

α	ionisation fraction	-
γ	activity coefficient	-
ρ	bulk density	kg/m^3
ρ_d	dry density	kg/m^3

Chapter 1

Introduction

Sasol is one the largest and most successful industrial companies in South Africa, and currently supplies 41% of South Africa's liquid fuel requirements. Sasol Synfuels (Pty) Ltd in Secunda, South Africa, operates the world's only commercial coal-based manufacturing facility. The principal feedstock used to produce this liquid fuel is a low grade coal, which is converted into value-added hydrocarbons through unique Fischer-Tropsch process technologies. In this process the coal is gasified in the presence of oxygen and steam, producing ash (fine and course) as a by-product. On average, approximately 132 tons of fine ash and 690 tons of course ash are produced per hour. In addition to this ash from gasification, fly ash and bottom ash are produced by the coal-based power stations (steam plants) operated within the two chemical plants, Sasol 2 (West) and Sasol 3 (East) in Secunda. On average, the production rate of the fly ash is roughly 312ton/h, and the production rate of the bottom ash is approximately 63ton/h. This fly ash and bottom ash, as well as the fine ash generated as a by-product from gasification, are all classified as 'fine ash' and are disposed of collectively by means of a closed-loop wet ash disposal system. The liquid phase used to transport the ash to the disposal sites[1] is an industrial effluent, consisting predominantly of recycled ash effluent, known as clear ash effluent (CAE), as well as a multitude of process waste streams often containing high concentrations of salts. Since some of the effluent, used to transport the ash, is recycled, as well as used as feedstock to the TRO[2] process, it is imperative that the majority of the salts entering the system (as well as those that are leached from the ash) are removed from the ash effluent during the disposal process.

[1] The Ash Dams

[2] Tubular Reverse Osmosis

Previous investigations have been conducted on the Secunda ash disposal system; however, the actual chemistry, which occurs throughout the disposal process, is still largely unknown. The focus of this study was therefore, to investigate the chemical reactions that occur when an industrial effluent, such as the one used by Sasol 2 and 3, is mixed with fine ash. The objectives of this investigation were:

- To identify the salts of primary concern to the operation of the Secunda ash disposal system.
- To evaluate the efficiency (in terms of salt retention[3]) of the disposal system under field conditions.
- To investigate the chemical changes, which occur from the time the fresh ash is mixed with the effluent, to the time the effluent is recycled to the plants; i.e. if certain salts are removed from the effluent during the disposal process, how are they removed, during what stage of the process are they removed, and how can their removal be enhanced.
- To relate the results of this study to other research carried out on the Secunda ash disposal system.

Taking all these objectives into consideration, the overall aim of the project was to obtain a comprehensive understanding of the functioning of the fine ash disposal system so that its efficiency can be improved upon, and furthermore, so that the ash dams can be utilised to their full potential as salt sinks[4].

The strategy of the investigation, in order to achieve the project objectives, consisted of four main aspects. Initially a literature survey was conducted to assess the scope of previous research that had been conducted on issues relevant to the Secunda ash disposal system (Chapter 2). Chapter 3 encompasses an investigation of the changes, which occur within the actual ash disposal system, using previous data generated by Sasol. Due to the

[3] Removal from the effluent

[4] A means of trapping salts in a stable form and therefore removing them from the effluent that is recycled.

complexity of the system and the lack of data for certain stages of the process, laboratory column experiments were performed to examine the ash/water chemistry in more detail (Chapter 4). In order to obtain a more comprehensive understanding of the salt holding capacity and efficiency of the ash dams under field conditions, boreholes were drilled into an active and inactive ash dam at Sasol, Secunda. Core samples were obtained from the ash fill material, as well as from the underlying vertisol material for analysis purposes, the results of which are presented in Chapter 5. The results of the four different aspects of the project were integrated, and are presented in this manner in Chapter 6.

Chapter 2

A Literature Review and Relevant Theory

The aqueous chemistry involved in the mixing of fly ash with an industrial effluent is relatively complex and involves a significant number of cations and anions, inorganic solids, as well as other materials. It is therefore imperative that, before tackling a specific ash disposal system, one understands the basic composition of fly ash. It is also important that one is aware of investigations carried out by other researchers relating to the disposal of ash using an effluent stream.

This chapter encompasses information pertaining to the composition and disposal of fly ash, as well as the chemistry of the main elements pertinent to a wet ash disposal system. Other relevant theory, applicable to discussions in the chapters to follow, has also been incorporated in this chapter.

2.1 The composition of fly ash

Fly ash is defined in cement and concrete terminology as "the finely divided residue resulting from the combustion of ground or powdered coal, which is transported from the firebox through the boiler by flue gas." The American Society for Testing and Materials (ASTM) in 1989 defined fly ash as the finely divided residue that results from the combustion of ground or powdered coal and does not include residue from the burning of municipal refuse (Combustion Products Management Inc., 2000).

During the combustion of coal in furnaces, high temperatures are reached (more than 1600°C) which results in the decomposition, fusion, and agglomeration of the mineral matter present in the parent coal. Fine silicates and iron oxides are carried out with the

flue (fly ash), while the agglomerates tend to fall to the bottom of the combustion chamber to be removed as bottom ash. Many trace elements are volatised during the combustion process, and tend to condense onto the surface of the fly ash in the cooler parts of the chamber. Since the ash used by Sasol in their wet ash disposal system consists mainly of fly ash, the focus of the literature survey will be on fly ash.

The composition of fly ash depends on several factors, which include:

- The differences in the inorganic components in the parent coal.
- How the coal is prepared for combustion as well as the actual conditions in the combustion chamber.
- The configuration of the furnace.
- The type and efficiency of emission control devices.
- The ash collection and disposal methods.

2.1.1 Physical properties of fly ash

Fly ash consists predominately of glass spheres ranging from 0.01 to 100μm in size (Swaine, 1995), with typical fly ash particles having a diameter of 50μm. Most are spherical in shape, indicating that they have fused during their brief time in the boiler. According to Mackechnie (1989), the non-combustible material melts while in suspension and cools rapidly as it leaves the furnace. It is this rapid cooling that causes the fly ash to form spherical particles, which are combinations of glassy crystalline phases. According to O'Brien (2000) and Swaine (1995) the spheres found in fly ash include solid glass spheres, hollow glass spheres (cenospheres) and hollow glass spheres containing other glass spheres that are 1μm or less in diameter (plerospheres). Even though these molecules are very small, they possess very high mechanical strengths. Fly ash, for the most part, is chemically inert and has a melting point of 1000°C. Table 2.1 presents typical physical properties of fly ash and bottom ash (Bezuidenhout, 1995).

Table 2.1: Physical Properties of Fly Ash and Bottom Ash

Physical Property	Fly ash	Bottom ash
Specific gravity	1.59 – 3.1	2.17 – 2.78
Dry bulk density (mg/m^3)	1.01 – 1.43	0.74 – 1.58
Specific surface area (m^2/kg)	200 – 3060	400
Coefficient of permeability (m/s)	$5e^{-8} – 1e^{-6}$	$2.5e^{-4} – 9.4e^{-4}$
Mean particle diameter (μm)	20 - 80	500 - 7000

2.1.2 Chemical and mineralogical properties of fly ash

In general, the major constituents or elements of fly ash are heterogeneous glassy and crystalline phases of silicon, aluminium, iron, calcium and magnesium. Chemical analyses of fly ash (XRF analyses) show the compounds occurring as oxides of these elements, however, they actually occur as aluminosilicate glass interspersed with a small fraction of crystalline compounds such as quartz, mullite, hematite, magnetite and elemental siliceous or aluminosilicate glass.

2.1.2.1 Minerals present in fly ash

The general composition of fly ash is described in section 2.1.2, however, it is important to support this description with a report of previous work done on the mineralogical composition of fly ash.

- The most common minerals found in fly ash are quartz and mullite ($Al_6Si_2O_{13}$) with smaller amounts of magnetite, maghemite, anhydrite and lime (Bezuidenhout, 1995). Bezuidenhout (1995) also reports that the main Fe-bearing compounds in fly ash are hematite and magnetite; the principal Ca-bearing compounds are anhydrite and lime; and the dominant crystalline compound of Mg is periclase; with further Fe, Ca and Mg also possibly present in the glassy phase.
- According to Swaine (1995) the main constituents of fly ash are glassy aluminosilicate phases with lesser amounts of mullite, quartz, hematite and 'carbon', present due to the incomplete oxidation of the coal. Other phases which may be present are anhydrite ($CaSO_4$), tricalcium aluminate ($Ca_3Al_2O_6$), lime (CaO),

merwinite ($Ca_3Mg(SiO_4)_2$), melilite (a complex of Ca, Al, Mg silicate) and periclase (MgO).

- According to Jones (1995), the majority of fly ash particles are glassy spheres with the remainder consisting of quartz, mullite, non-magnetic iron oxides, and magnetic iron spinels. In a study conducted by Bosch (1990) on fly ash from three South African Power Stations, the major phases present were found to be glass (45-75%), mullite (16-39%), and quartz (1.5-16%). It was further discovered (by means of electron microprobe analysis) that the glass consisted of SiO_2 (21-100%) and Al_2O_3 (0.1-49%), with significant quantities of CaO, TiO_2, Fe_2O_3 and MgO. Other mineral phases that were identified include lime, portlandite, hematite, and an Fe-oxide phase identified to be maghemite (γ-Fe_2O_3).

2.1.2.2 Changes that occur during combustion

During combustion, sulphide (pyrite and calcopyrite) and carbonate (calcite, siderite and dolomite) minerals are decomposed completely to form metal oxides as well as SO_2/SO_3 and CO_2, respectively. A portion of the sulphur oxide gases may recombine with CaO to form $CaSO_4$ (Jones, 1995). This can be seen from the XRD analyses performed on the fresh fine ash obtained from Sasol, where lime is definitely present and no calcite could be detected (section 5.2.6).

Mullite is formed by the decomposition of the aluminosilicate phases in the coal. The most common aluminosilicate mineral in coal is kaolinite, which decomposes according to the following reactions, to form mullite.

$$Al_2O_3.2SiO_2.2H_2O \xrightarrow{500°C} Al_2O_3.2SiO_2 + 2H_2O \qquad (2\text{-}1)$$

kaolinite metakaolin

$$3(Al_2O_3.2SiO_2) \xrightarrow{980°C} 3Al_2O_3.2SiO_2 + 4SiO_2 \qquad (2\text{-}2)$$

metakaolin mullite

Further effects of heat on the major minerals in coal are (Swaine, 1995):

$$pyrite \rightarrow iron\ (Fe^{3+})\ oxides + SO_x \quad (2\text{-}3)$$

$$calcite \rightarrow calcium\ oxide\ (CaO) + CO_2 \quad (2\text{-}4)$$

$$siderite \rightarrow iron\ (Fe^{2+})\ oxide + CO_2 \quad (2\text{-}5)$$

$$quartz \rightarrow softens \quad (2\text{-}6)$$

The CaO and iron (Fe^{2+}) oxide (FeO), shown in the above reactions, are relatively unstable and probably react to form glassy aluminosilicates. However, it is actually the fusion and agglomeration after the decomposition that dictates the actual composition of the bottom and fly ash.

2.1.2.3 Chemical composition

Major elements

As expected from the mineralogical constitution of fly ash, Si, Al, and to a lesser extent Fe are the dominant elements, being derived mainly from clays, quartz, and pyrite. When coal is burned, more than 80% of its mass is lost, thus it is not surprising that the concentrations of both major and trace elements are at least five fold higher than in the parent coal. According to Swaine (1995), fly ash from low-rank coals tends to have more Ca, Na and Mg and less Al than that from bituminous coals. The fly ash at Sasol, Secunda has more Ca (about 9% CaO) than Fe (3.6%), but not much Na (0.58%) or Mg (2.3%). Table 2.2 shows the chemical composition of different fly ash samples. All the fly ash samples presented in table 2.2 are from sources in South Africa. It is evident that although there are differences in composition of the different fly ashes, these differences are minimal. According to an investigation carried out by Swaine (1995), although there are in general wide ranges for the major elements found in fly ash, there are not great differences between the ranges for fly ashes from the UK, USA, and Australia.

Table 2.2: Comparison of Fly Ashes from Different Sources (mass %)

	Alberts (1996)	**Ritter (1991)**		**O'Brien (2000)**	**Willis (1987)**	**Campbell (1999)**	**Mackechnie (1989)**			**Rousseau (1997)**	
Component	Fly-ash	Ash A (Sasol 2, field 1)	Ash B (Sasol 2, field 4)	SASOL	SASOL	SASOL	Lethabo Field 2	Lethabo Classified	Matla Classified	Hendrina	Kriel
SiO2	50.1	49.2	44.3	54.3	61-67	53	50.9	53.2	47.3	56.9	52.0
Al2O3	28.3	25.4	30.2	29.9	23-27	28.5	36.0	32.4	28.6	27.6	26.0
CaO	8.19	9.95	9.91	5.4	6.1-7.1	6.40	4.66	4.98	9.40	2.90	11.00
Fe2O3	3.97	3.68	2.57	3.3	3.1-4.8	3.30	3.91	3.90	4.30	3.10	3.90
TiO2	1.52	1.35	1.81	1.60	1.2-1.4	1.70	1.80	1.95	-	1.50	1.60
MgO	2.00	2.02	2.45	1.00	1.4-1.7	1.40	1.36	1.20	2.90	1.00	2.20
P2O5	0.94	0.824	2.22	0.14	0.22-0.51	0.260	0.660	0.600	-	0.300	0.800
K2O	0.91	0.543	0.783	0.51	0.31-0.48	0.460	0.530	0.550	1.08	0.600	0.700
Na2O	0.500	0.000	0.563	0.12	0.76-1.3	0.400	0.320	0.300	0.400	0.000	0.000
L.O.I	2.30	4.40	1.95	3	-	4.400	0.400	0.230	0.900	3.900	0.700

2.1.3 Soil composition compared to fly ash composition

Bezuidenhout (1995) conducted an investigation to determine the differences in the major elements found in soil compared to ash. He found that ash has lower levels of Al, Ca, and Fe than soil, but could be enriched in Mg, K, Na and S. According to Swaine (1995), the major elemental composition of fly ash is similar to that of soils, with the exception being Al, which tends to be higher in the fly ash. Thus, both Bezuidenhout (1995) and Swaine (1995) report that as far as major elements are concerned, the composition of fly ash is very similar to the composition of soil.

2.1.4 Trace elements

As was the case with the major elements found in fly ash, it is not surprising that the concentrations of trace elements in the ash are much higher than in the parent coal; since the coal loses about 80% of its mass during combustion. Combustion is also the cause for the redistribution of trace elements. Some trace elements may be volatised during combustion and then recondense on the surface of the ash particles thus making them more accessible for leaching. Another possibility is that during the high temperature combustion of the coal, phase transformation of the mineral matter occurs, which may render the trace elements present in the coal more susceptible to leaching.

Trace elements can either be situated on the surface of the ash particles (in association with the major surface phases), or within the ash matrix. The release of the trace elements depends on where they are situated. If they are situated within the ash matrix, the rate of the dissolution of the bulk phase will be the determining factor. If they are located on the surface of the ash particles, the primary and secondary phases will determine the leachability of these trace elements. The *primary phases* are produced as a result of the combustion process, whereas *secondary phases* are produced when the ash reacts with the water in which it is in contact with. According to Godbeer and Swaine (1995), this distribution, as well as the abundance of trace elements in the by-product

streams (fly ash, bottom ash and vapour phase) from coal fired power stations, depends on:

- The chemical properties of the individual elements (especially volatility).
- The boiler type and load.
- The operating conditions.
- The operation of the particle attenuation equipment.

Swaine (1995) suggests that the trace elements in coal are found enhanced in fly ash by a factor related to the ash yield of the parent coal. He also found that with most of the trace elements found in fly ash, there is an increase in concentration with a decrease in particle size. He found this to be particularly true for the more volatile elements or their oxides. This research was done on fly ash produced from an Australian bituminous coal, and obviously the type of coal used, as well as factors such as: the operating condition of the boiler, the type of boiler, the age of the sample, and the means of separation into the different particle sizes could influence these results. One should however, keep in mind this suggestion of the enrichment of some trace elements on the smaller particle size, since it could enhance the leachability of these trace elements from waste disposal areas.

Jones (1995) found that some trace elements are preferentially enriched on the surface of the ash particles. These elements are: As, B, Cd, Cu, Hg, Mo, Sb, Se, V and Zn. Therefore, since they are located on the surface of the ash particles, the primary and secondary phases will determine the leachability of these trace elements. On the other hand, he found that Ba, Co, Cr, Mn, Ni and Pb tend to be more evenly distributed between the surface and underlying matrix.

In general, trace elemental concentrations for South African coals are reported to be lower than those in coals from the USA, Germany, Belgium and Australia (Rousseau, 1997). However, it is not in essence the concentrations of the trace elements that are of concern, but rather the mobility of these elements. Thus, the potential that these trace elements have to leach from the ash, needs to be explored.

2.1.4.1 Leaching of trace elements from fly ash

According to Jones (1995), the fundamental chemical processes, which control the leaching of trace elements from coal ash, are identical to those that apply to soils, sediments and other types of solid waste. The initial concentration of a trace element in the leachate will depend on a number of factors such as:

- The concentration and form of the element on the exposed surface of the ash particles.
- The way in which it is chemically bonded to the major phases in the ash.
- The pH of the surrounding environment.

It is thus not surprising that the concentration of an element in the fly ash is not a good indication of its potential for its dissolution into the water phase. Since it is the phases containing the major elements that provide the substrate for the environmentally more sensitive trace elements (Jones, 1995), it is imperative to understand the behaviour of the major mineral phases present in the ash during leaching. It is the dissolution of the primary phases and the formation of the secondary phases that have a major influence on the concentrations of the trace elements in the leachate.

Jones (1995) reports that a number of surveys have indicated that the following trace elements are likely to be of potential concerns in solid wastes from coal: As, B, Cd, Cr, Cu, Ni, Hg, Mo, Pb, Se and Zn. Of these, As, Cd, Pb and Se appear to be the trace elements most commonly found in ash leachates at concentrations high enough to be an environmental concern. Boron is only likely to be of concern if there is any discharge of the leachate to fresh water systems, even though it is reported to be one of the most mobile elements in ash disposal systems. Jones (1995) also expressed that Ca may play a role in controlling the solubility of B, since borate can be incorporated into $CaCO_3$. (Based on the work done by Hollis et al., 1988).

In leaching experiments performed by Fernandez et al. (1994), and reported by Rousseau (1997), Cd, Cu, Co and Zn were the elements found to be most readily leached from the fly ash when it was contacted with water. It is evident that both Jones (1995) and Fernandez et al. (1994), through their research, have identified Cd to be of potential

environmental concern when dealing with leachates associated with fly ash. Groenewald et al. (1984) have, however, found that at a pH of 6.5 – 7.0 and higher, heavy metals such as cadmium and lead tend to precipitate as hydroxide carbonates.

2.1.4.2 Solubility of the trace elements

According to Jones (1995), the solubilities of Cd, Cu, Mn, Ni, Pb and Zn tend to decline as the pH increases due to the fact that these ions appear to be adsorbed on the major aluminosilicate and iron oxide phases, and due to the precipitation of hydroxide and carbonate compounds. On the other hand, As, B, Mo, Sb, Se and V tend to be more mobile in neutral to moderately alkaline environments. However, Jones also found that the solubility of these oxyanionic trace elements was reduced at higher and lower pH's. He also reports that there is a dramatic reduction (over several orders of magnitude) in the solubility of all oxyanionic for a pH greater than 12, which coincides with a reduction in the solution concentrations of Al, Si and SO_4. This reduction could be attributed to the precipitation of ettringite ($Ca_6Al_2(SO_4)_3(OH)_{12}.26H_2O$), however, ettringite is unstable with respect to recarbonation reactions and thus cannot be seen as a potential sink for oxyanions in environments exposed to the atmosphere where CO_2 is in abundance. In general, Jones states that the primary variables determining the extent of dissolution of the elements will be pH and the liquid to solid ratio of the primary leach medium.

2.1.5 Types of fly ash

There are two types of fly ash, class F and class C. These different fly ashes are described below and the difference in composition (mass %) of the two classes is shown in table 2.3.

Class F fly ash

Class F fly ash is produced by burning anthracite and bituminous coal. Class F ash contains silica, aluminium and iron in combinations of greater than 70%.

Class C fly ash

Burning lignite or sub-bituminous coal produces class C fly ash. Class C fly ash generally contains more calcium and less iron, with its lime (CaO) content in the range of

15% to 30%. This makes the Class C fly ash cementitious in addition to pozzolanic (A pozzolanic material is one which possesses hydraulic cementing properties when mixed with water in the presence of $Ca(OH)_2$.)

Table 2.3: Comparison of Class F and Class C Fly Ash (mass %)

	Class F	Class C
SiO_2	49.1	53.79
Al_2O_3	16.25	15.42
Fe_2O_3	22.31	5
TiO_2	1.09	1.68
CaO	4.48	18
MgO	1	3.4
Na_2O	0.05	0.5
K_2O	1.42	0.5
SO_3	0.73	1.44
LOI	2.55	0.8
Other	1.02	0.27

According to Bezuidenhout (1995), in South Africa, most of the coal burned is bituminous coal producing 20-35% ash. Thus, the ash produced in South Africa would be classified as class F fly ash.

2.2 The disposal of fly ash and related issues

Ash, resulting from the combustion of coal, is one of the major wastes produced from industry. This waste poses as a significant disposal problem and expense, but on the other hand, can also be a potentially useful material. There are basically two different methods that can be used to dispose of fine ash. The first is dry ash disposal, which basically consists of landfills that receive dry ash directly from the power plant. Wet ash disposal systems involve the slurrying of the fine ash with an effluent. The ash is then transported in a slurry mixture to "tailings" dams where the ash is separated from the water. The water can either be recycled for re-use in the ash disposal system, or disposed in a controlled manner. According to Jones (1995), recycling of sluice water is most commonly associated with inland power stations that draw fresh water from rivers. The

slurrying of ash in a wet ash disposal system can lead to the leaching of certain elements during the transport phase, as well as due to further seepage of leachate through the ash deposit. Work done by Hodgson and Van Niekerk (reported by Bezuidenhout, 1995) at the Kriel Power Station in South Africa revealed that the wet ash disposal system used, did not pose as an environmental risk as far as contamination of underground water was concerned. The reason for this was that they found that the soils in the vicinity of the settling ponds had the capacity to act as an impermeable layer to the leachate. They also found a reduction in the various elemental concentrations, the conductivity, and the pH of the ash water, with the possible explanation being the formation of $CaCO_3$ and $CaSO_4$ precipitates.

The ash disposal system used by Sasol 2 and 3 in Secunda, South Africa, is a wet ash disposal system where the ash water is recycled (see section 3.1). It is therefore a closed system and no ash water is directly disposed of to a water source. Since the ash water is recycled, there is the possibility that certain elements could leach from the ash into the water and build up in the system. Therefore, an understanding of the leaching, and consequent chemical reactions, associated with an ash water system is essential to the efficient operation of a wet ash disposal system.

2.2.1 Leaching that occurs during the disposal process

The process of leach generation within an ash deposit is simply the dissolution of soluble substances from the solid waste material (ash) into the water percolating through it. The process of leach generation is complex and can be based on the following aspects (Shen-Yu and Zwane, 2001; Dhanpat et al., 1986), i.e.:

- The bulk transport of the aqueous phase through the deposit.
- The diffusion of the dissolved species in the porous matrix of the ash.
- Aqueous heterogeneous chemical reactions.
- Particle coagulation and agglomeration mechanisms.
- Redox state, pH, and solids/ligands availability.
- Natural physical conditions like temperature.

- Salinity of the loading medium.
- Solid phase composition.
- Gaseous phases present.

According to Dhanpat et al. (1986), the solid phase composition is one of the most important aspects involved in leach generation. This is because the solid phases, through their solubility, control not only the aqueous concentrations of inorganic elements, but also the subsequent precipitation of secondary solid phases that may limit concentrations in the leachate. Solid phases also have the potential to provide large reactive surface areas on which the adsorption/desorption of aqueous constituents can occur. For example iron oxides and silicon-aluminium oxides. It is expressed in their work that a detailed characterisation of the ash can be used to predict the aqueous concentrations of an element in the initial leachates derived from the weathering of fresh ash.

It is also important to know the composition of the effluent used to transport the ash in a wet ash disposal system, since the quality of the ash water directly affects the leach generation behaviour of the ash deposits. The ash water, used by Sasol, varies depending on factors such as:

- The actual chemicals entering the ash water system from various process units.
- The efficiency and type of waste water management employed.
- The composition of the ash produced by both the power stations and from gasification.

As discussed in section 2.1.3, most of the major elements present in fly ash pose little risk to the environment (such as Si, Al, Ca, Mg, Fe, Na) since they are present in the ash at approximately the same proportions as are present in soil.. The more volatile trace elements (B, Cd, Cr, Co, Se, As), however, condense on the surface of the ash particles and are not only more susceptible to leaching but are also more toxic at lower levels than the major elements. According to Bezuidenhout (1995), the factors controlling the major and minor elemental concentrations in an ash water disposal system are:

- precipitation/dissolution,
- complex formation,

- adsorption/desorption, and
- redox reactions

According to Dhanpat et al. (1986), in order to quantify the adsorption/desorption reactions, information on the charge characteristics of the aqueous species is needed, as well as the quantity and nature of the complexation sites.

2.2.2 Previous investigations pertaining to fly ash disposal

2.2.2.1 Major elements present in fly ash leachate

Many people have investigated the leaching associated with the disposal of fly ash. In terms of the major elements associated with fly ash leachate, the following information was attained:

- Lee (1997) found that the fly ash leachate (collected from the fly ash disposal mound in one of the major UK coal-fired power stations) contained high concentrations of Ca, Na, and SO_4.
- Villaume et al. (1987) found that leachate chemistry (using fly ash) was clearly dominated by the strong base cations: Ca, Na, K, and Mg and the strong acid anion SO_4.
- Groenewald et al. (1984) found the leachate they worked with was typically alkaline and had very high Na and SO_4 concentrations. In underlying groundwater, contaminated by the ash disposal area, Na, SO_4 and TDS concentrations were found to be as high as 16 947mg/l, 36 820mg/l and 52 650mg/l, respectively. On average however, the Na and SO_4 concentrations remained relatively constant at values of 1500mg/l and 3350mg/l, respectively. These values are about three times higher than groundwater not contaminated with leachate.

2.2.2.2 Column experiments

Many people have performed column experiments to investigate the leaching associated with fly ash disposal. A point that came up in many of these investigations is that precaution should be taken when attempting to use the results obtained from laboratory scale batch experiments in the actual ash disposal system. These laboratory tests, in isolation, do not provide sufficient information regarding thermodynamic and kinetic

properties of the primary geochemical processes occurring in the actual ash disposal system. Petersen (1998) noted that in particular, slow reaction mechanisms may go unnoticed in short-term laboratory experiments, but may become significant in full-scale practice. The laboratory scale column experiments do, however, provide an insight into possible chemical reactions that could occur in a fly ash disposal system.

Hassett et al. (1985) found that with the sole exception of sulphate, solution concentrations at the end of one-day column experiments were a poor guide to the actual leaching behaviour of the ash under long-term contact with water. They also noted that a substantial amount of soluble ions could be extracted from the ash.

Studies carried out by Roy et al. (1984), and reported by Jones (1995), revealed that for alkaline systems, although the pH did not vary greatly over the 20 weeks during which the column experiments were conducted, there was a significant reduction in the concentrations of Al, B, Ca and SO_4. Thermodynamic modelling suggested that it was $CaSO_4$ and not $CaCO_3$ that controlled the solution concentration of Ca. More recent studies done by Fruchter et al. (1990), also suggest that it is gypsum ($CaSO_4.H_2O$), which initially controls the solubility of Ca.

Hassett et al. (1985) conducted leaching tests on highly alkaline gasification ashes. They performed a long-term leaching experiment (120 days) using distilled-deionised water and found that significant fractions of the Na, K, Al, S, As, Mo, Se and V in the ash were extracted. XRD analyses were performed on the ash after the leaching procedure and it was found that only a portion of the ash had reacted with the leaching solution. The reaction products were mainly non-crystalline but minor amounts of zeolites, calcite and gibbsite were identified. It was also suggested in their work that the formation of secondary solid phases appear to be important in controlling leachate concentrations.

Liquid to solid ratio

According to Hassett et al. (1985), L:S ratios are important in determining the elements extracted and in controlling the pH. According to their results, it appears that the lower the L:S ratio, the higher the pH of the resulting leachate:

- pH of about 13 using a L:S ratio of 2:1
- pH of just below 10 using a L:S ratio of 10:1.

These results correspond well with laboratory experiments conducted for this project – that is using a L:S ratio of 5:1, the pH of the resulting leachate is found to be about 12. They also concluded from their results that the different L:S ratio resulted in different leaching mechanisms. This they deduced from the behaviour of the pH during their long-term leaching experiments using L:S ratios of 2:1 and 20:1. In the 2:1 experiment the pH rose rapidly and then levelled off to about 12.7 within about 20 days. In the 20:1 experiment the pH also showed a rapid increase to about 11.3, however, it began to decrease within a few days to a value of approximately 9.8. If the leaching mechanisms in the two experiments had been identical then the pH behaviours would have paralleled one another only differing by a factor of 1.0 due to the ten-fold dilution.

pH

According to Jones (1995), the pH of fly ash is a particularly important property since pH is the master variable that controls the leachability of contaminants, as well as the solubility of many solids (Shen-Yu and Zwane, 2001). It is the relative amounts of the sulphide minerals and alkaline earth metals in the parent coal determine to a large extent the pH of the ash. Based on published material, about 70% of fly ashes produce a neutral to strongly alkaline leachate. According to work done by Hodgson and Van Niekerk (Bezuidenhout, 1995), in South Africa the coals used for combustion have a low S content and thus produce an alkaline leachate. This was confirmed in this investigation where it was observed that the fine ash slurry, associated with the fine ash produced by Sasol 2 and Sasol 3 in Secunda, South Africa, had a pH of approximately 12. Thus, at this high pH value, the slurry is not in equilibrium with atmospheric CO_2, and recarbonation occurs resulting in a decrease of the pH.

Column experiments have shown that there is an initial decline in the pH of the leachate, which can be attributed to the existence of an acidic surface adsorbed species such as SO_2. The rise in the pH after this initial decrease is due to the reaction of the water with the deeper layers of the ash particles (Jones, 1995). Jones (1995) also reports that both Pb and Cu display increased solubilities at pH values greater than 11.5, which can be attributed to the formation of anionic hydoxo-complexes. In general, Groot et al. (Jones, 1995), revealed that there was a drastic decline in the solution concentrations of the anionic trace elements only when leachate solutions exceeded a pH of 12.2. Work done by Turner et al. (Jones, 1995), suggests that acidic conditions favour the leaching of most trace elements from ash, however it appears more pronounced for Cd, Cu and Zn. Shen-Tu and Zwane (2001) also report that an acidic leaching environment results in elevated concentrations of the leached species in the final leachate. Therefore, since the conditions in the ash disposal system studied in this investigation can be classified as highly alkaline, one would expect the leaching of trace elements to be minimal.

2.3 Chemistry of specific components

2.3.1 Calcium

2.3.1.1 A literature review

Calcium in the solid and aqueous phase is present in the +2 oxidation state. Calcium is not appreciably volatised during combustion, and therefore the amount of calcium in the ash is very similar to that in the parent coal. Since calcium is not volatile, it is not found to be preferentially enriched in fly ash or associated with the smallest particle size fraction. According to Dhanpat et al. (1986), the majority of calcium in coal is present in the inorganic phase, as carbonates, sulphates and silicates, although a small amount maybe present in the organic phase. A lot of information, pertaining to the calcium chemistry occurring in ash disposal systems, can be found in literature.

According to Dhanpat et al. (1986), due to the fact that Ca forms relatively stable compounds, it is present in ash predominately as discrete solids. They also report that not

many studies have been performed to try to quantify the specific Ca solid phases present. The possible Ca solid phases that could be present in fly ash are given in table 2.4.

Table 2.4: Possible Ca Solid Phases Present in Fly Ash (Dhanpat et al., 1986)

Unweathered Ash		Weathered Ash		
Predicted	**Observed**	**Predicted**	**Observed**	**Mineral name**
$CaCO_3$	$CaCO_3$	$CaCO_3$	$CaCO_3$	Calcite
$CaSO_4$	$CaSO_4$	$CaSO_4$		Anhydrite
CaO	CaO			Lime
	$CaSO_4.2H_2O$		$CaSO_4.2H_2O$	Gypsum
	$Ca(OH)_2$	$Ca(OH)_2$	$Ca(OH)_2$	Portlandite
	Ca-Ferrite			
	Ca_2SiO_4			Bredigite
	Ca_3SiO_5			
	$Ca_3Al_2O_6$			
	$CaSiO_3$			Wollastonite
	$CaMgSi_2O_6$			Diopside
	$Ca_2MgSi_2O_7$			Melilite
	$Ca_3Mg(SiO_4)_2$			Merwinite
	Ca_3SiO_5			Alite
	$Ca_6Al_4Fe_2O_{15}$			Brownmillerite
	$CaMg(CO_3)_2$	$CaMg(CO_3)_2$		Dolomite
		$CaAl_2Si_4O_{12}.4H_2O$		Laumontite
		$Ca_6Al_2(SO_4)_3(OH)_{12}.26H_2O$	$Ca_6Al_2(SO_4)_3(OH)_{12}.26H_2O$	Ettringite
			Ca-silicate	
			Ca-aluminate	

The origin and form of Ca in ash

Solids such as CaO, $CaSO_4$, and Ca-ferrite must result from the high temperature alteration of the original compounds present in coal since these compounds are not reported to be present or stable in coal. The origin and form of Ca in the ash is confirmed by the following citations in literature:

- The origin of the lime (CaO) in the ash, according to Dhanpat et al. (1986), is from the decarbonisation of the $CaCO_3$ that is found in the coal.
- The major forms of Ca in fresh ash, reported by Jones (1995), are $CaSO_4$ and CaO which may occur either as small discrete particles with a higher density than the primarily aluminosilicate or glassy spheres, or attached to the surface of the larger glassy spheres.

- Work done by Kaufher et al. in the USA (Jones, 1995) indicated that Ca and S are enriched on the surface of the fly ash. They reported that the S appeared to be in stoichiometric excess to that required for $CaSO_4$, which suggested that adsorbed SO_2 was present on the surface.

The solubility and leaching of Ca

If one compares the following three calcium compounds: CaO, $CaCO_3$, and $CaSO_4.2H_2O$; the most soluble is CaO. In an alkaline environment $CaCO_3$ is the least soluble and thus will precipitate rapidly. Dhanpat et al., 1986, suggest that it is this compound that controls the aqueous Ca concentration in weathered fly ash over long periods of time, provided the environment is an alkaline one. If the environment is acidic, it will be the $CaSO_4.2H_2O$ that controls the Ca concentration. They also suggest that during the earlier stages of weathering, compounds that are more soluble than $CaCO_3$ and $CaSO_4.2H_2O$ may control the Ca concentration in a solution. An example of one of these such compounds is $Ca(OH)_2$, which forms rapidly due to the hydrolysis of CaO in very alkaline and CO_2-defficient environments. However, due to the presence of CO_2 in the air, the $Ca(OH)_2$ and other metastable compounds in alkaline conditions will eventually convert to $CaCO_3$. These reactions, pertaining to the calcium carbonate chemistry, are:

$$CaO_{(s)} + H_2O \rightarrow Ca(OH)_2 \qquad (2\text{-}7)$$

$$CO_2 + H_2O \rightarrow H_2CO_3 \qquad (2.8)$$

$$Ca(OH)_2 + H_2CO_3 \rightarrow CaCO_{3(s)} \qquad (2.9)$$

Many people support the calcium carbonate chemistry as described by reactions (2-7), (2-8) and (2-9):

- Villaume et al. (1987) performed a principal component analysis, which looks at the interrelationships among constituents, and the results suggested an inverse grouping of calcium with carbonate at high pH values, and therefore the possible presence of a calcium carbonate solid phase. They also suggested that the formation of this solid may be controlled by the availability of atmospheric carbon dioxide in the carbonate deficient test cell that they used in their study.

- According to Dhanpat et al. (1986), calcite and $CaSO_4.H_2O$ are commonly reported to be present in both weathered and unweathered wastes.
- Hassett et al. (1984) suggest, from their research, that calcite is the phase controlling the solubility of Ca. Since the solubility of calcite is strongly pH dependent, if the solubility of Ca is controlled by calcite, then the solubility of Ca is also pH dependent.
- Bezuidenhout (1995) reports that in his study of an ash water system, he found the activity of Ca in the solution to be consistent with wollastonite, calcite, fluorite and portlandite.
- Bezuidenhout (1995) reported findings, by Sakata, that an alkaline leachate containing relatively high concentrations of Ca, and SO_4, will move downward through an ash heap forming gypsum (which has a low solubility) during the process. He further reports the suggestion by Roy and Griffen, that the Ca activity is controlled by the solubility of anhydrite. Bezuidenhout (1995) also reported findings by Fruchter and Zachara; that Ca concentrations are controlled by gypsum, calcite, anhydrite, and at pH values in excess of 12, portlandite. Fruchter and Zachara found the activities of Ca to be independent of the pH, which suggests that calcite and portlandite are not the solubility controlling solids, and therefore gypsum and anhydrite must be controlling the solution concentration of Ca.

In terms of leaching of the Ca from the ash, Dhanpat et al. (1986) found the following to be true:

- The amount of Ca leached varies greatly depending on the leaching medium (i.e. the pH of the medium).
- The rate of Ca leaching decreases with time.
- Long-term leaching produces steady-state Ca concentrations.

2.3.1.2 Theoretical calcium chemistry

Calcium is a component of particular importance in the Sasol ash water system at Secunda, and therefore, it will be discussed in more detail than the other components. Furthermore, the Ca chemistry, occurring in an ash water system, is well documented in the literature.

Langelier Saturation Index

If total alkalinity, pH, and calcium concentration of a particular water are measured, it is possible to calculate whether or not a water is saturated with respect to calcium carbonate – that is, whether or not the solubility product equation for $CaCO_3$ is satisfied. When the product of the active concentration of calcium and carbonate ions exceeds the solubility product constant, the water is over saturated with respect to $CaCO_3$, and the $CaCO_3$ will precipitate out. On the other hand, when the solubility product is not exceeded, the water is under saturated with respect to $CaCO_3$. From theoretical considerations, Langelier developed a 'saturation index', which, by its sign, establishes whether a water is over or under saturated with respect to $CaCO_3$.

Calculation of the Langelier Saturation Index

(Benefield, 1982)

The solubility equilibrium constant expression for calcium carbonate has the form

$$K_s' = [Ca^{2+}][CO_3^{2-}] \qquad (2\text{-}10)$$

Since carbonic acid is a weak acid, the distribution of the various carbonic species depends on the pH of the solution. Thus, ionisation fractions, α, are defined with represent the fraction of the total carbonic species concentration, C_T, present as a given species.

For example,

$$\alpha_2 = \frac{[CO_3^{2-}]}{C_T} \qquad (2\text{-}11)$$

Therefore, $\left[CO_3^{2-}\right]$ can be expressed as $C_T\alpha_2$. Equation (2-10) can thus be written as

$$K_s^{'} = \left[Ca^{2+}\right]\alpha_2 C_T \tag{2-12}$$

where α_2 is defined as

$$\alpha_2 = \frac{1}{\frac{\left[H^+\right]^2}{K_1^{'}K_2^{'}} + \frac{\left[H^+\right]}{K_2^{'}} + 1} \tag{2-13}$$

Before going any further, it is necessary to define some terms, which will be used in the derivation of the Langelier Saturation Index.

$$K_1 = \frac{\left[H^+\right]\left[HCO_3^-\right]}{\left[H_2CO_3^*\right]} \tag{2-14}$$

where $H_2CO_3^*$ is the sum of the concentrations of dissolved CO_2 and H_2CO_3.

$$K_2 = \frac{\left[H^+\right]\left[CO_3^{2-}\right]}{\left[HCO_3^-\right]} \tag{2-15}$$

The total carbonic species is defined in terms of the mass balance expression

$$C_T = \left[H_2CO_3^*\right] + \left[HCO_3^-\right] + \left[CO_3^{2-}\right] \tag{2-16}$$

The ionic activity coefficient for ionic chemical species can be estimated, according to Benefield et al. (1982) from the following relationship:
The Davies relationship for solutions whose ionic strengths do not exceed 0.5M.

$$\log\gamma = -AZ^2\left(\frac{\sqrt{I}}{1+\sqrt{I}} - 0.3I\right) \qquad (2\text{-}17)$$

where:

$$I = ioinc\ \ strength = \left(2.5\times10^{-5}\right)(TDS) \text{ in moles/l} \qquad (2\text{-}18)$$

TDS = total dissolved solids concentration of the water in mg/l – this equation applies when the TDS concentration is less than 1000mg/l.

However, Kemp (1971) indicates that the activity coefficient, γ , is relatively insensitive to small changes in ionic strength and as a result this equation generally provides a reasonable approximation of the ionic strength of a solution.

$Z =$ oxidation number of the chemical species of interest

$$A = 1.82\times10^{6}(DT)^{-3/2} \qquad (2\text{-}19)$$

where T = temperature of the solution (K)

D = dielectric constant for water, which is generally taken to have a value of 78.3

Using the activity correction illustrated in equation (2-17), equations (2-14) and (2-15) can be correctly expressed as

$$K_1 = \frac{\gamma_m\left[H^+\right]\gamma_m\left[HCO_3^-\right]}{\left[H_2CO_3^*\right]}$$

or (2-20)

$$K_1' = \frac{K_1}{(\gamma_m)^2}$$

And

$$K_2 = \frac{\gamma_m [H^+] \gamma_D [CO_3^{2-}]}{\gamma_m [HCO_3^-]}$$

or (2-21)

$$K_2' = \frac{K_2}{\gamma_D}$$

The thermodynamic equilibrium constant values are for standard state conditions, which implies 25°C. To develop an apparent equilibrium constant, the 25°C constant is first adjusted for temperature, and then the ionic strength corrections are applied. The equilibrium constant K_1 and K_2 may be adjusted for temperature by applying the following relationships (Loewenthal and Marais, 1976):

$$pK_1 = \frac{17052}{T} + 215.21(\log T) - 0.12675(T) - 545.56 \quad (2\text{-}22)$$

$$pK_2 = \frac{2902.39}{T} + 0.02379(T) - 6.498 \quad (2\text{-}23)$$

Now that the necessary terms have been defined, it is possible to write an expression for the Langelier Saturation Index.

Substituting equation (2-13) into equation (2-12) gives

$$K_s' = \frac{[Ca^{2+}] C_T}{\frac{[H^+]^2}{K_1' K_2'} + \frac{[H^+]}{K_2'} + 1} \quad (2\text{-}24)$$

This equation illustrates the relationship between calcium carbonate solubility and pH and indicates that the solubility will increase with decreasing pH.

The Langelier index (LI), is defined on the basis of the saturation pH.

$$\text{Langelier index (LI)} = \text{pH} - \text{pH}_s \qquad (2\text{-}25)$$

Where pH = measured pH of the water, and

pH_s = calculated saturation pH of the water.

A negative LI indicates water that is undersaturated with respect to $CaCO_3$; a positive LI indicates water that is oversaturated with respect to $CaCO_3$. A LI of zero indicates water that is just saturated with respect to $CaCO_3$.

Calculation of pH_s

Loewenthal and Marais (1976) developed an equation that is needed for the calculation of pH_s, the derivation of which is summarised below:

The alkalinity, based on the assumption that it is due to the presence of a strong base in a carbonic acid solution, can be expressed as

$$[Alk]_e = [CO_3^{2-}]_e + [HCO_3^-]_e + [OH^-]_e - [H^+]_e \qquad (2\text{-}26)$$

where $[\ ]_e$ represents the concentration, of the particular component, in terms of equivalents per litre.

In terns of Moles per litre, equation (2-23) can be written as

$$2[Alk] = 2[CO_3^{2-}] + [HCO_3^-] + [OH^-] - [H^+] \qquad (2\text{-}27)$$

where $[H^+]$ is the molar hydrogen ion concentration. This value is calculated from the measured pH value by employing the following equation

$$[H^+] = \frac{10^{-pH}}{\gamma_m} \tag{2-28}$$

Solving equation (2-27) for $[CO_3^{2-}]$ and substituting for $[HCO_3^-]$ in equation (2-27) from equation (2-21) gives

$$[CO_3^{2-}] = [Alk] - \frac{[H^+][CO_3^{2-}]}{2K_2'} - \frac{1}{2}[OH^-] + \frac{1}{2}[H^+]$$

rearranging gives (2-29)

$$[CO_3^{2-}] = \frac{[Alk] - \frac{1}{2}[OH^-] + \frac{1}{2}[H^+]}{\left[1 + \frac{[H^+]}{2K_2'}\right]}$$

If the denominator of equation (2-29) is multiplied by $\frac{2K_2'[H^+]}{2K_2'[H^+]}$, then the following equation is obtained;

$$[CO_3^{2-}] = \frac{K_2'\{2[Alk] - [OH^-] + [H^+]\}}{[H^+]\left[\frac{2K_2'}{[H^+]} + 1\right]} \tag{2-30}$$

For any equilibrium calcium concentration, the carbonate required for saturation may be computed by rearranging the solubility equilibrium constant expression into the form

$$[CO_3^{2-}]_s = \frac{K_s'}{[Ca^{2+}]} \qquad (2\text{-}31)$$

where $[CO_3^{2-}]_s$ is the concentration required for saturation at a specified calcium concentration (moles/l).

For a specific total carbonic species concentration, the carbonate concentration is dependent only on pH. Equation (2-30) can therefore be written as;

$$[CO_3^{2-}]_s = \frac{K_2' \{2[Alk] - [OH^-]_s + [H^+]_s\}}{[H^+]_s \left[\frac{2K_2'}{[H^+]_s} + 1\right]} \qquad (2\text{-}32)$$

where $[H^+]_s$ and $[OH^-]_s$ represent the saturation hydrogen ion and hydroxyl ion concentrations, respectively.

Substituting for $[CO_3^{2-}]_s$ in equation (2-32) from equation (2-31), and rearranging gives

$$K_s' = \frac{[Ca^{2+}]K_2' \{2[Alk] - [OH^-]_s + [H^+]_s\}}{[H^+]_s \left[\frac{2K_2'}{[H^+]_s} + 1\right]} \qquad (2\text{-}33)$$

Rearranging equation (2-33) and taking the logarithm of both sides yields the following equation:

$$-\log[H^+]_s = \log K_s' - \log K_2' - \log[Ca^{2+}] - \log\{2[Alk] - [OH^-]_s\} + \log\left[\frac{2K_2'}{[H^+]_s} + 1\right]$$

(2-34)

Since

$$pH_s = -\log[\gamma_m [H^+]_s]$$
$$pK_s' = -\log K_s'$$
$$pK_2' = -\log K_2'$$
$$pCa^{2+} = -\log[Ca^{2+}]$$

equation (2-34) reduces to

$$pH_s = pK_2' + pCa^{2+} - pK_s' - \log\{2[Alk] - [OH^-]_s + [H^+]_s\} + \log\left[\frac{2K_2'}{[H^+]_s} + 1\right] - \log\gamma_m$$

(2-35)

According to Loewenthal and Marais (1976), equation (2-35) can be simplified when the pH is in the range 6.5 to 9.5. Within this pH range the $[H^+]_s$ and $[OH^-]_s$ terms in the sum $\{2[Alk] - [OH^-]_s + [H^+]_s\}$ and the $2K_2'/[H^+]_s$ term in the sum $[2K_2'/[H^+]_s + 1]$ are negligible.

Equation (2-35) therefore reduces to

$$pH_s = pK_2' + pCa^{2+} - pK_s' - \log(2[Alk]) - \log\gamma_m \qquad (2\text{-}36)$$

In order to solve equation (2-35) the following procedure was followed:

pK_w was calculated using the following equation:

$$pK_w = \frac{4787.3}{T} + 7.1321(\log T) + 0.010365(T) - 22.801 \qquad (2\text{-}37)$$

From this K_w and K_w' were calculated:

$$K_w^{'} = \frac{K_w}{(\gamma_m)^2} \tag{2-38}$$

The term $[H^+]_s$ and $[OH^-]_s$ in equation (2-35) were then expressed as follows:

$$[H^+]_s = \frac{10^{-pH_s}}{\gamma_m} \tag{2-39}$$

and

$$[OH^-]_s = \frac{K_w^{'}}{[H^+]_s} \tag{2-40}$$

Substituting equations (2-39) and (2-40) into equation (2-35) yields:

$$pH_s = pK_2^{'} + pCa^{2+} - pK_s^{'} - \log\left(2[Alk] - \frac{K_w^{'}}{10^{-pH_s}/\gamma_m} + \frac{10^{-pH_s}}{\gamma_m}\right) + \log\left(\frac{2K_2^{'}}{10^{-pH_s}/\gamma_m} + 1\right) - \log\gamma_m \tag{2-41}$$

Equation (2-41) can be solved using a trial-and-error method (or the solver function in Excel).

The pH_s values were calculated using equation (2-41) as well as the simplified equation (2-36), even though all the pH values for the water samples were not in the range 6.5 to 9.5, as required.

Possible Reactions and Equilibrium Formulae

From Pourbaix (1966), the following information was obtained in relation to the reactions associated with Ca.

Table 2.5: Different forms of Ca

CALCIUM			
	Oxidation Number	Considered	Name
Solid Substances	-2	CaH_2	calcium hydride
	0	Ca	calcium
	+2	CaO hydr.	hydrated calcium oxide $Ca(OH)_2$ or hydroxide
	+2	CaO anh.	Anhydrous calcium oxide CaO
Dissolved Substances	+4	CaO_2	calcium peroxide
	+2	Ca^{++}	divalent calcium ion

Reactions

Two Solid Substances

$$CaH_2 \leftrightarrow Ca + 2H^+ + 2e^- \quad (2\text{-}42)$$

$$CaH_2 + H_2O \leftrightarrow CaO + 4H^+ + 4e^- \quad (2\text{-}43)$$

$$Ca + H_2O \leftrightarrow CaO + 2H^+ + 2e^- \quad (2\text{-}44)$$

$$CaO + H_2O \leftrightarrow CaO_2 + 2H^+ + 2e^- \quad (2\text{-}45)$$

One Solid Substance and One Dissolved Substance

$$Ca^{2+} + H_2O \leftrightarrow CaO + 2H^+ \quad (2\text{-}46)$$

$$CaH_2 \leftrightarrow Ca^{2+} + 2H^+ + 4e^- \quad (2\text{-}47)$$

$$Ca \leftrightarrow Ca^{2+} + 2e^- \quad (2\text{-}48)$$

$$Ca^{2+} + 2H_2O \leftrightarrow CaO_2 + 4H^+ + 2e^- \qquad (2\text{-}49)$$

Stability of Calcium

The alkaline earth metals in general, including calcium, exert an extremely low solution potential. As the whole of their domain of stability lies well below that of water (see figure 2.1), these metals are very unstable in the presence of aqueous solutions of any pH. They are extreme base metals and powerful reducing agents, having a large affinity to react with water, which they decompose with the evolution of hydrogen. By examining the potential-pH diagram for calcium (figure 2.1), one can see that calcium is unstable with respect to the anhydride CaH_2, which itself is unstable in the presence of water.

Stability of the oxides and hydroxides of calcium

In the presence of water, the anhydrous oxide, CaO, is very unstable with respect to the corresponding hydroxide, $Ca(OH)_2$. They therefore tend to become hydrated according to the reaction $CaO + H_2O \leftrightarrow Ca(OH)_2$ (equation (2.7)). As is well known, this hydration reaction takes place very rapidly. Figure 2.2 shows the influence that pH has on the solubility of calcium hydroxide.

Stability of the hydride of calcium

As can be seen in the Pourbaix diagram (Figure 2.1), the hydride of calcium is thermodynamically unstable in the presence of water and aqueous solutions, in which it will decompose with the formation of hydrogen and the cation Ca^{2+}.

The numbers displayed in figures 2.1 and 2.2 relate to the reactions 2-42 to 2-49 in the manner shown in table 2.6.

Table 2.6: Numbers in figures 2.1 and 2.2, and corresponding reaction

Number in figures 2.1 and 2.2	Corresponding reaction
1	(2-42)
2	(2-43)
3	(2-44)
4	(2-45)
5	(2-46)
6	(2-47)
7	(2-48)
8	(2-49)

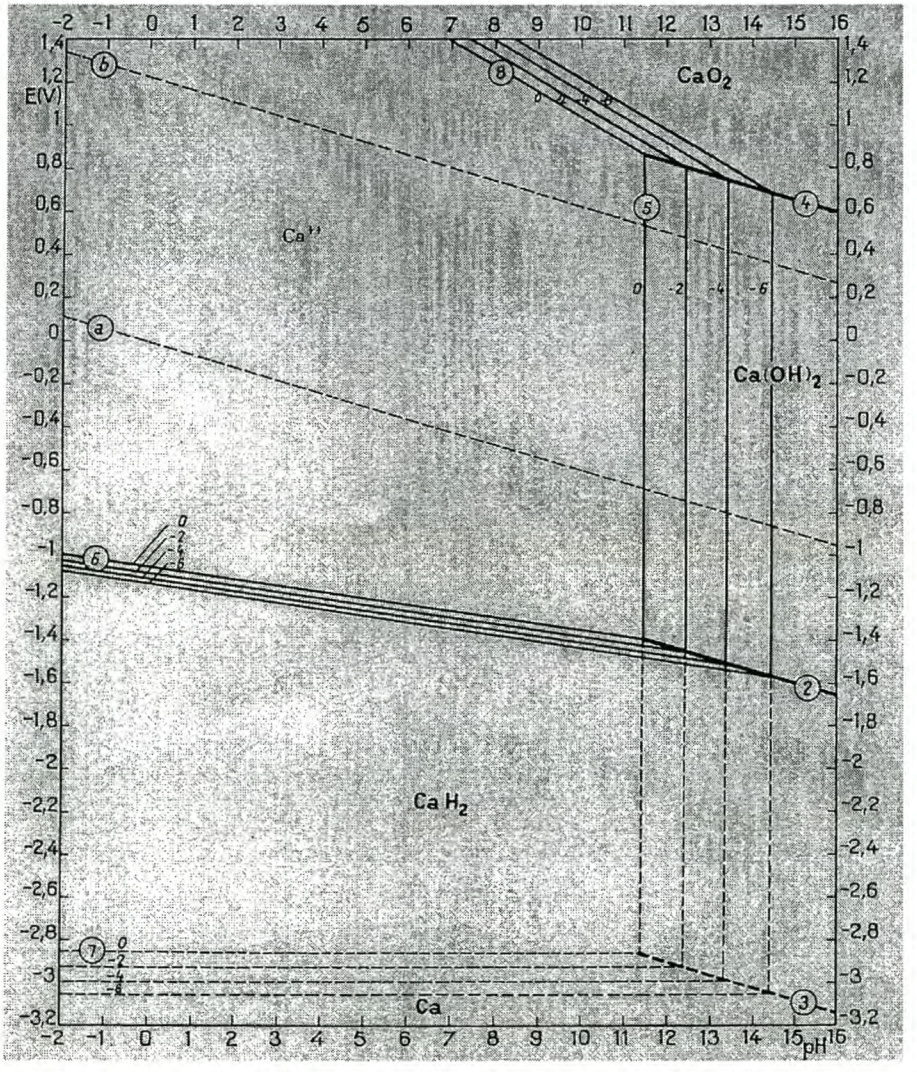

Figure 2.1: Potential-pH equilibrium diagram for the calcium-water system, at 25°C (Pourbaix, 1966)

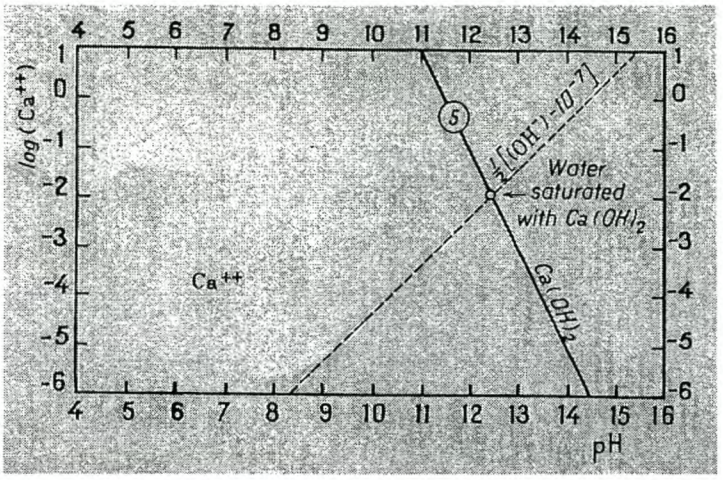

Figure 2.2: Influence of pH on the solubility of $Ca(OH)_2$ at 25°C (Pourbaix, 1966)

2.3.2 Sodium

2.3.2.1 A literature review

Hassett et al. (1985), found sodium to be the most abundant metallic element in solution. They also found that the maximum amount of Na that was extracted from the ash, using distilled water, was 47% (L:S = 20:1), and 38% (L:S = 2:1). They found that at some stage in their leaching experiments, the rate of leaching of the Na decreased considerably, suggesting that either most of the Na had been leached by that stage, or the formation of a secondary solid phase was controlling the concentration of the dissolved Na through its saturation behaviour.

The form of Na in the ash

The possible Na containing phases in fly ash are identified by Hassett et al. (1985) to be:

- Carnegieite
- Nepheline
- Sodalite
- Melilite
- Glass

Hassett et al. (1984) found both K and Na in nepheline, carnegieite, Ca-Na-silicates, sodalite-phase, plagioclase, zeolites and the glass phase. The zeolites detected were Na-aluminosilicate and would be expected to exchange Na and K when contacted with water containing divalent cations. They suggested that the foremost mechanism for the release of Na and K from the aluminosilicates is ion exchange.

The solubility and leaching of Na

It is proposed by Jones (1995) that Na, K, Mg and Ca are all excluded from the structures of mullite and quartz since these phases crystallise from the molten state. It is the amorphous glassy phases appear to contain the major portion of Na and K, and lesser amounts of Ca and Mg. If the Na were enriched in the glassy phases, one would expect the initial leachate to contain Na, since the glassy phases are preferentially dissolved compared to the more resistant crystalline phases.

2.3.2.2 Theoretical sodium chemistry

Possible Reactions and Equilibrium Formulae

From Pourbaix (1966), the following information was obtained in relation to the reactions associated with Na.

Table 2.7: Different forms of Na

SODIUM			
	Oxidation Number	Considered	Name
Solid Substances	-1	NaH	sodium hydride
	0	Na	sodium
	+1	Na_2O	sodium monoxide
	+1	NaOH	sodium hydroxide
	+2	Na_2O_2	sodium peroxide
Dissolved Substances	+1	Na^+	sodium cation

Reactions

Two Solid Substances

$$NaH \leftrightarrow Na + H^+ + e^- \qquad (2\text{-}50)$$

One Solid Substance and One Dissolved Substance
(Solubility of the solid substances)

$$NaH \leftrightarrow Na^+ + H^+ + 2e^- \qquad (2\text{-}51)$$

$$Na \leftrightarrow Na^+ + e^- \qquad (2\text{-}53)$$

Stability and Formation of Sodium

Since the whole of the domain of stability of sodium is situated very much below the domain of the stability of water (figure 2.3), it is extremely unstable in the presence of aqueous solutions of any pH. The oxide of Na is very soluble, and Na metal will decompose aqueous solutions vigorously with the evolution of hydrogen.

Stability and Formation of Sodium Hydride

From the potential-pH diagram (figure 2.3) it is evident that sodium hydride is less unstable in the presence of water than sodium. Although it still reacts vigorously with water forming hydrogen, it is perfectly stable in the absence of water and oxygen.

The numbers displayed in figure 2.3 relate to the reactions 2-50 to 2-52 in the manner shown in table 2.8.

Table 2.8: Numbers in figure 2.3 and corresponding reactions

Number in figure 2.3	Corresponding reaction
1	(2-50)
2	(2-51)
3	(2-52)

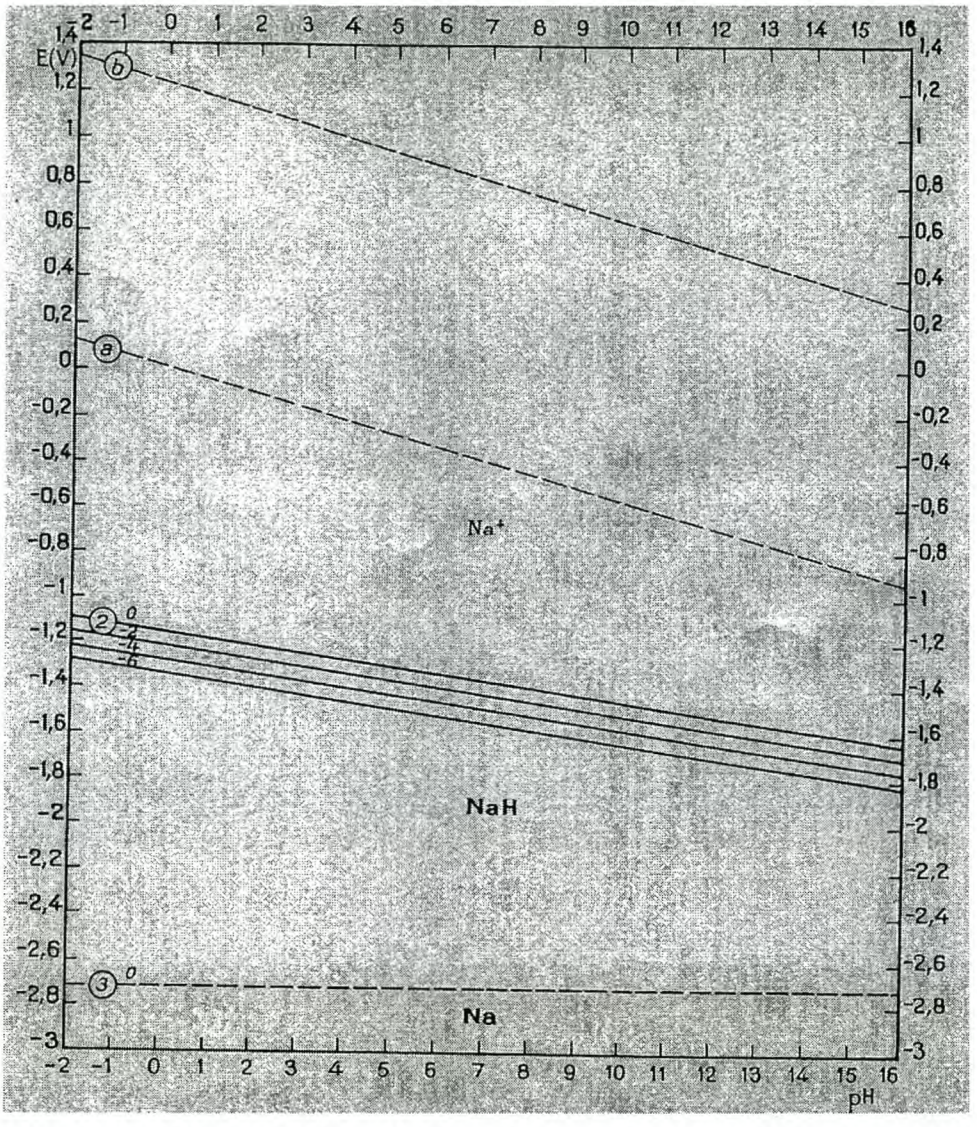

Figure 2.3: Potential-pH equilibrium diagram for the sodium-water system, at 25°C (Pourbaix, 1966)

2.3.3 Sulphur

2.3.3.1 A literature review

According to Hassett et al. (1985), sulphur is present in the ash largely as sulphate. They also found that they were able to extract substantial amounts of sulphate from the ash even after the first day of column leach experiments. This initial drastic leaching of the sulphates from the ash could be explained by the possible presence of a compound such

as sodium sulphate (or a more complex phase) that is unstable at a high pH. They also found that the concentration of the sulphate in the leachate remained constant after the first few days, suggesting that either all the leachable sulphur was extracted from the ash in the first few days, or, more likely, a secondary solid phase controlled the sulphur concentration through its saturation behaviour. Initial experiments conducted during this study revealed that 313mg/l of sulphate was leached from the ash after a week.

Bezuidenhout (1995) found a decrease in the SO_4 concentration, which was difficult to explain since the MINTEQA2 speciation (based on solution composition data) indicated that the solution was undersaturated with respect to gypsum. He suggested that another possible reason for the decrease in the SO_4 concentration could be due to the reduction of sulphate to sulphide by anaerobic sulphate reducing bacteria. He found the reducing environment, required for this process, in the topsoil of the soil profile beneath the actual ash dam. A further possible explanation for the reduction in the sulphate concentration could be the precipitation of a mineral less soluble than gypsum, possibly ettringite.

2.3.4 Potassium

2.3.4.1 A literature review

Hassett et al. (1985) found K to behave similarly to Na. A maximum of 13% of the K in the ash was extracted (using a L:S ratio of 20:1) and 7% using a L:S ratio of 2:1. Due to the fact that less K was extracted in their experiments than Na, it was suggested that the phases containing K are less leachable than those containing Na.

The form of K in the ash

Hassett et al. (1984) found both K and Na in nepheline, carnegieite, Ca-Na-silicates, sodalite-phase, plagioclase, zeolites and the glass phase. The zeolites detected were Na-aluminosilicate and would be expected to exchange Na and K when contacted with water containing divalent cations. They suggested that the foremost mechanism for the release of Na and K from the aluminosilicates is ion exchange.

The solubility and leaching of K

It is proposed by Jones (1995) that Na, K, Mg and Ca are all excluded from the structures of mullite and quartz since these phases crystallise from the molten state. It is the amorphous glassy phases appear to contain the major portion of Na and K, and lesser amounts of Ca and Mg. If the K were enriched in the glassy phases, one would expect the initial leachate to contain K, since the glassy phases are preferentially dissolved compared to the more resistant crystalline phases.

2.3.5 Aluminium

2.3.5.1 A literature review

Hassett et al. (1984) found Al to be present in the following phases:

- glass
- ferrite spinel
- nepheline
- carnegieite
- melilite
- the sodalite-phase
- zeolites.

The solubilities of all these phases are relatively low, and therefore the solubility of Al is more likely to be controlled by its oxyhydroxides and hydroxide species thus making it pH dependent. Hassett et al. (1984) also reports that the solubility of Al increases at lower pH values, which would explain why there is very little Al present in the leachate from the fine ash studied in this investigation (highly alkaline ash water).

Warren and Dudas concluded, from the research they did, that the leachate characteristics after moderate weathering were characterised by the release of relatively high levels of Si and Al from the surface glass (Bezuidenhout, 1995).

2.3.6 Silicon

2.3.6.1 A literature review

According to work done by Hassett et al. (1984), kinetically, it is probably the glass phase that controls the solubility of Si in the early stages of leaching. Only later during the leaching process will compounds such as nesosilicates (C_2S, merwinite), sorosilicates (melilite) and tectosilicates (nepheline, carnegieite, sodalite) begin to show significant solubility. Bezuidenhout (1995) found that above a pH of 10, the activity of Si in the leachate was consistent with the stability of wollastonite ($CaSiO_3$).

2.3.7 Magnesium

2.3.7.1 A literature review

The form of Mg in the ash

Hassett et al. (1984) found Mg to be present in:

- Merwinite
- Ferrite spinel
- Periclase (MgO)
- The C_2S phases
- Melilite
- The glass phases.

The solubility and leaching of Mg

According to Jones (1995) and Hassett et al. (1984), MgO is the primary soluble form of Mg in a strongly alkaline fly ash. When the ash comes into contact with water, the MgO will hydrate and thus the initial concentration of Mg will be controlled by the solubility of $Mg(OH)_2$, which is pH dependent.

Jones (1995) found an increase in the Mg concentration of the leachate at lower pH values. Based on this finding, one would not expect to find very high Mg concentrations in the ash water used in the ash water system at Sasol, Secunda, since this water is highly alkaline.

2.3.7.2 Theoretical magnesium chemistry

Possible Reactions and Equilibrium Formulae

From Pourbaix (1966), the following information was obtained in relation to the reactions associated with Mg (see table 2.9 and equations (2.53) to (2.55)).

Table 2.9: Different forms of Mg

MAGNESIUM				
	Oxidation Number	Considered	Not Considered	Name
Solid Substances	-2		MgH_2	magnesium hydride
	0	Mg		magnesium
	+1		Mg_2O	magnesium sub-oxide
	+2	MgO hydr.		magnesium hydroxide $Mg(OH)_2$
	+2	MgO anh.		magnesium oxide
	+4		MgO_2	magesium peroxide
Dissolved Substances	+1		Mg+	magnesous ion
	+2	Mg^{2+}		magnesic ion

Reactions

Two Solid Substances

$$Mg + H_2O \leftrightarrow MgO + 2H^+ + 2e^- \qquad (2\text{-}53)$$

One Solid Substance and One Dissolved Substance
(solubility of magnesium and magnesium oxide)

$$Mg^{2+} + H_2O \leftrightarrow MgO + 2H^+ \qquad (2\text{-}54)$$

$$Mg \leftrightarrow Mg^{2+} + 2e^- \qquad (2\text{-}55)$$

Stability of Magnesium

As can be see in the potential-pH diagram (figure 2.4), the whole of the domain of stability of magnesium is well below that of water; magnesium is therefore an string base metal and an extremely powerful reducing agent. At all pH's it has a great affinity to

react with water, which it reduces with the evolution of hydrogen, dissolving as Mg^{+} and Mg^{2+} ions.

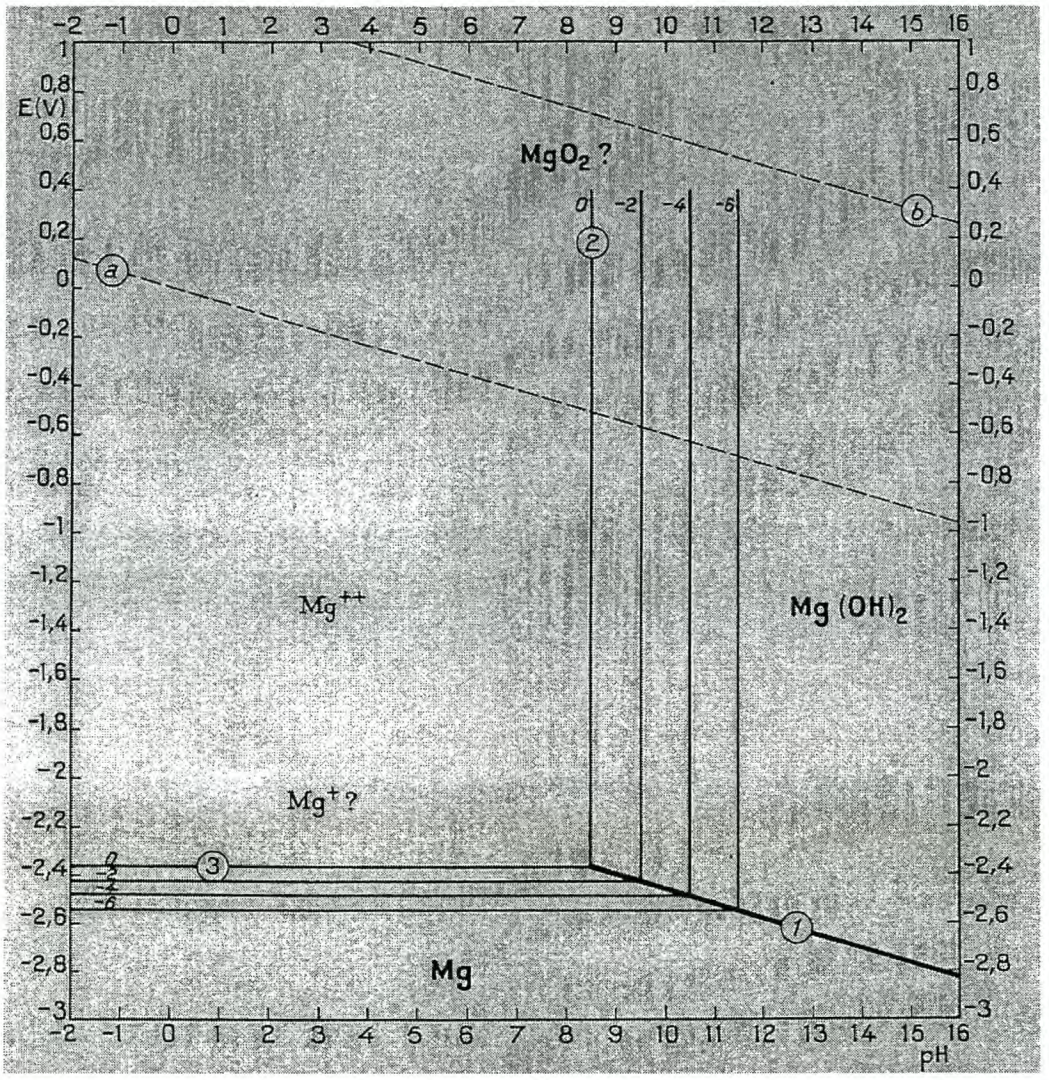

Figure 2.4: Potential-pH equilibrium diagram for the magnesium-water system, at 25°C (Pourbaix, 1966)

Stability of the magnesium oxides

From the potential-pH diagram (figure 2.4) one can see that the oxidation of magnesium in an alkaline solution can give rise to the formation of the oxide MgO and the hydroxide $Mg(OH)_2$, neither of which possess any amphoteric (can act as either an acid

or a base) character. Since the free enthalpy of formation of $Mg(OH)_2$ at 25°C (-142 580 cal/gmol MgO) is below the free enthalpy of formation of anhydrous MgO (-136 130 cal), $Mg(OH)_2$ is thermodynamically more stable than MgO in the presence of water. The oxide can therefore theoretically be hydrated according to the following reaction:

$$MgO + H_2O \rightarrow Mg(OH)_2 \qquad (2.56)$$

The influence of pH on the solubility of MgO and $Mg(OH)_2$ can be seen in figure 2.5.

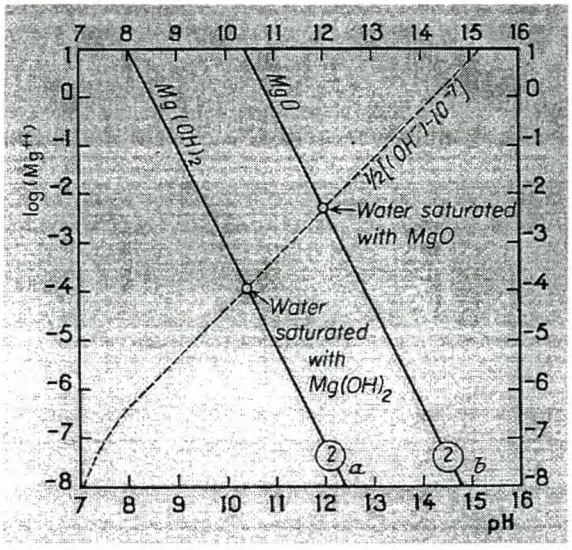

Figure 2.5: Characteristics of solutions of MgO and $Mg(OH)_2$ in pure water (Pourbaix, 1966)

The numbers displayed in figures 2.4 and 2.5 relate to the reactions 2-53 to 2-55 in the manner shown in table 2.10.

Table 2.10: Numbers in figures 2.4 and 2.5, and corresponding reactions

Number in figures 2.4 and 2.5	Corresponding reaction
1	(2-53)
2	(2-54)
3	(2-55)

2.3.8 Iron

2.3.8.1 A literature review

Iron in fly ash occurs in many phases, and Hassett et al. (1984) suggest that the solubility of Fe is controlled by the oxyhydroxides and hydroxides of Fe.

Jones (1995) reports that the outer 'glass' layer of the fly ash particles is enriched with Fe along with Ca, Mg, and Al. This is based on the theory that the majority of the fly ash particles consist of a core of mullite surrounded by a glassy matrix.

2.4 Electrochemistry

Electrochemical thermodynamics can, within certain limits, provide assistance to electrochemistry in a similar manner to that in which chemistry assists chemical thermodynamics. The potential-pH diagrams (Pourbaix diagrams) have the essential purpose of supplying a thermodynamic framework for electrochemical reactions involving aqueous solutions. If one knows the potential and pH of water, then this point can be located on the potential-pH diagram. All the reactions with equilibrium potentials below the potential of this point can take place only in the oxidation direction; all the reactions whose equilibrium potentials are above the potential of this point, can take place only in the reduction direction.

The letters *a* and *b* on all the Pourbaix diagrams represent the limits of the domain of the stability of water. Line *a* represents the equilibrium conditions for the reduction of water (or its H^+ ions) to gaseous hydrogen, and line *b* represents the oxidation of water to gaseous oxygen; when the partial pressure of hydrogen or oxygen is 1atm at 25°C. These limits are reproduced on all the potential-pH diagrams since all aqueous solutions contain water.

A detailed discussion of potential-pH diagrams for specific components was presented in section 2.3.

2.5 Water Alkalinity

A qualitative test of an alkaline substance is its ability to neutralize acids; a test of an acid is its ability to neutralize bases. To quantitatively test for the amount of alkaline substance in water it is common to reduce the alkalinity with a known concentration of acid to prescribed end points (titration). In water chemistry, the convenient end points are those produced by phenolphthalein and methyl orange indicators. Figure 2.6 illustrates that if an acid is added to reach the methyl orange end point (at a pH of about 4.3), the total alkalinity of the water is determined. This methyl orange alkalinity, or "M alkalinity (MAlk)", therefore represents total alkalinity.

Since there is no simple way of checking for specific ions such as bicarbonate or carbonate ions that could contribute to this, the phenolphthalein end point (at a pH of about 8.2 – 8.4) is also used. Empirically it has been determined that his "P alkalinity (PAlk)" represents all of the hydroxide ions present plus one half of all the carbonate ions.

When the pH exceeds 8.2 – 8.4, the free CO_2 disappears and the bicarbonate ions begin to convert to carbonate ions. This progresses until a pH of about 9.8 – 10 is reached, at which point all the CO_2 originating alkalinity is essentially in the form of carbonates. It is convenient to use a shorthand method to easily calculate the balance between HCO_3^-, CO_3^{2-} and OH^-, based on P and M alkalinities. These expressions are as follows:

Below pH 9.8 – 10.0 (where PAlk is less than ½ MAlk):

$$CO_3^{2-} = 2xP \tag{2-57}$$

$$HCO_3^- = M - CO_3^{2-} = M - 2P \tag{2-58}$$

$$OH^- = zero \tag{2-59}$$

Above pH 9.8 – 10.0 (where PAlk exceeds ½ MAlk):

$$CO_3^{2-} = 2(M - P) \tag{2-60}$$

$$OH^- = 2P - M \tag{2-61}$$

$$HCO_3^- = zero \tag{2-62}$$

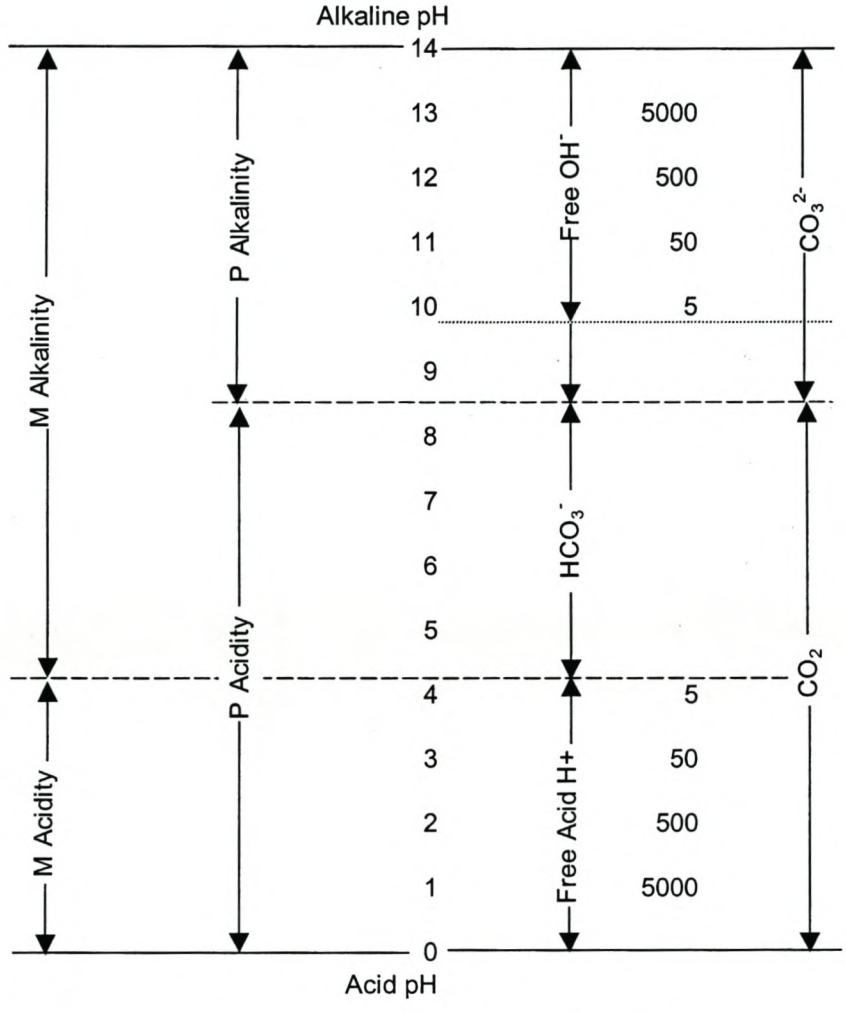

Figure 2.6: Schematic representation of the MAlk and PAlk

There is also a direct correlation between pH and the amount of hydroxide or mineral acids in a water (see figure 2.6). For example, a pH of 11 indicates that the water contains 50 ppm of hydroxide ions (expressed in terms of $CaCO_3$). A pH of 2 indicates

that 500 ppm of free mineral acid is present (in terms of $CaCO_3$). This chart can therefore, be used to convert free mineral acidity or hydroxide alkalinity to pH, or visa versa.

2.6 Geochemical modelling

PHREEQC (Parkhurst, 1995) is a computer program that has been designed to cope with a wide range of low-temperature aqueous geochemical calculations. It is written in the C programming language and can be used for:

- speciation,
- batch-reaction,
- one-dimensional transport, and
- inverse geochemical calculations.

The program is based on equilibrium chemistry of aqueous solutions interacting with minerals, gases, solid solutions, exchangers, and sorption surfaces. It is also capable to model kinetic reactions with rate equations that are completely user specified in the form of BASIC statements. As part of this investigation, PHREEQC was used as a speciation program to calculate saturation indices and the distribution of aqueous species in solution.

Even though PHREEQC is a general program and is applicable to many hydro-geochemical environments, it does have limitations that need to be considered. As far as the aqueous model is concerned, PHREEQC uses ion-association and Debye Huckel expressions to account for the non-ideality of aqueous solutions. This type of model is appropriate for solutions with a low ionic strength, but may not be applicable at higher ionic strengths (in the range of seawater and above). Another limitation of the aqueous model is the lack of internal consistency in the data in the databases. The databases available are *phreeqc.dat*, *wateq4f.dat* *and minteq.dat*. In this study, the database *phreeqc.dat* was used for all speciation calculations performed on the ash water (section 3.9.2).

2.7 Statistical methods

Very basic statistical methods were used in this investigation, the purpose being to identify "outliers" in plant data. The boxplot method was chosen since it provided the necessary statistical output needed to discard some of the plant data analyses.

2.7.1 The Boxplot

The boxplot provides a quick display of some important features of the data. According to Vining (1998), the boxplot gives the analyst a formal tool for discriminating outliers during preliminary data analysis. It is constructed by measuring the centre of the data and the spread of the data based on the *median* and *quartiles* (once it has been arranged in ascending order), which are resistant or insensitive to the presence of outliers.

2.7.1.1 Definitions

- The *median* is the middle value of the data set once it has been arranged in ascending order.
- Once a data set has been arranged in ascending order, the *quartiles* are those views that divide the data set into four equal parts. Q_1 represents the lower quartile (or first quartile), Q_3 represents the upper quartile (of third quartile). The median is the second, or middle quartile, Q_2.
- The *interquartile* range can be defined as:
  $IQR = Q_3 - Q_1$ (2-63)
  and is sometimes used as a measure of the variability in the data.
- The *inner fences* define the bounds for the unquestionably good data. By "unquestionably good" it is meant that the data values that fall within the inner fences cannot be seen as outliers. The *upper inner fence (UIF)* and *lower inner fence (LIF)* can be calculated as follows:

$$step = 1.5 \times (IQR) \quad (2\text{-}64)$$

$$UIF = Q_3 + step \quad (2\text{-}65)$$

$$LIF = Q_1 - step \tag{2-66}$$

At a glance therefore, a boxplot provides one with the following:

- the centre of the data set,
- where most of the data falls,
- the spread of the "unquestionably good" data, and
- possible outliers.

2.8 Summary

The literature survey provided one with an overview of fly ash: how it is produced, how it is disposed of, and the general chemical and mineralogical composition of fly ash. Furthermore, previous research carried out on similar systems was investigated; with the general observation being that although the chemical, physical and mineralogical properties of fly ash are well documented, the actual chemistry involved in the mixing of fly ash with a water source, is to a large extent unknown. The reason for this is two-fold: Firstly, every wet ash disposal system is unique; the composition of fly ash varies due to many different factors, the composition of the effluent used to transport the ash differs from one system to another and may even fluctuate over time within a specific system, some wet ash disposal systems are open whereas others are closed (with a recycle effluent stream), and lastly, the operation of the system (e.g. retention time in the dams, size of the ash dams, L:S ratio) varies from system to system. Secondly, not all fly ash is disposed of by means of slurrying the ash with an effluent; some power stations utilise dry ash disposal, therefore the focus of a lot of the published research was found to be based on the leaching that occurs as a results of precipitation on dry ash heaps. However, although the specific chemical and mineralogical changes that occur in an ash disposal system differ, some consistency was identified in the observations made by previous researchers:

- The major constituents or elements of fly ash are heterogeneous glassy and crystalline phases of silicon, aluminium, iron, calcium and magnesium. The main mineralogical

phases that have been identified by previous researchers are quartz and mullite, with lesser amounts of iron-containing phases such as hematite.

- Leachate associated with fly ash was found to contain high concentrations of Ca, Na, and SO_4.
- Column experiments that were conducted revealed a reduction in the Ca and SO_4 ions in solution, and calcite was identified as one of the crystalline reaction products formed during the experiments.
- pH is an important variable associated with the leaching of elements from fly ash.
- As far as major elements are concerned, the composition of fly ash is very similar to the composition of soil.

This chapter also provides one with an overview of the electrochemistry, water alkalinity, geochemical modelling and statistical methods referred to in the chapters that follow.

Chapter 3

The Actual Ash Disposal System

The wet ash disposal system used by Sasol 2 and 3 in Secunda, South Africa, is a complex process involving many different variables. It is a closed system, implying that no water from the system is directly disposed of to a receiving water source. Instead the ash water (CAE) is recycled back to the plants for re-use in the transportation of the fine ash. The ash disposal system is also used to co-dispose various process waste streams that often have very high salt loadings. The entire system, as it is currently operated, serves as a salt sink and is able to adequately buffer the variations in salt loadings of the inlet streams. However, over the last 15 years, a change has been seen in the composition of the effluent used to transport the ash (CAE). It is thus imperative that one understands the working of the system properly in order to utilise it to its maximum potential.

The ash water system serves both Sasol 2 (West) and Sasol 3 (East). The ash disposal system is identical for both plants, and eventually, before the effluent is recycled to the plants for re-use, the two disposal systems merge into one system. For the purpose of this investigation, the two systems were analysed separately where applicable, since the 'foreign' waste streams entering the system differ for Sasol 2 and Sasol 3. Three different phases in the ash disposal system have been identified during which time the ash/water chemistry of the system may differ. Thus, the plant data has been analysed on the basis of these three phases.

The objective of this investigation was to determine, if possible, what changes are occurring in the ash disposal system currently used by Sasol 2 and Sasol 3 in Secunda. It also served to highlight the 'knowledge gaps' pertaining to the monitoring of the system, and identify areas that require further scrutinization.

3.1 Overall description of the system

The ash disposal system utilised by Sasol in Secunda is a wet ash disposal system, with recycle. There are two separate ash-handling plants, one for Sasol 2 (West) and one for Sasol 3 (East). These two disposal systems are identical in their operation, and eventually merge at the evaporation and CAE (clear ash effluent) dams before the ash water is recycled to the plants for re-use. The ash disposal system is designed to handle ash from both the Gasification Section, U43/243, (fine ash) and from the Steam Plant, U10/201 (bottom ash and fly ash). The entire ash disposal system (figure 3.1) is divided into two sections, namely, Inside Ash and Outside Ash. Detailed diagrams of both Inside and Outside Ash are given in Appendix B1. Included in these diagrams are the various samples points referred to throughout this chapter.

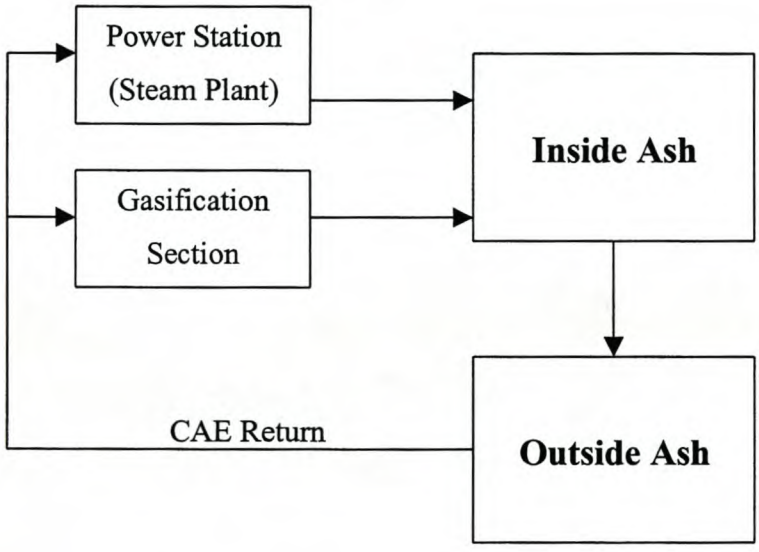

Figure 3.1: Diagrammatic representation of the Secunda Ash Disposal System

At Inside Ash, the course ash is separated from the fine ash, the former of which is then transported by means of conveyor belts to ash heaps. The fine ash as pumped a slurry to ash dams, where the ash settles and is separated from the water. The majority of the water leaves the dams by means of a penstock-overflow, and some percolates through the ash and leaves via the toe drains. All the water leaving the ash dams passes first to

evaporation dams, and then to the so-called CAE dams. Both the evaporation and CAE are basically holding dams before the water is recycled to the factory. However, important chemical reactions occur during this stage of the ash water system, and therefore their role in the entire process is crucial.

A relatively small quantity of water contained in the course ash is collected and transferred to the CAE dams.

3.1.1 Inside Ash

The ash water system serves as a sink[1] for various waste streams from Sasol 2 and Sasol 3. These streams enter the ash water system at Inside Ash, and have very serious implications on the water and salt balance in the entire ash water system. The streams entering the system for Sasol 2 and Sasol 3 are different, and thus all data presented in this chapter was divided into data obtained for the ash water system of Sasol 2 and Sasol 3, separately.

3.1.1.1 Basic Description

As mentioned previously, diagrammatic representations of the ash disposal system are given in Appendix B1, and Appendix A3 contains a description of the various process units referred to in the text. Coal, which is fed to the gasifiers via wet screening, is gasified in the presence of oxygen and steam. The ash produced as a result of this process is dropped into an ash-lock from where it is discharged to the sluiceways situated beneath the gasifier. In these sluiceways, ash water is used to cool and transport the ash to Inside Ash, where the ash is dewatered and also where the course and fine ash are separated. A bypass pond is used when problems are encountered at Inside Ash. At the classifiers, the water recovered is transported to a sump from where it is recycled where it is mixed once again with the ash. The dewatered course ash is transported via a conveyor belt system from the vibrating classifiers to ash heaps.

---

[1] A means of disposing of the waste streams, i.e. they are disposed of in the ash water system and the salts, present in the waste streams, are retained in the ash dams.

Ash from the Steam Plant (fly ash and bottom ash) is also handled at Inside Ash by two classifiers. The slurry is then sent to thickeners (residence time of about an 1½ hours). The overflow from these thickeners is returned to the sumps, and the underflow is sent to a slurry sump from where it is pumped in a slurry form to the fine ash dams. Some waste streams enter the ash water system at this slurry sump, such as catalyst from U20 and blow-down from U45. The other process waste streams (salty water from U44, sludge from U55 and wash water overflow from U10) enter Inside Ash via the by-pass dam. Water from this dam then enters the entire ash water system by various means (e.g. at the screens). Examples of other process waste streams entering the system at Inside Ash are salty water from the new demineralisation plant, wastewater from the TRO (Tubular Reverse Osmosis) plant, and salty water from U66.

3.1.1.2 Foreign streams entering the system

The simplified block diagram (figure 3.2) identifies the foreign streams entering the ash water system at Inside Ash. Table 3.1 gives a more thorough explanation of these streams.

Table 3.1: Description of Foreign Process Waste Streams

Stream	Description
1	Wastewater from the TRO (tubular reverse osmosis desalination) plant
2	Water from the sump at U66 (salty water system)
3	Salty water from the new demineralisation plant
4	Blow-down from U45 (process cooling water)
5	Spent catalyst from Synthol
6	Salty water from hot lime treatment process units, demineralisation plant – cation regeneration waste
7	Sludge from the flocculation units
8	Wash-water overflow from gasification
9	Overflow effluent from the wet screening plants

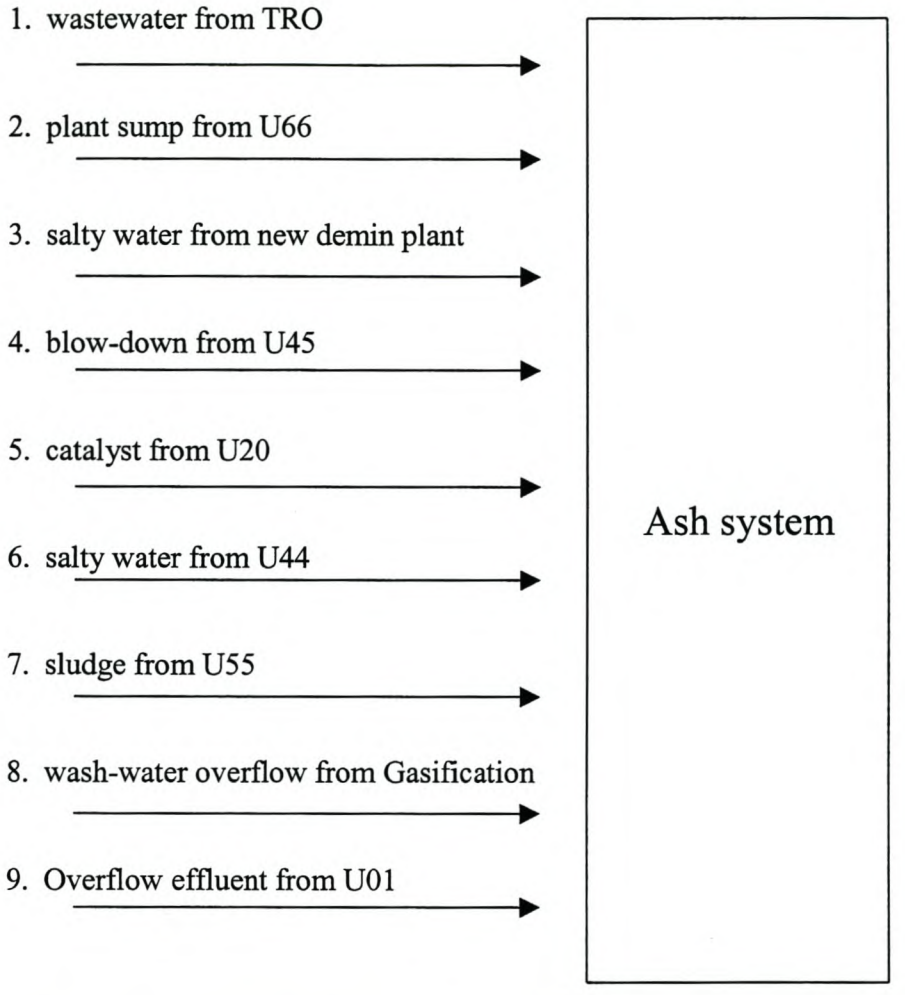

Figure 3.2: Diagrammatic representation of foreign process streams entering ash system

3.1.2 Outside Ash

The concentrated slurry from Inside Ash is pumped to the fine ash dams (figure 3.3). Fine ash dam 3 handles ash from Sasol 2, and fine ash dam 4 handles ash from Sasol 3 (see Appendix B1). There are 2 other ash dams, fine ash dam 1 and fine ash dam 2, but they are both inactive dams (no longer in commission). There is also a new fine ash dam (FAD), FAD 5, which came into operation in 2001. Once the slurry is pumped onto these ash dams, the ash settles out and the majority of the water flows from the dams via a penstock overflow (see figures 3.4 and 3.5) to the relevant evaporation dam. From the

evaporation dams, the clear effluent water (known as clear ash effluent, CAE) flows to the CAE dams before returning to the plants for re-use. These ash water ponds (figure 3.6) are common for both Sasol 2 and Sasol 3. The small fraction of water transported with the course ash to the course ash dams, is collected in a course ash dam and then directed to the CAE dams.

Figure 3.3: Pumping of slurry onto a fine ash dam

Figure 3.4: Penstock overflow on fine ash dam 3

Figure 3.5: Penstock overflow from fine ash dam 3 into evaporation ponds

Figure 3.6: View of evaporation and CAE dams

3.1.2.1 Dam volumes and surface areas

The dam volumes, surface areas, and surface area to volume ratios are given in table 3.2.

Table 3.2: Dam Volumes and Surface Areas

Dam	Volume	Surface Area (m^2)	Surface Area: Volume (m^2/m^3)
Fine Ash Dam 3	$15x10^6 m^3$	-	-
Fine Ash Dam 4	$22x10^6 m^3$	-	-
Emmet Dam	178 M*l*	97 000	0.545
Evaporation Dam 1	618 M*l*	220 000	0.356
Evaporation Dam 2	488 M*l*	180 000	0.369
CAE Dam 1	284 M*l*	110 000	0.387
CAE Dam 2			
CAE Dam 3			

3.1.2.2 Water to ash ratio of slurry stream

The specific gravity of the slurry streams taking the ash to the ash dams is approximately 1.2 (the slurry lines were designed to handle a SG of 1.3, but the slurry is generally pumped to the dams at a SG of 1.2). Thus, the water: ash ratio of the slurry stream is about 5:1.

3.2 Ash production

The ash produced by Sasol 2 and Sasol 3 in Secunda can be broken down as displayed in figure 3.7.

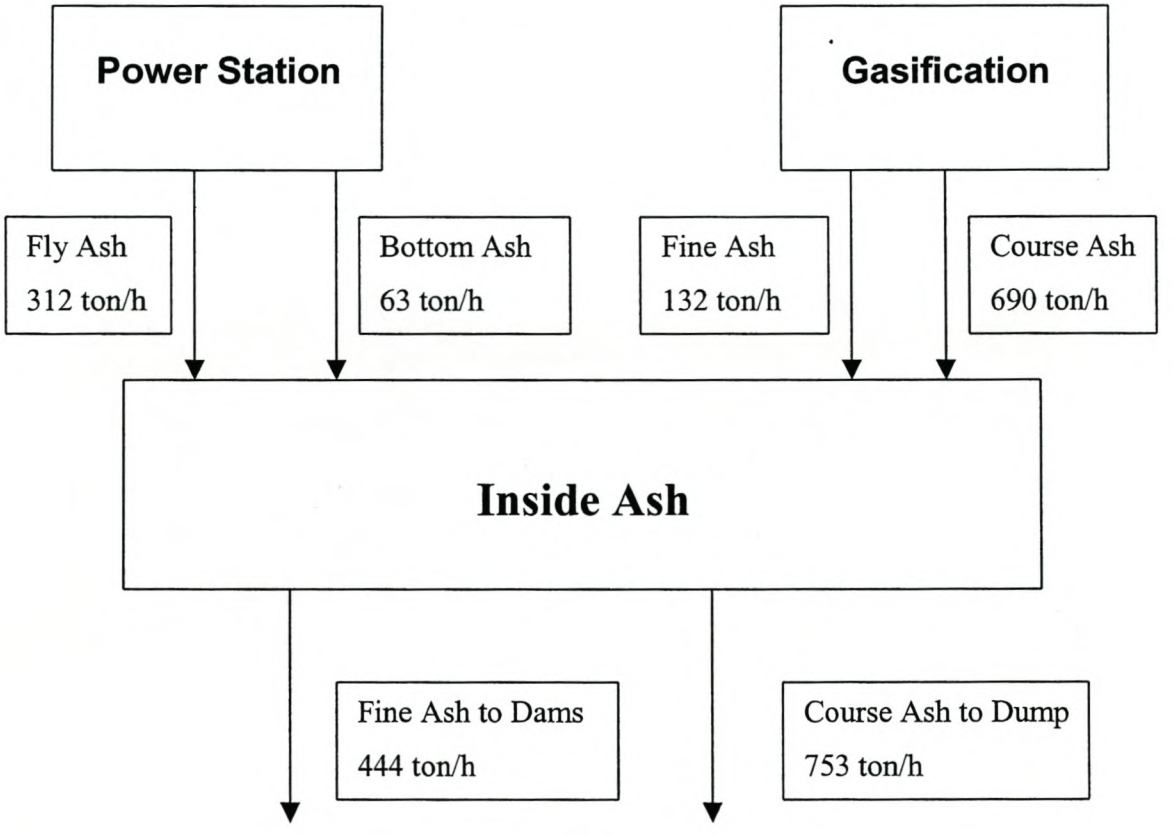

Figure 3.7: Schematic representation of ash production

3.2.1 Fine ash

The fine ash referred to in this report is a combination of fly ash and bottom ash from the coal fired power stations, as well as fine ash from gasification. The approximate percentages of these three types of ash, making up the fine ash, are:

62% fly ash

26% fine ash from gasification

12% bottom ash

3.3 Fine ash composition

As mentioned in section 2.1, one of the important factors that determine the composition of the fine ash is the parent coal from which the ash originates. An investigation was therefore carried out to assess the difference in composition of the coal used by the Power Station and Gasification, and the fine ash produced by these units. The data used for the average coal composition was obtained from the five coalmines, which serve Sasol Synthetic Fuels (SSF) in Secunda. The +6mm fraction is sent to Gasification, while the -6mm faction is sent to the Power Station. The fine ash was obtained from the point in the system just before it is mixed with the FAM (fine ash make-up water, the effluent that is mixed with the fine ash). Figures 3.8 to 3.10 display the elemental distributions of the various elements in the coal and in the fine ash.

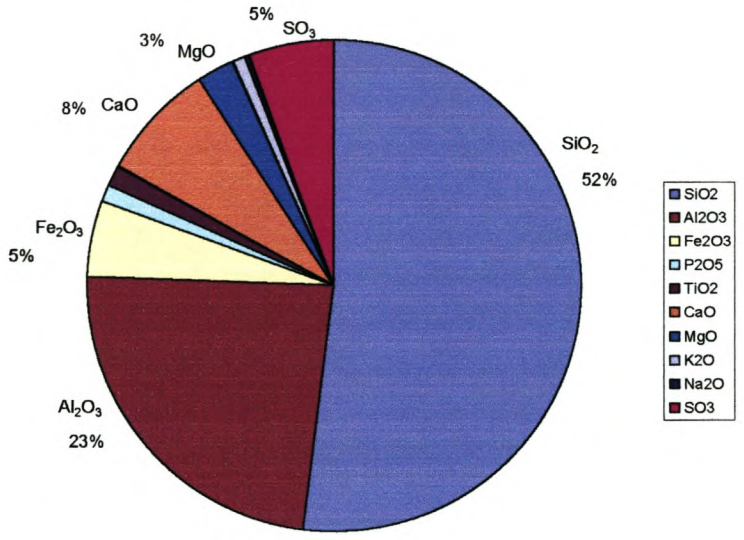

Figure 3.8: Distribution of main elements in +6mm fraction of coal

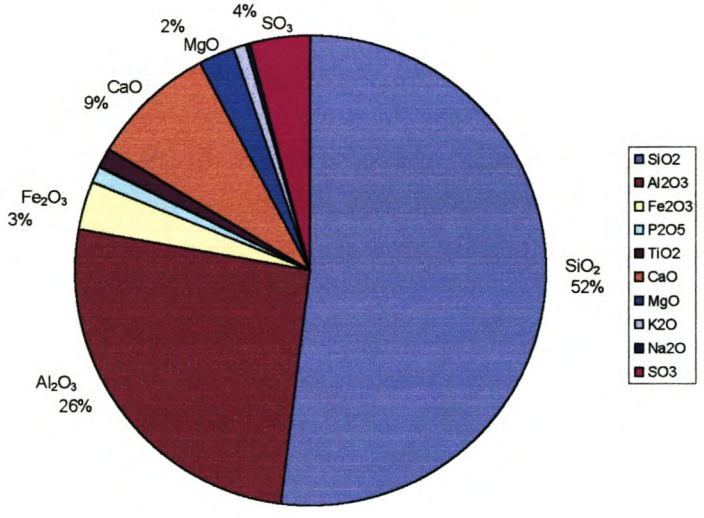

Figure 3.9: Distribution of main elements in -6mm fraction of coal

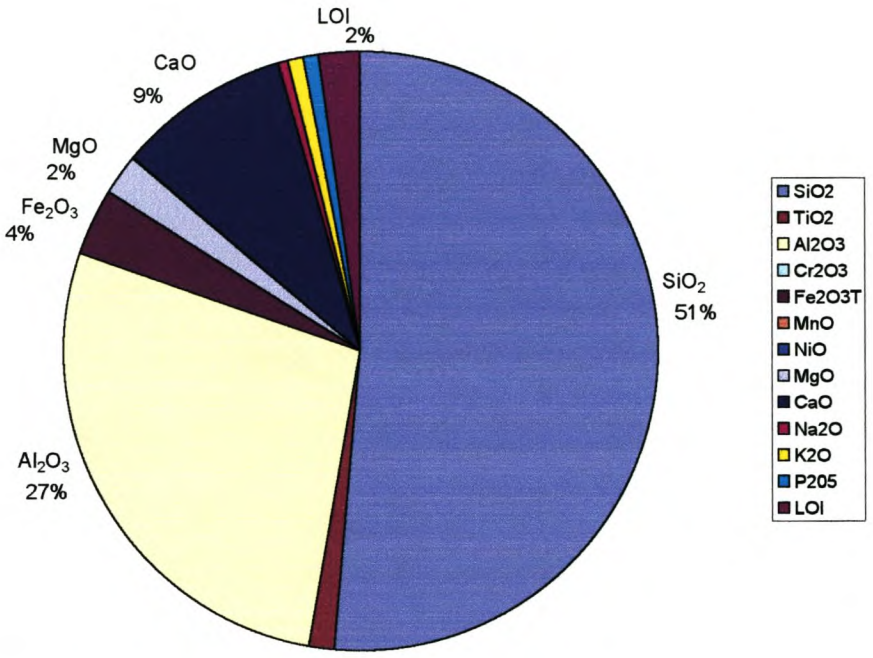

Figure 3.10: Distribution of main elements in the fresh fine ash

It is evident from the data presented in figures 3.8, 3.9 and 3.10 that the elemental distribution in the fine ash is practically the same as that seen in the parent coal. Table 3.3 and figure 3.11 present a summary of the data in figures 3.8, 3.9 and 3.10.

Table 3.3: Distribution of Main Elements in Coal and Fine Ash

	Coal (+6mm) %	Coal (-6mm) %	Fine Ash %
SiO_2	52	52	51
TiO_2	1.4	1.5	1.5
Al_2O_3	23	26	27
Fe_2O_3T	5.0	3.4	4
MgO	2.5	2.4	2
CaO	7.8	8.6	9
Na_2O	0.4	0.5	1
K_2O	0.8	0.7	1
P_2O_5	0.9	1.0	1
LOI/SO_3	5.5	4.0	2

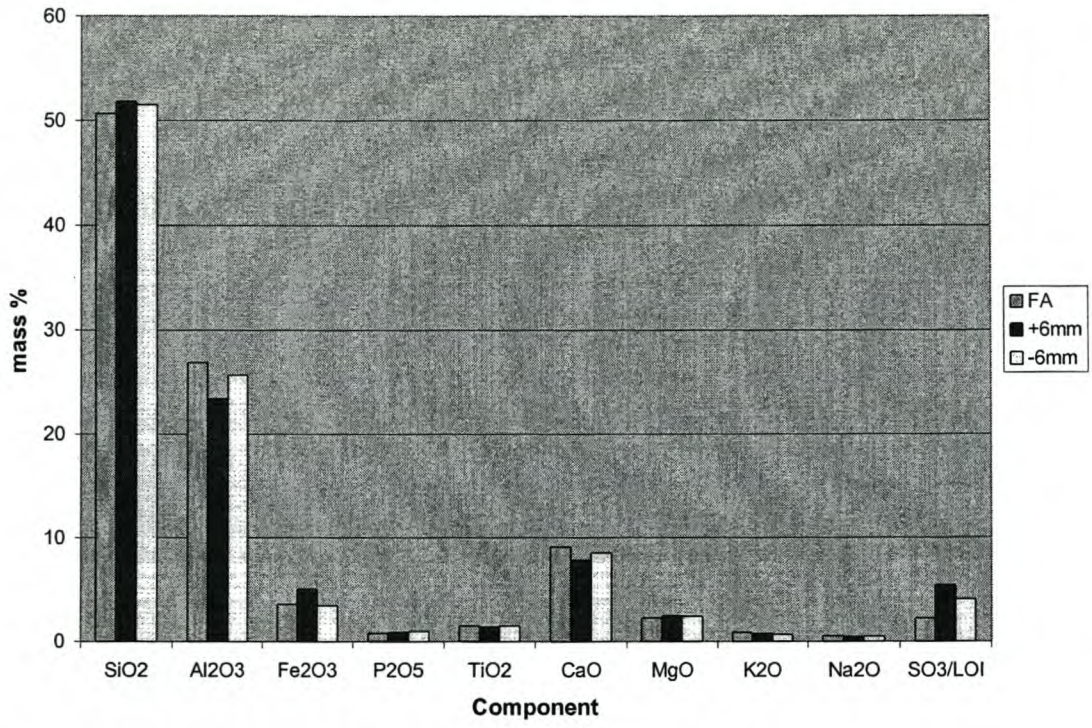

Figure 3.11: Distribution of Main Elements in Coal and Fine Ash

3.4 Sample point identification

A selection of sample points was identified at the beginning of this study. A number was assigned to each of these sample points for the convenience of future reference and also to aid with the reporting of data. The location of these sample points can be seen on the diagrams in Appendix B1. Table 3.4 gives a brief description of all the sample points.

Table 3.4: Sample Point Identification and Description

Sample Point	Description	Figure In Appendix B1
1	Penstock over-flow from FAD 3 to evaporation ponds	B1&B3
2	Penstock over-flow from FAD 4 to Emmet Dam	B1&B2
5	From CAE dams to Sasol 2 (west)	B1&B3
6	From CAE dams to Sasol 3 (east)	B1&B2
7e	Fine ash slurry (line A) from Sasol 3 (east)	B2
7w	Fine ash slurry (line A) from Sasol 2 (west)	B3
9e	Fine ash slurry (line C) from Sasol 3 (east)	B2
9w	Fine ash slurry (line C) from Sasol 2 (west)	B3

These samples points are the main sample points that were used in the assessment of Outside Ash as far as actual plant data is concerned. There was ample data, in the form of samples collected and analysed on a regular basis, for sample points 1, 2, 5, and 6. On the other hand very little data (chemical analyses) was available for the slurry streams leaving Inside Ash (sample points 7e&w, and 9e&w). Thus, one should bear in mind throughout the reporting of the actual plant data, that the trends observed using sample points 1, 2, 5 and 6 (Phase 3) are much more reliable than those involving points 7 and 9 (Phase 2).

The mention of "Phases" has already been alluded to and will be discussed further in section 3.4.1.

3.4.1 Phase Identification

In the whole ash water system three phases were identified, during which time different chemical reactions/mechanisms could possibly occur. These phases are shown diagrammatically in figure 3.12, and can be described as:

Phase 1: The initial contact of the ash with the ash water.

Phase 2: The time the ash spends in contact with the water (i.e. from the point where the slurry is pumped from Inside Ash, to the penstock over-flow from the ash dams).

Phase 3: The period of time the ash water spends in the evaporation and CAE dams before being recycled to the factories for re-use in the ash water system.

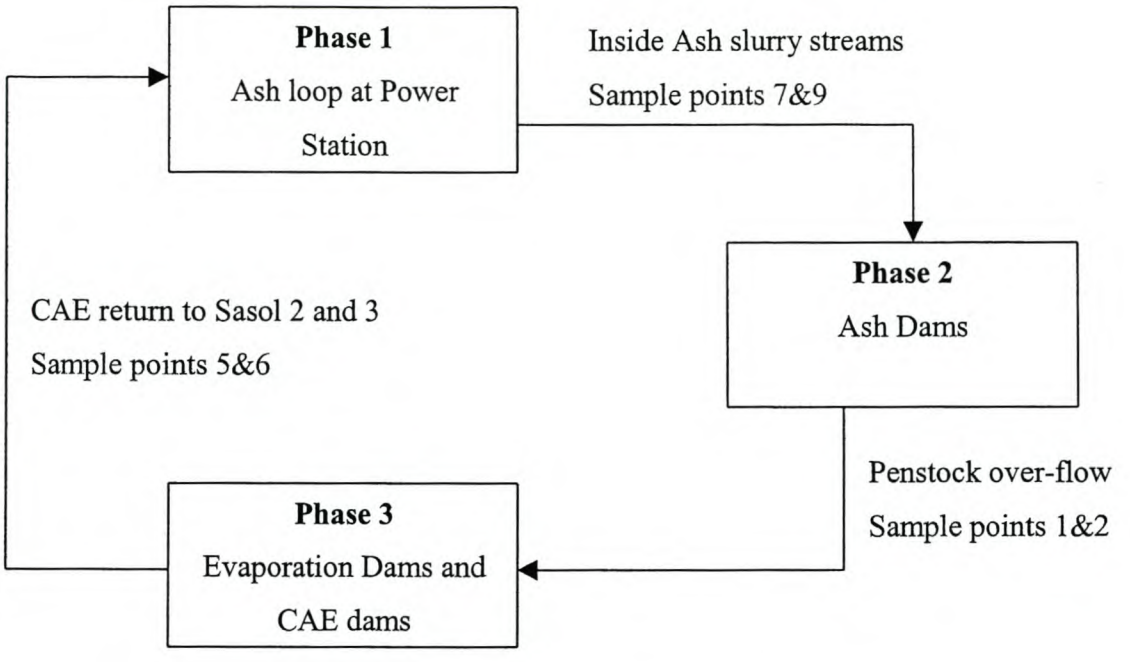

Figure 3.12: Phase Identification Diagram

3.4.2 Sasol 2 and Sasol 3/ Sasol West and Sasol East

Throughout this chapter pertaining to the analysis of the actual plant data, the words east and west will be used to denote the 2 disposal systems for the two plants. As mentioned previously, even though the operation and set-up of these systems are identical, it is possible that the actual chemistry could differ slightly since the process waste streams entering the two systems are not identical. However, sample points 5 (west) and 6 (east) are in essence the same point as the CAE dams are common to both Sasol 2 (West) and Sasol 3 (East) – the CAE being sent from Outside Ash to the two factories is the same. The difference in the analyses of these two sample points can be seen in the graphs given in Appendix B2, and a principal component analysis of the difference in the two sample points is given in Appendix E. Therefore, for all the calculations performed pertaining to concentration variations for phase 3, the average values of sample points 5 and 6 were used for both the west and the east system.

Sample points 7 and 9 (on both the east and the west side) are also in essence the same. The ash/water slurry flowing in lines 7 and 9 both originate from the slurry sumps, line 7 is just from sump A and line 9 from sump C. Therefore, in all the analyses pertaining to trends in concentration variation, average values of points 7 and 9 were used. The east and the west lines were, however, not combined, so average values were calculated for 7e&9e and then 7w&9w.

3.5 Ash water quality

3.5.1 Ash water quality in general

According to an internal report on the ash water system at Sasol, Secunda in 1991 (Billik and Mashike, 1991), the quality of the ash water has deteriorated since the start-up of the two plants (Sasol 2 and Sasol 3). They looked at a time period from 1984 to 1990 when comparing the change in the composition of the ash water. The streams that they identified to be contributing to this deterioration are:

- the excess salty water,
- the cation exchange regeneration water, and
- the blow-down of the process cooling water.

Obviously the contaminants in the ash also contribute to the ash water quality.

Table 3.5: Variation in ash water quality over a period of approximately 20 years

Constituent in ash water	units	1984 average	1990 average	2000 average	% change 1984-1990	% change 1990-2000
COD	mg/l	465	445	242	-4.4	-59
pH		12.05	11.59	10.21	-3.9	-13
SO_4	mg/l	1029	1728	2496	51	36
Cl	mg/l	175	743	699	124	-6.1
F	mg/l	11.34	15	11.02	28	-31
Na	mg/l	435	958	1194	75	22
Ca	mg/l	1240	704	445	-55	-45
M alkalinity	mg/l as $CaCO_3$	718	454	165	-45	-93
Conductivity	mS/cm	4000	4430	6534	10	38

Table 3.5 shows the changes in the ash water quality over a period of approximately 20 years. The 1984 and 1990 data was obtained from the report by Billik and Mashike (1991), thus only the elements they had data for could be compared to the current ash water. Examining these elements reveals that there is a definite increase in the SO_4 and Na concentrations, and also in the conductivity. However, there is an overall decrease in the COD, pH, Ca concentration and the M alkalinity. According to Ginster (1997), with lower Ca concentrations, and higher Na, SO_4 and Cl concentrations in the ash water, the more soluble Na salts will begin to dominate the overall salinity status of the ash water system as opposed to the less soluble Ca salts. Another constituent to be noted in table 3.5 is F. There was a concern about the rising F levels in the ash water, however, as one can see, even though there was a general increase in the F concentration for the period 1984-1990, there was an overall decrease for the period 1990-2000. One can see from this data that currently the concentration of F in the ash water is at about the same level as it was in 1984.

Ginster (1997) also reported that the monitoring of the ash water over a period of 15 months showed that the water entering the ash water system had a much larger variability compared to the water leaving the system to be re-used in the factory (CAE). This shows that the ash water system is able to adequately buffer the effects of altering loadings to the system, which at times can be very high.

Table 3.6 displays the average composition of the CAE leaving the CAE dams for the period January 2000 to March 2001. Appendix B2 contains graphs to illustrate the variation in the composition of the CAE during this time period.

Table 3.6: Average Composition of the Ash Water

Constituent	Value	Units
Ca	443	mg/l
Cl	721	mg/l
COD	257	mg/l
F	10.9	mg/l
Fe	0.504	mg/l
K	97.5	mg/l
Mg	6.70	mg/l
Na	826	mg/l
Con	6693	mS/cm
pH	10.20	
Malk	162	mg/l as $CaCO_3$
PAlk	88.3	mg/l as $CaCO_3$
SS	216	mg/l
SO_4Tot	2623	mg/l
Si	13.0	mg/l
TDS	5184	mg/l

3.5.2 Ash water quality with mine water addition to the system

From June 2001 mine water was added to the ash water system. This water was added directly into the CAE dams. The ratio of the CAE to mine water going to the factories is approximately 10:1 and the salts concentration of the mine water is much lower than that of the CAE, thus it was assumed that the addition of the mine water would not have a marked influence on the working of the ash water system. However, a comparison was done to compare the quality of the water being returned to the factories, with and without the mine water addition.

The data used for this comparison was:

- January '00 to March '01 (without mine water).
- June '01 to October '01 (with mine water).

The results of these comparisons show that the addition of the mine water to the ash water system does not significantly affect the quality of the CAE being returned to Sasol 2 and Sasol 3. These results are displayed in figures 3.13, 3.14 and 3.15.

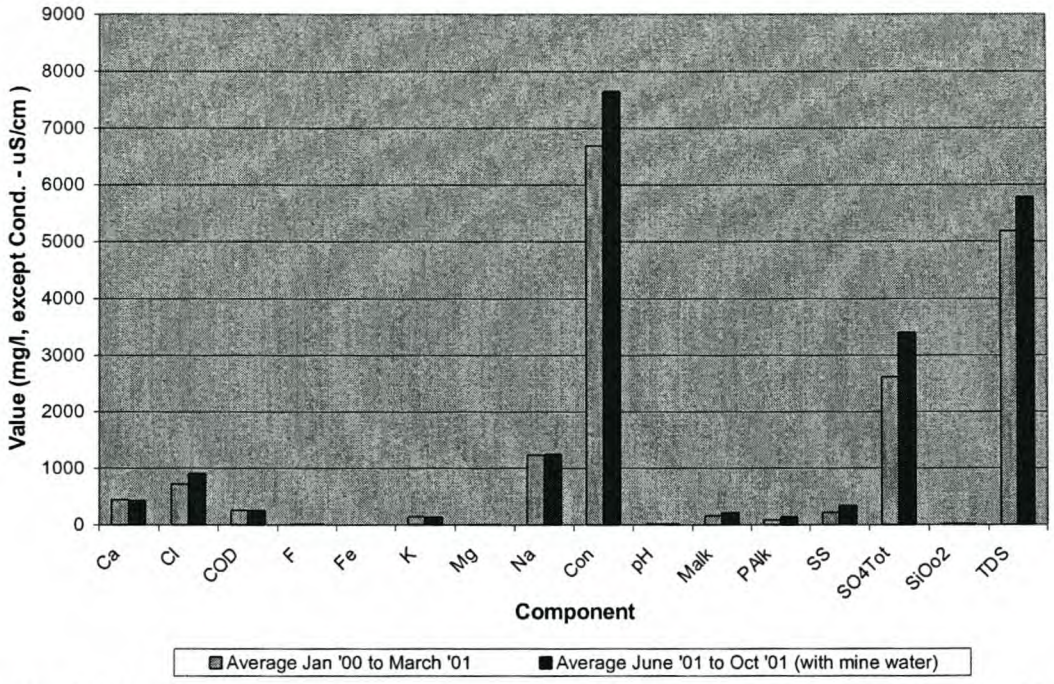

Figure 3.13: Average value comparison at sample point 5&6 (CAE), with and without mine water

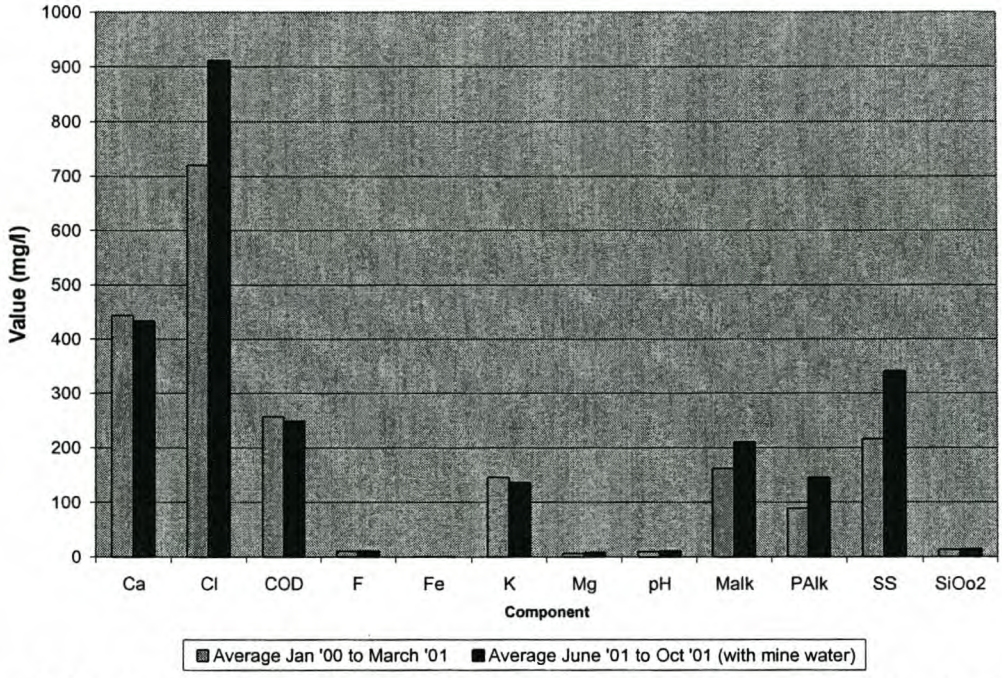

Figure 3.14: Average value comparison at sample point 5&6 (CAE), with and without mine water (values < 1000mg/l)

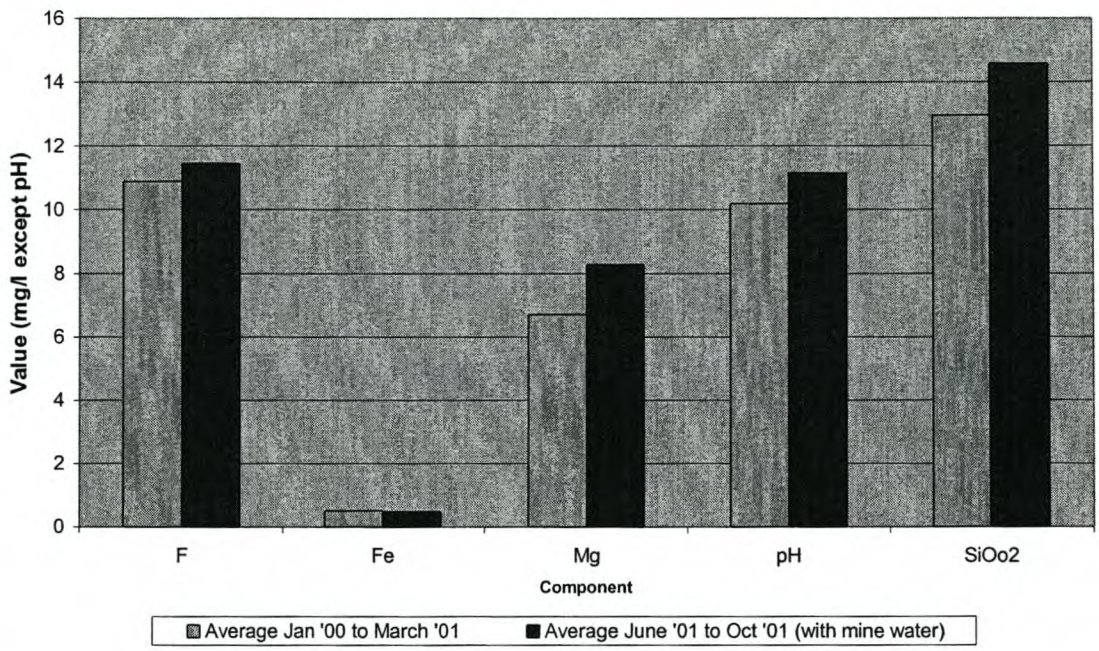

Figure 3.15: Average value comparison at sample point 5&6 (CAE), with and without mine water (values < 20mg/l)

3.5.3 Elemental scan

Table 3.7 displays the elemental scan performed on three different samples of FAM. This elemental scan serves to highlight all the elements present in the FAM, even if they are present in very small quantities.

Table 3.7: Elemental Scan of the FAM

	FAM sample a	FAM sample b	FAM sample c		FAM sample a	FAM sample b	FAM sample c
Component	**Conc.**	**Conc.**	**Conc.**	**Component**	**Conc.**	**Conc.**	**Conc.**
Li (mg/L)	9.4	9.7	9.6	In (ng/L)	64	21	47
Be (ng/L)	290	<20	<20	Sn (ng/L)	1800	560	410
B (µg/L)	3600	1200	1200	Sb (ng/L)	1700	130	120
Na (mg/L)	1957	**2002**	**2060**	**Te (ng/L)**	700	<230	<230
Mg (mg/L)	3.762	0.040	0.064	I (µg/L)	1000	1000	990
Al (mg/L)	**5.038**	**22 µg/L**	**24 µg/L**	Cs (µg/L)	14	16	15
Si (mg/L)	**10.10**	**16.60**	**13.19**	Ba (mg/L)	0.218	0.177	0.164
K (mg/L)	**204.0**	**202.7**	**209.0**	La (µg/L)	6.600	0.190	0.150
Ca (mg/L)	**466.5**	**900.5**	**908.5**	Ce (µg/L)	12.000	0.089	0.081
Sc (ng/L)	1300	510	420	Pr (ng/L)	1300	13.0	5.7
Ti (µg/L)	220	11	13	Nd (ng/L)	5000	45	49
V (mg/L)	0.050	1.3 µg/L	1.3 µg/L	Sm (ng/L)	1200	<28	<28
Cr (mg/L)	0.083	0.418	0.440	Eu (ng/L)	180	18	<7.5
Mn (mg/L)	0.042	1.1 µg/L	<0.01	Gd (ng/L)	810	<24	29
Fe (mg/L)	**2.663**	**3.522**	**3.626**	Tb (ng/L)	120	<3.6	<3.6
Co (µg/L)	2.80	2.40	2.30	Dy (ng/L)	770	<14	<14
Ni (mg/L)	0.045	0.030	0.030	Ho (ng/L)	140	<3.8	<3.8
Cu (mg/L)	0.042	0.040	0.044	Er (ng/L)	330	<12	<12
Zn (mg/L)	5.6 ug/L	10 µg/L	0.012	Tm (ng/L)	60	<3.9	<3.9
Ga (µg/L)	13.0	6.0	5.2	Yb (ng/L)	340	<15	<15
Ge (ng/L)	7300	2900	3300	Lu (ng/L)	52	<3.9	<3.9
As (µg/L)	26	13	13	Hf (ng/L)	450	<19	<19
Se (µg/L)	81	61	49	Ta (ng/L)	50	<4.1	<4.1
Br (mg/L)	3.20	3.10	3.20	W (µg/L)	81	2.400	2.100
Rb (µg/L)	210	210	210	Re (ng/L)	1100	1300	1100
Sr (mg/L)	25.430	48.380	48.320	Os (ng/L)	<25	<25	<25
Y (µg/L)	4.500	0.560	0.590	Ir (ng/L)	<8.7	<8.7	<8.7
Zr (µg/L)	14	0.230	0.014	Pt (ng/L)	54	85	<19
Nb (ng/L)	1400	<6	8.5	Au (ng/L)	240	180	190
Mo (µg/L)	400	440	440	Hg (ng/L)	610	930	490
Ru (ng/L)	85	120	100	Tl (ng/L)	350	120	130
Rh (µg/L)	0.250	0.600	0.470	Pb (mg/L)	2.9 µg/L	9.7 µg/L	10 µg/L
Pd (µg/L)	8.4	16.0	16.0	Bi (ng/L)	1500	73	73
Ag (ng/L)	1200	1100	760	Th (ng/L)	2300	79	32
Cd (ng/L)	380	170	310	U (ng/L)	1300	10	10

3.6 Main component identification

For analysis purposes, the main constituents of the ash water need to be identified. This was done by looking at what components are present in the ash water in the highest concentrations (at all sample points), and also by means of a literature search. The focus of the literature search was to determine, from other work done on ash water disposal systems, what elements were deemed to be the most important. Figure 3.16 illustrates the main components found in the ash water at the various sample points.

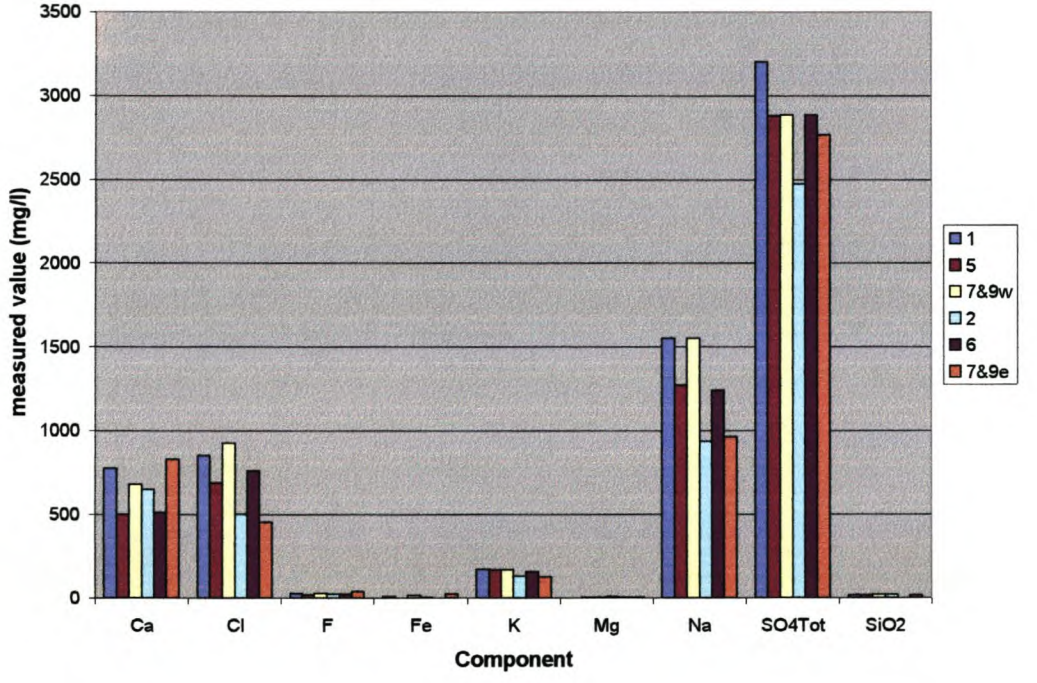

Figure 3.16: Actual measured value comparison for the various sample points

From figure 3.16, one can see that clearly Ca, Cl, Na and SO_4 are present in the highest concentrations at all points in the ash water system.

From literature, the following information pertaining to major elements, was obtained:

- Lee (1997), found that the fly ash leachate (collected from the fly ash disposal mound in one of the major UK coal-fired power stations) contained high concentrations of Ca, Na, and SO_4.
- Villaume et al. (1987), found that leachate chemistry (using fly ash) was clearly dominated by the strong base cations: Ca, Na, K, and Mg and the strong acid anion SO_4.
- Groenewald et al. (1984) found the leachate they worked with was typically alkaline and had very high Na and SO_4 concentrations.

Thus, the literature supports what is seen from the actual plant data, that the main components to consider when investigating a wet ash water disposal system are: Ca, Na and SO_4. For the purposes of this study, Cl was included as a main component, since it is also present in the Secunda ash water system in relatively high concentrations.

3.7 Analysis of actual plant data

3.7.1 Analysis procedure

As mentioned previously, the actual plant data available was not as comprehensive for sample points 7 and 9 as it was for sample points 1, 2, 5, and 6. Thus, the data obtained can be divided into the following categories:

Phase 2: July 1999 – November 1999, and

Phase 3: January 2000 – March 2001.

This data was in the form of chemical analyses, which included the following:

- Calcium (Ca)
- Chloride (Cl)
- Sodium (Na)
- Sulphate (SO_4)
- Total Dissolved Solids (TDS)
- Suspended Solids (SS)

- Magnesium (Mg)
- Potassium (K)
- Silicon (in the form of SiO_2)
- Fluoride (F)
- Iron (Fe)
- M Alkalinity
- P Alkalinity
- Chemical Oxygen Demand (COD)
- Conductivity
- PH

Unfortunately, no flow rates were available for either of these two time periods; therefore only trends on the basis of concentration could be explored.

3.7.1.1 Concentration variations

All the analyses available were divided into the various months and an average concentration was calculated for that month, for a specific sample point. These monthly averages were then plotted graphically for the different phases. For example, the average concentration for Ca in January at sample point 1 was plotted against the average concentration for Ca in January at sample point 5/6; overall representing phase 3 west. All these monthly trends for a specific phase and element were plotted on the same graph. From these graphs it was evident that there were certain "outliers". These visible "outliers" to the general tend observed were confirmed by mean of simple box and whisker plots. Once they were confirmed as an "outlier" they were discarded from the calculations regarding the overall trend for a specific phase and element.

Figure 3.17 illustrates the analysis of the concentration data for Ca, phase 3 (Sasol 2, West). As you can see there is a general decrease in the Ca concentration during phase 3, except for the months July'00, August'00, September'00, and Ocotber'00. According to the box and whisker plots, the average readings for July'00, August'00, and September'00 can all be classified as "outliers". Thus, these data points were not

included in the calculations of the overall trends for Ca, phase 3 west. The black line in figure 3.17 represents the average trend for the decrease in the Ca concentration over phase 3 west.

The same procedure as explained above was performed for all the constituents of the effluent that analyses were available for, and are discussed further in the relevant sub-sections.

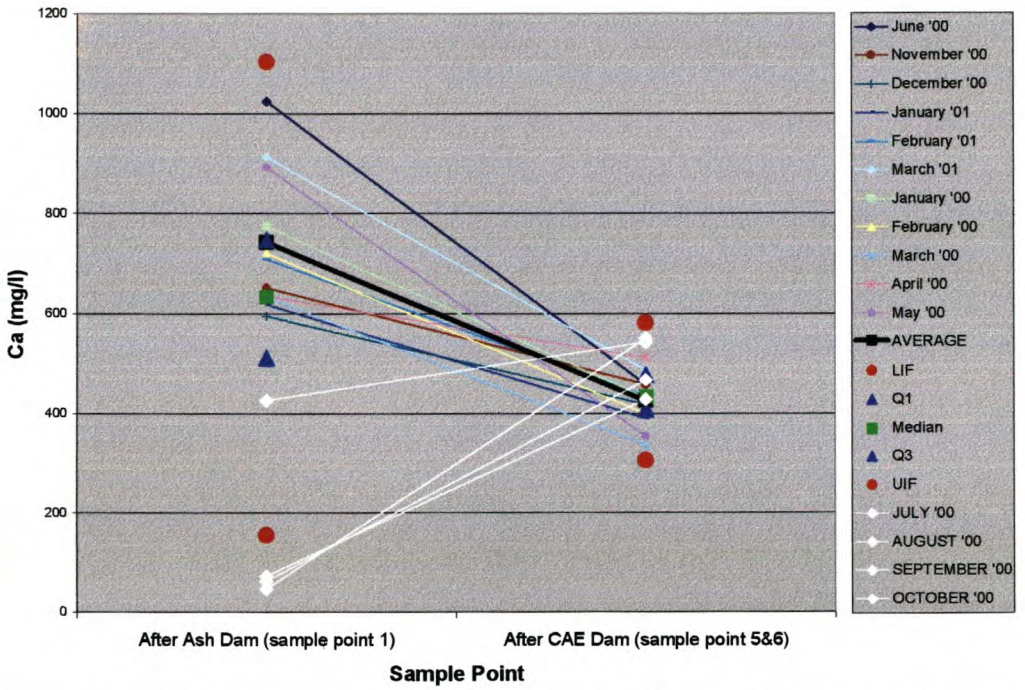

Figure 3.17: Concentration Variation for Ca Phase 3 West (including box and whisker plot)

3.7.1.2 Seasonal Variations

Another aspect concerning the analysis of the plant data was to divide the available data into "wet" and "dry" months, to determine if rainfall had a significant impact on the general trends observed.

The "wet" months were determined to be May to October, and the "dry" months were determined to be November to April. The actual rainfall for the time period March 1999 to May 2001 is given in table 3.8 and figure 3.18.

Table 3.8: Rainfall in Secunda Region

	1999	2000	2001	Units
January		199.7	42	mm
February		205.5	116	mm
March	37.5	159	16	mm
April	18.6	147	38	mm
May	32	67	39	mm
June	5	0		mm
July	0	0		mm
August	0	0		mm
September	15.3	32		mm
October	40.4	90		mm
November	82.5	168		mm
December	200.5	50.5		mm

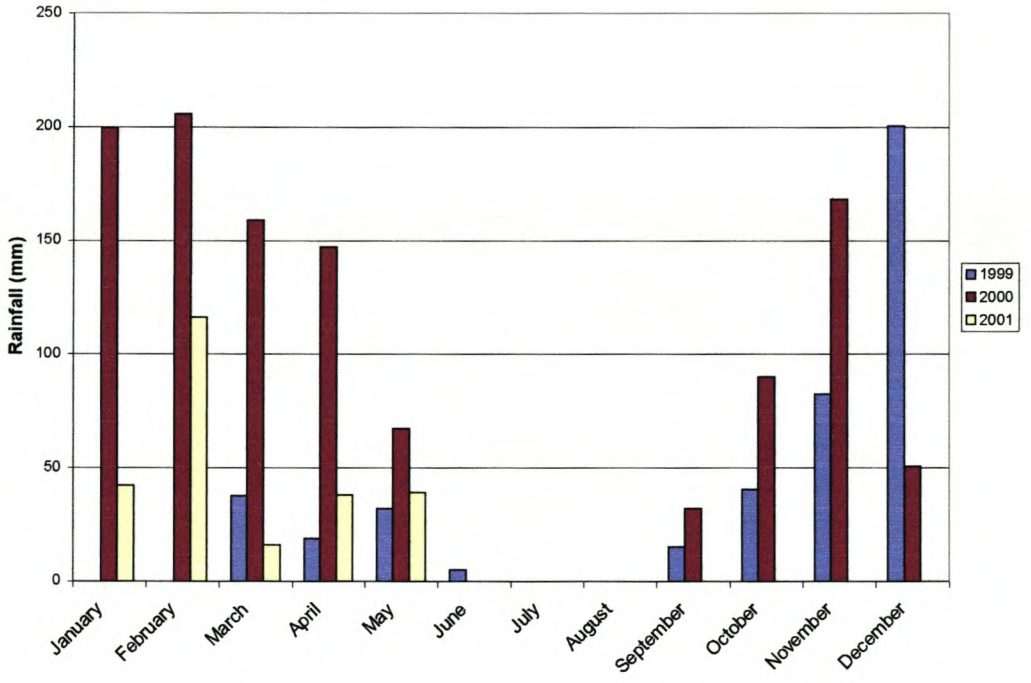

Figure 3.18: Rainfall in Secunda Area from March 1999 to May 2001

3.7.2 Component trends

The trends for Ca, Na, SO_4, Cl, K, TDS, totally alkalinity, pH, OH, and CO_3 are discussed in this section, the trends for the other components mentioned in section 3.7.1, are given in Appendix B3. Furthermore, a principal component analysis based on the 1999 data for phase 2 and phase 3 is given in Appendix E. The assumptions that were made for these components are:

- There were no readings for sample points 9e and 9w Oct, Nov '99; therefore the values for just 7e and 7w were used instead of the average of 7e&9e and 7w&9w.
- There was no TDS data for sample point 6 (1999), this is why there is no change in concentration shown for phase 3 east on figure 3.39.
- There were also no TDS analyses for point 6 for 2000/2001, therefore an average value for point 5 and 6 combined could not be calculated. The trends for phase 3 are therefore based on the TDS concentrations at point 5 and not the average of 5&6.

Data that was excluded from the average reduction/increase calculations for the various components (on the basis that they were determined, by statistical means, to be outliers[2]) are:

- The average value for the reduction in Ca for phase 3 west is excluding the readings for July, Aug, Sept '00.
- The average value for the reduction in SO_4 for phase 2 east is excluding the readings for Nov '99 7e and 9e.
- The average value for the reduction in Na, Cl and MAlk for phase 2 east is excluding the reading for Nov '99 7e.
- The average value for the increase in K for phase 2 east is excluding the reading for Aug '99 7e & 9e, and the average value for the increase in K for phase 2 west is excluding the readings for Aug '99 7w & 9w.

[2] Data that lies beyond the inner fences (which define the bounds for unquestionably good data).

3.7.2.1 Calcium

The trends seen for calcium can be summarised as follows:

Phase 2

On the east side there is a 17% average reduction in the calcium concentration from the time the ash water slurry leaves inside ash, to the time it leaves the ash dams (i.e. before going to the evaporation dams). On the west side there is a 24% average increase in the calcium concentration from the time the ash water slurry leaves inside ash, to the time it leaves the ash dams (i.e. before going to the evaporation dams). These results are displayed in figure 3.19.

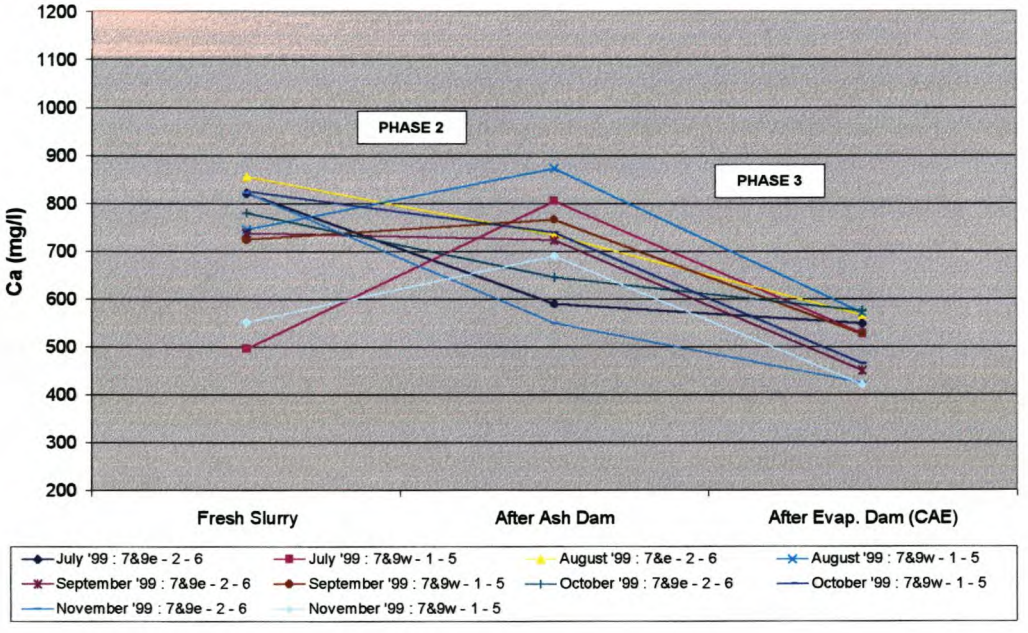

Figure 3.19: Concentration variation for Ca phase 2&3 east and west (1999 data)

Figure 3.19 shows data for both phase 2 and 3 for 1999. Even though there is no correlation between the trends for the east and the west side for phase 2, one can clearly see that overall, for phase 2 and 3, there is a decrease in the Ca concentration.

Phase 3

On the east side there is a 32% average reduction in the calcium content of the ash water from point 2 to 5/6 (i.e. from after the ash dams to after the CAE dams – before being returned to Sasol 3). On the west side there is a 38% average reduction in the calcium content of the ash water from point 1 to 5/6 (i.e. from after the ash dams to after the CAE dams – before being returned to Sasol 2).

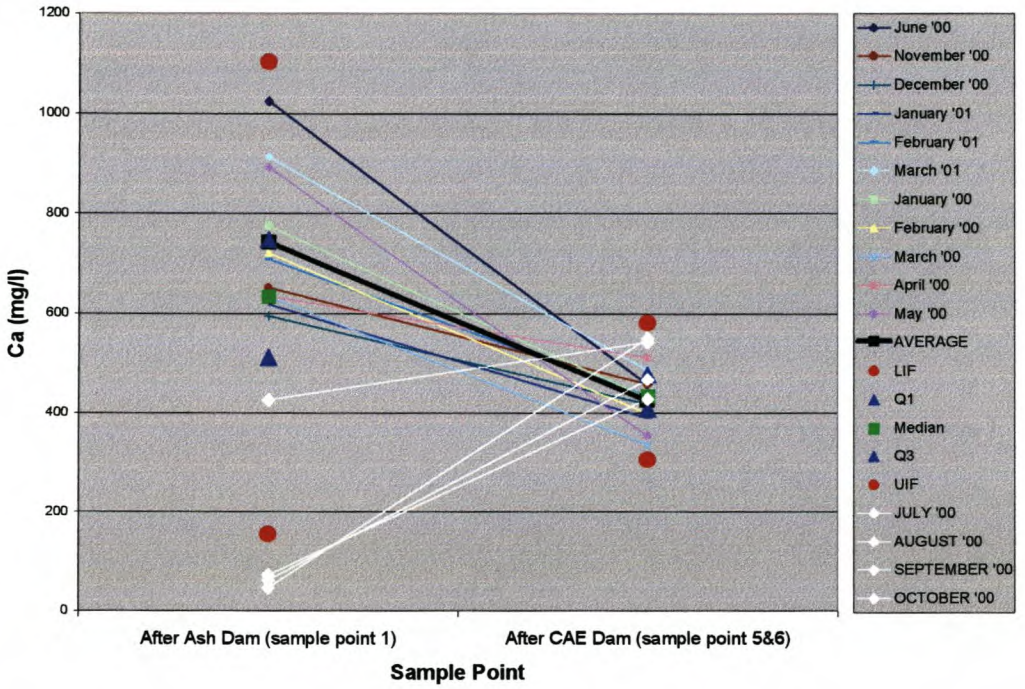

Figure 3.20: Concentration variation for Ca phase 3 west (including box and whisker plot)

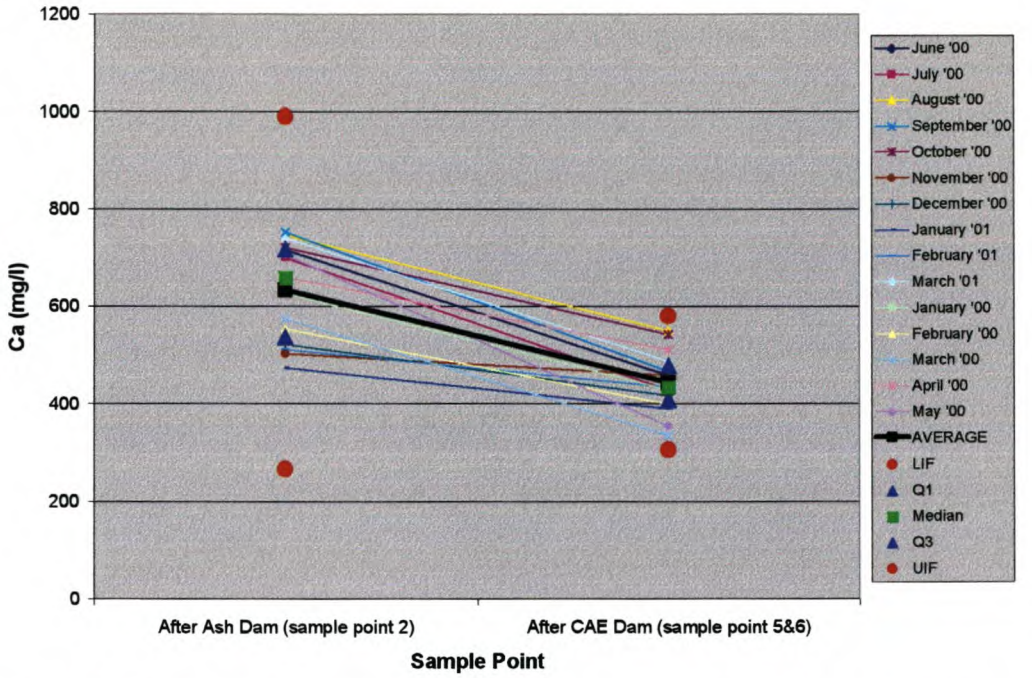

Figure 3.21: Concentration variation for Ca phase 3 east (including box and whisker plot)

Separation into seasons

Figure 3.22 displays the data divided into the "wet" and "dry" months[3]. If one examines figure 3.22 it is apparent that there still seems to be a general trend of a decrease in the calcium for phase 3 (points 1 and 2 to 5 and 6 (phase 3). The only increase in the calcium content of the ash water was seen for the dry months point 1 to 5&6, this could be explained by the increase in calcium concentration for the months of July, Aug, Sept, Oct '00 (as excluded above). This increase cannot be attributed to evaporation during the "dry" months since as can be seen in the box and whisker plot (figure 3.20), it is the low concentrations for Ca at point 1 rather than higher concentrations at points 5/6 that result in an overall increase in Ca concentration for these months. If the concentration of the Ca at points 5&6 was higher for the dry months, then one could relate this back to evaporation of water from the CAE and Evaporation Dams.

[3] The wet months are November to April, and the dry months May to October.

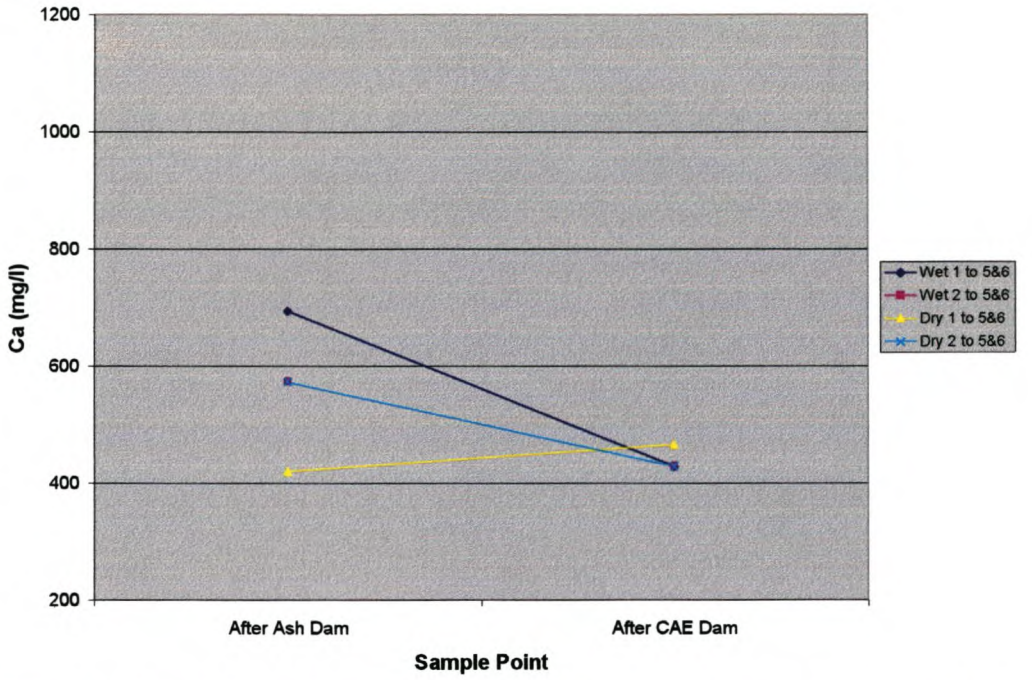

Figure 3.22: Comparison of variation in Ca concentration for the wet and dry months for phase 3 east and west

3.7.2.2 Sodium

The trends observed for the variation in the sodium concentration can be summarised as follows:

Phase 2

On the east side of the disposal system, from the time the ash water slurry is pumped to the ash dams, to the time the effluent leaves the dams via the penstock overflow, there is a 10% average reduction in the sodium concentration. However, on the west side there is a 6% average increase in the sodium concentration during phase 2. These results are displayed in figure 3.23.

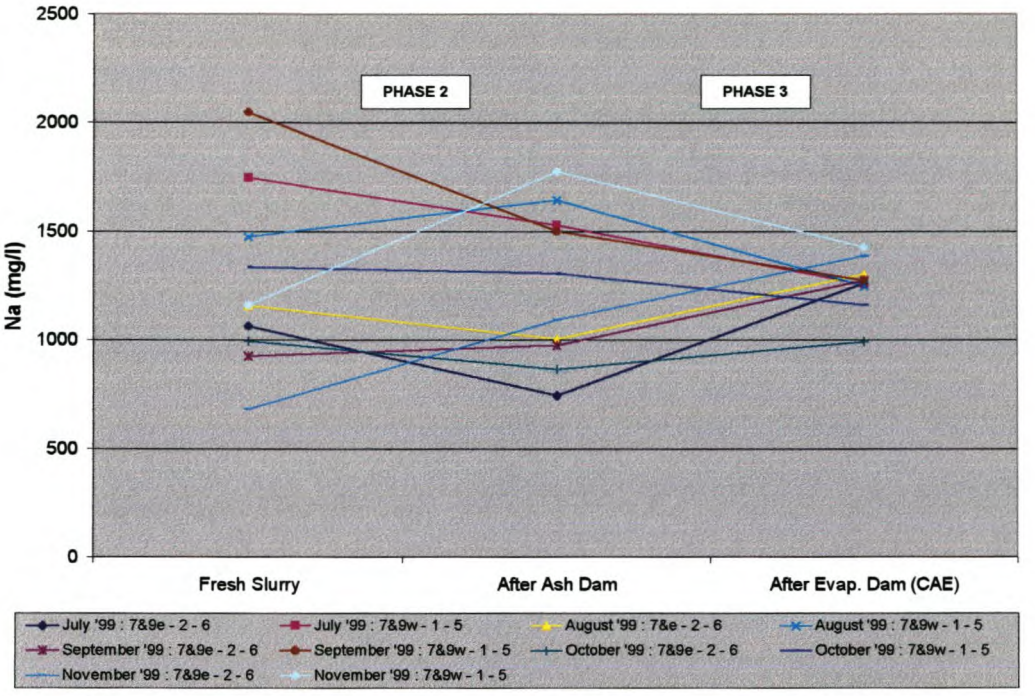

Figure 3.23: Concentration variation for Na phase 2&3 east and west (1999 data)

In figure 3.23 one can see that overall, for phase 2 and 3 combined, there is no drastic change in the concentration of the Na. This does not mean that there is not an overall increase or decrease of the Na content of the water. A mass balance and therefore flow rates would be needed to investigate this. One can, however, see from figure 3.23 that for phase 3 west there is a general decrease in the Na concentration, and for phase 3 east, a general increase.

Phase 3

If one examines figures 3.24 and 3.25, it is evident that although there is a slight increase in the Na concentration on the east and the west wide, (1% and 3%, respectively), this change is so small that it can be classified as negligible.

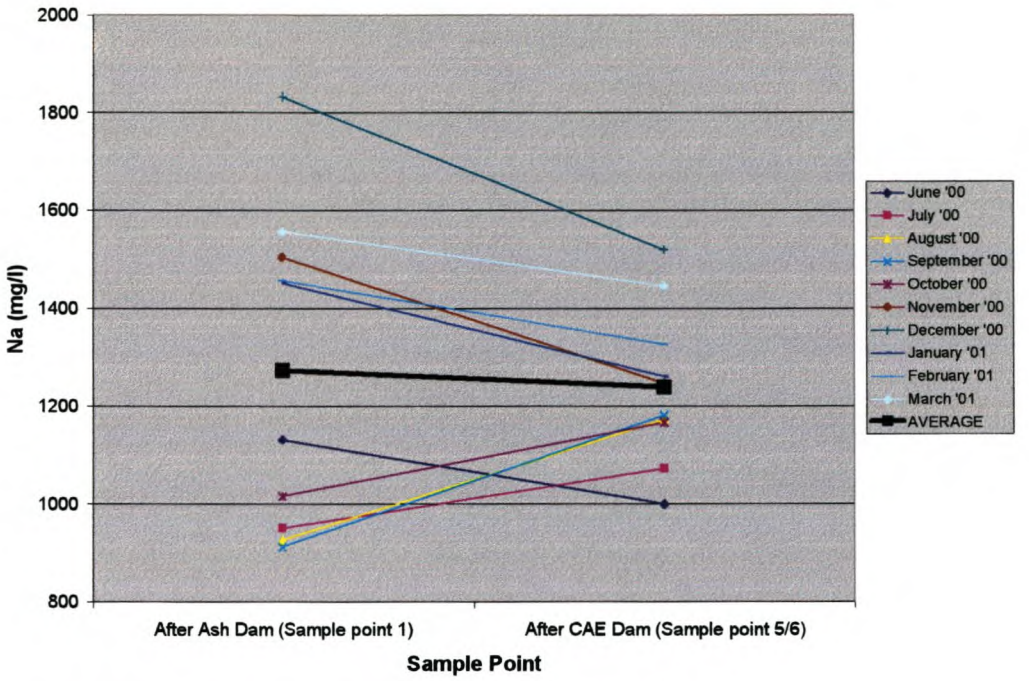

Figure 3.24: Concentration variation for Na phase 3 west

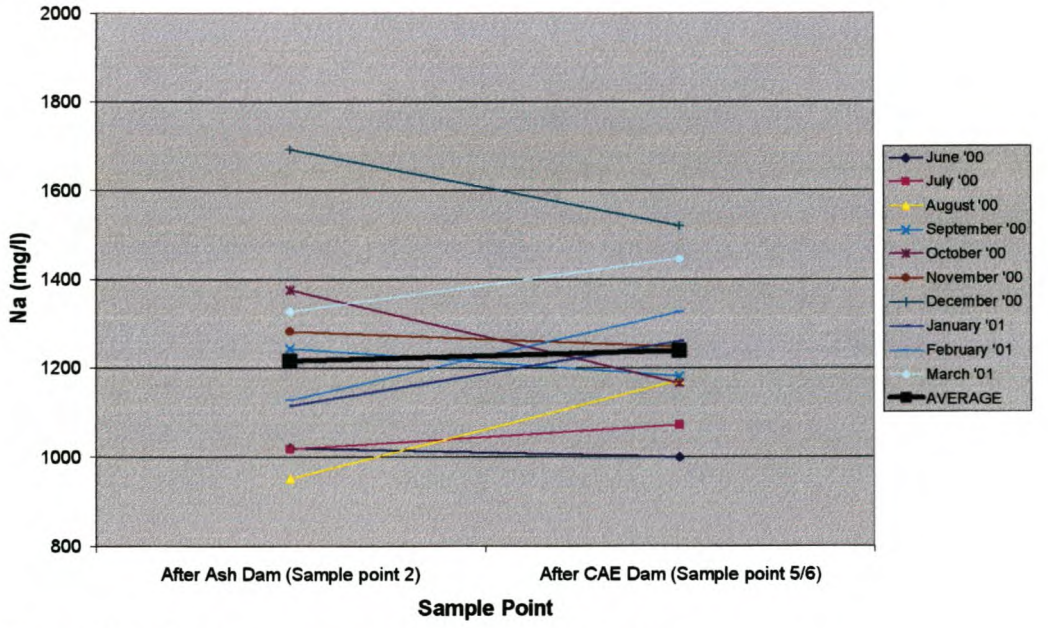

Figure 3.25: Concentration variation for Na phase 3 east

Separation into seasons

If one examines the variation in the Na concentration for the different seasons (figure 3.26), it is apparent that there is on average a slight decrease in sodium for the wet months, and a slight increase for the dry months. This overall increase in the Na concentration in the dry months as opposed to the wet months could be due to more evaporation and less precipitation occurring in the CAE and Evaporation Dams during the dry months. A decrease in the amount of water present could result in an increase in the Na concentration at the outlet of the CAE dams, i.e. points 5 and 6. It could be argued from the other angle as well, that in the wet months the increase in precipitation results in a dilution effect in the CAE and Evaporation Dams thus in essence lowering the concentration of the Na at points 5 and 6.

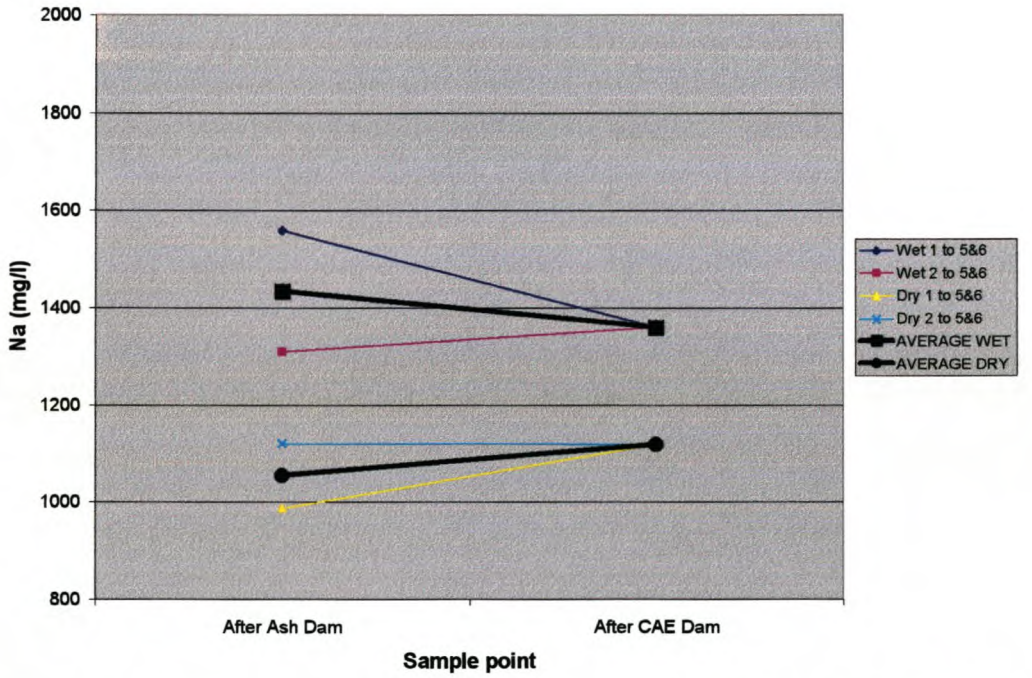

Figure 3.26: Comparison of variation in Na concentration for the wet and dry months for phase 3 east and west

3.7.2.3 Sulphate

The trends seen for sulphate are given in figures 3.27 to 3.30, and can be summarised as follows:

Phase 2

If one examines figure 3.27 it is evident that on the east side there is a 15% average reduction in the SO_4 (from the time the ash water slurry leaves inside ash, to the time it leaves the ash dams), whereas on the west side there is practically no change in the SO_4 concentration (1% average increase).

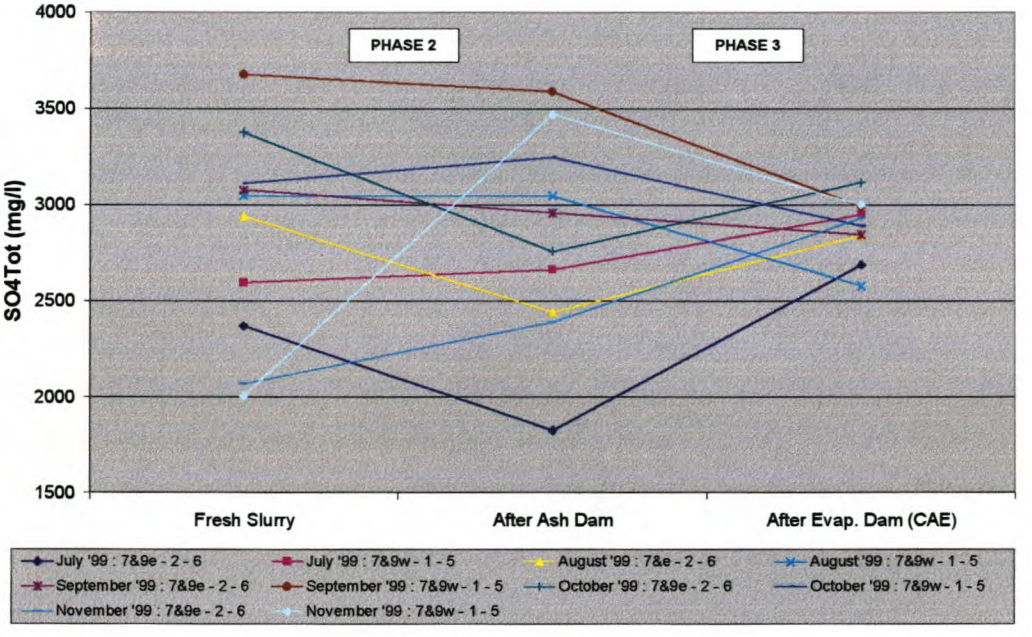

Figure 3.27: Concentration variation for SO_4 phase 2&3 east and west (1999 data)

Figure 3.27 does not show any major change in the SO_4 concentration overall for phase 2 and 3 combined (i.e. Outside Ash), however, one should bear in mind that these are changes in concentration and not changes in the actual SO_4 content. One can see for phase 3 (1999 data, figure 3.27) that there is apparent increase in the SO_4 concentration

for phase 3 east and a general decrease for phase 3 west. These trends correlate to the findings for phase 3 using the more comprehensive data for 2000/2001 (figures 3.28 and 3.29)

Phase 3

If one examines figures 3.28 and 3.29 it is apparent that opposite trends, for the variation in the SO_4 concentration, exist on the east and west side of the disposal system. On the east side there is an 18% average increase in the SO_4 content of the ash water, whereas on the west side there is a 9% average reduction.

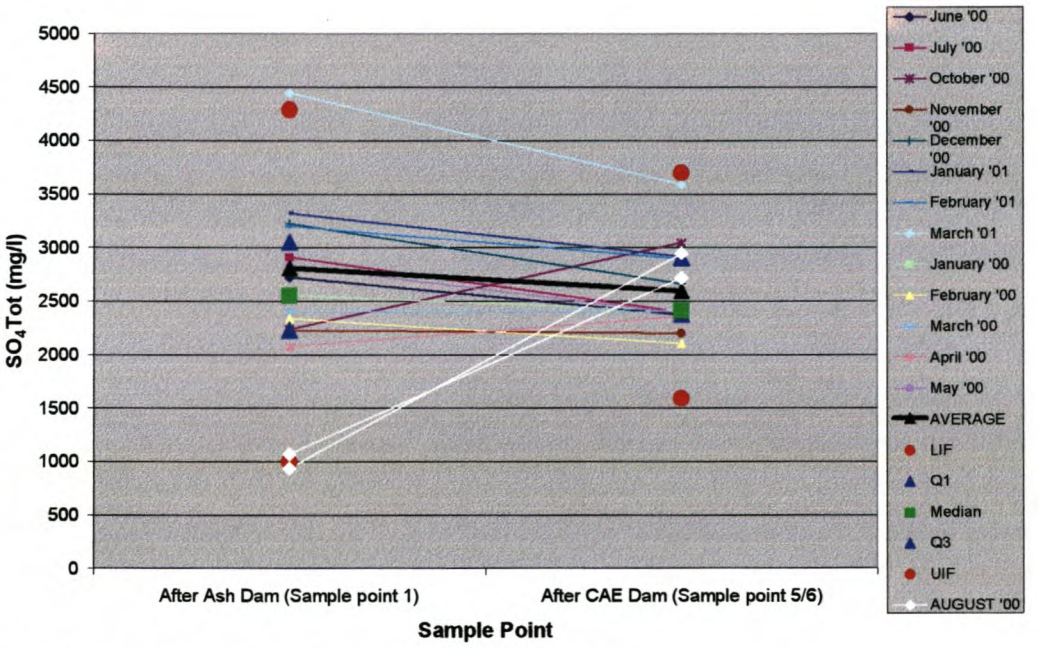

Figure 3.28: Concentration variation for SO_4 phase 3 west

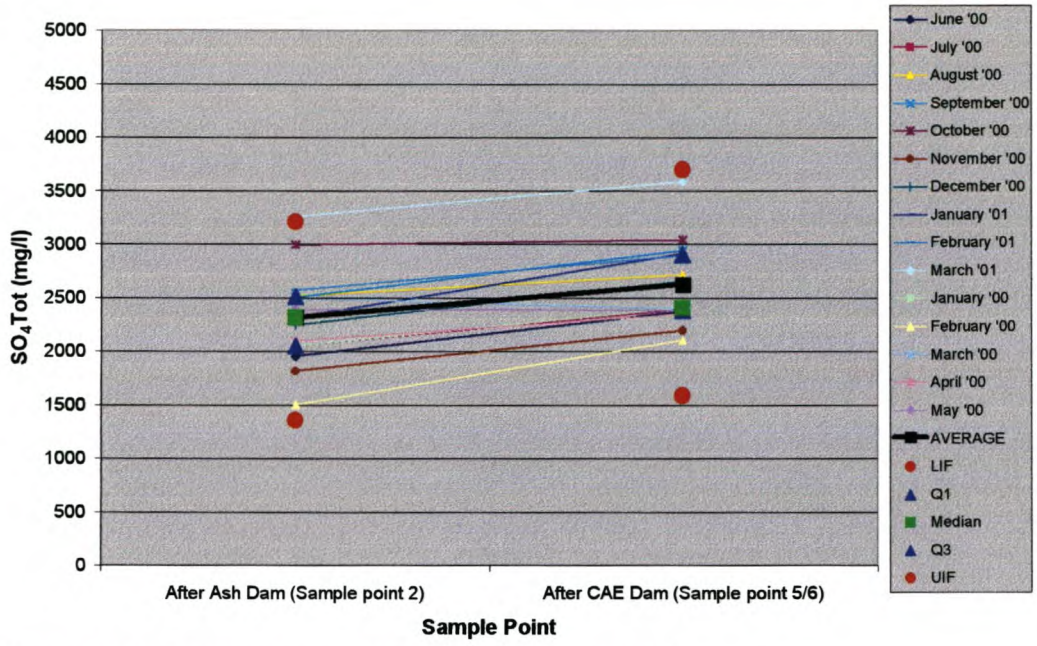

Figure 3.29: Concentration variation for SO_4 phase 3 east

Separation into seasons

When the data is divided into "wet" and "dry" months (figure 3.30), it is evident that there is an increase in the SO_4 concentration for all the seasons except during the wet months for sample points 1 to 5&6. The fact that an overall reduction is observed for the west side, is due to the fact that the readings for Aug, Sept '00 (1 to 5&6) were left out – these displayed large increases in SO_4. If in fact these readings are included, is can be seen that there is an overall increase in the SO_4 concentration for both the wet and dry months.

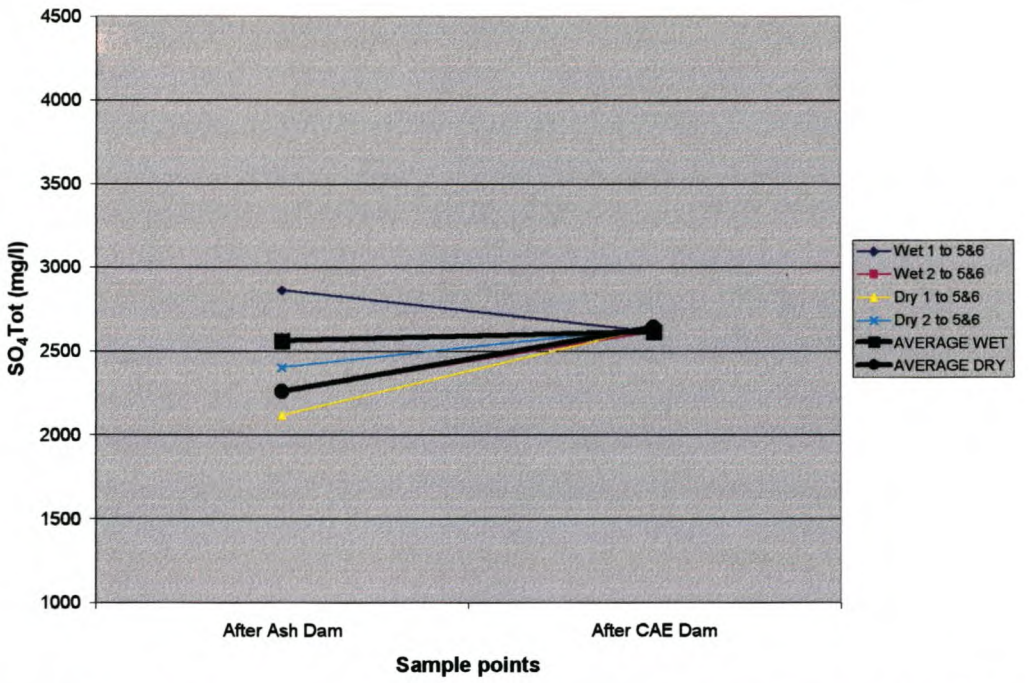

Figure 3.30: Comparison of variation in SO_4 concentration for the wet and dry months for phase 3 east and west

3.7.2.4 Chloride

For chloride, the trends in the actual plant data are displayed in figures 3.31 to 3.34, and can be summarised as follows:

Phase 2

Figure 3.31 illustrates that on the east side there is a 4% average increase in the chloride ion concentration over phase 3, whereas on the west side there is a 3% average reduction in the chloride ion concentration.

Besides illustrating the trends for phase 2, figure 3.31 also indicates the trends for phase 3 based on data from 1999. It is evident that there is an overall increase in the chloride ion concentration for phase 3 east and an overall decrease for phase 3 west. This is reinforced the findings for phase 3 using the 2000/2001 data (figures 3.32 and 3.33).

Thus, it appears that in general there is an increase in the Cl ion concentration over the Outside Ash for the east system, and a general decrease for the west system.

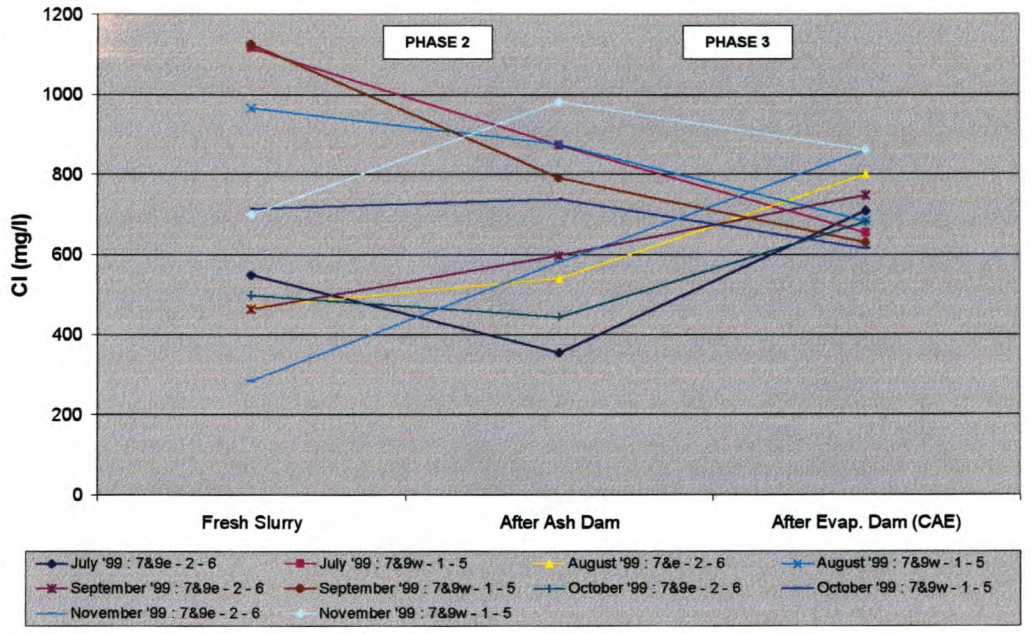

Figure 3.31: Concentration variation for Cl phase 2&3 east and west (1999 data)

Phase 3

From the 2000/2001 data (figures 3.32 and 3.33) it is evident that for phase 3, on the east side, there is an 8% average increase in the chloride ion concentration of the ash water (from point 2 to 5/6). However, on the west side there is a 7% average reduction in the chloride ion concentration of the ash water (from point 1 to 5/6).

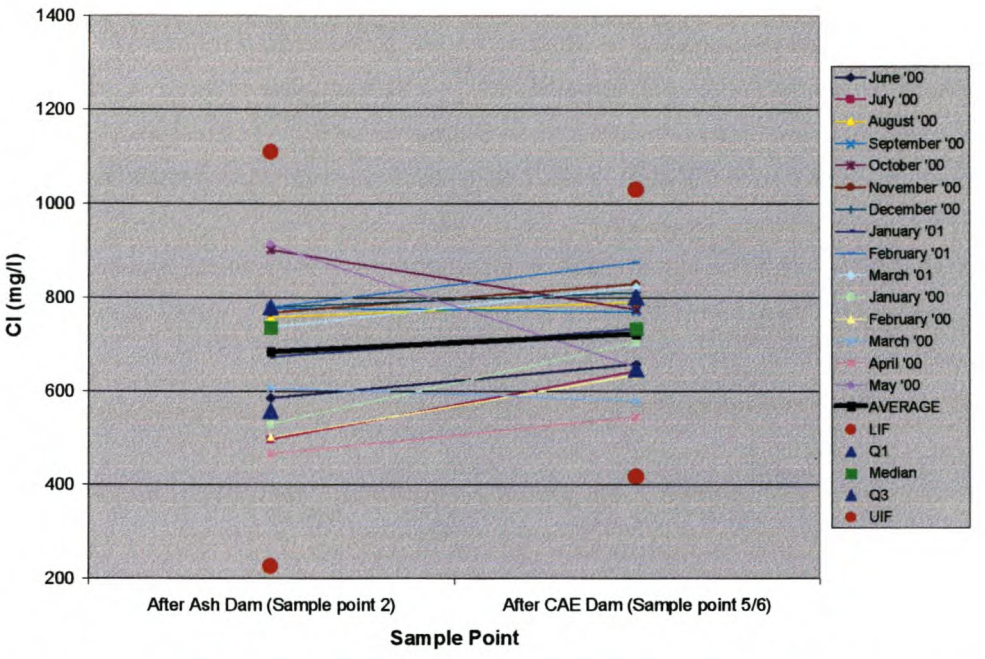

Figure 3.32: Concentration variation for Cl phase 3 east (including box & whisker plot)

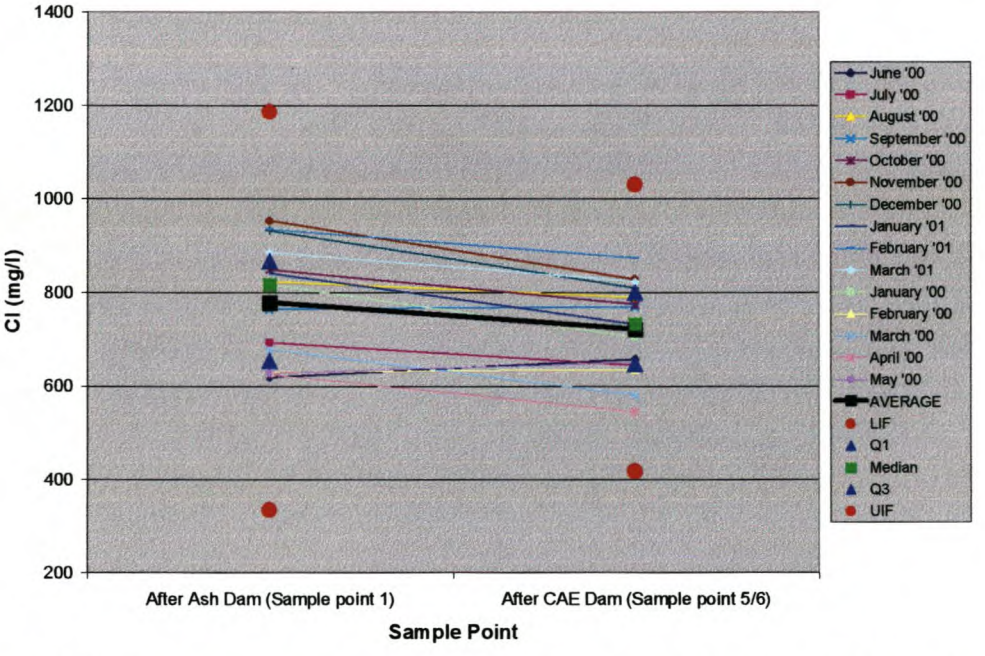

Figure 3.33: Concentration variation for Cl phase 3 west (including box & whisker plot)

Separation into seasons

A separation of the data into seasons reveals that there is an overall decrease in the Cl for the dry moths from points 1 and 2 to 5&6. For the wet months, however, there is an increase in the chlorine from 2 to 5&6 and a decrease from 1 to 5&6. The variations in the Cl are much more drastic in the wet months than in the dry months – whether it be an increase or a decrease. Therefore, when the data for the wet and dry months is combined (figure 3.34), then for points 2 to 5&6 the overall trend appears to be an increase in chlorine since the increase in the wet months is much greater than the decrease in the dry months.

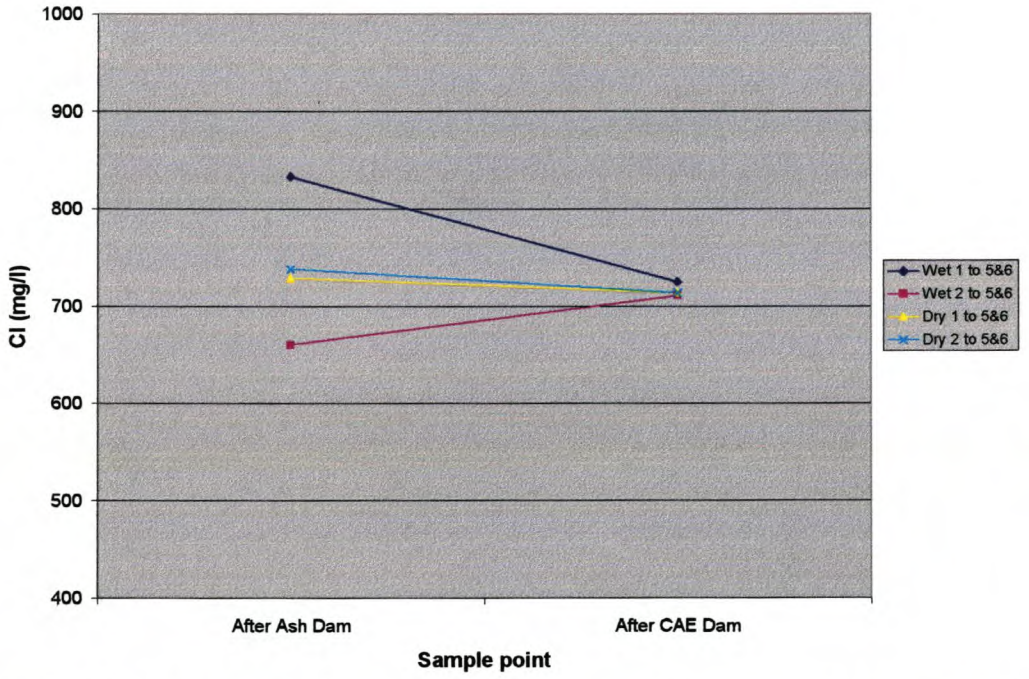

Figure 3.34: Comparison of variation in Cl concentration for the wet and dry months for phase 3 east and west

3.7.2.5 Potassium

The variations in the K concentration in the ash water system are presented in figures 3.35 to 3.38, and can be summarised as follows:

Phase 2

From figure 3.35 it is apparent that on the east side there is a 11% average increase in the potassium from the time the ash water slurry leaves inside ash, to the time it leaves the ash dams; on the west side there is also an increase (13%) in the potassium concentration.

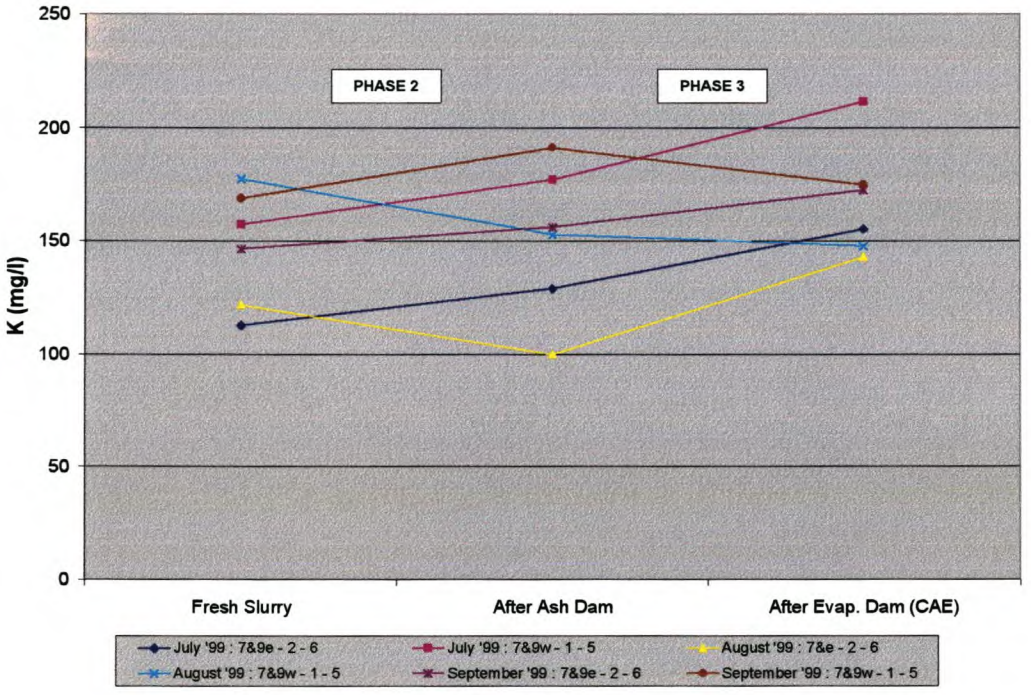

Figure 3.35: Concentration variation for Mg phase 2&3 east and west (1999 data)

From figure 3.35 one can see that there is in general an overall increase in the K concentration over both phase 2 and phase 3. This increase in concentration for phase 3 is reinforced by the trends seen using the 2000/2001 data (figures 3.36 and 3.37).

Phase 3

For phase 3, using the 2000/2001 data, it is evident that there is an increase in the potassium content of the ash water on the east and the west side. On the east side there is a 25% average increase (figure 3.36) and in the west side, a 20% average increase (figure 3.37).

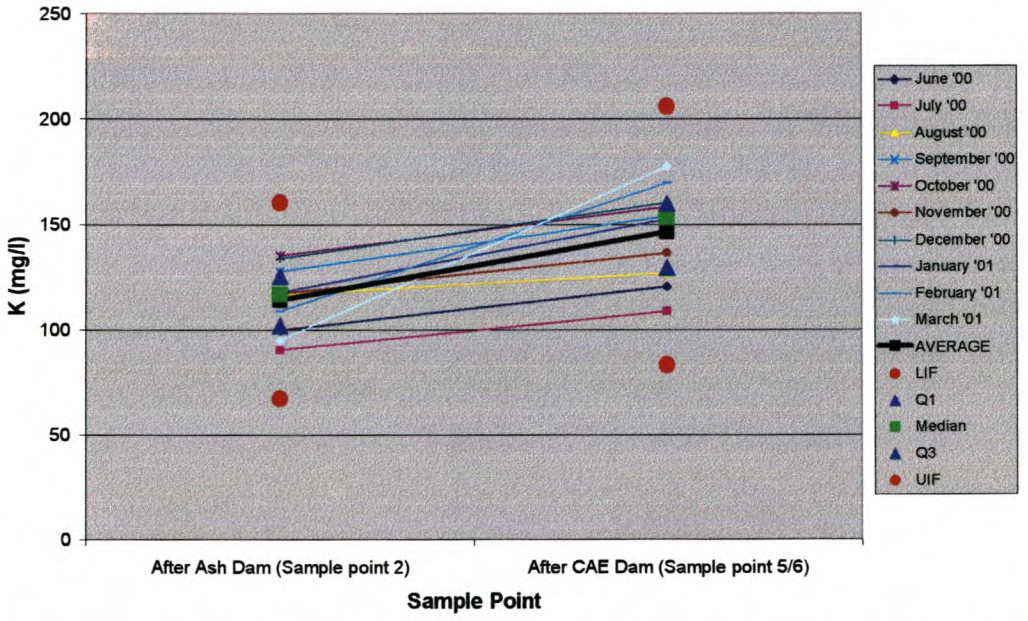

Figure 3.36: Concentration variation for K phase 3 east (including box and whisker plot)

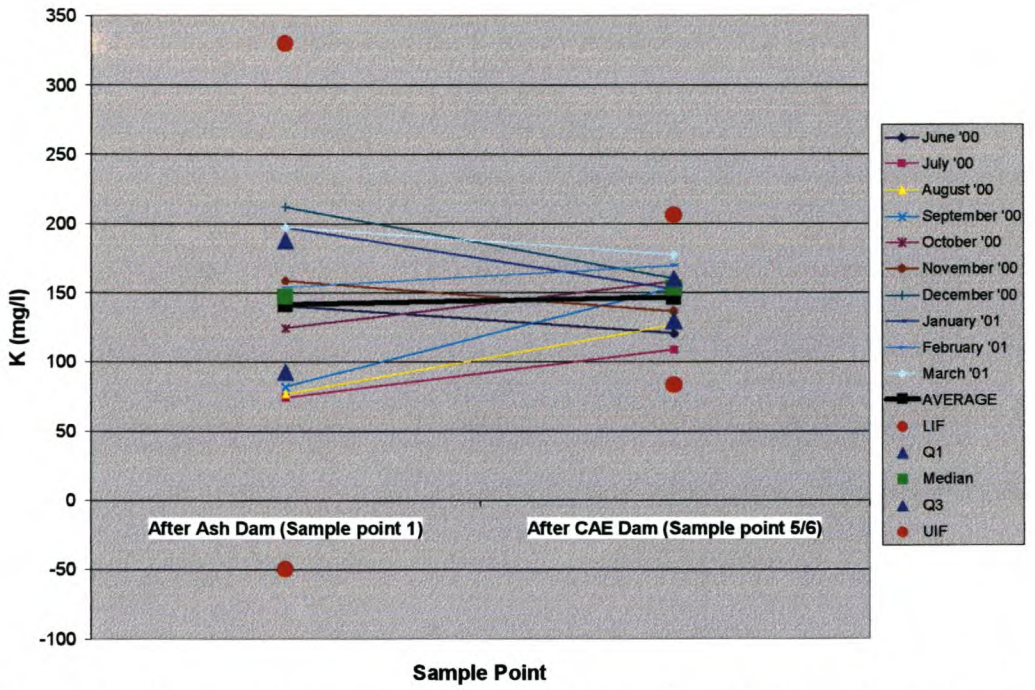

Figure 3.37: Concentration variation for K phase 3 west (including box and whisker plot)

Separation into seasons

If the plant data is divided into wet and dry months, there is still an overall increase in the potassium concentration over phase 3, except a decrease is seen for the wet months data for points 1 to 5&6. For these wet months a decrease is seen for all months (Nov '00, Dec '00, Jan '01, Mar '01) except Feb '01. The only other month out of all the data for which a decrease is seen is for June '00 (dry month).

The decrease observed for the wet months for the west side, phase 3, appears to have more to do with the concentration of the K being higher at the penstock over-flow (sample point 1), than the concentration being lower in the CAE dams (due to excess rainfall). Thus, it the variation in the K concentration for the wet months (west side, phase 3) cannot be attributed to rainfall.

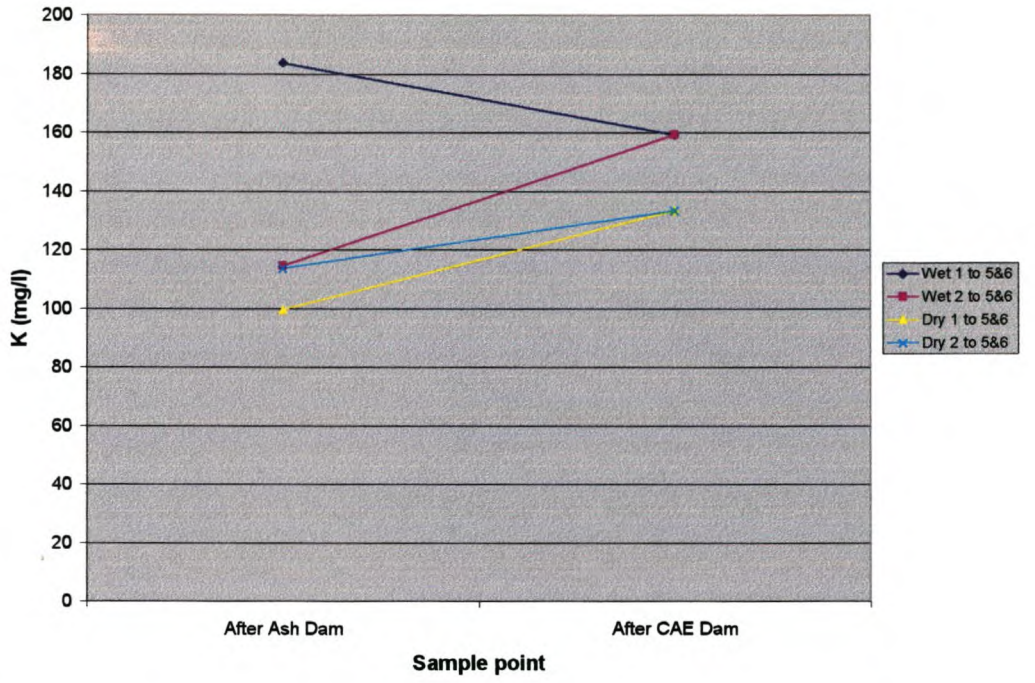

Figure 3.38: Comparison of variation in K concentration for the wet and dry months for phase 3 east and west

2.7.2.6 Total Dissolved Solids

The variation in the concentration of the total dissolved solids provides one with a good idea of the change in the overall salt content of the ash water as it passes through the disposal system. The trends observed for the total dissolved solids are given in figures 3.39 to 3.42, and can be summarised as follows:

Phase 2

There is a decrease in the TDS on the east and the west side, however, the magnitude of the decrease is far greater for the east side (40%) than for the west side (4%). These results are displayed graphically in figure 3.39.

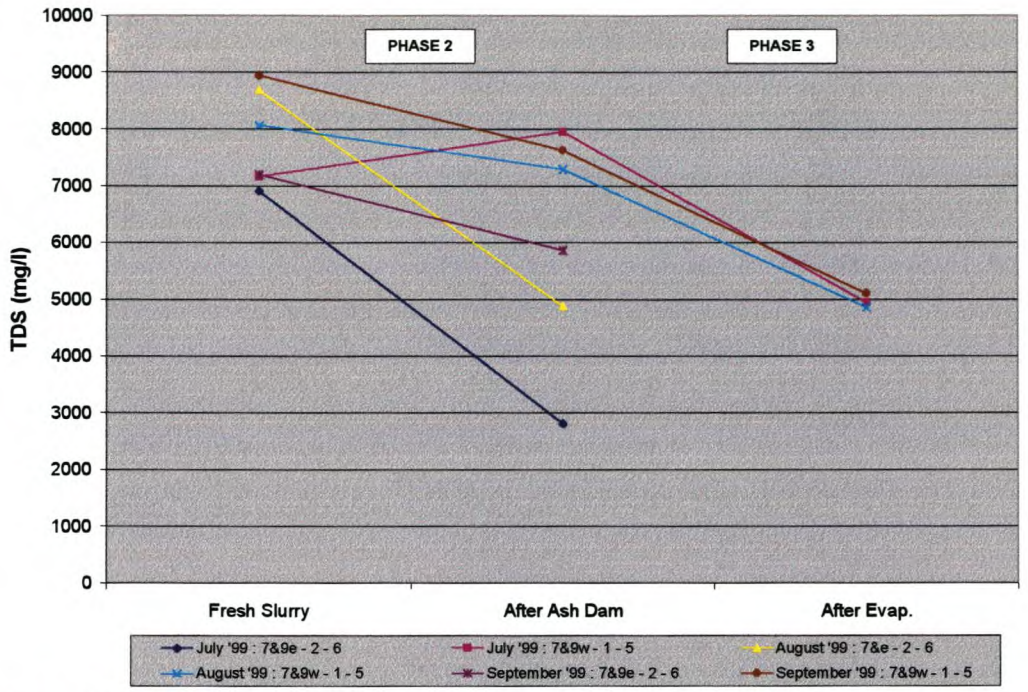

Figure 3.39: Concentration variation for TDS phase 2&3 east and west (1999 data)

Figure 3.39 shows that besides the decrease in TDS concentration for phase 2 east and west, there is also an overall decrease in the TDS concentration over the entire Outside Ash system (phase 2 and 3 combined).

Phase 3

If one examines the 2000/2001 data, it is apparent that there is a 3.5% decrease in the TDS on the east side (figure 3.40), whereas on the west side there is practically no reduction in the TDS from point 1 to 5 (figure 3.41). The fact that overall, no change in the TDS concentration is observed for the west side, can be attributed to there is an increase for the months of July, August September, and October '00. The trends for TDS could therefore possibly be explained according the annual rainfall pattern – the increase in TDS was for the "dry months".

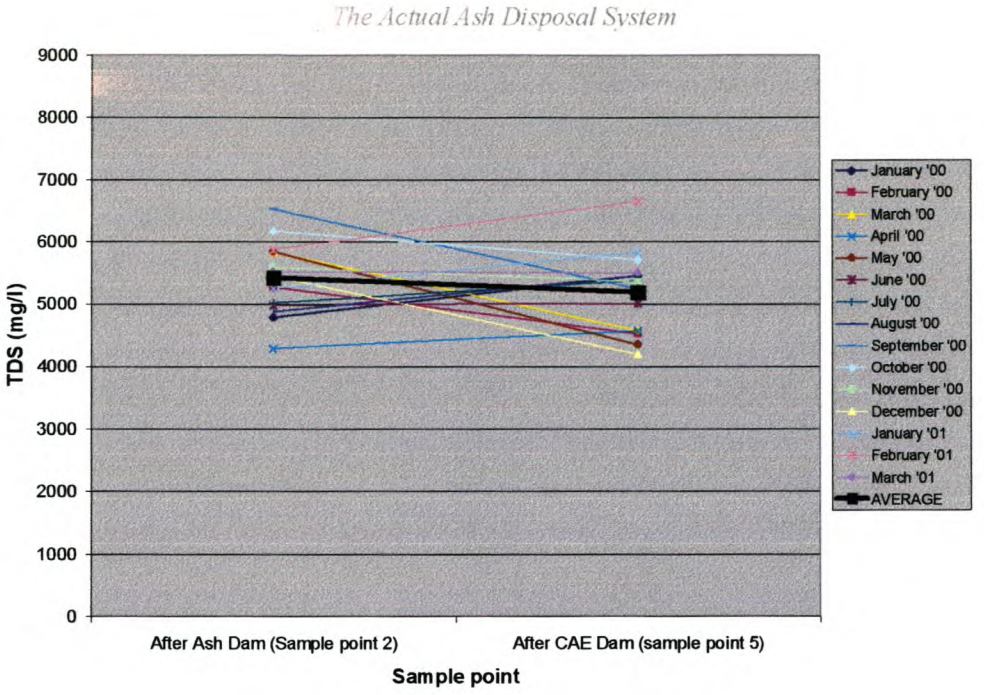

Figure 3.40: Concentration variation for TDS phase 3 east

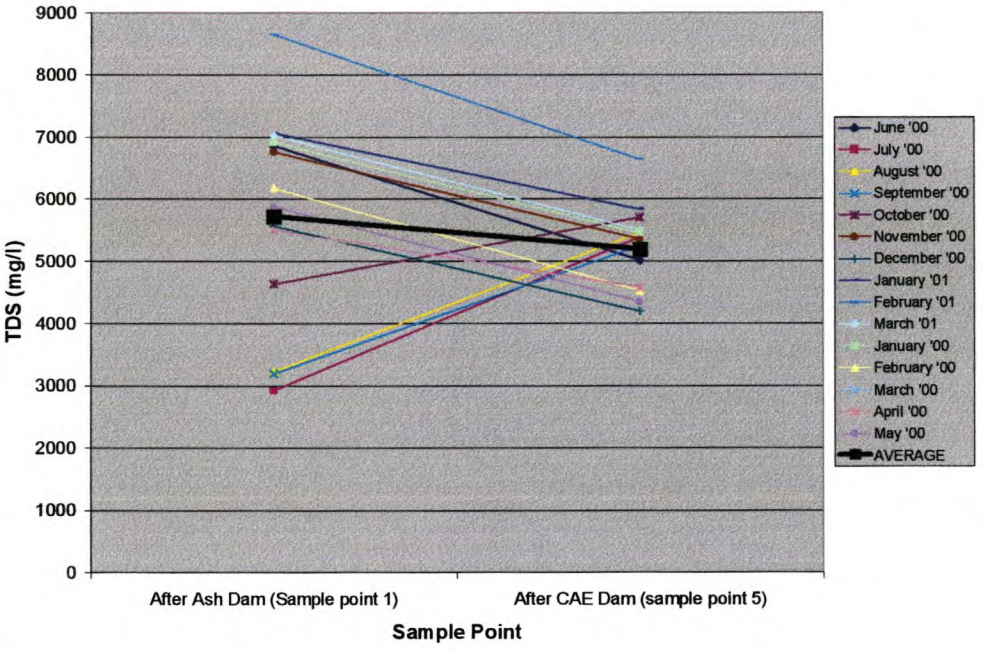

Figure 3.41: Concentration variation for TDS phase 3 west

Separation into seasons

If the TDS data is divided into "wet" and "dry" months, there is a decrease in the TDS for all the seasons except for "dry" 1 to 5 (figure 3.42). This is due to the fact mentioned above – there is an increase in TDS for the months of July, August, September, and October '00 from point 1 to 5&6. However, these same patterns are not seen for points 2 to 5. A possible reason could be because there was no data available for point 6, so in fact only the data from point 5 was used. If in fact there was data from point 6 available, then the same trends may have been observed, i.e. a decrease in TDS for the wet months, and an overall increase in the dry months. The question one needs to ask is whether one can in fact use data for point 5 instead of point 6? Well as can be seen with the data given in Appendix B2, there is not much difference between these two sampling points, but it is probably still safer not to draw any hard and fast conclusions from these results.

However, as far as the increase for the dry months for phase 3 west is concerned, this could be attributed to an increase in the concentration at point 5 due to more evaporation and less precipitation occurring in the CAE and Evaporation Dams during the dry months.

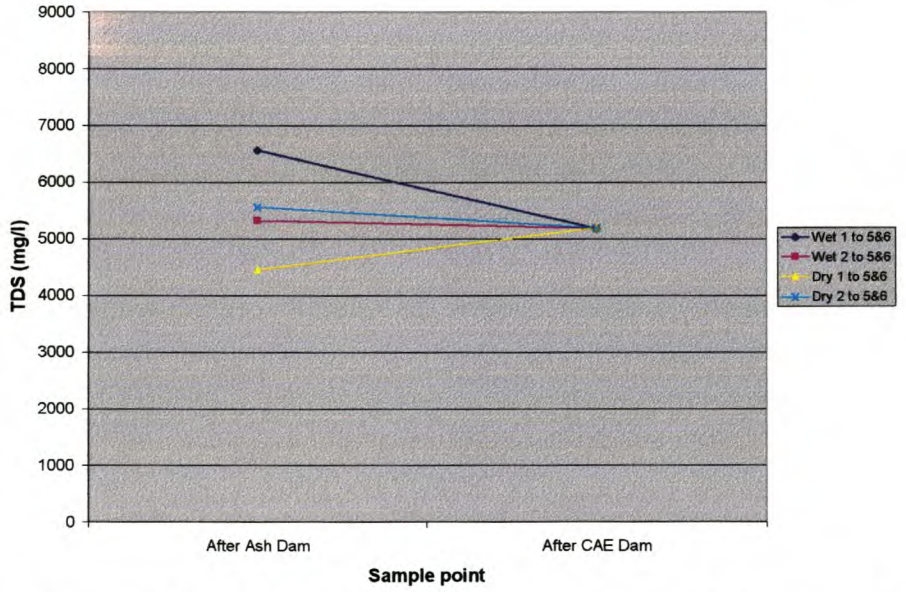

Figure 3.42: Comparison of variation in TDS concentration for the wet and dry months for phase 3 east and west

3.7.2.7 Total Alkalinity

The total alkalinity of the effluent is represented by the M alkalinity (see section 2.5). The variation in the M alkalinity through the Secunda ash water system is displayed in figures 3.43 to 3.46, and can be summarised as follows:

Phase 2

On the east and the west side there is an average reduction in the MAlk from the time the ash water slurry leaves inside ash, to the time it leaves the ash dams (figure 3.43). On the east side there is a 28% reduction, and on the west a 7% reduction.

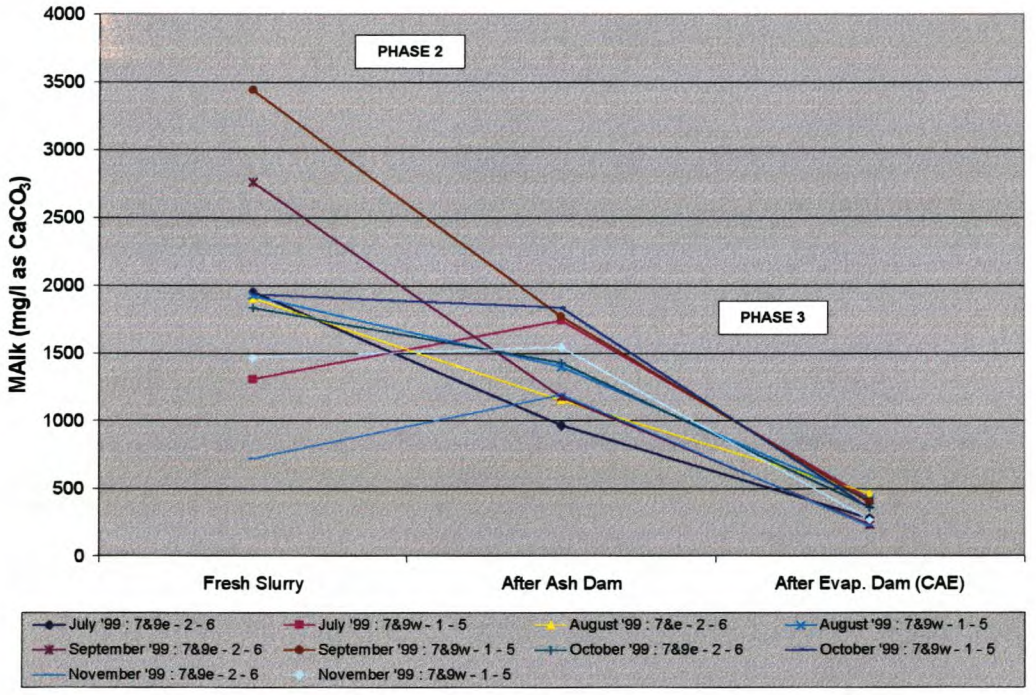

Figure 3.43: Concentration variation for MAlk phase 2&3 east and west (1999 data)

From figure 3.43 it is evident that overall (phase 2 and 3 combined), for Outside Ash on the east and the west side, there is a decrease in the total alkalinity of the ash water.

Phase 3

For phase 3, using the 2000/2001 data, it is evident that the change in the MAlk on the east and the west side is very similar. On the east side there is an 84% average reduction in the MAlk of the ash water from point 2 to 5/6 (figure 3.44), and on the west side there is an 85% average reduction in the MAlk of the ash water from point 1 to 5/6 (figure 3.45).

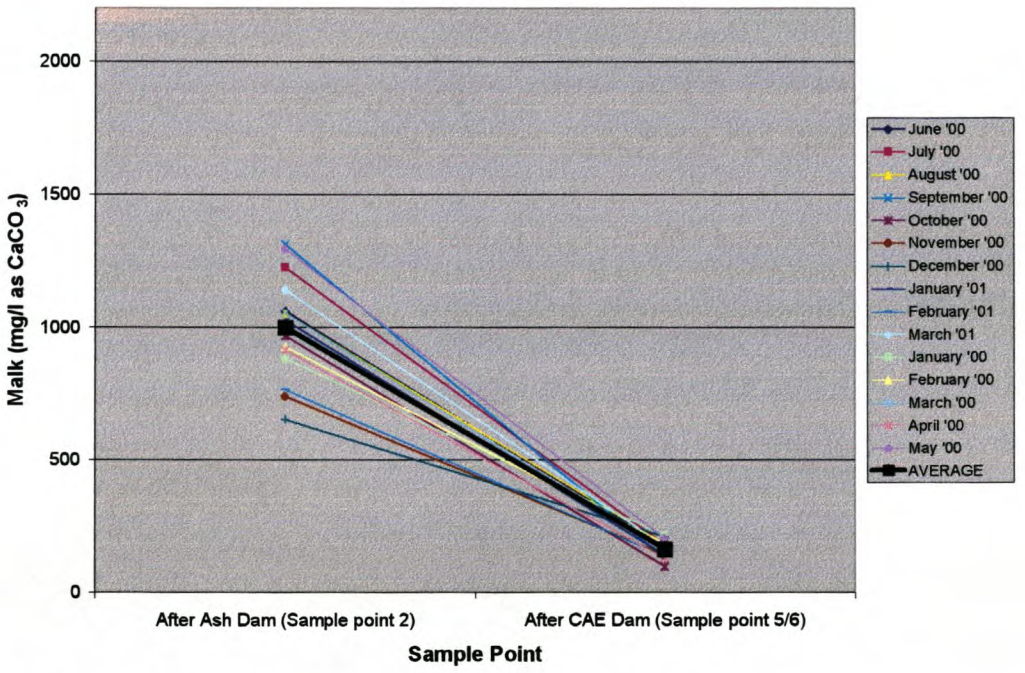

Figure 3.44: Concentration variation for MAlk phase 3 east

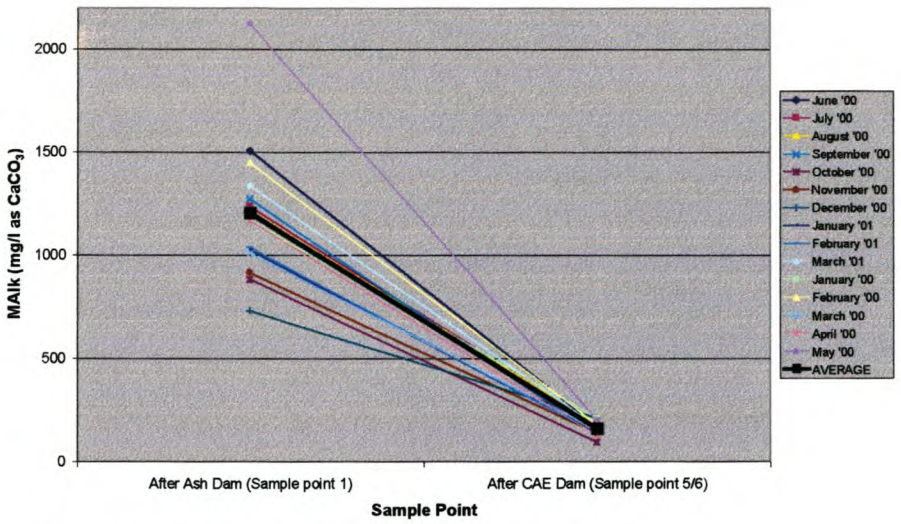

Figure 3.45: Concentration variation for MAlk phase 3 west

Separation into seasons

When dividing the data up into "wet" and "dry" months there is still an average reduction in the MAlk from points 1 and 2 to 5&6 (phase 3). There is no major difference in the reduction for the wet and dry months.

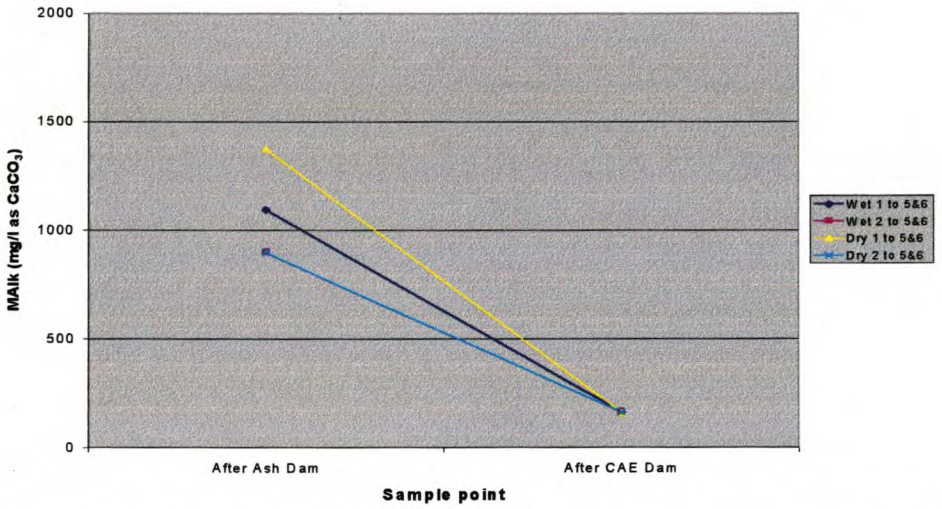

Figure 3.46: Comparison of variation in the MAlk concentration for the wet and dry months for phase 3 east and west

3.7.2.8 pH

As far as the change in pH is concerned, average values could not be calculated in the same manner as for the other components, since it is based on a logarithmic scale.

Thus, in order to assess the variation of the pH at different points in the ash system, scatter plots of the actual pH readings were drawn and evaluated. Figure 3.47 shows the variation of the pH at the slurry sample points (7e&w, and 9e&w). This graph is based on the data from 1999, and covers a period of 20 weeks.

Figure 3.48 displays the variation in the pH for sample points 1, 2, 5 and 6 (i.e. at the penstock over-flow, and at the point where the CAE is returned to the factories). The data used in this graph covers a time period of 26 months (1999-2001).

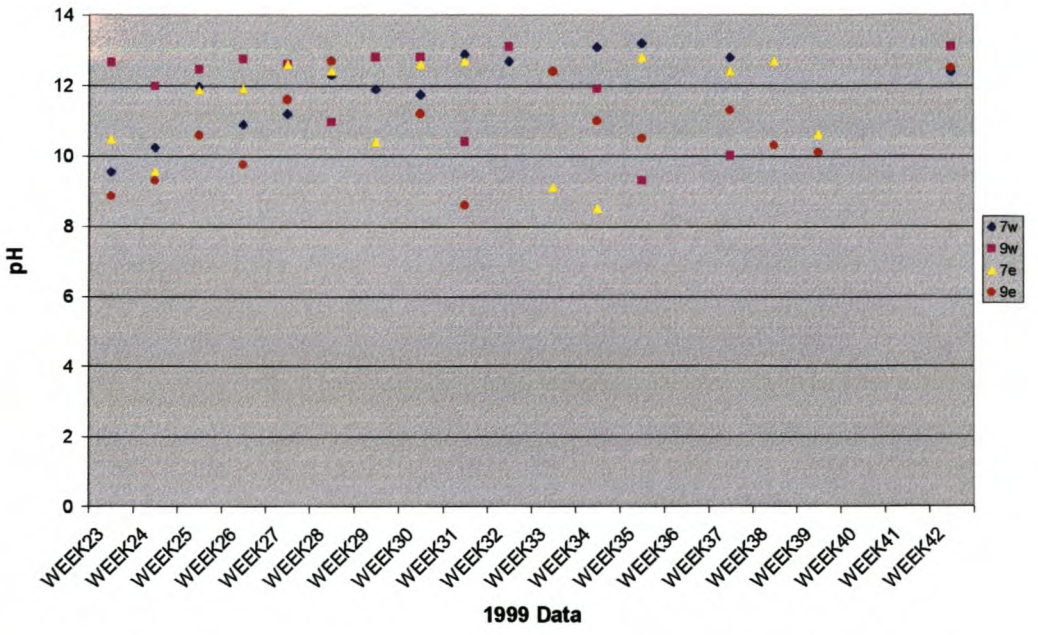

Figure 3.47: pH variation at slurry sample points

The data in figure 3.47 shows that the pH varies between about 8 and 13 for the ash water slurry; the average being close to about 12.

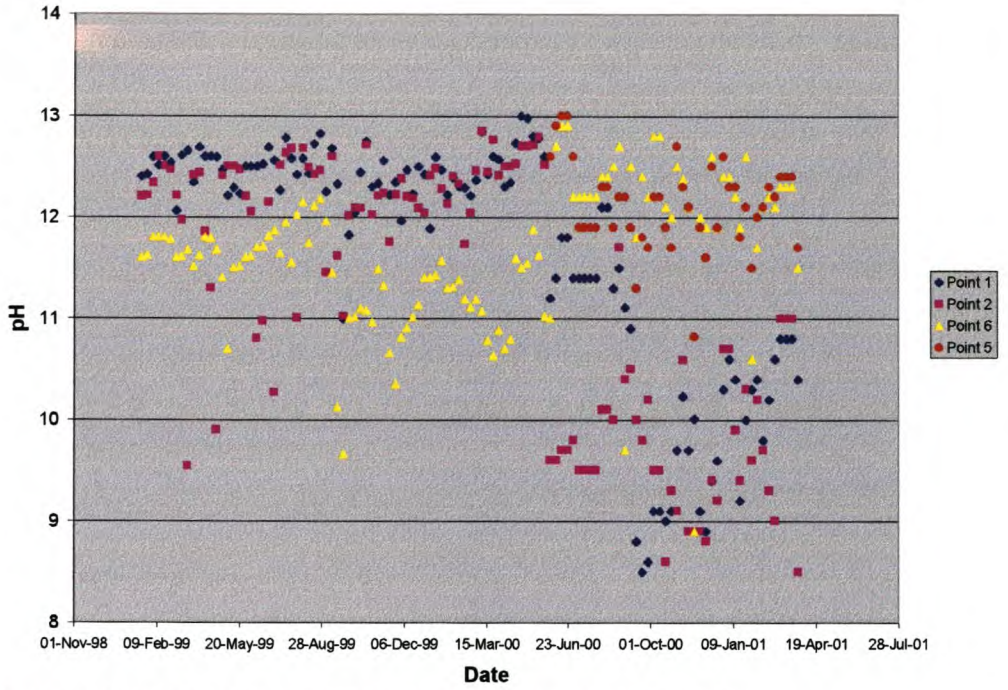

Figure 3.48: pH variation for phase 3 east and west (1999-2001)

From figure 3.48 it is evident that the pH at both points 1 and 2 has changed quite considerably over the 2 year time period (1999-2001). Up until about April 2000 the pH was at about 12.5 for both points 1 and 2 (penstock over-flow for ash dams 3 and 4 respectively). After about April 2000, the pH dropped to an average value of approximately 10 and has stayed within that range (8.5 to 11) until April 2001 (the last data point used in this analysis). Thus, one can assume that the pH stays fairly constant at the penstock over-flow, provided the operating conditions of the ash system remain constant.

Examining the more recent data for phase 3 (April 2000 – April 2001), the pH at the CAE dams is higher than the pH at the penstock over-flow (for both the east and the west side). Looking at this time period, the pH is just above 12 for the return lines to Sasol 2 and 3 (sample points 5 and 6), and approximately 10 for the penstock over-flow points (sample points 1 and 2). There hasn't been a drastic change in the pH of the CAE during the time period Feb 1999 to April 2001, although from about June 2000 it does appear to increase slightly (based on the data from sample point 6).

Thus, overall one can say that the variation of the pH at Outside Ash lies in the range 8 to 13 (slurry streams, penstock over-flow, and CAE return to factories). The pH lies within the same range for both the east and the west system, and also any changes that have occurred in the pH (from 1999 – 2001) have taken place on both the east and the west side.

3.7.2.9 Hydroxide and Carbonate Ion Variation

The data, in the form of M alkalinity and P alkalinity (section 2.5), can be used to calculate the concentration of OH^- and CO_3^{2-} ions in solution. For pH values above pH 9.8 – 10.0 (where PAlk exceeds ½ MAlk):

$$CO_3^{2-} = 2(M - P) \tag{2-60}$$

$$OH^- = 2P - M \tag{2-61}$$

$$HCO_3^- = zero \tag{2-62}$$

Thus, the relevant OH^- and CO_3^{2-} concentrations were calculated for all the sample points at Outside Ash (i.e. the ash slurry streams, the penstock over-flows, and the CAE return to the plants.). The trends determined are displayed in figures 3.49 and 3.50.

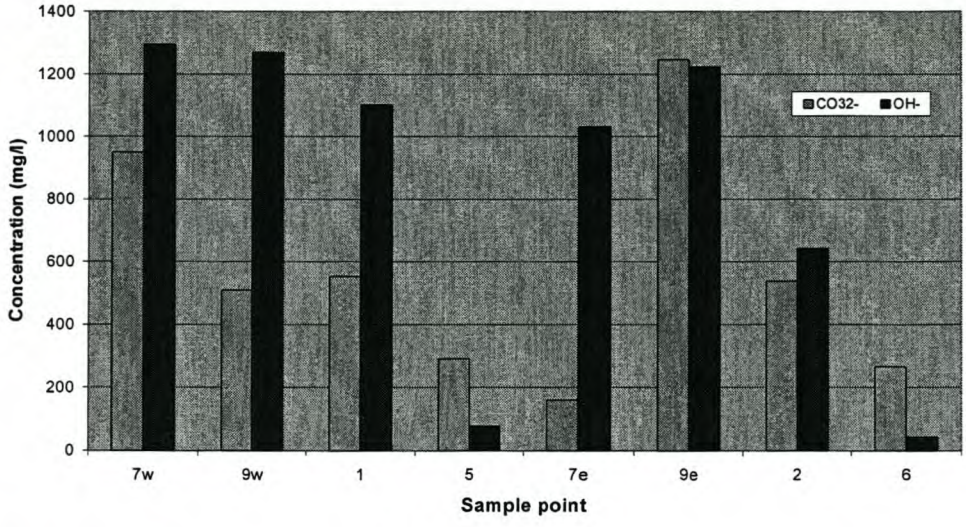

Figure 3.49: Average values of OH^- and CO_3^{2-} concentrations at various sample points (east and west)

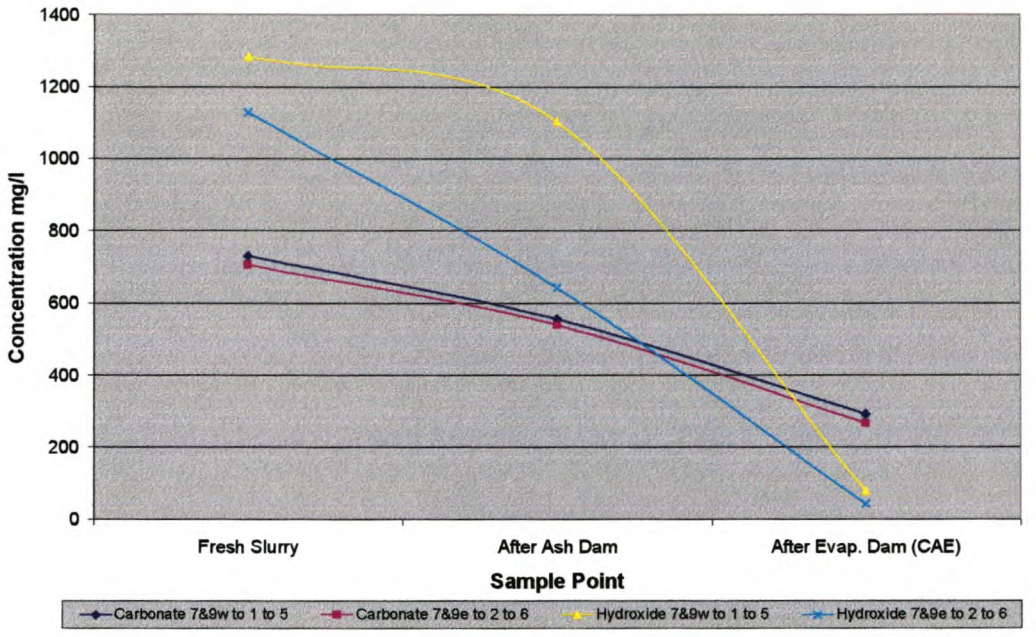

Figure 3.50: Variation in OH^- and CO_3^{2-} concentrations at Outside Ash

From figures 3.49 and 3.50 it is evident that there is a decrease in both the OH^- and CO_3^{2-} concentrations from the slurry streams, to the penstock over-flows, to the CAE dams. This supports the calcium chemistry that the precipitation of calcite is occurring in the ash system. One can also see that at the point where the ash water slurry leaves inside ash, the OH^- concentration exceeds the CO_3^{2-} concentration. It still exceeds the CO_3^{2-} concentration at the penstock over-flow, but in the CAE dams the CO_3^{2-} concentration exceeds the OH^- concentration. This can also be explained by the fact that the majority of the calcite precipitation occurs in the Evaporation and CAE dams. Also from the time the ash water leaves the ash dams (via the penstock over-flow), the water is no longer in contact with the ash, thus the following reaction will cease to occur (since the CaO is present in the ash).

$$CaO_{(s)} + H_2O \rightarrow Ca(OH)_2 \qquad (2\text{-}7)$$

3.7.3 Identified 'outlier' months

From the analysis of the component trends discussed in section 3.7.2, it was evident that some months in particular were discarded repeatedly due to the fact that they were identified as "outliers". The following months were identified to be 'outlier' months in terms of concentration variations, i.e. for more than one component, or at more than one sample point, it was during these months that a deviation from the general trend was seen. The number in brackets is the number of times that this month was discarded from the calculation of the average increase or decrease of a specific component for a certain phase, as described in section 3.7.2.

November 1999 [10]

August 2000 [7]

September 2000 [6]

August 1999 [4]

October 2000 [4]

December 2000 [3]

Thus, it is evident that November 1999 was discarded the most number of times, suggesting that something must have happened in the ash water system during this month to cause so many deviations from the norm. From reports by Smit (1999, 2000 and 2001), on the ash dam levels of the Secunda ash water system, certain incidents were cited that could possibly explain why some of these months, mentioned above, are seen as 'outlier' months.

November 1999

- During November 1999, there was less rainfall than was predicted (58mm less). Less rainfall could possibly mean higher concentrations than usual at Outside Ash.
- The product flow from U66 and U67 (the salty water system) was 3M*l*/day more than what was expected. Obviously an increase in the salty water entering the system will affect the trends seen for the changes in concentration of the various elements.

August 2000

- During August 2000, ash water was pumped to the black products dams (fine coal dams).
- Fine ash slurry was pumped to the course ash heaps.

September 2000

- In mid September (about the 18th), the pumping of ash water to the fine coal dams was terminated.

December 2000

- Fine ash slurry was once again pumped onto the course ash heaps.
- An increase in the PCWBD (process cooling water blow-down) from SSF East to the ash system was observed during the period December 2000 to April 2001.

These observed 'outlier' months were presented to plant personnel in order to ascertain whether they could identify certain occurrences within the system to explain why they could be seen as 'outliers'. Unfortunately, since the system is so complex, and involves many different process units, no particular incidents could be identified. This further emphasises the need for a close monitoring of the entire ash disposal system at all times.

3.8 Mass balances

3.8.1 Phase 1

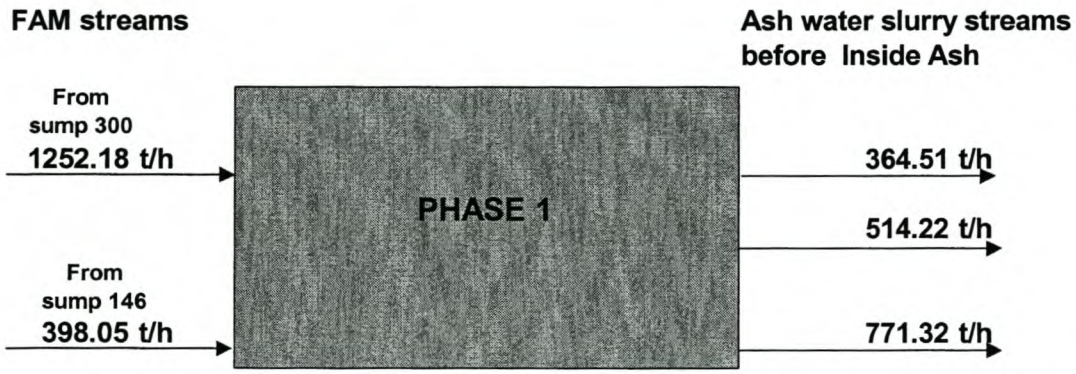

Figure 3.51: Basic flow diagram for phase 1

The flow data shown in figure 3.51 was combined with the sample analyses from the following dates in order to perform mass balances over phase 1.

- 29th August 2001
- 30th August 2001
- 31st August 2001
- 6th September 2001
- 13th September 2001

This data, used in performing the mass balances, was obtained from a study done by Marais, E., 2002 on the Sasol, Secunda, Ash Water System. The chemical composition of the streams used was calculated by taking an average value of the analyses from the five dates mentioned above. Mass balances were calculated on both a kg/h basis and g/kg ash basis. For the calculations based on the g/kg ash basis, an ash flow rate of 177 000kg/h was used (the approximate ash flow rate associated with the ash water flow rates shown in figure 3.51). The results of these calculations are shown in tables 3.9 and 3.10.

Table 3.9: Mass balance results for phase 1

Component	Units	IN	OUT	IN - OUT	
Cl	**kg/h**	**1709**	**1911**	**-201**	**leached**
COD	kg/h	653	645	8.1	retained
F	kg/h	30.1	22.7	7.4	retained
Ammonia	kg/h	135	159	-25	leached
Nitrate	kg/h	22.5	18.8	3.7	retained
Phosphate	kg/h	4.35	0.50	3.9	retained
Sulphate	**kg/h**	**3572**	**3136**	**435**	**retained**
SS	kg/h	1704	50571	-48866	leached
TDS	**kg/h**	**12322**	**16119**	**-3797**	**leached**
Na	**kg/h**	**2285**	**2809**	**-524**	**leached**
Mg	kg/h	1.03	1.82	-0.8	leached
Al	kg/h	0.68	0.51	0.2	retained
Si	kg/h	22.8	26.7	-3.9	leached
K	kg/h	233	269	-37	leached
Ca	**kg/h**	**642**	**546**	**96**	**retained**
Mn	kg/h	0.28	0.22	0.1	retained
Fe	kg/h	2.85	1.26	1.6	retained
Sr	kg/h	37.2	41.3	-4.2	leached
Ba	kg/h	0.90	0.83	0.1	retained

Table 3.10: Mass balance results for main components based on g/kg ash basis

Component	kg/h	g/kg ash	
Cl	-201	-1.14	leached
Sulphate	435	2.46	retained
TDS	-3797	-21.5	leached
Na	-524	-2.96	leached
Ca	96	0.541	retained

One can see from these results that there is an overall leaching of salts into the ash water during phase 1 (TDS increases). The Na and Cl mass balances also reveal an overall leaching from the ash into the water; however, Ca and SO_4 show that they are retained. These results should be interpreted as preliminary results since they are based on the stream compositions from only five days. It is suggested that further samples of the streams relating to phase 1 be taken and analysed, in order to enhance the reliability of the mass balance results.

3.8.2 Phase 2

Using flow data (Marais, 2002) measured towards the end of 2001 (shown in figure 3.52), mass balances for the different components of the ash water could be calculated.

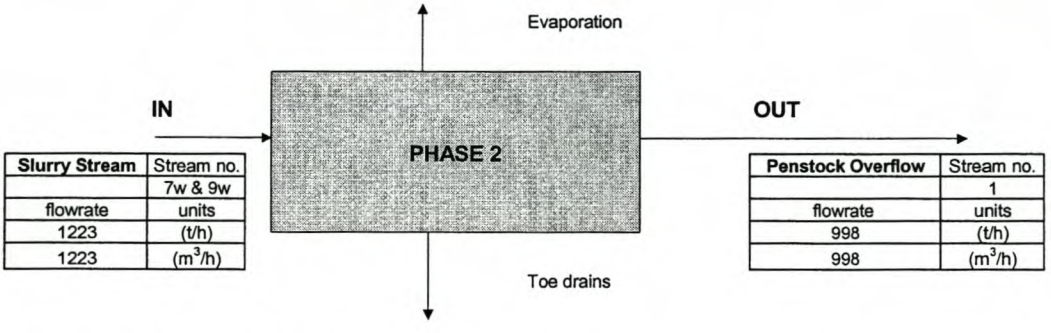

Figure 3.52: Basic flow diagram for phase 2

Table 3.11 displays the results for mass balances based on the average values of samples collected on the following days (Marais, 2002):

- 29th August 2001
- 30th August 2001
- 31st August 2001
- 6th September 2001
- 13th September 2001

Table 3.12 represents the results obtained using the data from 1999. More thorough mass balances could not be performed since the slurry streams are not sampled on a regular basis.

Table 3.11: Mass Balances for Phase 2 (Data from Aug/Sept 2001: Marais, 2002)

Component	Units	IN	OUT	IN - OUT	
Cl	**kg/h**	**1643.59**	**1073.85**	**570**	**retained**
COD	kg/h	544.24	369.86	174	retained
F	kg/h	21.99	16.21	5.78	retained
Ammonia	kg/h	139.30	35.33	104	retained
Nitrate	kg/h	18.04	18.96	-0.92	leached
Phosphate	kg/h	0.37	0.32	0.04	retained
SO_4Tot	**kg/h**	**3442.75**	**3463.06**	**-20.3**	**leached**
SS	kg/h	262891.19	533.93	262357	retained
TDS	**kg/h**	**20935.19**	**7829.91**	**13105**	**retained**
Na	**kg/h**	**1883.36**	**1309.08**	**574**	**retained**
Mg	kg/h	0.23	0.02	0.21	retained
Al	kg/h	0.45	0.03	0.42	retained
Si	kg/h	15.19	6.60	8.59	retained
K	kg/h	223.77	126.28	97.5	retained
Ca	**kg/h**	**594.02**	**492.73**	**101**	**retained**
Mn	kg/h	0.17	0.13	0.04	retained
Fe	kg/h	2.16	1.61	0.55	retained
Sr	kg/h	38.35	24.83	13.5	retained
Ba	kg/h	0.67	0.54	0.14	retained

These results show an overall retention of the Cl, Na, Ca and TDS, but a slight leaching of the SO_4. One should bear in mind that the data used for these mass balances is only an

average of five readings taken over a relatively short time period, and only for the west side of the ash disposal system (i.e. sample points 7w&9w to 1).

Table 3.12: Mass Balances for Phase 2 (Data from 1999)

Component	Units	IN	OUT	IN - OUT	
Ca	**kg/h**	**831.27**	**772.53**	**59**	**retained**
Cl	**kg/h**	**1128.72**	**848.60**	**280**	**retained**
F	kg/h	30.22	25.89	4.33	retained
Fe	kg/h	15.17	4.58	10.6	retained
K	kg/h	205.23	168.96	36.3	retained
Mg	kg/h	2.22	0.97	1.24	retained
Na	**kg/h**	**1897.77**	**1546.37**	**351**	**retained**
SO_4Tot	**kg/h**	**3529.96**	**3196.19**	**334**	**retained**
Si	kg/h	21.22	16.02	5.21	retained
TDS	**kg/h**	**9846.37**	**7446.08**	**2400**	**retained**

The results from the mass balances for 1999 show an overall retention of Cl, Na, Ca, SO_4 and the TDS. Thus, all the major elements appear to be retained in the ash dams.

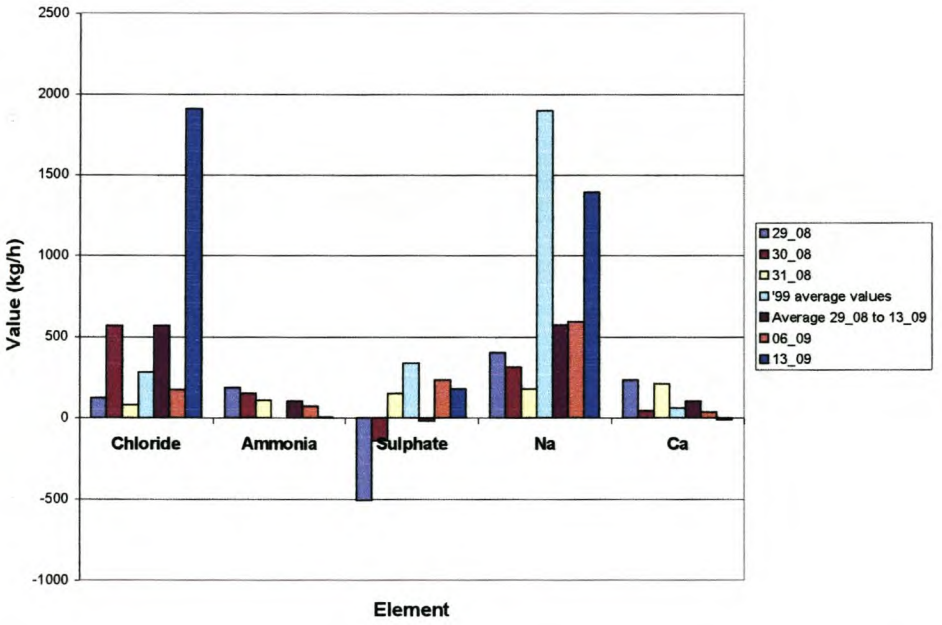

Figure 3.53: Comparison of mass balance results for phase 2 (positive ⇒ retention)

From figure 3.53 one can see that there is an overall retention of the main components (Ca, Na, Cl and SO_4), in the ash dams.

Assumptions

- No flow data was available for 1999; therefore for the purpose of determining the trends rather than exact quantitative mass balances results, the flow data from 2001 was used to perform the mass balances based on the chemical analyses from 1999.
- The concentrations of the various elements in the slurry stream were assumed to be an average of stream 7w and 9w, as explained in section 3.4.2.

3.9 Calcium Carbonate Chemistry

3.9.1 Langelier Saturation Index

If total alkalinity, pH, and calcium concentration of a water sample are measured, it is possible to calculate whether or not the water is saturated with respect to calcium carbonate – that is, whether or not the solubility product equation for $CaCO_3$ is satisfied. When the product of the active concentration of calcium and carbonate ions exceeds the solubility product constant, the water is over saturated with respect to $CaCO_3$, and the $CaCO_3$ will precipitate out. On the other hand, when the solubility product is not exceeded, the water is under saturated with respect to $CaCO_3$. From theoretical considerations, Langelier developed a 'saturation index', which, by its sign, establishes whether a particular water is over or under saturated with respect $CaCO_3$. The derivation of this 'saturation index' is explained in section 2.3.1.2. The pH_s values were calculated using equation (2-41) as well as the simplified equation (2-36), even though all the pH values for the water samples were not in the range 6.5 to 9.5 as required. These results are displayed in table 3.13, further details pertaining to these calculations can be found in Appendix B4. From these results it is evident that the simplified equation can be used for the calculation of pH_s, which is needed for the calculation of the Langelier Index (LI), since the difference in results from the two different equations is minimal.

Table 3.13: Comparison of the Calculated Saturation Indices

sample point	pH_s eq. (2-36)	pH_s eq. (2-41)	LI eq. (2-36)	LI eq. (2-41)	difference between 2 pH_s's		
					units	%	
average 1	5.9098	5.9099	6.32	6.32	5.33E-05	0.00090	ppt
average 2	6.0523	6.0524	6.16	6.16	8.72E-05	0.00144	ppt
average 5&6	7.0005	7.0015	3.20	3.20	9.77E-04	0.01395	ppt
average 7&9e	5.7164	5.7164	6.45	6.45	2.69E-05	0.00047	ppt
average 7&9w	5.7763	5.7763	6.60	6.60	4.06E-05	0.00070	ppt
average 1	6.0305	6.0306	6.20	6.20	7.69E-05	0.00127	ppt
average 2	6.1728	6.1729	6.04	6.04	1.16E-04	0.00188	ppt
average 5&6	7.1208	7.1220	3.08	3.08	1.18E-03	0.01664	ppt
average 7&9e	5.8380	5.8380	6.33	6.33	4.53E-05	0.00078	ppt
average 7&9w	5.8981	5.8981	6.48	6.48	5.97E-05	0.00101	ppt

The results shown in table 3.13 indicate that all the streams around phase 2 and phase 3 are over-saturated with respect to $CaCO_3$, thus suggesting the precipitation of $CaCO_3$ at each of these sample points. These saturation indices can also be calculated using computer programs designed to perform geochemical calculations. An example of such a program is PHREEQC-2, the use of which is discussed further in section 3.9.2.

3.9.2 The application of PHREEQC-2 to the ash water system

Speciation calculations were performed using PHRREQC-2 to calculate the distribution of the aqueous species at the various sample points. An input file was written for the following sample points:

- Sample point 1: Penstock overflow from Fine Ash dam 3 to evaporation dams
- Sample point 5: CAE supply to Sasol 2 (West) Factory
- Sample point 2: Pen-stock overflow from Fine Ash dam 4 to Emmet dam
- Sample point 6: CAE supply to Sasol 3 (East) Factory

The input files as well as an example of the output file (for sample point 1) can be found in Appendix B5. A comparison of the saturation indices obtained from PHREEQC-2 for the various mineral phases is displayed in table 3.14. Obviously a positive saturation index (SI) indicates that the water at that point is super-saturated with respect to that particular mineral, a negative SI indicates sub-saturation, and a SI of zero indicates that the mineral is in equilibrium.

Table 3.14: Saturation Indices Calculated Using PHREEQC-2

		SI at each sample point			
Phase	**Formula**	**1**	**5**	**2**	**6**
Anhydrite	$CaSO_4$	-0.37	-0.31	-0.32	-0.3
Aragonite	$CaCO_3$	2.78	2.05	2.72	1.82
Calcite	**$CaCO_3$**	**2.94**	**2.21**	**2.87**	**1.97**
Chalcedony	SiO_2	-1.9	-0.66	-2.14	-0.07
Chrysotile	$Mg_3Si_2O_5(OH)_4$	11.98	7.93	12.19	4.44
Dolomite	**$CaMg(CO_3)_2$**	**3.24**	**2.67**	**3.22**	**2.3**
$Fe(OH)_3(a)$	$Fe(OH)_3$	1.34	2.3	1.17	2.99
Fluorite	**CaF_2**	**1.85**	**1.51**	**1.91**	**1.52**
Goethite	FeOOH	7.23	8.19	7.06	8.88
Gypsum	**$CaSO_4$:$_2$H2O**	**-0.12**	**-0.06**	**-0.07**	**-0.05**
Hematite	Fe_2O_3	15.05	17.1	14.73	18.49
Jarosite-K	$KFe_3(SO_4)_2(OH)_6$	-16.9	-9.06	-17.58	-4.5
Melanterite	$FeSO_4$:$7H_2O$	-26.74	-22.5	-26.94	-20.14
Quartz	SiO_2	-1.42	-0.18	-1.66	0.4
Sepiolite	$Mg_2Si_3O_7.5OH$:$3H_2O$	5.29	4.6	5.03	3.26
Sepiolite(d)	$Mg_2Si_3O_7.5OH$:$3H_2O$	2.88	2.15	2.61	0.81
Siderite	$FeCO_3$	-19.15	-15.69	-19.47	-13.57
SiO2(a)	SiO_2	-2.81	-1.56	-3.04	-0.97
Talc	$Mg_3Si_4O_{10}(OH)_2$	11.62	10.08	11.36	7.78

These results confirm the precipitation of calcite (a positive SI at all points), and are clearly consistent with the LI calculations discussed in section 3.9.1. It is also evident that all the sample points are super-saturated with respect to dolomite and fluorite, suggesting the precipitation of these two mineral phases along with the precipitation of calcite. The CAE sample points, sample points 5 and 6, both appear to be in equilibrium

with respect to gypsum, not super-saturated as was anticipated as a possible explanation for the removal of SO_4 from the ash water.

3.9.3 Analysis of precipitate found in the dams

During a visit to the site, a precipitate was found in an empty CAE dam. This precipitate was consequently analysed using XRD (X-ray diffraction), with the result being that calcite was the dominant mineral present. This precipitate collected is shown in figures 3.54 and 3.55.

Figure 3.54: Top view of the precipitate

Figure 3.55: Front view of the precipitate

The diffractogram for this precipitate is given in figure 3.56. The red vertical lines show where peaks for calcite should be. It is evident that all the peaks shown on the diffractogram are accounted for by the presence of calcite in the precipitate. There may, however, be other minerals present but in much smaller quantities so that they do not feature as prominently on this diffractogram.

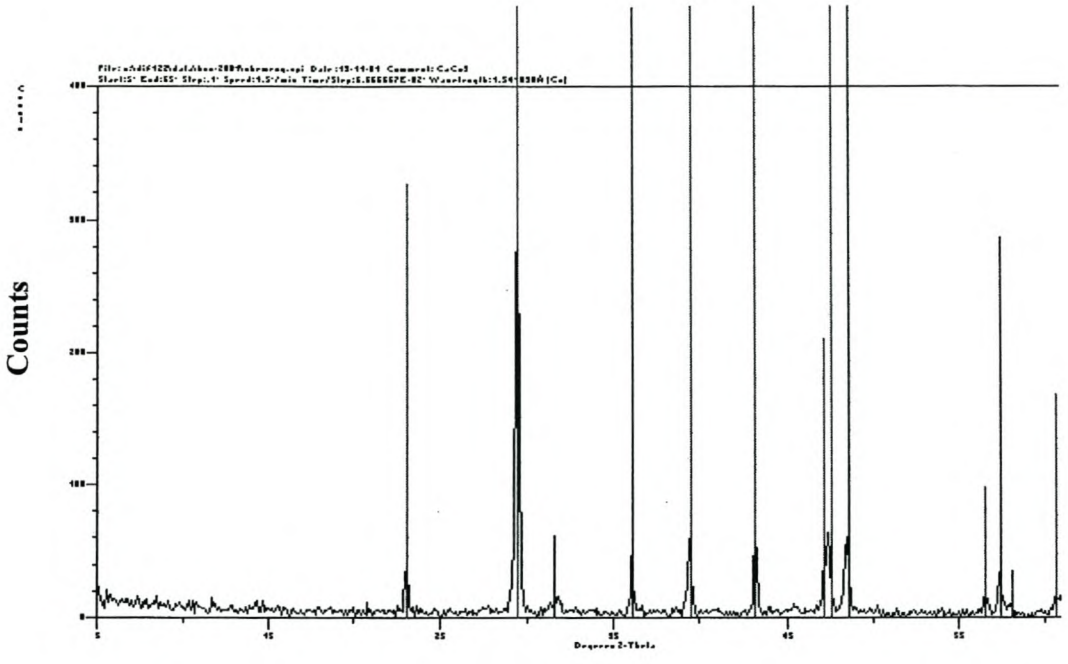

Figure 3.56: Diffractogram of precipitate from CAE dam 3

As part of the study undertaken by Ginster (1997), to assess the long-term changes in the quality of the ash water system at Secunda, sediment deposits from the bottom of selected ash water dams were sampled. These samples were analysed by means of XRD to identify the major mineral phases present. These results showed that the samples collected were mainly composed of calcite, calcium oxide and quartz. Lesser quantities of Fe and S were also identified in the samples analysed. In a study conducted by Pretorius (2001), the crystalline mineral phases present in a variety of precipitates were identified. The results, displayed in table 3.15, reveal that the main crystalline mineral phase present in all the precipitates was calcite.

Table 3.15: Crystalline Phases of Precipitates Found at Outside Ash

Sample	Mass % crystalline phase			
	Lime	Calcite	Mullite	Quartz
From surface of weathered fine ash dam	None	100%	None	None
Precipitate from pent-stock overflow canal	None	100%	None	None
Precipitate from evaporation dam	None	100%	None	None

3.10 Previous work performed on the Secunda ash water system

Billik and Mashike (1991), analysed the Secunda ash water system with the emphasis being on evaluating the performance of the system as both a salt sink and a fine ash disposal system combined. As far as the quality of the ash water is concerned, they found that there was an increase in the concentration of Cl, Na and SO_4 in the CAE from 1984 to 1991, as well as an increase in the conductivity of the water. They also found that there was no major change in the pH and COD of the CAE, and there was a decrease in the total alkalinity of the CAE from 1984 to 1991. They concluded that since start-up, the ash water quality had deteriorated; and that the 'foreign' streams entering the system contribute significantly to the decline in the quality of the ash water as well as to the positive water balance (as of 1991).

Ginster (1997), conducted a study to assess the long-term changes in the water quality of the Secunda ash water system. He found the ash water system was able to adequately buffer the effects of erratic high chemical loadings to the system. This was based on the monitoring of the 'inlet' and 'outlet' water streams to the ash system, phase 3, over a period of 15 months. The water leaving the system (CAE) for re-use in the factory, showed very little variation in composition compared to the 'inlet' water streams, i.e. the inlet streams to phase 3 (penstock over-flows). He also found an overall reduction in the alkalinity, electrical conductivity, pH, COD, Ca and F over phase 3; and an increase in

the SO_4 concentration between in 'inlet' and 'outlet' streams for both the east and the west side of phase 3 of the ash disposal system. He expresses concern regarding the increase in the F concentration of the CAE from 1987 to 1997, and suggests that the solubility controlling mechanism for F needs to be determined. As far as studies on the solid phases in the ash system are concerned, Ginster (1997) reports that XRD analyses of sediment deposits on the bottom of selected ash water dams show that calcite calcium oxide and quartz are the dominant mineral phase present.

Marais (2002) performed mass balances across different parts of the Inside Ash Handling Plant, as well as across Gasification, the Power Station and Outside Ash. The purpose of these mass balances was to determine whether a salt sink exists in the ash system and if it does, where is it most significant? The results of these mass balances showed the following:

- At the Power Station, Ca appears to be removed from the water as a result of the addition of the ash to the CAE.
- At Gasification, Ca and Cl appear to be removed from the water as a result of the addition of the ash to the CAE.
- Overall at Inside Ash, Ca and SO_4 are leached from the ash into the water, and the alkalinity of the water increases.
- Over Thickener C (handles slurry from the Power Station) at Inside Ash, the Ca, SO_4 and Cl appear to be leached from the ash into the water, and the total alkalinity of the water increases. Sodium on the other hand appears to be removed from the water and retained in the ash.
- Over Thickener A/B (handle slurry from gasification) at Inside Ash, the Ca, SO_4, Cl and F appear to be leached from the ash and once again the alkalinity of the water increases. As was the case with Thickener C, the Na appears to be removed from the water phase.
- Over FAD3, it seems as if there is an overall retention of the Na and Ca in the ash dam.

Important data gained from this investigation was the flow rates at various points in the ash water system, which were previously non-existent.

3.11 Correlation between the past and the present

3.11.1 Ash water quality

Billik and Mashike (1991) report an increase in the Cl, Na and SO_4 concentrations of the CAE, as well as an increase in the conductivity for the period 1984 to 1991. As of 2000, there still appears to be an overall increase in the Na and SO_4 concentration, and conductivity of the CAE, however, from 1991 to 2000 it appears as if the overall Cl concentration has decreased. In the time period from 1991 to 2000 there is an overall decrease in the COD, pH, total alkalinity, and Ca concentration of the CAE. Billik and Mashike also report a decrease in the alkalinity for the period 1984 to 1991, as well as no change in the COD and pH of the CAE. The F concentration, which increases in the CAE from 1984 to 1991, has decreased again from 1991 to 2000 and is currently at the same level it was at in 1984. Therefore, concerns expressed in the report by Ginster (1997) regarding the increase of the F concentration of the CAE, can be dismissed on the grounds that there doesn't appear to be an accumulation of F in the CAE.

3.11.2 Phase 1

Mass balance results performed in this study of the ash system; show an overall retention of Ca and SO_4 over phase 1, and a leaching of the TDS, Na and Cl into the water phase from the ash. Marais (2002) also reports that there is a retention of the Ca at the Power Station, where the fine ash is mixed with the CAE. It is also reported by Marais (2002) that there is a retention of Ca at Gasification where the CAE is mixed with the fine ash produced there. One would expect the trends to be similar for both the Power Station and Gasification mass balances, since at both these stages, ash is mixed with the CAE.

3.11.3 Phase 2

Mass balance results performed in this study of the ash system; show an overall retention of Ca, Na, Cl and SO_4, as well as the fact that TDS are retained in the ash dams. The fact that the TDS are retained in the ash dams is reinforced by the trends seen in terms of

concentration variations rather than actual mass balances. These results show a decrease in the concentration of TDS from the time the slurry streams leave Inside Ash to the time the water leaves the ash dam via the penstock over-flow. Also on a concentration basis, the total alkalinity is shown to decrease over phase 2. Marais (2002) also reports a retention of Na and Cl in the ash dams.

3.11.4 Phase 3

According to the work done by Ginster (1997), there is an overall decrease in the Ca and F concentrations, as well as a decrease in the total alkalinity, conductivity, pH and COD, over phase 3. He also reports an increase in the SO_4 concentration for both the east and the west side over phase 3. From the results of this study, it was deduced that there was also an overall reduction in the Ca and F concentrations, as well as a reduction in total alkalinity, conductivity, pH and COD, over phase 3. As far as the change in SO_4 concentration is concerned, this investigation (2000-2001) showed that there was an increase in the SO_4 concentration over phase 3, but only for the east side; for the west side there was a decrease in concentration.

3.12 Summary

The actual ash water disposal system used by Sasol 2 and 3 in Secunda, South Africa, is a complex process involving many different variables. It is a closed system, implying that no water from the system is directly disposed of to a receiving water source. Instead the ash water (CAE) is recycled back to Sasol 2 and 3 for re-use in the transportation of the fine ash.

Very little flow data was available for the various streams involved in the ash water system, thus the most comprehensive results are based on variations in concentration of the different constituents of the ash water.

A lot of data, in the form of chemical analyses of the ash water streams, was available for phase 3; less data was available for phase 2; and very little data was exists for phase 1. With all the currently available data, the following conclusions can be drawn:

3.12.1 Ash water quality

The quality of the ash water has varied over the last 15 years; however, these variations are not drastic compared to the variations in composition and quantity of the 'foreign' streams entering the system.

- There is a gradual increase in the Na and SO_4 concentrations, as well as an increase in the conductivity of the CAE.
- A gradual decrease in the total alkalinity of the CAE has been observed over the past 15 years (1984 to 2000).
- For the time period 1991 to 2000, there appears to be a reduction in the Ca and Cl concentrations in the CAE, as well as a decrease in COD and pH.
- The initial increase in the F concentration that was observed during the time period 1984 to 1991 appears to have reversed from 1991 to 2000, where a decrease in the F concentration of the CAE can be seen. The concentration of the F in the CAE is currently at the same level it was at in 1984.

3.12.2 Phase 1

From the moderate plant data available for phase 1, one can conclude that there is an overall leaching of salts from the ash into the ash water, since there is an increase in the TDS over this phase. Specifically there appears to be a leaching of Na and Cl from the ash into the water, and a reduction in the Ca and SO_4 ions in solution. Further data should be obtained in order to confirm these findings.

3.12.3 Phase 2

Mass balance results over phase 2 reveal that there is an overall retention of salts (TDS) in the ash dams. Specifically, a retention of Ca, Na, Cl and SO_4 is observed. There is also a decrease in the total alkalinity of the ash water over phase 2.

As far as trends based on variations in concentrations are concerned, one can conclude that:

- For Ca, Cl, Na, SO_4, and F there was no correlation between the trends seen for the east and the west side of the ash disposal system. This finding reinforces the fact that the two sides to the disposal system, for phase 2 of the disposal process, possibly need to be considered separately.
- An increase in the K and Si concentrations is seen for the east and the west side, as well as an increase in the COD.
- There is an overall decrease in the TDS, SS, and Fe concentrations for the east and the west side, as well as a decrease in the conductivity.
- No conclusions could be made regarding the change in Mg concentration.

3.12.4 Phase 3

All the findings for phase 3 are based on variations in concentration, since no flow rates could be measured over this extremely complex phase. A lot of data was, however, available (samples taken on a regular basis around this phase) in the form of chemical analyses of the ash water. The trends seen for this phase are:

- An overall decrease in the Ca and F concentrations, as well as a reduction in the total alkalinity, conductivity, pH and COD of the water. These findings are confirmed by the work done by Ginster (1997).
- A decrease in concentration is also observed for Fe and the suspended solids on both the east and west side.
- There is an increase in the K, Na and Mg concentrations for both the east and the west side.

- For Cl, SO_4, and Si there was no correlation between in trends seen for the east and the west side of the ash disposal system.
- The results from the analysis of the TDS show a slight decrease in the TDS (on a concentration basis) for the east side, and practically no change for the west side.

One should bear in mind that once the ash water passes from the penstock over-flows into the respective dams for the east and the west side, there is a lot of mixing of the water from the two disposal systems in the evaporation and CAE dams. Thus, it is very hard to actually consider the east and west side as separate systems during phase 3. This inter-flow of the various dams, as well as all the side streams entering the system at phase 3 (e.g. mine water, water from black products area, flow from the toe drains of the ash dams), also make it impossible to perform a mass balance over phase 3.

3.13 Recommendations

From the results obtained pertaining to the actual plant data for the ash disposal system, the following recommendations can be made:

- More flow data is required, especially around phase 3 (the evaporation and CAE dams), in order to perform mass balances to ascertain exactly what is happening in this phase.
- More samples need to be taken for phase 1 and 2. There is currently insufficient data available to be able to draw any firm conclusions as to what is happening in these two phases.
- Since the ash water disposal system is constantly changing, due to variations in the 'foreign' inlet streams to the system, it is imperative that the entire system is monitored on a regular basis in order to understand the influence of various parameters.
- Due to the complexity and scale of the actual ash disposal system it will be necessary to design a pilot scale set-up of the system in order to fully understand the working of the system under field conditions.

In order to further investigate the chemistry, which occurs when an effluent is mixed with the fine ash, laboratory scale column experiments were performed. These allowed one to investigate the chemistry of certain components in more detail, as it was evident throughout this chapter that in the actual disposal system there are a lot of different factors which influence the working of the system. The complexity of the actual disposal system restricts one from fully understanding the changes that occur, since not even simple mass balances can be performed due to the lack of flow-rate data. The column experiments simulated the actual disposal system in terms of the three phases identified (section 3.4.1), and served to provide one with more insight into the chemical reactions that occur during the different phases. These column experiments are discussed in detail in chapter 4.

Chapter 4

Laboratory Column Experiments

The operation of the ash disposal system, under field conditions, has already been discussed in chapter 3. The results of this investigation divulged the necessity to explore the working of a wet ash disposal on a simpler and smaller scale. Therefore laboratory scale column experiments were performed, with the purpose being to simulate the actual ash disposal system in order to quantify the chemical changes that occur in terms of mass balances.

Each column experiments consisted of three phases, designed to simulate the three phases identified in the actual disposal system (section 3.4.1). In total, seventeen column experiments were performed, and the factors that were changed were: the ash/water mixing time, the liquid to solid ratio, the composition of the liquid phase, and the retention time of phase 3. The changes in the liquid phase as well as the solid phase were considered, which included liquid and solid phase mass balances for the pertinent elements.

Precaution should be taken when attempting to use the results obtained from laboratory scale batch experiments in the actual ash disposal system. These laboratory tests, in isolation, do not provide sufficient information regarding thermodynamic and kinetic properties of the primary geochemical processes occurring in the actual ash disposal system. They do, however, provide one with means of investigating the ash water chemistry on a manageable scale. The complexity of the actual ash disposal system restricts one from obtaining a thorough understanding of the working of the system – due to the difficulty of flow rate measurements, especially around Outside Ash, not even simple mass balances could be performed.

4.1 Materials and methods

4.1.1 Experimental procedure

The general experimental procedure for the column experiments is as follows, and was designed to simulate the actual ash disposal system:

The fresh fine ash was heated in a furnace to a temperature of ± 260°C (which is the temperature at which the fly-ash leaves the precipitators at the power station). It was then mixed with the liquid phase in a stainless steel tank by means of an electric stirrer (PHASE 1). This mixing was varied in some of the experiments, but the general time for the mixing was two and a half hours. Once the slurry had been mixed for the appropriate time, a sample of the slurry stream was collected, and the remaining slurry mixture was allowed to pass into the column. A small quantity of the slurry stream initially passed out of the bottom of the column, however, the ash settled very quickly, and combined with the glass wool, prevented any further ash from passing out the valve at the bottom of the column. Once the leachate leaving the column was free of ash, a sample was collected. The following day once the majority of the effluent had passed through the column, another sample was collected from the collecting dish (PHASE 2). The last sample was taken after a week, i.e. the leachate was allowed to stand exposed to the atmosphere for a week (PHASE 3). This method was used for experiments Trial 1, Exp 1 to 7 and Exp 9.

Variations to the above-mentioned method were used in experiments Exp 11, and Exp 13 to 17. In these experiments the exception to the described method was that a sample of the slurry mixture was taken from the stainless steel tank after 5 minutes of mixing time as well as after two and a half hours. The purpose of this was to determine the initial contact of the ash with the water.

Experiments 15, 16, and 17 were furthered varied in that instead of only leaving the leachate in the collecting dish for one week, it was left for five weeks and sampled on a weekly basis. The motivation for doing this was to simulate to actual retention time of the ash water in the Evaporation and CAE dams.

The experimental procedure used for experiments 4, 8, 10 and 12 was completely different than that procedure used for the other experiments. For these experiments the ash, used in the previous experiment, was merely flushed using distilled water. For example, Exp 4 involved the flushing of the ash (with distilled water) left in the column after Exp 3. The leachate was collected as it left the column in separate samples bottles based on time. The total amount of water that passed through the ash in each experiment was about five litres.

4.1.2 Experimental Set-up

The laboratory-scale column experimental set-up is shown schematically in figure 4.1.

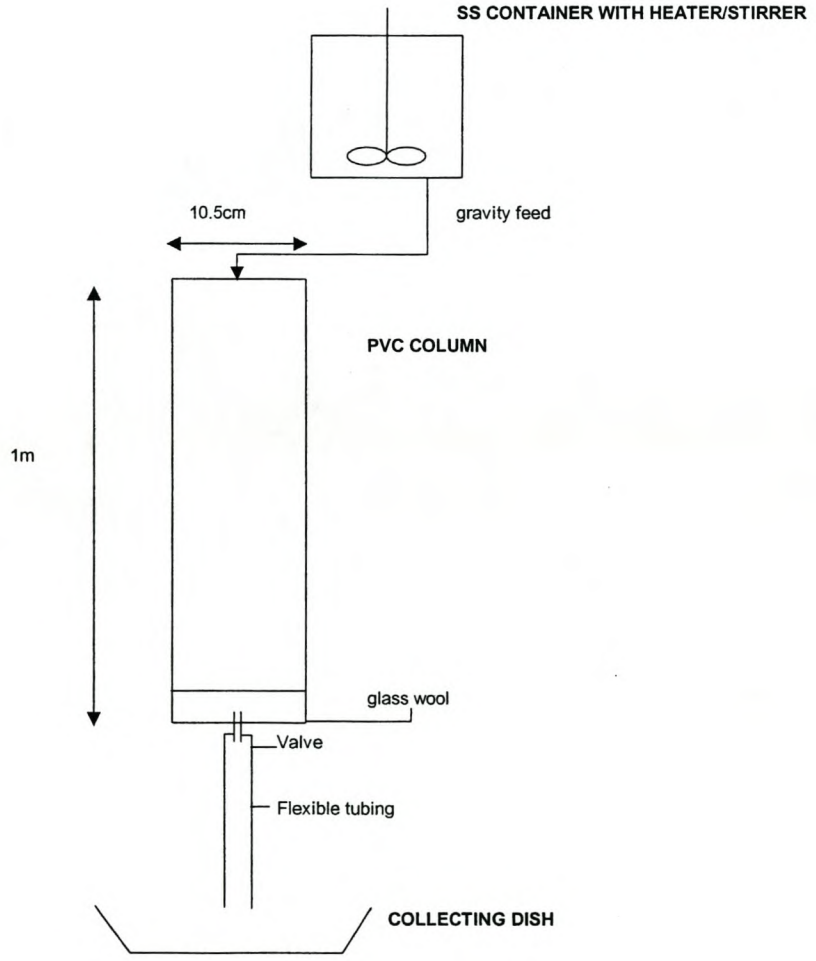

Figure 4.1: Basic laboratory column experimental set-up

4.1.3 Experiments Conducted

Table 4.1 displays the various laboratory column experiments performed in this investigation, as well as the specific conditions and factors used for each experiment.

Table 4.1: Laboratory scale column experiments conducted

Name	With	Mixing time	Start date	End date	L:S	Other
Trial 1	Distilled water	half hour	11-Feb	18-Feb	5:1	
Exp 1	CAE	half hour	04-Mar	11-Mar	5:1	
Exp 2	CAE	One and half hours	11-Mar	18-Mar	5:1	
Exp 3	CAE	Two and half hours	18-Mar	25-Mar	5:1	
Exp 4	Distilled water	flush Exp 3 ash	25-Mar	01-Apr		
Exp 5	FAM	Two and half hours	02-Apr	09-Apr	5:1	
Exp 6	FAM	Two and half hours	09-Apr	15-Apr	10:1	
Exp 7	FAM	Two and half hours	16-Apr	23-Apr	5:1	add salty stream to FAM slurry
Exp 8	Distilled water	flush Exp 7 ash	23-Apr	29-Apr		
Exp 9	new FAM	Two and half hours	30-Apr	07-May	5:1	
Exp 10	Distilled water	Flush Exp 9 ash	07-May	08-May		
Exp 11	new FAM	Two and half hours	08-May	15-May	5:1	add salty stream to new FAM
Exp 12	Distilled water	Flush Exp 11 ash	15-May	16-May		
Exp 13	Distilled water	Two and half hours	20-May	27-May	5:1	
Exp 14	Distilled water	Two and half hours	27-May	03-Jun	5:1	
Exp 15	new FAM	Two and half hours	03-Jun	08-Jul	5:1	left in collecting dish for 5 weeks
Exp 16	new FAM	Two and half hours	04-Jun	09-Jul	5:1	left in collecting dish for 5 weeks
Exp 17	new FAM	Two and half hours	05-Jun	10-Jul	5:1	left in collecting dish for 5 weeks

4.1.4 Methods of analysis

4.1.4.1 Calcium

Calcium was analysed for by means of Atomic Absorption Spectroscopy. Standards were prepared using a 10% nitric acid solution to preserve the standards. The standards used were 250ppm, 500ppm, 750ppm and 1000ppm. If the Ca concentration of the sample being tested was not in this range, the sample was diluted. A Varian 250 plus

Atomic Absorption Spectrophotometer as used to analyses the samples. A lamp with a current of 10mA, as well as a wavelength of 239.9nm and a spectral band pass of 0.2nm was used in conjunction with the specific standards mentioned, for all the samples. The fuel used was acetylene, with the support being nitrous oxide. Due to the precipitation of calcite when the samples were contacted with air, care was taken to keep a lid on all samples at all times, except when the actual analysis was being performed.

4.1.4.2 Sodium

Sodium was analysed for by means of Atomic Absorption Spectroscopy. Standards were prepared using a 10% nitric acid solution to preserve the standards. The standards used were 100ppm, 200ppm, 500ppm and 1000ppm. If the Na concentration of the sample being tested was not in this range, the sample was diluted. A Varian 250 plus Atomic Absorption Spectrophotometer as used to analyses the samples. A lamp current of 5mA, a wavelength of 330.3nm, and a spectral band pass of 0.5nm was used, in conjunction with the specific standards mentioned, for all the samples. The fuel used was acetylene, with the support being air.

4.1.4.3 Potassium

Potassium was analysed for by means of Atomic Absorption Spectroscopy. Standards were prepared using a 10% nitric acid solution to preserve the standards. The standards used were 50ppm, 100ppm, 200ppm and 500ppm. A Varian 250 plus Atomic Absorption Spectrophotometer as used to analyses the samples. A lamp current of 5mA, a wavelength of 404.4nm, and a spectral band pass of 0.5nm was used, in conjunction with the specific standards mentioned, for all the samples. The fuel used was acetylene, with the support being air.

4.1.4.4 Sulphate

The sulphate ions were analysed for using a Dionex Al450 Ion Chromatograph. . Due to the high concentrations of SO_4 present in the ash water, all the samples were diluted using distilled water (20 times dilution) before being analysed. Before the samples were injected into the Dionex apparatus they were filtered through a 0.45μm nylon Millipore

filter. The operating conditions pertaining to the Dionex Al450 Ion Chromatograph are given in table 4.2.

Table 4.2: Operating conditions for the Dionex Al450 Ion Chromatograph

Sample Loop Volume	Approx. 20µl
Guard Column	IonPac AG4A-SC 4mm
Separator Column	IonPac AG4A-SC 4mm
Eluant	1.80 mM Na_2CO_3, 1.70 mM $NaHCO_3$
Eluant flow rate	2.0ml/min
Suppressor	Anion Micro Membrane
Regenerant	25 mM H_2SO_4
Regenerant flow rate	3 ml/min
Expected background conductivity	14 to 18 µS

4.1.4.5 Chloride

The chloride ions were also analysed for using a Dionex Al450 Ion Chromatograph. The operating conditions are the same as those for the SO_4 analysis and are shown in table 4.2. Due to the high concentrations of Cl present in the ash water, all the samples were diluted using distilled water (20 times dilution) before being analysed. Before the samples were injected into the DIONEX apparatus they were filtered through a 0.45µm nylon Millipore filter.

4.1.4.6 Aluminium, Strontium, Chromium, Magnesium, Iron and Silicon

All measurements for Al, Sr, Cr, Mg, Fe and Si were performed on a Varian Liberty II Series Radial Air Path Inductively Coupled Plasma Atomic Emission Spectrometer (ICP-AES), with 1.8 kW RF power at a frequency of 40 MHz. It uses a 750mm focal length Czerny-Turner monochromator with 1800 lines per mm holographic diffraction grating.
The operating parameters were as follows:
Power: 1.1 kW
Plasma gas flow: 15 L/min
Aux. gas flow: 1.5 L/min
Sample aspiration: 1 ml/min
Nebulizer: V-groove
Integration time: 3 s

No additional sample treatment was performed, and the standards were prepared and diluted from high purity 1000ppm standards. The relative standard deviations between replicate readings per element varied between 0.1 and 2%.

4.1.4.7 Total Dissolved Solids

The TDS were analysed by calculating the mass of dissolved solids per 100ml of effluent. 100ml of each sample was measured and filtered using a vacuum filter. The filtrate was placed on a hot plate in a porcelain dish where the majority of the water was evaporated from the samples. The dishes were then placed in an oven at 180°C for an hour, after which they were dried over silica gel and then weighed.

4.1.4.8 Conductivity and pH

The conductivity of the samples was measured using an EC 215 conductivity meter. The probe was made of glass with four corrosion resistant platinum rings and had a built-in temperature sensor that automatically compensated for temperature changes. The pH was measured using a Beckman Φ360 pH meter with automatic temperature compensation (ATC). Each time the pH meter was used it was calibrated using a two-point calibration at pH 4 and pH 7.

4.1.4.9 Comparison between analysis techniques

Table 4.3 shows a comparison between the methods used to analyse the various constituents of the laboratory column experiments performed in this study; and the techniques employed by the labs at Sasol to analyse the water samples from the ash disposal system.

Table 4.3: Comparison between University and Sasol analysis techniques

Component	University of Stellenbosch Method	Sasol Method
Ca	AA	ICP
Fe	AA	ICP
Mg	AA	ICP
Na	AA	ICP
K	AA	ICP
Cl	Dionex	TITRINO
F	Dionex/electrode	Fluoride Meter
SO_4Tot	Dionex	AUTO ANALYSER
pH	pH meter	pH meter
Conductivity (uS/cm)	Cond meter	Cond meter
Malk (mg/l as $CaCO_3$)		Titration
Palk (mg/l as $CaCO_3$)		Titration
COD		AUTO ANALYSER
SS		oven
TDS	hotplate/oven	hotplate/oven
Si		ICP
NH3		AUTO ANALYSER
Nitrate		AUTO ANALYSER
Cr	AA/ICP	ICP
Zr	ICP	ICP
Sr	ICP	ICP

4.2 Results and discussion: the liquid phase

Mass balances were performed on the liquid phase for the components displayed in figure 4.2. It is evident that the main elements to consider when looking at the change in composition of the effluent are: Ca, Na, Cl, and SO_4Tot. This finding is reinforced by the work done by Villaume et al. (1987), who found that the pore water and the leachate chemistry were clearly dominated by the strong base cations: Ca, Na, K, and Mg and the strong acid anion SO_4. Lee (1997) also found that the fly ash leachate they worked with (collected from the fly ash disposal mound in one of the major UK coal-fired power stations) contained high concentrations of Ca, Na, and SO_4. Results from the actual plant data also reveal that Ca, Na, Cl and SO_4 are the main salts to consider when dealing with the ash water system used by Sasol, Secunda. The results in figure 4.2 reveal an overall leaching of the Ca into the liquid phase, and an overall retention of the Na, Cl, and SO_4 in

the ash. **Throughout chapter 4, a positive value indicates an increase of a specific component in the liquid phase (leaching from the ash), and a negative value represents a removal of that component from the liquid phase.**

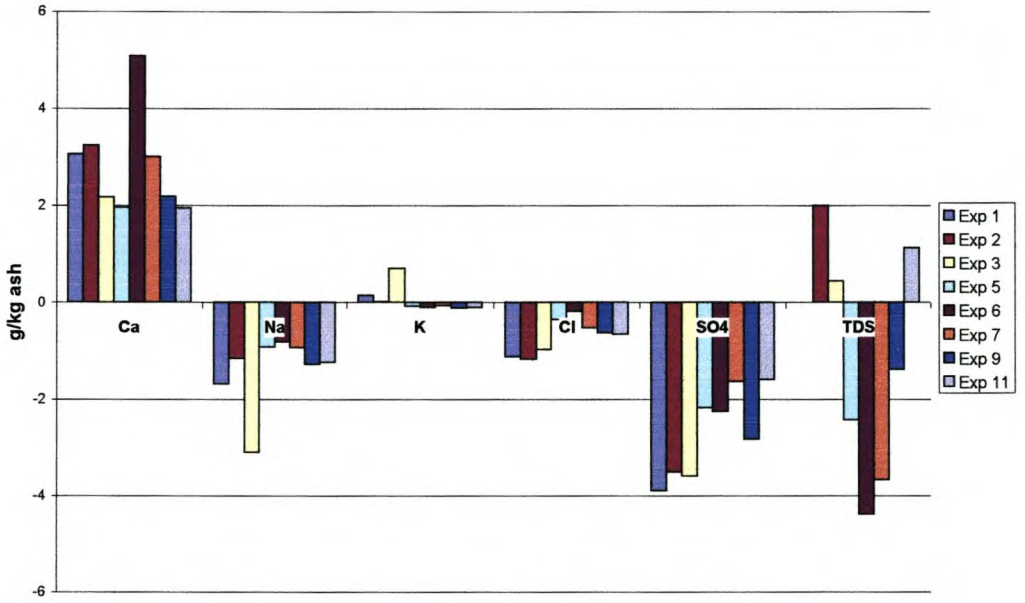

Figure 4.2: Comparison of Liquid Phase Mass Balance Results

Table 4.4: Average Values for Mass Balance Results

Average Values		
Element	**g/kg ash**	
Ca	2.8	leached
Na	-1.4	retained
Cl	-0.7	retained
SO_4	-2.7	retained

The overall leaching of the Ca from the ash into the water is based on the experiments where the collecting dish was only left to stand for one week. It was felt that this was not enough time to allow for the calcium carbonate chemistry to influence the overall

concentration of Ca in the system. The estimated retention time of the water in the evaporation and CAE, (in the actual ash disposal system), is estimated to be about five to six weeks. Further experiments were therefore conducted to attempt to simulate to actual situation more closely. Three identical experiments were performed, using the same sample of FAM, the same mixing time, and the same L:S ratio. Instead of leaving the collecting dish for on a week, all three were left for a period of five weeks. These experiments, and the results thereof, are discussed further in section 4.2.2.

The retention of Na, Cl, and SO_4, as evident in figure 4.2 and table 4.4, was explored further by means of 'flushing' experiments. The purpose of these experiments was to determine if the salts, which are retained in the ash, are merely retained due to hydraulic retention, or if they are in some way (precipitation, ion exchange, etc.) bound in the ash. Distilled water was used to flush the ash in the column that had been used in a previous experiment. The leachate was collected and the total amount of each of the salts, mentioned above, flushed out of the ash, was determined. These experiments and results are discussed further in section 4.2.4.

4.2.1 General column experiments

The overall experimental results have already been discussed, however, more details pertaining to the general column experiments performed, are discussed in this section. Table 4.5 and figure 4.3 display the mass balance results for the complete experiment, i.e. after the collecting dish was left exposed to the atmosphere for one week. Table 4.6 and figure 4.4 represent the mass balance results after the leachate had only been in the collecting dish, exposed to the atmosphere, for 24 hours (i.e. on day two of the experiment).

Table 4.5: Overall Mass Balance Results

	Exp 1	Exp 2	Exp 3	Exp 5	Exp 6	Exp 7	Exp 9	Exp 11	Average	Units
Ca	3.06	3.24	2.17	1.97	5.08	3.01	2.19	1.95	**2.83**	g/kg ash
Na	-1.684	-1.152	-3.106	-0.916	-0.817	-0.929	-1.272	-1.236	**-1.39**	g/kg ash
K	0.156	0.0235	0.71	-0.0711	-0.104	-0.0605	-0.119	-0.103	**0.054**	g/kg ash
Cl	-1.124	-1.173	-0.972	-0.346	-0.177	-0.526	-0.634	-0.654	**-0.70**	g/kg ash
SO4	-3.889	-3.515	-3.598	-2.179	-2.252	-1.627	-2.827	-1.594	**-2.69**	g/kg ash
TDS	-	2.012	0.446	-2.432	-4.382	-3.6740	-1.379	1.130	**-1.18**	g/kg ash

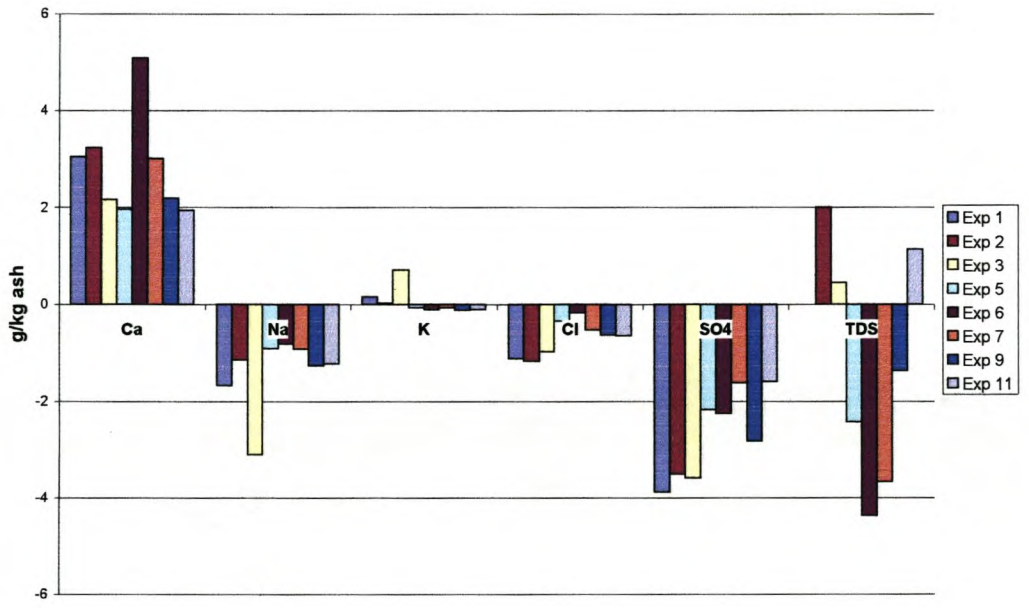

Figure 4.3: Overall mass balance results

Table 4.6: Mass Balance Results after 24 hours

	Exp 1	Exp 2	Exp 3	Exp 6	Exp 7	Exp 9	Exp 11	Average	Units
Ca	3.43	3.96	4.43	6.21	2.99	3.65	4.39	**4.15**	g/kg ash
Na	-4.93	-1.13	-0.443	-0.757	-1.387	-1.498	-1.682	**-1.69**	g/kg ash
K	-0.0888	0.158	0.711	-0.0875	-0.119	-0.117	-0.940	**-0.069**	g/kg ash
Cl	-0.962	-1.132	-0.942	-0.127	-0.877	-0.681	-0.521	**-0.75**	g/kg ash
SO4	-3.375	-3.188	-3.088	-1.446	-2.033	-2.243	-1.395	**-2.40**	g/kg ash
TDS	-	2.92	3.427	-2.53	-4.3060	0.538	2.127	**0.36**	g/kg ash

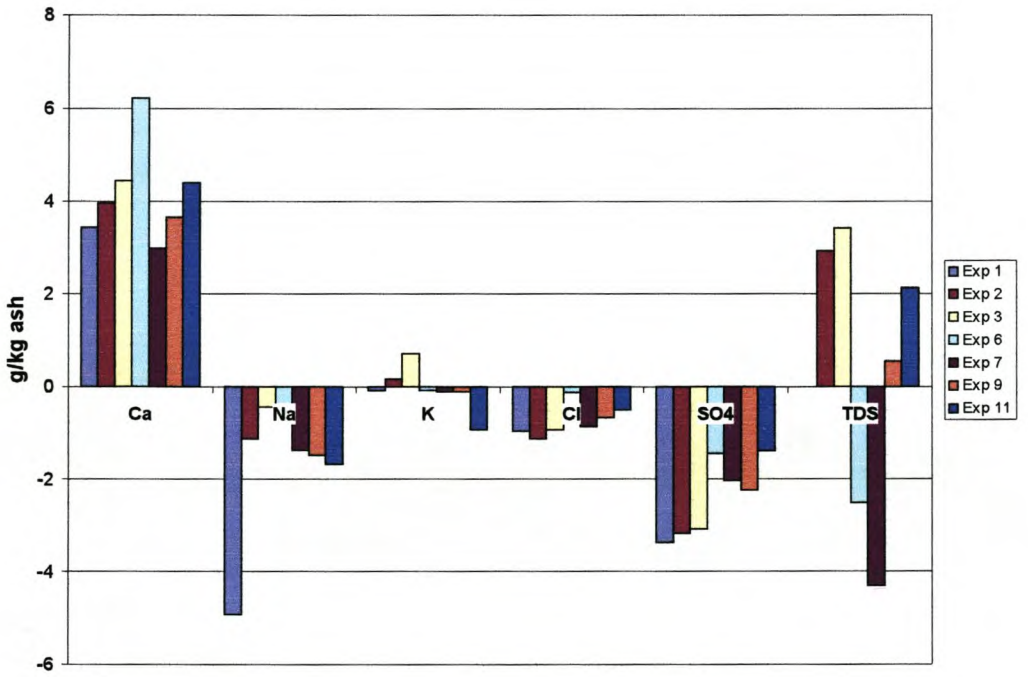

Figure 4.4: Mass balances results after 24 hours

Table 4.7 displays the comparison between the average values for the mass balance results after 24 hours and after one week.

Table 4.7: Comparison of Mass Balance Results after 24 hours and after 1 week

	After 24 hours	One week	Units
Ca	4.15	2.83	g/kg ash
Na	-1.69	-1.39	g/kg ash
K	-0.069	0.054	g/kg ash
Cl	-0.75	-0.70	g/kg ash
SO_4	-2.40	-2.69	g/kg ash
TDS	0.36	-1.18	g/kg ash

It is evident from these results that some of the Ca initially leached from the ash into the water, is removed when the leachate is left in the collecting dish for a week. This finding is discussed further in section 4.2.2.2. There is also a slight increase in the amount of SO_4 removed from the leachate that it is left in the collecting dish during this first week. The TDS, which are initially leached from the ash into the water, are further removed from the water phase during the week the leachate is left exposed to the atmosphere. This is probably largely due to the removal of Ca from the leachate in the form of calcite precipitation. Section 4.2.2.2 explores these results in more detail.

4.2.1.1 Variation in pH

Figure 4.5 displays the variation in pH for all the column experiments conducted. The most consistent results are for Exp 15, Exp 16 and Exp 17, since these three experiments were identical in terms of FAM composition, mixing time, and L:S ratio. For the majority of the experiments, figure 4.5 shows that there is an initial increase in the pH during the mixing stage; then a fairly constant pH for the time the water spends percolating through the ash column and for the first 24 hours that the leachate spends in the collecting dish; and finally after a week there is a reduction in the pH of the leachate. As discussed in section 4.2.2.7, for experiments 15, 16 and 17, this change in the pH of the leachate is a gradual decrease for four weeks, and during the 5^{th} week there is a drastic reduction in the pH. For all the other experiments, there is no consistency in the change in pH during the time (one week) the leachate spends in the collecting dish. A decrease in pH is seen for Exp 1, Exp 5 and Exp 11, whereas Exp 2, Exp 3, Exp 6, Exp 7 and Exp 9 all show an overall increase in pH of the leachate during the first week spent in the collecting dish. It is expected that if the leachate of all the experiments were allowed

to stand for five weeks, then overall the change in the pH would have been the same. The reason for this being that the chemistry, which occurs during phase 3, takes a lot longer than one week to reach equilibrium.

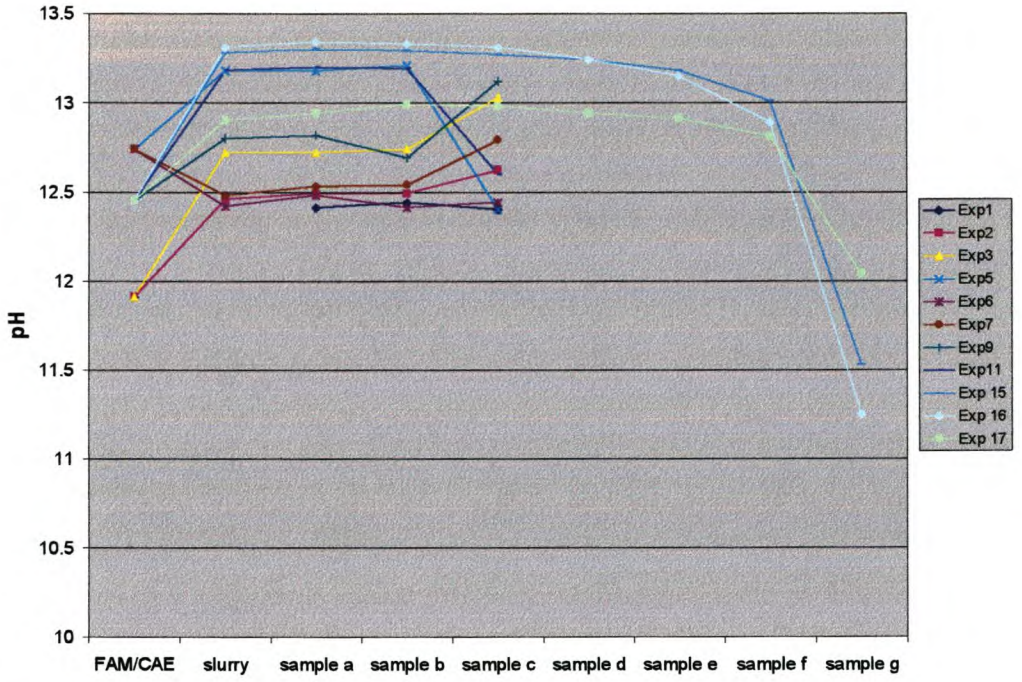

Figure 4.5: Variation in pH for all experiments

4.2.1.2 Variation in Conductivity

Examining figure 4.6 once again highlights the necessity to allow a longer retention time for phase 3 of the ash disposal process in the column experiments. It is clearly evident that it is only after a week of the leachate being left exposed to the atmosphere that any major chemical reactions occur, which in turn affects the composition of the leachate. During the mixing stage, a definite increase in the conductivity is seen for all the experiments. This is expected due to the leaching of certain elements from the ash into the water phase.

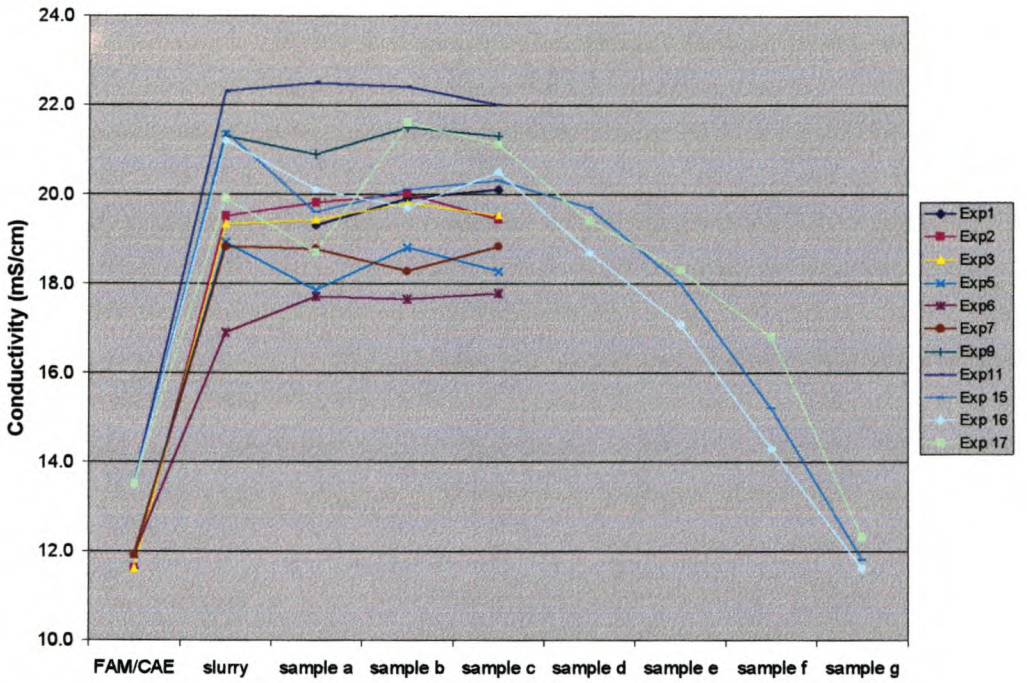

Figure 4.6: Variation in conductivity for all experiments

4.2.1.3 Changes in experimental factors

Mixing time

The mixing time of the ash and the water was initially varied (Exp 1, Exp 2 and Exp 3). However, since it was suspected, and later proved, that the majority of the changes that occur during the mixing stage occur during the initial contact of the ash with the water, this mixing time was kept constant for the rest of the experiments (at the estimated ash/water contact time of the actual ash disposal system – 2½ hours).

Liquid:Solid ratio

The actual L:S ratio utilised in the ash disposal system is 5:1. This ratio was changed to 10:1 for Exp 6. The motivation behind this was from the work done by Hassett et al. (1985). They found that L:S ratios are important in determining the elements extracted, and in controlling the pH. According to their results, it appears that the lower the L:S

ratio, the higher the pH of the resulting leachate. The reason why only one experiments was conducted with a variation in the L:S ratio was because it was found that at this higher L:S ratio, a lot of the ash passed out the bottom of the column before the combined effect of the glass wool and the fast settling ash could prevent the flow of the slurry straight out of the column. It was also reasoned that there were more important factors to investigate, and since the current ash disposal system has slurry lines designed to handle a slurry with a SG of about 1.3, the L:S ratio used in the actual set-up would not be easy to change.

Experiments with an added 'salty stream'

It was evident from the first column experiments conducted, that Na and Cl were removed from the effluent. The process waste stream, entering the ash system, from the salty water pits at Unit 44 (Demineralisation Plant) has a high Na and Cl content. It was therefore decided that an investigation should be conducted to determine the effect of higher Na and Cl concentrations in the effluent on the working of the ash column as a sink for these salts. The Na and Cl concentrations in this stream are shown in table 4.8.

Table 4.8: Na and Cl concentrations in salty stream from U44

Date Sampled	Cl (mg/l)	Na (mg/l)
29th Aug 2001	16 478	5 300
30th Aug 2001	231	666
31st Aug 2001	7 189	6 005
6th Sept 2001	879	2 660
AVERAGE	**6 194**	**3 658**

The ratio of the flow rate of this stream compared to the FAM used to transport the ash is approximately 1:12 (U44:FAM = 135:1650ton/h). Therefore, the liquid phase used for these experiments consisted of 4615m*l* FAM and 385m*l* NaCl mixture (3.581g NaCl in 385m*l* distilled water; Na = 3657mg/l, Cl = 5644mg/l). Two experiments, Exp 7 and Exp 11, were conducted with this added 'salty stream'. Figure 4.7 shows the overall Na and Cl retention (removal from the effluent) for these two experiments compared to the Na and Cl retention for the other column experiments. The results for Exp 7 should actually

only be compared to those for Exp 5, and Exp 11 compared to Exp 9 (experimental conditions identical in terms of FAM used, mixing time and L:S ratio). If one compares the experiments on this basis, it is evident that there is not much difference between the overall results for the removal of Na and Cl from the effluent if a concentrated Na and Cl stream is added to the ash water slurry. More experiments need to be conducted in order to confirm these preliminary results.

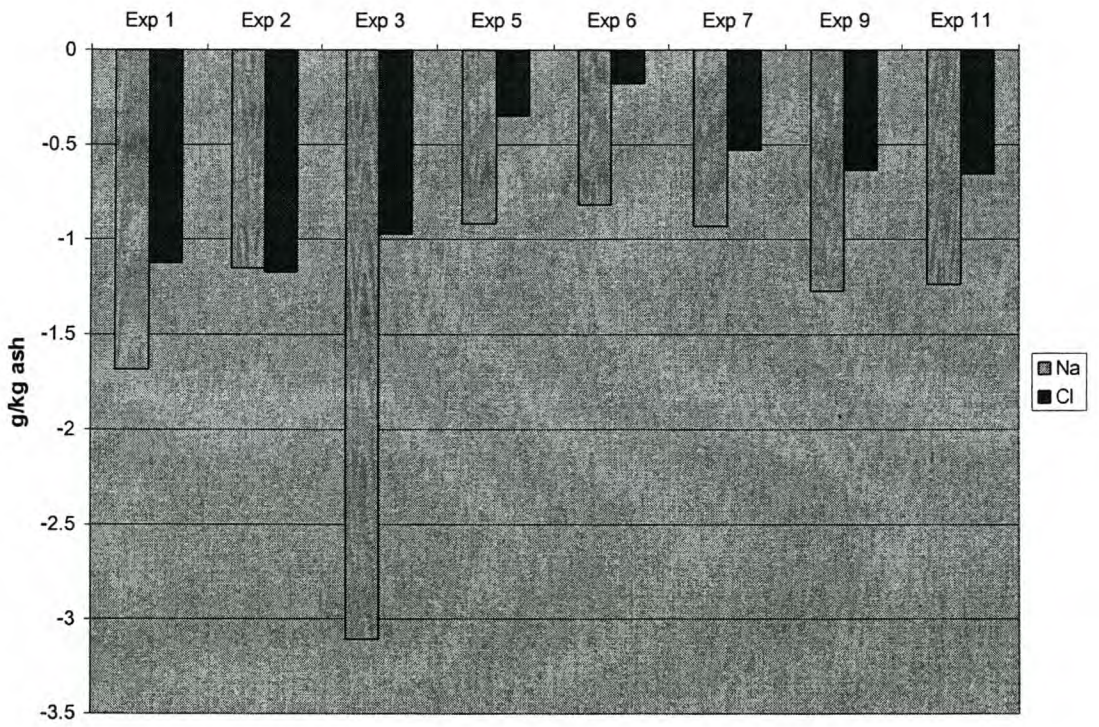

Figure 4.7: Na and Cl removal from the effluent for all column experiments

After the ash, used in these two experiments, was flushed with distilled water, there was still an overall retention of Na in the ash, however, all the Cl initially retained appeared to be flushed out by the distilled water. These specific results are given below, however, more details pertaining to the flushing experiments are given in section 4.2.4.

Table 4.9: Na and Cl Retention after Flushing with Distilled Water

	Exp 3&4	Exp 7&8	Exp 9&10	Exp 11&12	units
Na	2.59	**0.13**	0.43	**0.34**	g/kg ash
Cl	0.71	**-0.038**	0.089	**-0.039**	g/kg ash

As mentioned previously, one should actually compare Exp 11 to Exp 9 since these two experiments were identical (besides the addition of the NaCl stream to Exp 11). Thus, if one compares the results of the flushing of these two ash columns, it is evident that overall more Na is retained in the ash when no NaCl is added to the initial ash water slurry. This could, however, be as a result of the actual ash sample used, even though all the ash used in the column experiments was collected on the same day. It is interesting to examine how much Na and Cl are flushed out of the ash on the basis of the exact amount of water passing through the ash column. These results are presented in table 4.10 on the basis of litres of leachate collected.

Table 4.10: Na and Cl Flushed Out of the Ash Column per litre of Leachate Collected

	Exp 4	Exp 8	Exp 10	Exp 12	units
Na	444	172	173	174	mg/l total leachate collected
Cl	180	116	105	121	mg/l total leachate collected

Firstly, if one compares the results from Exp 8 and Exp 12 (flushing of Exp 7 and Exp 11 ash, respectively), it is evident that the amount of Na and Cl flushed out of the ash per litre of water that passed through the column, is very similar. If one compares the results from the flushing of Exp 9 ash (Exp 10), and Exp 11 ash (Exp 12), then it is clear that when a concentrated NaCl stream is added (Exp 7 and Exp 11) to the ash water slurry, more Cl is flushed from the ash. The amount of Na flushed from the ash, on the basis of the amount of water passing through the ash, is the same for both the experiment with the added NaCl stream (Exp 11&12) and the experiment without the addition of a NaCl stream (Exp 9&10). Thus, it appears from these preliminary results, that if Cl is added to the ash water slurry, it is retained in the ash, but has the potential to be completely flushed out. Na on the other hand will only be flushed out to a certain extent, probably depending on the hydraulic retention of the ash. This amount that is flushed out does not appear to be influenced by the addition of Na to the initial ash water slurry.

The heating of the ash

For all the experiments conducted the ash was heated in a furnace to a temperature of 260°C. When the ash was added to the effluent (at room temperature, ± 20°C) the temperature of the mixture was measured to be ± 30°C. It is thus clear that the ash is quenched very quickly by the effluent, and does not retain its temperature of 260°C once mixed with the effluent. Due to the rapid quenching of the ash to a temperature not that much higher than room temperature, the heating of the ash was considered to not be of utmost importance to the chemical reactions which occur in the ash/water slurry. If, when the ash was added to the effluent, the mixture had reached a temperature much higher than 20°C, then the chemistry of the slurry mixture may have been affected. However, since this was not the case, altering the temperature to which the ash was heated was not included in the column experiments performed. For consistency sake, the ash was heated to 260°C before each experiment.

4.2.1.4 Other components tested for but not reported

Initially a variety of components were tested for in the effluent samples, however, some of the components tested for were present in the effluent at concentrations that were too low to be detected by the specific test method available.

- F could not be tested for using the Dionex Al450 Ion Chromatograph that was used to test for Cl and SO_4. The reason for this is that it was vital that at least a 20-times dilution of the effluent samples was used due to the high concentrations of Cl and SO_4. At such a high dilution, the F could not be detected. Moreover, according to plant data from the actual ash disposal system, F is not an element of major concern; therefore it was not tested for in the column experiments.
- Fe, Al, Cr, Si and Mg were all tested for using an Inductively Coupled Plasma Atomic Emission Spectrometer (ICP-AES). The results of these analyses were that all the components mentioned were present in the effluent samples at very low concentrations: Fe<0.5ppm, Al< 0.5ppm, Cr<0.1ppm, Si<0.1ppm and Mg<0.1ppm. Therefore, for the purpose of the column experiments conducted in this investigation, these components were not analysed for in the leachate produced.

4.2.2 Experiments with a longer retention time for phase 3

4.2.2.1 Overall

The experiments conducted, to confirm the Ca chemistry occurring during phase 3, were Exp 15, Exp 16 and Exp 17. In each of these experiments approximately 1kg of ash and 5*l* of water was used. (L:S = 5:1). The ash was heated to 260°C and then mixed with the effluent (new FAM). After five minutes a sample of the slurry mixture was taken (slurry I), as well as after 2½ hours (slurry II), just before the slurry was allowed to pass into the column. The small initial amount of slurry, which passed through the glass wool, was weighed, noted and discarded, and the first leachate sample was then collected (sample a). Once sample (a) was collected, the collecting dish was placed under the column to collect the rest of the leachate. After 24 hours a sample (sample b) was taken from the collecting dish, and the dish containing the leachate was weighed. After one week, another sample was collected (sample c), and this procedure was repeated for a period of 5 weeks (samples were taken on a weekly basis).

The results from these experiments are reported on the basis of mass balances. Even though the focus of the three experiments was to determine the calcium chemistry occurring during phase 3, mass balances for all the main components were also calculated. The overall results are shown in table 4.11 and figure 4.8.

Table 4.11: Mass Balance Results for Exp 15, Exp 16 and Exp 17 (g/kg ash)

Component	Exp 15 (g/kg ash)	Exp 16 (g/kg ash)	Exp 17 (g/kg ash)	
Ca	-1.34	-1.60	-1.67	Removal from ash water
CO_3	-0.244	-0.236	-0.203	Removal from ash water
SO_4	-4.26	-4.48	-5.86	Removal from ash water
Na	-1.42	-1.43	-1.57	Removal from ash water
Cl	-0.74	-0.73	-0.84	Removal from ash water

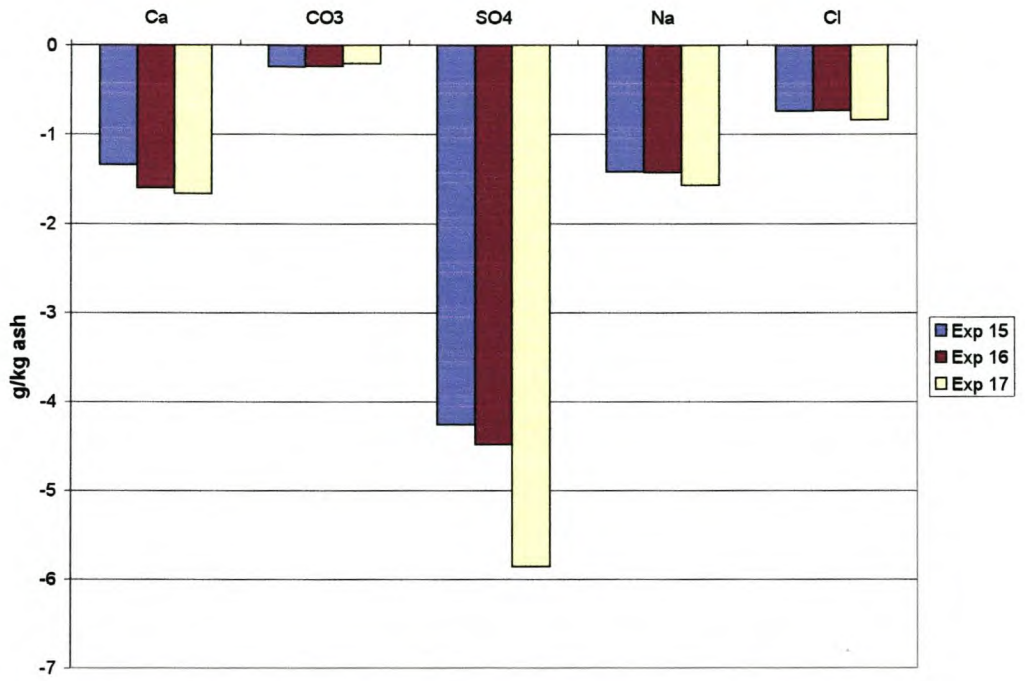

Figure 4.8: Overall mass balance results for Exp 15, Exp 16 and Exp 17

These results show that all the salts mentioned are actually removed from the water phase and either retained in the ash, or removed as a precipitate. Since the molecular weights of the different salts vary, these mass balance results are also reported on a mmol/kg ash basis in table 4.12.

Table 4.12: Mass Balance Results for Exp 15, Exp 16 and Exp 17 (mmol/kg ash)

Component	Exp 15 (mmol/kg ash)	Exp 16 (mmol/kg ash)	Exp 17 (mmol/kg ash)	
Ca	-34	-40	-42	Removal from ash water
CO_3	-4	-4	-3	Removal from ash water
SO_4	-44	-47	-61	Removal from ash water
Na	-62	-62	-68	Removal from ash water
Cl	-21	-21	-24	Removal from ash water

It is clear from the figures given in tables 4.11 and 4.12 that the results for the three experiments are very consistent, and can thus be deemed as reliable. The results for the different phases of the experiments will be discussed further in the sections that follow.

4.2.2.2 Calcium

Mixing Stage (Phase 1)

Table 4.13 displays the results for the mixing stage of the experiment.

Table 4.13: Mass Balance Results for Ca Phase 1

	First 5 minutes		After 2½ hours	
	mg	g/kg ash	mg	g/kg ash
Exp 15	3 038	3.04	355	0.41
Exp 16	2 065	2.07	769	0.86
Exp 17	1 886	1.87	86	0.097

One can clearly see that there is an initial leaching of the Ca from the ash into the water during the mixing stage. It is also evident that the majority of the leaching occurs very rapidly – i.e. in the first five minutes of water/ash contact. This point is discussed further in section 4.2.5.1.

Column (Phase 2)

Figure 4.9 diagrammatically represents the values used in the mass balance calculations for phase 2.

From the values for Ca shown in figure 4.9, one can calculate that there is an overall retention of Ca in the column for all three experiments.

Table 4.14: Mass Balance Results for Ca Phase 2

	mg	mmol	kg ash	g/kg ash	mmol/kg ash	
Exp 15	-3939	-98	0.747	**-5.27**	-132	Retention in column
Exp 16	-2856	-71	0.786	**-3.63**	-91	Retention in column
Exp 17	-1380	-35	0.772	**-1.79**	-45	Retention in column

Obviously one of the explanations for the retention of the Ca in the column is due to hydraulic retention. Performing a water mass balance around the column, after 24 hours, revealed that 0.583*l*, 0.576*l*, and 0.579*l* was retained for experiments 15, 16 and 17, respectively. These values were calculated taking into account the evaporation for the 24

hours that the collecting dish was exposed to the atmosphere (measured by a control collecting dish to be 19ml/day).

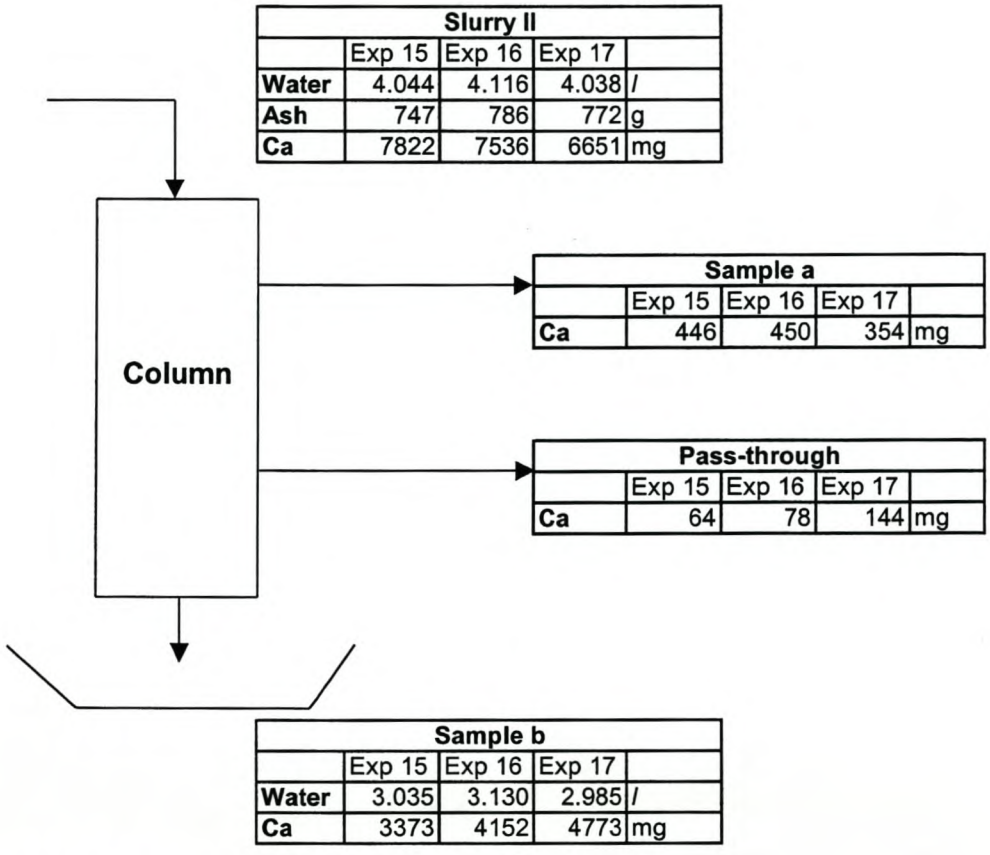

Figure 4.9: Mass balance values for phase 2 for Ca

Collecting Dish (Phase 3)

After 24 hours it was evident that there was no more leachate passing from the column into the collecting dish. Therefore, the valve at the bottom of the column was closed, and a sample (sample b) was taken from the collecting dish. The rest of the leachate, which was left in the collecting dish for 5 weeks, is that which was used to determine the changes during phase 3. Samples were taken on a weekly basis, weighed and analysed. Mass balance results over this phase reveal that there is an overall removal of Ca from the leachate. These results are shown in table 4.15.

Table 4.15: Mass Balance Results for Ca Phase 3

	mg	mmol	kg ash	g/kg ash	mmol/kg ash
Exp 15	-798	-20	0.747	**-1.07**	-27
Exp 16	-1586	-40	0.786	**-2.02**	-50
Exp 17	-2020	-51	0.772	**-2.62**	-65

Since there was no ash in contact with the leachate at this stage, the only plausible reason for the removal of Ca must be due to precipitation. This possibility was reinforced by the presence of a white precipitate in the collecting dish. It was found mainly on the surface of the leachate (until the dish was disturbed to take a sample, then the precipitate sunk to the bottom), suggesting that it was calcite (CO_2 from the atmosphere). Besides the fact that this precipitate was tested by means of XRD and found to be predominantly calcite, a mass balance was performed on the CO_3 in the system to determine if there was also a reduction in the carbonates.

4.2.2.3 Carbonate

Mixing Stage (Phase 1)

Table 4.16 displays the results for the mixing stage of the experiment.

Table 4.16: Mass Balance Results for CO_3 Phase 1

	First 5 minutes		After 2½ hours	
	mg	g/kg ash	mg	g/kg ash
Exp 15	301	0.3	-117	-0.14
Exp 16	261	0.26	36	0.040
Exp 17	330	0.33	-173	-0.19

It is evident, from the mass balance results given in table 4.16, that there is an initial overall increase of CO_3 in the water during the mixing stage. However, after 2½ hours there appears to be an overall removal of CO_3 from the water. Obviously one cannot measure the amount of CO_2 entering the slurry mixture, but still there is an overall reduction in the carbonate ions in solution. This would suggest that precipitation (possibly as calcite) is already occurring at this stage.

Column (Phase 2)

Figure 4.10 diagrammatically represents the values used in the CO_3 mass balance calculations for phase 2.

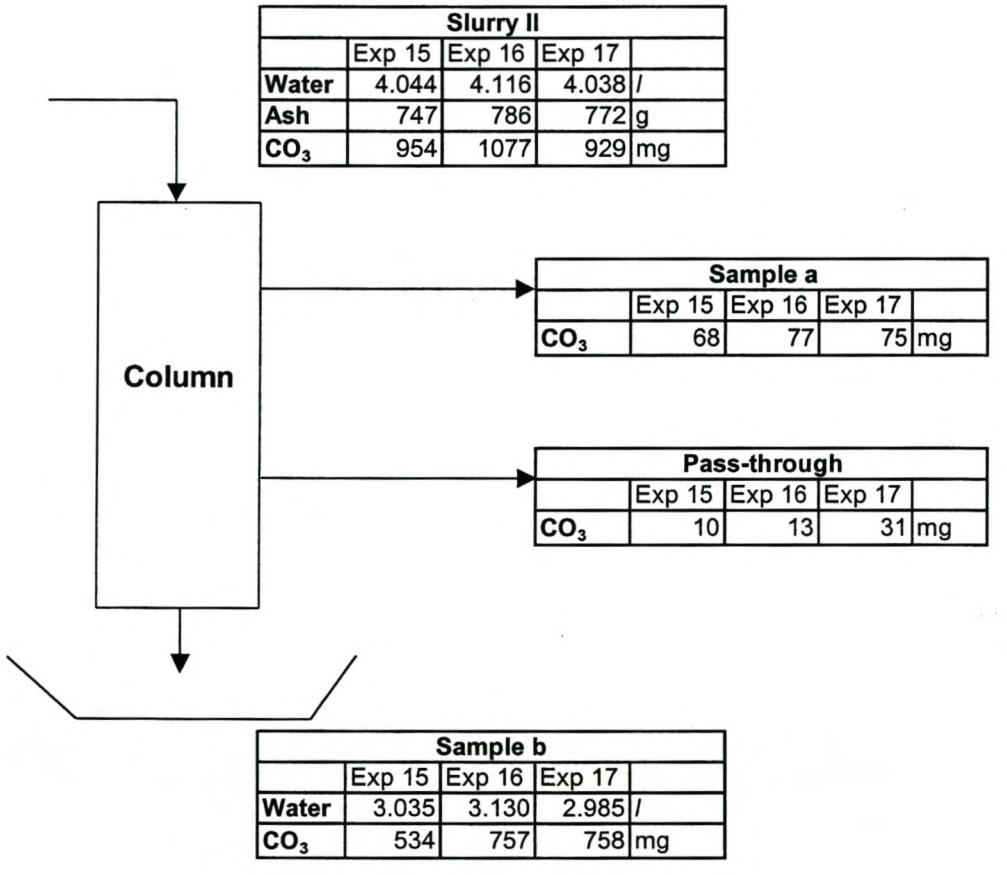

Figure 4.10: Mass balance values for phase 2 for CO_3

If one utilises the values for CO_3 shown in figure 4.10, one can calculate that, for all three experiments, there is an overall retention of CO_3 in the column.

Table 4.17: Mass Balance Results for CO_3 Phase 2

	mg	mmol	kg ash	g/kg ash	mmol/kg ash	
Exp 15	-342	-5.7	0.747	**-0.46**	-7.6	Retention in column
Exp 16	-230	-3.8	0.786	**-0.29**	-4.9	Retention in column
Exp 17	-65	-1.1	0.772	**-0.08**	-1.4	Retention in column

Obviously, as mentioned in section 4.2.2.2, part of this retention is due to mere hydraulic retention within the ash column. What is interesting to note is the variation in retention for the different experiments, compared to the Ca retention in the column for those same experiments (table 4.14). The same pattern is seen for the Ca and the CO_3 retention, maximum retention for Exp 15 and the least retention for Exp 17. This further suggests a correlation between the Ca and CO_3 chemistry.

Collecting Dish (Phase 3)

The description given for the sampling of phase 3 is the same as that for Ca (section 4.2.2.2). Mass balance results over this phase reveal that there is an overall removal of CO_3 from the leachate. These results are shown in table 4.18.

Table 4.18: Mass Balance Results for CO_3 Phase 3

	mg	mmol	kg ash	g/kg ash	mmol/kg ash
Exp 15	-104	-1.7	0.747	**-0.14**	-2.3
Exp 16	-304	-5.1	0.786	**-0.39**	-6.4
Exp 17	-295	-4.9	0.772	**-0.38**	-6.4

These values do not take into account the additional CO_2 that enters the leachate from the atmosphere. However, even though there is CO_2 entering the leachate, there is still an overall reduction in the CO_3^{2-} ions in solution. As mentioned in section 4.2.2.2, these results just further confirm the precipitation of calcite during phase 3. Thus, even though the general result from the column experiments (figure 4.2) show a leaching of Ca from the ash into the water; the results for these three experiment highlight the fact that overall, Ca is removed from the system in the form of calcite. The one week (as opposed to the five weeks used in these experiments) allowed for phase 3 initially, was not long enough to show this overall removal of Ca from the liquid phase.

4.2.2.4 Sulphate

Mixing Stage (Phase 1)

Table displays the results for the mixing stage of the experiment.

Table 4.19: Mass Balance Results for SO_4 Phase 1

	First 5 minutes		After 2½ hours	
	mg	g/kg ash	mg	g/kg ash
Exp 15	1 026	1.03	-530	-0.61
Exp 16	-92	-0.092	-350	-0.39
Exp 17	-2 176	-2.18	-411	-0.46

From the results presented in table 4.19 it is apparent that there is an overall decrease in SO_4 ions in solution during the mixing stage, suggesting that as soon as the water is in contact with the ash reactions occur which remove the SO_4 from the water.

Column (Phase 2)

Figure 4.11 diagrammatically represents the values used in the SO_4 mass balance calculations for phase 2. The values, presented in figure 4.11, can be used to determine that there is an overall retention of SO_4 in the column for all three experiments.

Table 4.20: Mass Balance Results for SO_4 Phase 2

	mg	mmol	kg ash	g/kg ash	mmol/kg ash	
Exp 15	-5985	-62.3	0.747	**-8.01**	-83.5	Retention in column
Exp 16	-5819	-60.6	0.786	**-7.40**	-77.1	Retention in column
Exp 17	-2375	-24.7	0.772	**-3.08**	-32.0	Retention in column

Obviously, as mentioned in sections 4.2.2.2 and 4.2.2.3, part of this retention is due to mere hydraulic retention within the ash column. Moreover, what is interesting to note is the variation amount of SO_4 retained for the different experiments, compared to the Ca retention in the column for those same experiments (table 4.14). The same pattern is seen for the Ca and SO_4 retention, maximum retention for Exp 15 and the least retention for Exp 17. This suggests the possibility of $CaSO_4$ precipitation in the ash column.

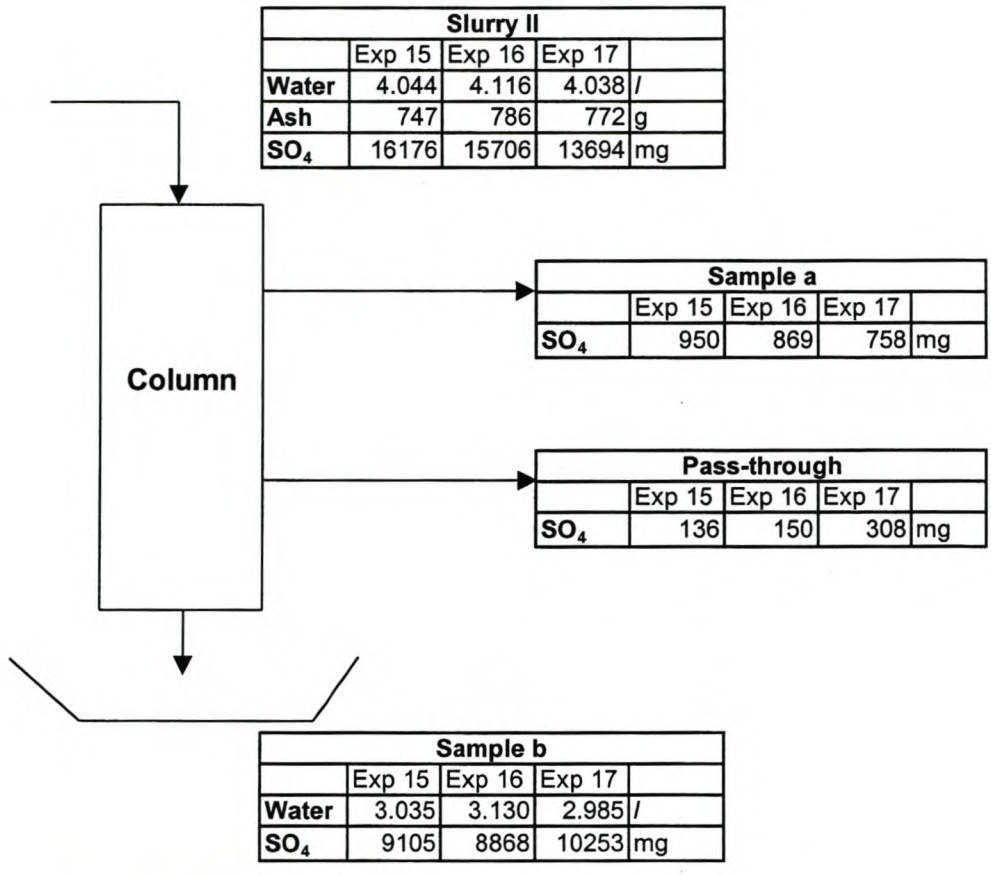

Figure 4.11: Mass balance values for phase 2 for SO_4

Collecting Dish (Phase 3)

The description given for the sampling of phase 3 is the same as that for Ca (section 4.2.2.2). During the 5 weeks period in which in the leachate was left in the collecting dish, it appears as if the amount of SO_4 ions in solution increased. These results are shown in table 4.21.

Table 4.21: Mass Balance Results for SO_4 Phase 3

	mg	mmol	kg ash	g/kg ash	mmol/kg ash
Exp 15	1227	12.8	0.747	**1.64**	17.1
Exp 16	1754	18.3	0.786	**2.23**	23.2
Exp 17	908	9.5	0.772	**1.18**	12.3

In order to investigate this increase in SO_4 in the leachate further, the period of 5 weeks was broken up into one week periods, and mass balance were performed to determine when the increase occurred, and if there was a decrease, when did that occur. Table 4.22 and figure 4.12 present these results.

Table 4.22: Mass Balance Results per week for SO_4

	1st week	2nd week	3rd week	4th week	5th week	
Exp 15	2562	-665	-584	-299	-14	mg
Exp 16	2554	-275	-276	-200	-52	mg
Exp 17	-30	-723	-391	-18	253	mg

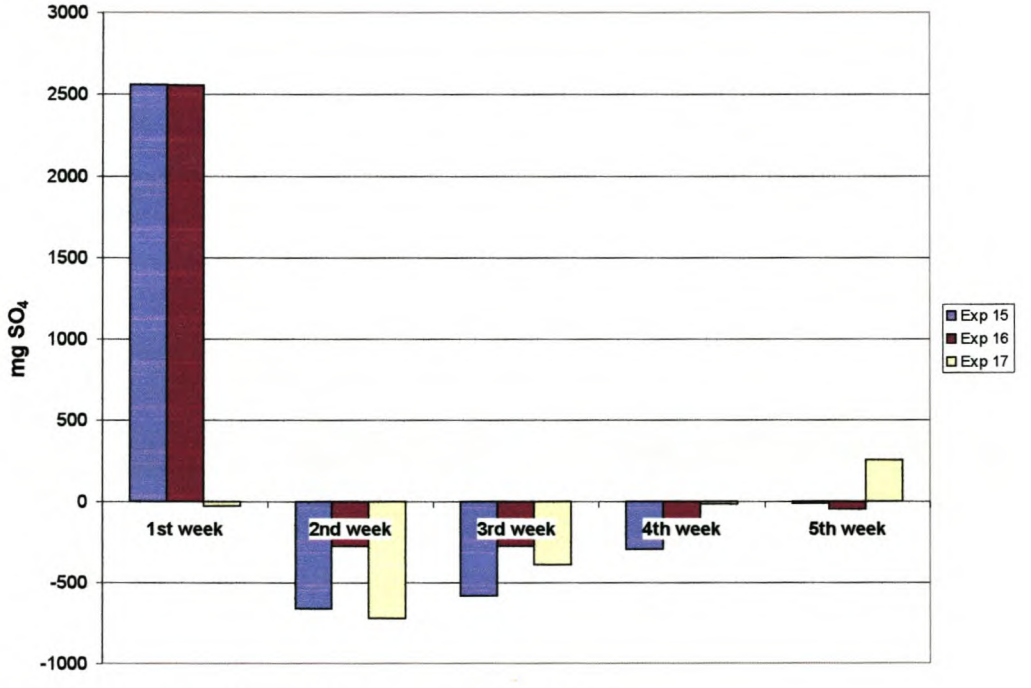

Figure 4.12: Mass Balance Results per week for SO_4

It is evident that in general, it is during the first week of the leachate being left in the container that there was an increase in the SO_4 ions in solution. After a week it appears as if they are removed from the liquid phase, however, this removal (over the 4 weeks) is less and the initial increase. Therefore, when looking at the 5-week period as a whole,

one sees an overall increase in SO_4 ions in solution during phase 3. A possible explanation for the very low values for SO_4 removal for Exp 15 and Exp16, and increase for Exp 17 during week 5 could be due to the low pH of the leachate at this stage.

4.2.2.5 Sodium

Mixing Stage (Phase 1)

The mass balance results for the mixing stage of the experiments are given in table 4.23.

Table 4.23: Mass Balance Results for Na Phase 1

	First 5 minutes		After 2½ hours	
	mg	g/kg ash	mg	g/kg ash
Exp 15	74	0.074	64	0.074
Exp 16	187	0.19	237	0.27
Exp 17	297	0.30	-31	-0.035

It is evident that there is an increase in the Na ions in solutions during the mixing stage, but these values are a lot lower than those for Ca (table 4.13). There also doesn't appear to be significantly more Na leaching during the first 5 minutes compared to after 2½ hours. These values were investigated further, combined with the results from the other experiments, and are discussed in section 4.2.5.3.

Column (Phase 2)

Figure 4.13 diagrammatically represents the values used in the Na mass balance calculations for phase 2. From the values for Na shown in figure 4.13, one can calculate that there is an overall retention of Na in the column for all three experiments (table 4.24). Part of this retention is probably due to mere hydraulic retention within the ash column. The retention of Na in the ash column for all three experiments is very similar.

Table 4.24: Mass Balance Results for Na Phase 2

	mg	mmol	kg ash	g/kg ash	mmol/kg ash	
Exp 15	-1060	-46.1	0.747	-1.42	-61.7	Retention in column
Exp 16	-1241	-54.0	0.786	-1.58	-68.6	Retention in column
Exp 17	-1092	-47.5	0.772	-1.41	-61.5	Retention in column

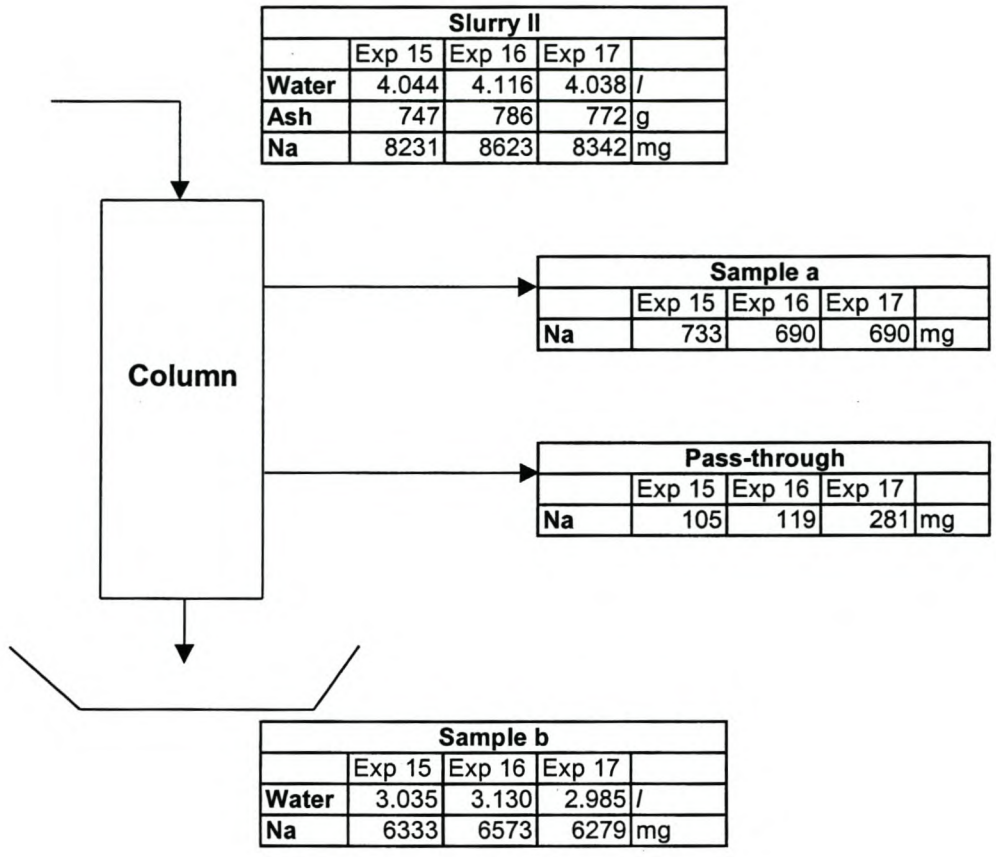

Figure 4.13: Mass balance values for phase 2 for Na

Collecting Dish (Phase 3)

Mass balance results over this phase reveal that there is an overall decrease of Na ions in solution during the 5 weeks, suggesting that they must be precipitating out together with one of the anions in solution, possibly $NaHCO_3$. These results are shown in table 4.25.

Table 4.25: Mass Balance Results for Na Phase 3

	mg	mmol	kg ash	g/kg ash	mmol/kg ash
Exp 15	-503	-21.9	0.747	-0.67	-29.3
Exp 16	-619	-26.9	0.786	-0.79	-34.2
Exp 17	-745	-32.4	0.772	-0.97	-42.0

4.2.2.6 Chloride

Mixing Stage (Phase 1)

The mass balance results for Cl during the mixing stage of the column experiments are presented in table 4.26. from these results it is evident that very little changes occur with respect to the Cl ions in solution during the mixing stage, suggesting that the Cl in the ash is not in a form that can be easily leached. Even for Exp 17, overall there is practically no change in the Cl content of the water after 2½ hours of mixing; the initial decrease is compensated for by the further increase during the full 2½ hours of mixing.

Table 4.26: Mass Balance Results for Cl Phase 1

	First 5 minutes		After 2½ hours	
	mg	g/kg ash	mg	g/kg ash
Exp 15	0	0	0	0
Exp 16	0	0	60	0.067
Exp 17	-250	-0.25	108	0.12

Column (Phase 2)

The values used in the Cl mass balance calculations for phase 2 are presented diagrammatically in figure 4.14.

The mass balance results, using the values for Cl shown in figure 4.14, are given in table 4.27. These results reveal that for all three experiments, there is an overall retention of Cl in the column. Furthermore, the retention of Cl in the ash column for all three experiments is very similar.

Table 4.27: Mass Balance Results for Cl Phase 2

	mg	mmol	kg ash	g/kg ash	mmol/kg ash	
Exp 15	-774	-21.8	0.747	-1.04	-29.2	Retention in column
Exp 16	-752	-21.2	0.786	-0.96	-27.0	Retention in column
Exp 17	-681	-19.2	0.772	-0.88	-24.8	Retention in column

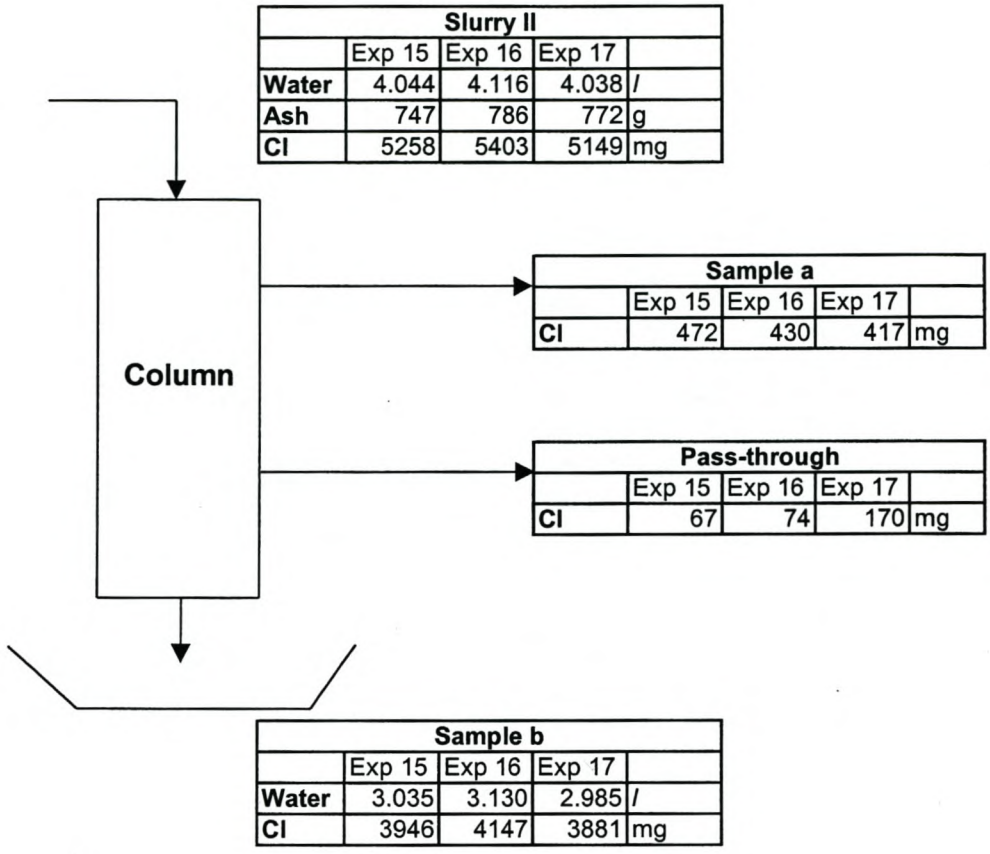

Figure 4.14: Mass balance values for phase 2 for Cl

Collecting Dish (Phase 3)

Mass balance results over this phase reveal that there is practically no change in the Cl ions in solutions during the 5 weeks. These results are presented in table 4.28.

Table 4.28: Mass Balance Results for Cl Phase 3

	mg	mmol	kg ash	g/kg ash	mmol/kg ash
Exp 15	31	0.9	0.747	0.04	1.2
Exp 16	-42	-1.2	0.786	-0.05	-1.5
Exp 17	-18	-0.5	0.772	-0.02	-0.7

4.2.2.7 pH

One can see from figure 4.15 that there is an initial increase in the pH of the effluent when the ash is added (in the first five minutes). It then remains at a fairly constant value for about a week, and after a week of exposure to the atmosphere, the pH begins to decrease. This can be attributed to the calcium carbonate chemistry occurring in the leachate. It is also evident that in the 5th week there is a sudden drop in the pH.

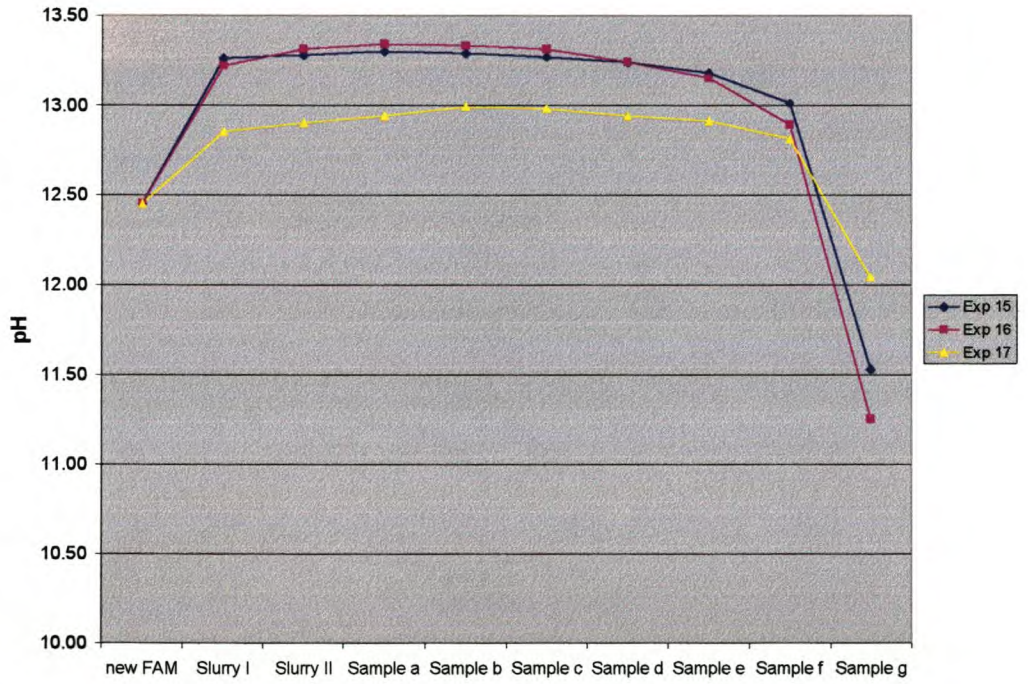

Figure 4.15: Variation in pH during Exp 15, Exp 16 and Exp 17

4.2.2.8 Conductivity and Total Dissolved Solids

As one can see from figure 4.16, the variation in conductivity is basically the same as the variation in TDS. There is an initial increase for both the conductivity and the TDS during the mixing stage, and then a drop for the first sample of leachate collected. Thereafter there is an overall increase for a period of about one week, after which time there is again a decrease, thus further emphasising the calcium carbonate chemistry occurring in the leachate. It was also evident that after a week the pH of the leachate

began to decrease. The initial increase in conductivity and TDS is probably related to the increase in SO_4 ions in solution seen during this time period (see table 4.22 and figure 4.12).

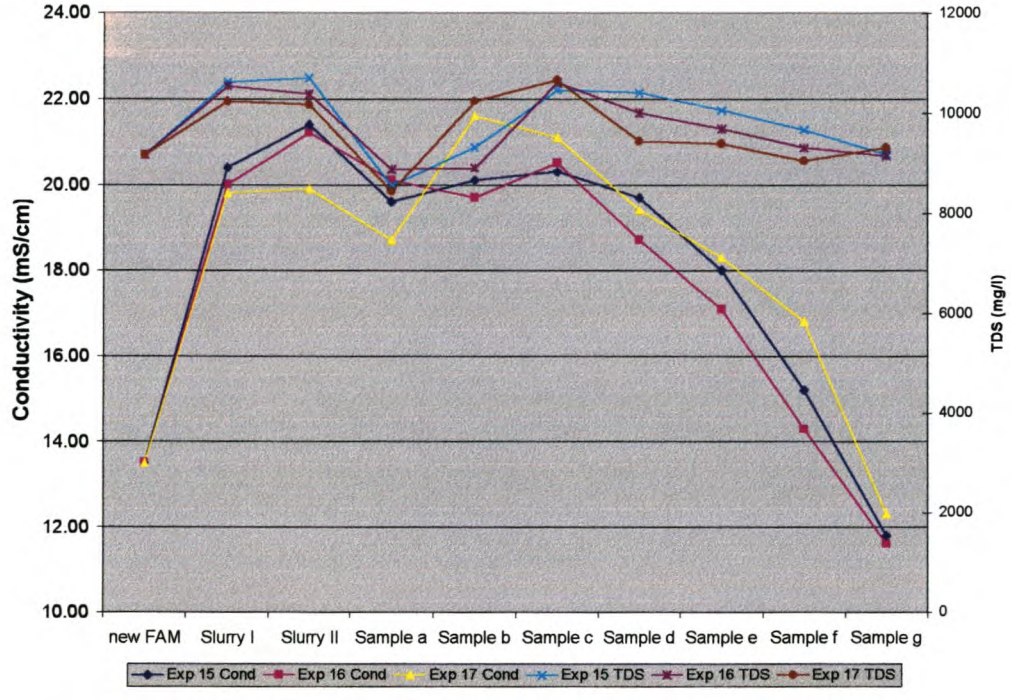

Figure 4.16: Conductivity and TDS variation for Exp 15, Exp 16 and Exp 17

4.2.3 Experiments with distilled water as the liquid phase

Two identical experiments (Exp 13 and Exp 14) were performed in order to assess the leaching of the main elements from the ash. In both these experiments approximately 1kg of ash and 5*l* of water was used (L:S = 5:1), with a mixing time of 2½ hours. Mass balances were performed in order to determine the amount of each of the main elements leached from the ash. These results are shown in table 4.29 and figure 4.17.

Table 4.29: Overall Mass Balance Results for Column Experiments with Distilled Water

	Exp 13	Exp 14	units
Ca	5.10	4.89	g/kg ash
Na	0.20	0.11	g/kg ash
K	0.0090	0.010	g/kg ash
Cl	0	0	g/kg ash
SO4	1.13	1.14	g/kg ash
TDS	10.5	10.0	g/kg ash

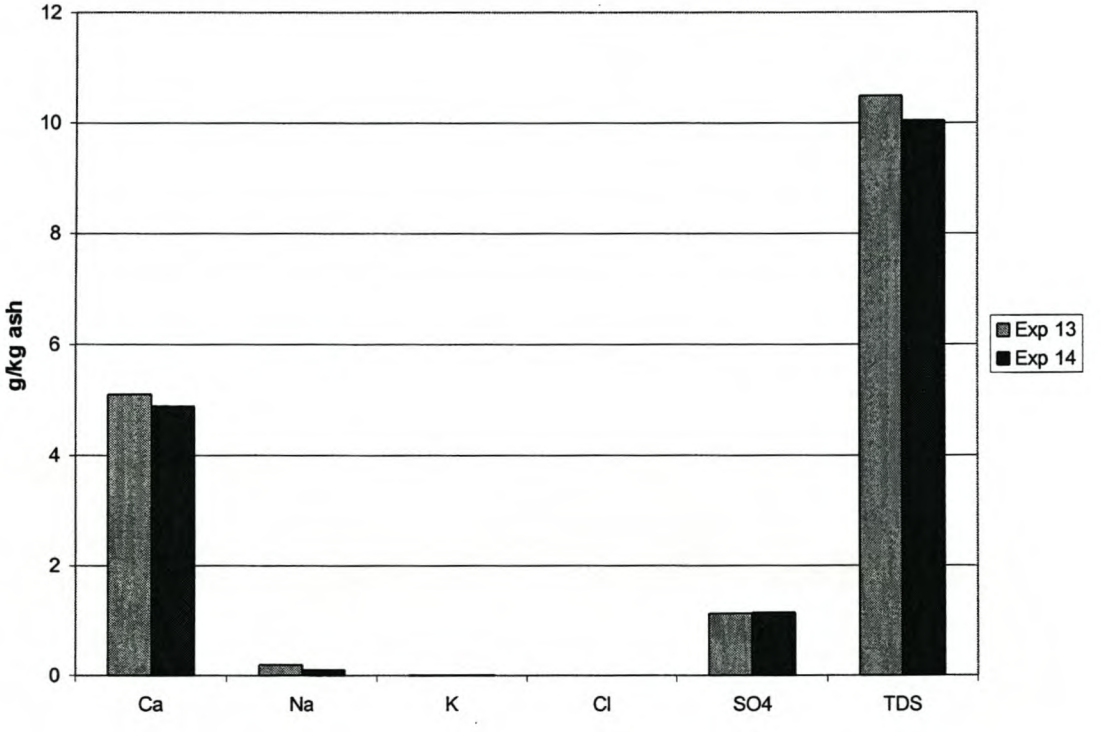

Figure 4.17: Graphical representation of mass balance results for column experiments with distilled water

One can see clearly that there is an overall leaching of each of the main components Ca, Na and SO_4, into the liquid phase from the ash. These results are also apparent for the same two experiments when only the mixing stage (phase 1, section 4.2.5.6) was examined. It is interesting to compare the leaching that occurs during the mixing stage and the overall mass balance results; to see what changes occur during the movement of

the water through the ash column (phase 2), and the time the leachate spends in the collecting dish (phase 3). Table 4.30 and figure 4.18 display these results.

Table 4.30: Comparison between Phase 1 and Overall Results

	Phase 1		Overall		Units
	Exp 13	Exp 14	Exp 13	Exp 14	
Ca	6.8	6.2	5.10	4.89	g/kg ash
Na	0.091	0.083	0.20	0.11	g/kg ash
Cl	0	0	0	0	g/kg ash
SO4	1.12	0.97	1.13	1.14	g/kg ash
TDS	11.7	12.4	10.5	10.0	g/kg ash

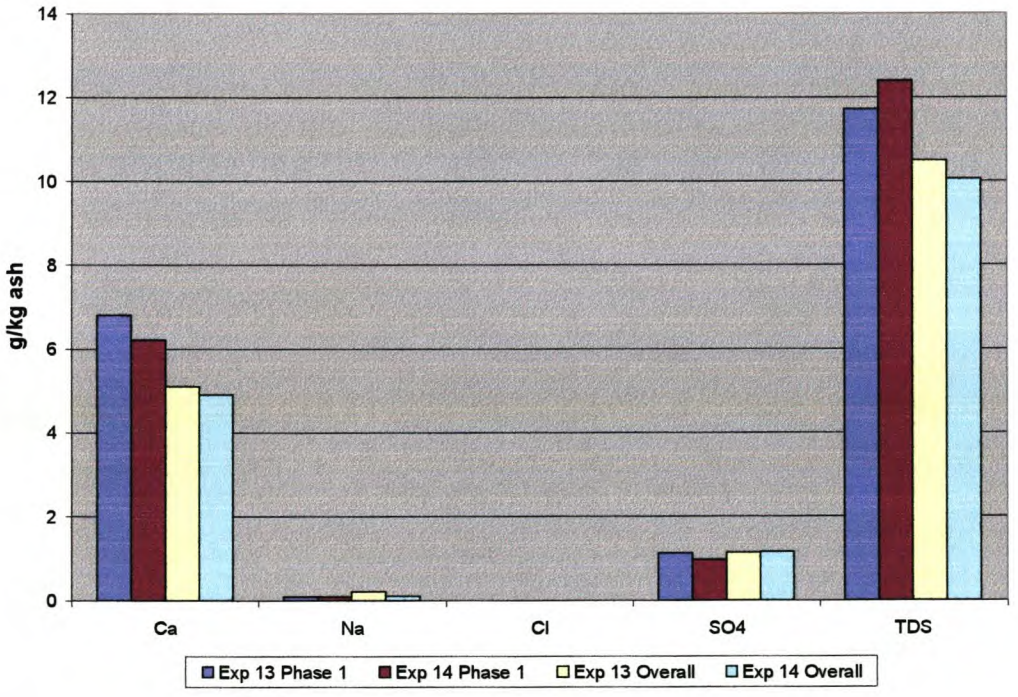

Figure 4.18: Leaching during mixing stage vs. overall mass balance results

- It is evident that some of the Ca, leached from the ash during the mixing stage, is further removed from the water during phase 2 and phase 3. Thus, the overall Ca

content of the water after the experiment is less than it was after just the mixing stage (phase 1).

- This decrease in Ca content would explain the overall decrease in the TDS of the water from after phase 1 to after phase 3.
- No major changes are observed for the SO_4 content of the water during phase 2 and 3 compared to phase 1.
- There is no Cl leached from the ash during phase 1, nor during phases 2 and 3.
- The amount of Na leached increases during phases 2 and 3, thus the overall Na content of the water after the experiment is higher than it was after just the mixing stage (phase 1).

4.2.4 Flushing Experiments

4.2.4.1 Overview

In order to determine whether the salts (Na, Cl, and SO_4), which appeared to be retained in the ash column, were retained merely due to hydraulic retention (the void fraction of the ash was found to be about 0.7), flushing experiments were performed. Four flushing experiments were carried out (Exp 4, Exp 8, Exp 10 and Exp 12). The ash from the previous experiments (i.e. Exp 3, Exp 7, Exp 9 and Exp 11) was left in the column after the experiment; distilled water was then passed through the ash column and the leachate was collected. If one assumes plug flow of the water through the ash column, then one would expect that the initial sample collected should basically be that water which is retained due to hydraulic retention. One would therefore, expect the composition of the initial leachate to be similar to that of the final sample taken from the previous experiment. The variation in concentration of the leachate, for Na, Cl and SO_4, is shown in figures 4.19 to 4.21. The variation observed for the other components is given in Appendix C2, since it is the retention of the Na, Cl and SO_4 that need to be assessed in this section.

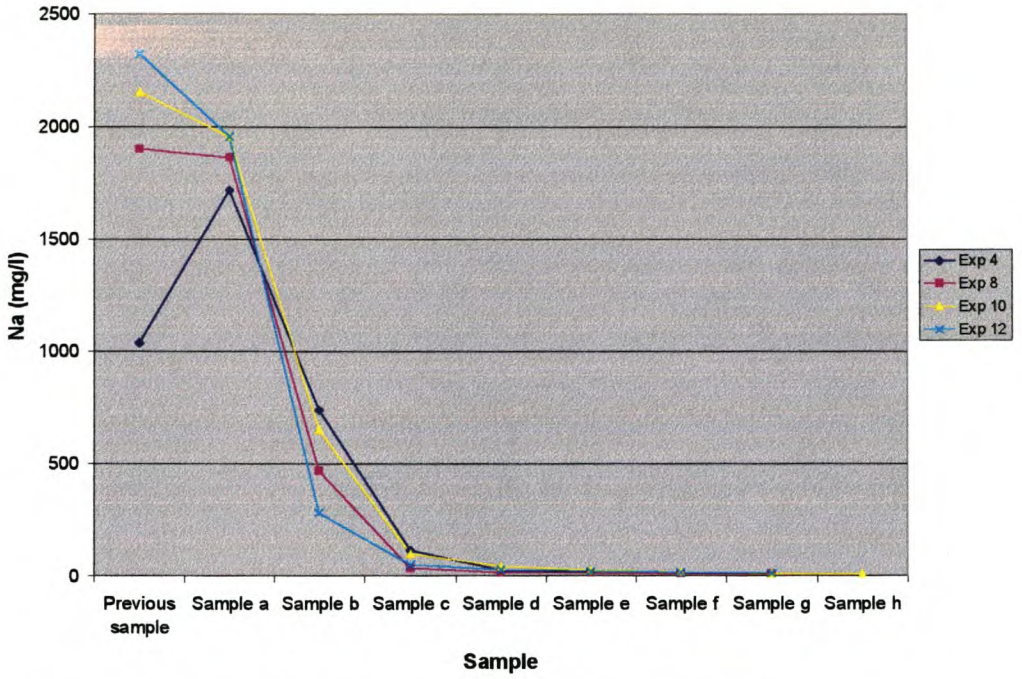

Figure 4.19: Variation in Na concentration for flushing experiments

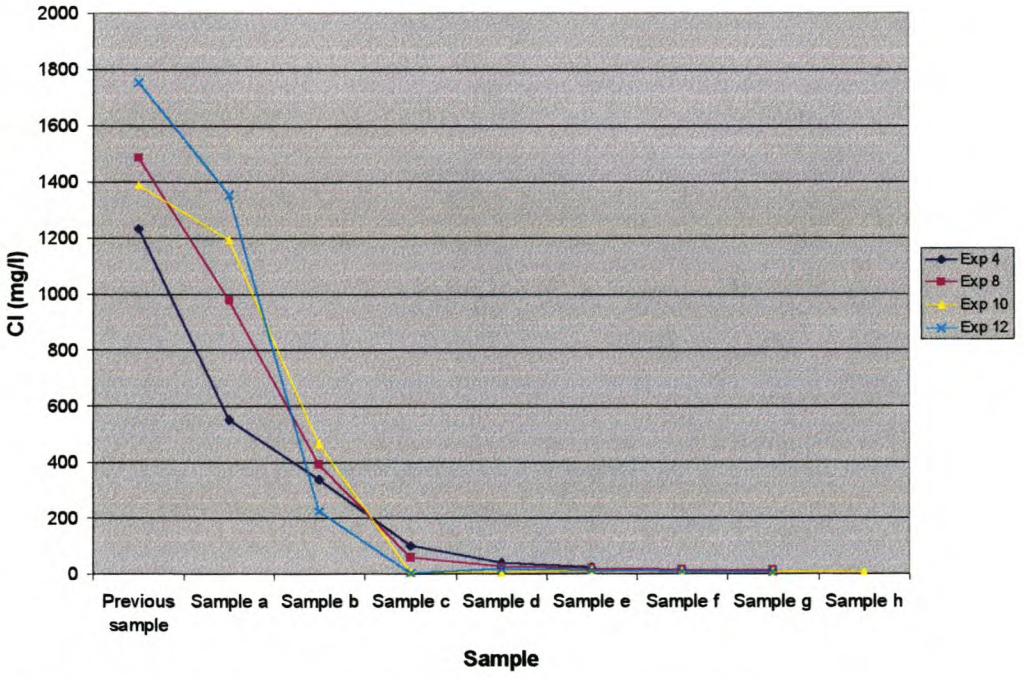

Figure 4.20: Variation in Cl concentration for flushing experiments

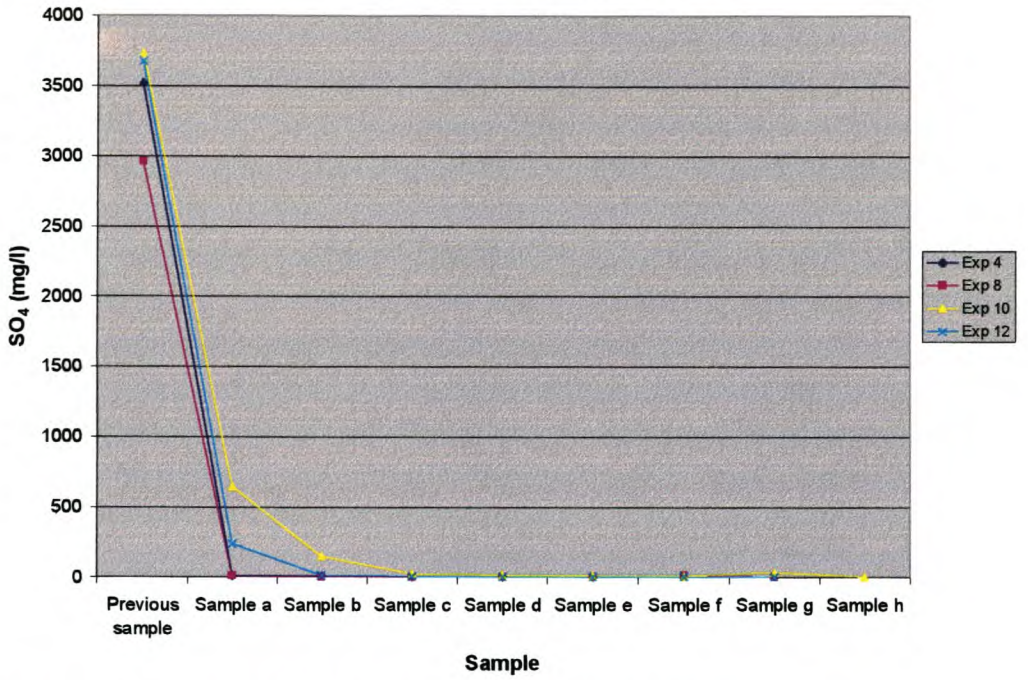

Figure 4.21: Variation in SO_4 concentration for flushing experiments

Obviously it is necessary to perform mass balances on the different salts to determine exactly how much of each salt is retained in the ash even after it has been flushed with distilled water. The amount of each salt retained in the ash before flushing commenced was determined by mass balances for Exp 3, Exp 7, Exp 9 and Exp 11. The total amount of each salt flushed from the ash was determined and compared to the original amount that was retained in the ash in Exp 3, Exp 7, Exp 9 and Exp 11. These results are displayed in table 4.31.

Table 4.31: Mass Balance Results After Flushing

		Exp 3&4	Exp 7&8	Exp 9&10	Exp 11&12	units
SO_4	Mass originally retained	3462	1625	1598	2840	mg
	Mass flushed out	7	30	123	355	mg
	Mass still retained in ash	**3455**	**1595**	**1475**	**2485**	**mg**
Na	Mass originally retained	2988	928	1277	1239	mg
	Mass flushed out	877	824	935	983	mg
	Mass still retained in ash	**2111**	**104**	**342**	**256**	**mg**
Cl	Mass originally retained	936	526	637	655	mg
	Mass flushed out	354	556	567	685	mg
	Mass still retained in ash	**582**	**-30**	**70**	**-30**	**mg**

Since the amount of ash in each experiment differed slightly, these results are also expressed on a g/kg ash basis, in table 4.32.

Table 4.32: Summary of Mass Balance Results after Flushing (g/kg ash basis)

	Exp 3&4	Exp 7&8	Exp 9&10	Exp 11&12	units
SO_4	4.24	2.01	1.87	3.27	g/kg ash
Na	2.59	0.13	0.43	0.34	g/kg ash
Cl	0.71	-0.038	0.089	-0.039	g/kg ash

It is evident from the data in tables 4.31 and 4.32 that the SO_4 cannot be easily flushed out of the ash once it is retained there. It can therefore, be concluded that the SO_4 must have in some way reacted with the ash, and is not merely held in the ash by means of hydraulic retention. Some of the Na is flushed out of the ash column using distilled water, however, even after about five litres of distilled water has been passed through the ash bed (about 800g), there is still an overall retention of the Na within the ash. Thus, the Na must also be retained in the ash by means other than hydraulic retention. As far as the Cl is concerned, a reasonable proportion of that which was originally retained in the ash during the experiments was flushed out with distilled water. The apparent leaching of Cl from the ash for Exp 7&8 and Exp 11&12 needs to be interpreted with care, since if one examines table 4.1 it is evident that a concentrated NaCl stream (2174mg Cl added) was actually added to the effluent used in Exp 7 and Exp 11. This suggests that some of the Cl in the water reacts with the ash and is retained within the ash column, however, the rest is retained by hydraulic retention and can be flushed out. Thus, over-loading the ash system with Cl ions in solution does not appear to be viable.

4.2.4.2 Summary of the results

- The SO_4 that is removed from the water and retained in the ash, in all the experiments, appears to be retained in a stable form within the ash and cannot be easily flushed out. This suggests that the ash system could act as a possible salt sink for SO_4.
- Some of the Na that is retained in the ash is flushed out, but there is still an overall retention of Na within the ash column.

- Most of the Cl retained in the ash can be flushed out with distilled water; suggesting that it is either retained by means of hydraulic retention, or else as a precipitate which easily dissolves in the distilled water.

4.2.5 Investigation of the initial ash/water contact: Phase 1

According to Jones (1995), during the initial mixing period where the ash in mixed vigorously to create a slurry, the composition of the liquid phase will be determined by the process with fast reaction kinetics. In wet ash systems where the transport medium is recycled and therefore, already saturated with calcite and/or dolomite, it is possible for the precipitation of secondary mineral phases to occur on the surface of the ash particles during the mixing stage.

The results of the mixing stage (phase 1) of the laboratory scale experiments performed in this investigation are discussed in detail below. For all these experiments, ash effluent was used as the liquid phase unless stated otherwise.

4.2.5.1 Calcium

Tables 4.33 and 4.34 display the mass balance results for Ca during the mixing stage of the experiment. The mass balance results for Ca are very consistent; there is an overall increase in the Ca content of the effluent during the mixing stage. From the results shown in table 4.33 it is evident that the majority of the leaching of the Ca from the ash into the water occurs during the first five minutes. Overall, for the 2½ hours of mixing, there is an average increase of 4.26g Ca per kg ash (106mmol Ca per kg ash).

Table 4.33: Mass Balance Results of Slurry I vs Slurry II for Ca

	First 5 minutes (Slurry I)		After 2½ hours (Slurry II)	
	mg	g/kg ash	mg	g/kg ash
Exp 11	5 154	5.15	690	0.78
Exp 15	3 038	3.04	355	0.41
Exp 16	2 065	2.07	769	0.86
Exp 17	1 886	1.87	86	0.097

Table 4.34: Overall Mass Balance Results for Ca After 2½ hours of Mixing

	mg	g/kg ash
Exp 3	5309	5.31
Exp 5	4078	4.08
Exp 6	3357	6.49
Exp 7	4586	4.59
Exp 9	3545	3.55
Exp 11	5844	5.93
Exp 15	3393	3.45
Exp 16	2834	2.93
Exp 17	1972	1.97

4.2.5.2 Sulphate

The mass balance results for SO_4, during the mixing stage of the experiments, are presented in table 4.35 and 4.36.

Table 4.35: Mass Balance Results of Slurry I vs. Slurry II for SO_4

	First 5 minutes (Slurry I)		After 2½ hours (Slurry II)	
	mg	g/kg ash	mg	g/kg ash
Exp 11	830	0.83	-34	-0.039
Exp 15	1 026	1.03	-530	-0.61
Exp 16	-92	-0.092	-350	-0.39
Exp 17	-2 176	-2.18	-411	-0.46

Table 4.36: Overall Mass Balance Results for SO_4 After 2½ hours of Mixing

	mg	g/kg ash
Exp 3	-678	-0.68
Exp 5	-123	-0.12
Exp 6	524	1.01
Exp 7	714	0.71
Exp 9	113	0.11
Exp 11	796	0.79
Exp 15	496	0.42
Exp 16	-442	-0.48
Exp 17	-2587	-2.64

It is evident from the data in tables 4.35 and 4.36 that results of the mass balances for SO_4 for the different experiments are not consistent. For the experiments listed in table 4.36 it apparent that 60% (6/10) show an overall increase of SO_4 ions in solution, whereas 40% (4/10) show a reduction of SO_4 ions in solution. These variations in results could not be attributed to different experimental conditions (i.e. different samples of FAM used), since the experimental conditions for Exp 15, Exp 16 and Exp 17 are exactly the same and yet still show different results. More experiments should be conducted to confirm the SO_4 mass balances for phase 1.

4.2.5.3 Sodium

Tables 4.37 and 4.38 display the mass balance results for Na during the mixing stage of the experiment. Even though some of these mass balance results for Na show that the Na is removed from the water, there is still an overall increase in the Na ion in solution during the mixing stage.

Table 4.37: Mass Balance Results of Slurry I vs. Slurry II for Na

	First 5 minutes (Slurry I)		After 2½ hours (Slurry II)	
	mg	g/kg ash	mg	g/kg ash
Exp 11	-284	-0.28	0	0
Exp 15	74	0.074	64	0.074
Exp 16	187	0.19	237	0.27
Exp 17	297	0.30	-31	-0.035

Table 4.38: Overall Mass Balance Results for Na After 2½ hours of Mixing

	mg	g/kg ash
Exp 3	1449	1.45
Exp 5	-613	-0.61
Exp 6	212	0.41
Exp 7	126	0.13
Exp 9	-123	-0.12
Exp 11	-284	-0.28
Exp 15	138	0.148
Exp 16	424	0.46
Exp 17	266	0.27

The average increase in Na ions in solution, based on the mass balance results for the experiments listed in table 4.38, is 0.21g Na per kg ash (9.0mmol Na per kg ash). As mentioned in section 4.2.2.5 (where just experiments 15 to 17 were evaluated), there doesn't appear to be significantly more Na leaching during the first 5 minutes compared to after 2½ hours, as is the case with the leaching of Ca.

4.2.5.4 Chloride

The mass balances results, for Cl, during the mixing stage of the experiments are given in tables 4.39 and 4.40. As was the case with the mass balance results for Na, even though some of the mass balance results for Cl show that the Cl is removed from the water, there is still an overall increase in the Cl ion in solution during the mixing stage. The average increase in Cl ions in solution, based on the mass balance results for the experiments listed in table 4.40, is 0.15g Cl per kg ash (4.3mmol Cl per kg ash). It is interesting to note that for some of the experiments there was no change in the Cl content of the effluent during the mixing stage. This observation is discussed further in section 4.2.5.6 where distilled water was mixed with the ash in order to determine the leaching of certain elements from the ash into the liquid phase.

Table 4.39: Mass Balance Results of Slurry I vs. Slurry II for Cl

	First 5 minutes (Slurry I)		After 2½ hours (Slurry II)	
	mg	g/kg ash	mg	g/kg ash
Exp 11	239	0.24	167	0.19
Exp 15	0	0	0	0
Exp 16	0	0	60	0.067
Exp 17	-250	-0.25	108	0.12

Table 4.40: Overall Mass Balance Results for Cl After 2½ hours of Mixing

	mg	g/kg ash
Exp 3	-270	-0.27
Exp 5	158	0.16
Exp 6	345	0.67
Exp 7	382	0.38
Exp 9	72	0.072
Exp 11	406	0.43
Exp 15	0	0
Exp 16	60	0.067
Exp 17	-142	-0.13

4.2.5.5 Summary of the results using ash effluent as the liquid phase

- Ca is leached from the ash into the effluent during the mixing stage of the experiments. The average value of this leaching, for the 2½ hours of mixing, is 4.26g/kg ash. The majority of the Ca is leached from the ash during the first five minutes of mixing.
- The mass balance results for SO_4 do not show either a general increase or a general decrease in the SO_4 ions in solution during the mixing stage. Since the results are not consistent, no conclusion can be made with respect to the change in SO_4 content of the effluent during the initial contact of the ash with the water.
- There appears to be a general increase in the Na ions in solution during the mixing stage. The average value of this leaching of Na from the ash, for the 2½ hours of mixing, is 0.21g/kg ash.
- There appears to be a general increase in the Cl ions in solution during the mixing stage. The average value of this leaching of Cl from the ash, for the 2½ hours of mixing, is 0.15g/kg ash.

4.2.5.6 Initial leaching using distilled water as the liquid phase

Two identical experiments were conducted using distilled water as the liquid phase, in order to determine what elements are leached from the ash. The overall results of these experiments are discussed in section 4.2.3. In this section it is the initial contact of the ash with the distilled water that was investigated further. Figures 4.22 and 4.23 show the change in the composition of the liquid phase of the slurry mixture. Slurry 1 represents the composition after 5 minutes of mixing, and slurry 2 after 2½ hours of mixing. Obviously the composition of the liquid phase to start with is zero for all the components, since distilled water was used.

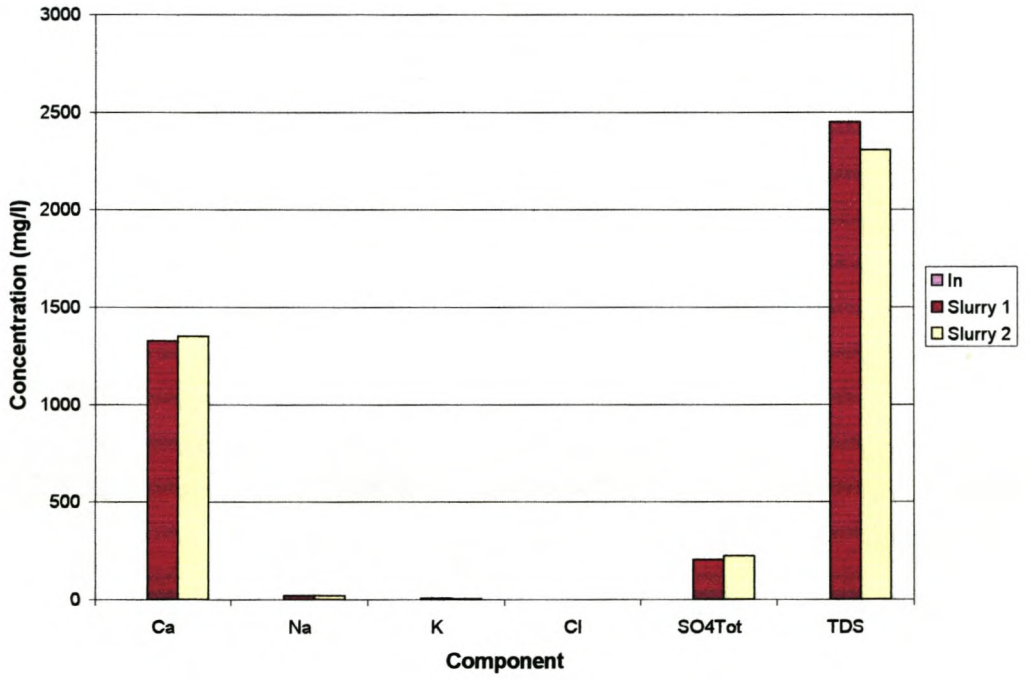

Figure 4.22: Change in liquid phase slurry composition for Exp 13

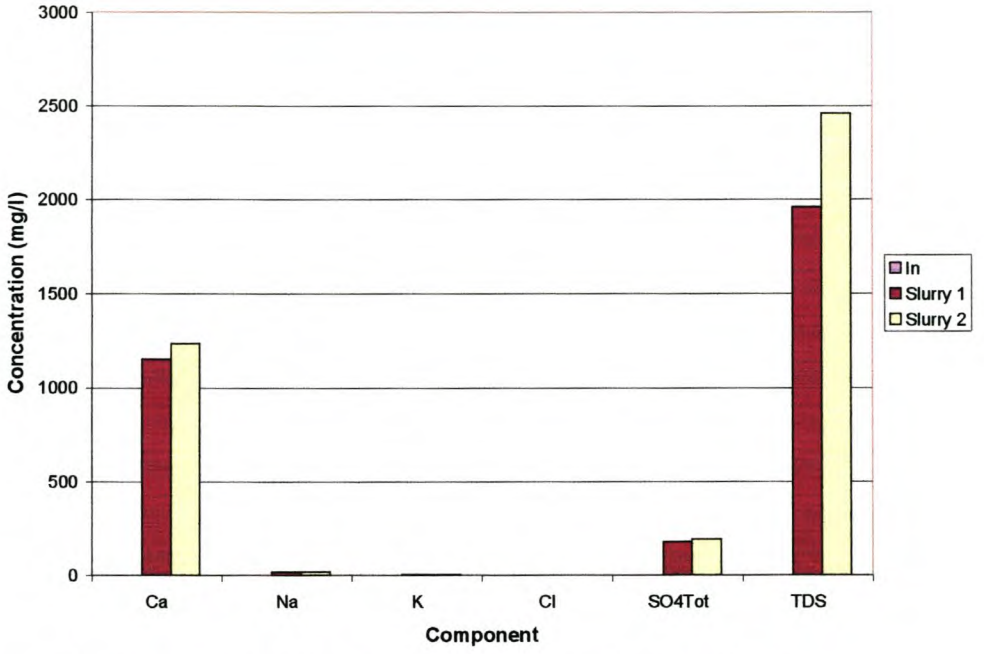

Figure 4.23: Change in liquid phase slurry composition for Exp 14

It is interesting to note that there is no leaching of Cl from the ash into the water, and very little Na and K leach into the water. It is also apparent that there is a drastic change in the composition of the water during the first 5 minutes of mixing. For both experiments there is a dramatic increase in the Ca, SO_4 and TDS concentrations during the first five minutes. Mass balances were performed for the mixing stage of the experiments in order to quantify this change. Figure 4.24 displays all these results.

Table 4.41: Overall Mass Balance Results of Exp 13 and Exp 14 for Phase 1

Component	Experiment	First 5 minutes		After 2½ hours		Overall
		mg	g/kg ash	mg	g/kg ash	g/kg ash
Ca	Exp 13	6720	6.7	111	0.13	6.8
	Exp 14	5789	5.8	348	0.40	6.2
Na	Exp 13	100	0.10	-8	-0.0094	0.091
	Exp 14	83	0.083	0	0	0.083
Cl	Exp 13	0	0	0	0	0
	Exp 14	0	0	0	0	0
SO_4	Exp 13	1014	1.01	95	0.11	1.12
	Exp 14	879	0.88	78	0.090	0.97
TDS	Exp 13	12 408	12.4	-633	-0.73	11.7
	Exp 14	9836	9.8	2236	2.58	12.4

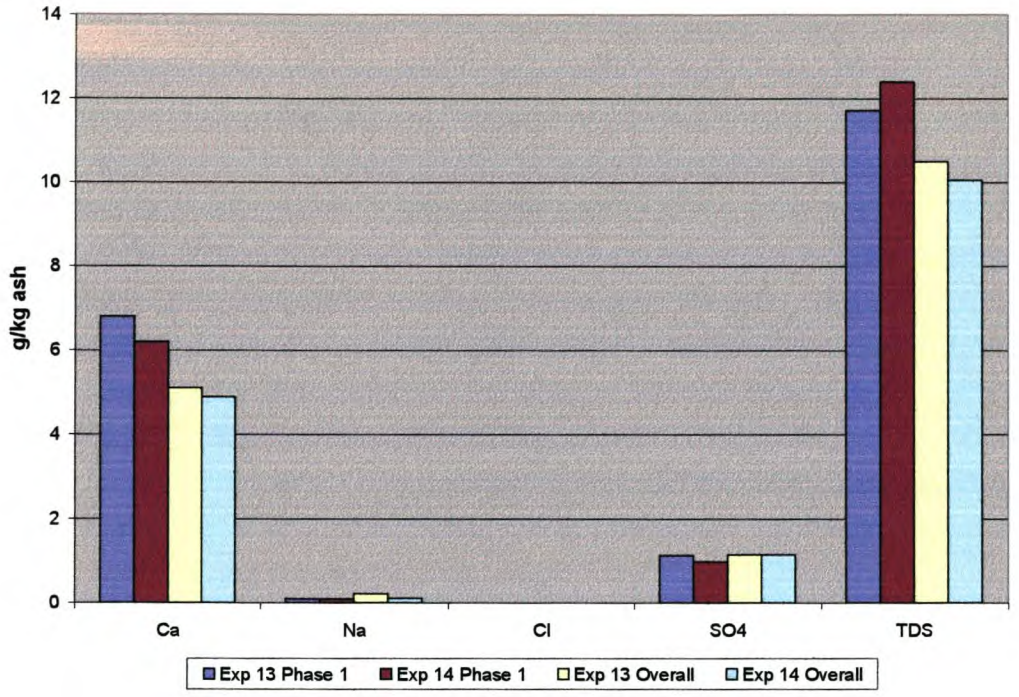

Figure 4.24: Mixing stage and overall mass balance results

It is evident that overall for the mixing stage of the experiment, the mass balance results for the two experiments are very similar. There is an overall increase in the Ca, Na, SO_4, and TDS content of the water, implying that they are leached from the ash into the water. The majority of the leaching for Ca, Na and SO_4 occurs during the first five minutes. Even though there appears to be a decrease in the TDS for the second stage of mixing for Exp 13, the overall result is that there is an increase in the TDS of the water. This overall value (11.7g/kg ash) compares well to the overall value for Exp 14 (12.4g/kg ash). Cl does not appear to leach from the ash when the ash is mixed with distilled water.

4.2.5.7 Combined results: Ash effluent and distilled water as the liquid phase

- Ca, Na and SO_4 appear to have the potential to be leached from the fine ash when it is mixed with water. The composition (e.g. Distilled water or FAM) of the water will determine if in fact these elements are leached from the ash into the water, or if they are in fact removed from the liquid phase due to reactions with the ash.

- Experimental results show that if fine ash is mixed with distilled water, Ca, Na and SO_4 will be leached from the ash into the water (TDS of the water therefore, also increases), with the majority of the leaching occurring during the first five minutes of ash/water contact. Cl is not leached from the ash when distilled water is used as the liquid phase.
- When the industrial effluent FAM is used as the liquid phase, Ca, Na and Cl are leached from the ash. There does not appear to be any trend in the change in SO_4 content of the ash water when FAM is used. These experimental results also show that the majority of the Ca leaching occurs during the first five minutes of ash/water contact.

4.2.6 Trace element analysis

The only trace element, which was detected in the effluent samples from the column experiments, at concentrations high enough to justify further investigation, was strontium. As mentioned in section 4.1.4.6, Sr was tested for using an Inductively Coupled Plasma Atomic Emission Spectrometer (ICP-AES). The mass balance results for Sr are presented in table 4.42 and figure 4.25. In keeping with the presentation of the results for the liquid phase. In all these experiments ash effluent was used as the liquid phase.

Table 4.42: Liquid Phase Mass Balance results for Sr

Exp 1	16.5	mg/kg ash
Exp 2	-7.7	mg/kg ash
Exp 3	16.5	mg/kg ash
Exp 5	86.2	mg/kg ash
Exp 6	44.7	mg/kg ash
Exp 7	69.2	mg/kg ash
Exp 9	-66.4	mg/kg ash
Exp 11	-1.0	mg/kg ash

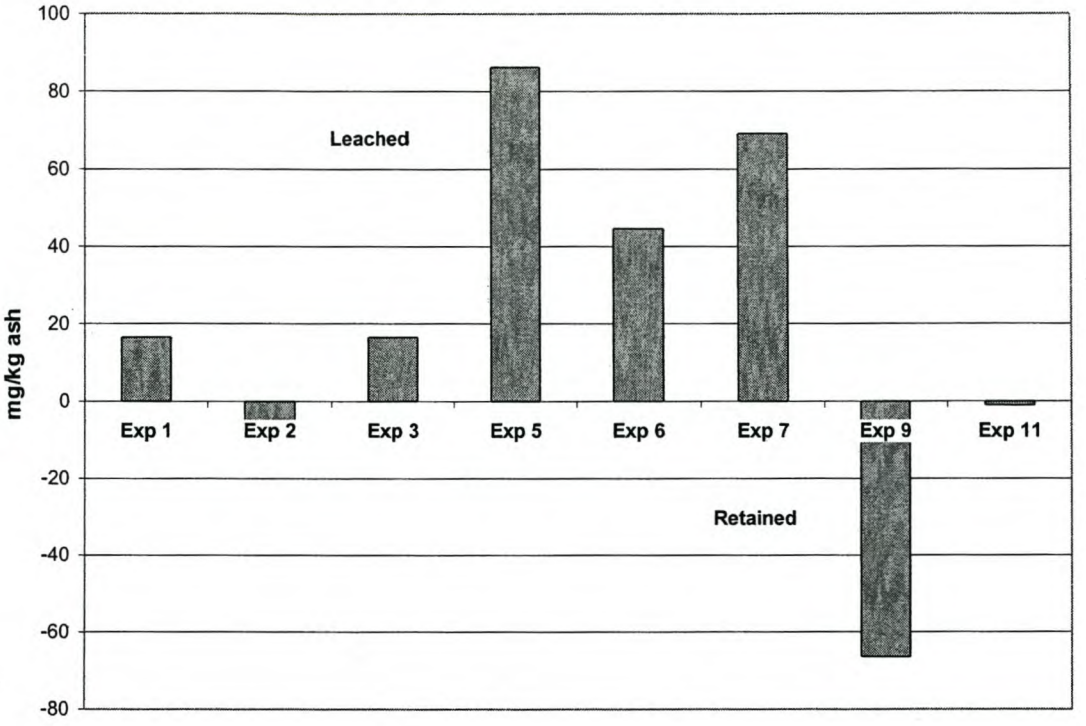

Figure 4.25: Graphical representation of liquid phase mass balance results for Sr

The results shown in table 4.42 and figure 4.25 reveal that according to the liquid phase mass balance results, there is an overall leaching of the Sr from the ash into the effluent.

4.2.7 Comparison to previous laboratory tests conducted

4.2.7.1 Overview

Pretorius (2002) also performed laboratory column experiments to try to simulate the Secunda ash disposal system. The different experiments conducted by Pretorius (2002) can be summarised as follows:

- Basic column leach tests.

  These experiments involved a three-step test process. Firstly the ash and water were mixed for 2½ hours in a mechanical shaker. The second phase involved the transfer of the solid suspension (generated during step 1) into a 50 mm diameter Plexiglas column where the ash solids were allowed to settle. The resulting water layer that

formed above the settled ash was then allowed to freely percolate through to a sample collection bottle. The third step was to force the residual water out of the column by high-pressure nitrogen to prevent secondary reactions.

- Column leach tests under different atmospheres.

  These tests were conducted to investigate the formation of $CaCO_3$ (seen in the basic column experiments) further. Therefore, it was the effect of CO_2, on the weathering process and the salt retention, which was investigated. Experiments were carried out under three different atmospheres, namely, air (some CO_2), CO_2 (100% CO_2) and N_2 (no CO_2). The initial ash water contact was conducted in air, but from the time the slurry passed into the column, it was kept under the specific atmospheres mentioned above.

- The liberation of CO_2.

  These experiments were conducted to confirm the results from the column experiments under different atmospheres. The aim was to determine the presence of carbonate minerals in the ash bed after the respective experiments. This was done by treating the ash with acid and testing for the liberation of CO_2. This liberation of CO_2 can be described by the following reaction:

  $$CaCO_{3(s)} + 2HCl \rightarrow H_2O + CaCl_2 + CO_{2(g)} \qquad (4\text{-}1)$$

- Remobilisation of retained salts by rainwater.

  These tests were conducted to investigate to what extent the salts, retained in ash contact experiments, would be mobilised by rainwater. Rainwater was collected and applied to the columns once all the test water had passed through the ahs bed. The amount of rainwater added was the amount equivalent to a storm evident of 40mm.

4.2.7.2 Discussion of results

Pretorius (2002) used a selection of different ash samples (fresh fine ash, weathered fine ash, fresh course ash, and weathered course ash) with a variety of water samples (FAM, distilled water, and TRO brine) in his column experiments. However, for the purpose of comparison to the results from this investigation, only the combination of fine ash with FAM and distilled water will be discussed.

Basic column experiments

Table 4.43 and table 4.44 compare the results obtained from the column experiments performed in this investigation to those results obtained by Pretorius (2002). Table 4.43 displays the results using FAM and fine ash, and table 4.44 shows the results using distilled water and fine ash.

Table 4.43: Comparison of Column Experiment Results using FAM

Component	Koch (2002)	Pretorius (2002)	Average	Units	
TDS	-1.2	-1.2	-1.2	g/kg ash	Retained in ash
Na	-1.4	-0.49	-0.95	g/kg ash	Retained in ash
Ca	2.8	2.2	2.5	g/kg ash	Leaching from the ash

Table 4.44: Comparison of Column Experiment Results using Distilled Water

Component	Koch (2002)	Pretorius (2002)	Average	Units	
TDS	10.3	10.5	10.4	g/kg ash	Leaching from the ash
Na	0.15	0.15	0.15	g/kg ash	Leaching from the ash
Ca	5.0	4.4	4.7	g/kg ash	Leaching from the ash

It is evident from the results displayed in tables 4.43 and 4.44 that there is a good correlation between the experimental results obtained during this investigation, and those obtained by Pretorius (2002).

Column tests under different atmospheres

The results from these experiments confirmed that the calcium chemistry is affected by the presence of CO_2. Sodium on the other hand does not appear to be affected by the amount of CO_2 available. A summary of the results that Pretorius (2002) found for these experiments is given in table 4.45.

Table 4.45: Comparison of Column Tests Under Different Atmospheres

Component	Carbon Dioxide	Air	Nitrogen	Units
TDS	-9.85 (retained)	-0.72 (retained)	-0.03 (retained)	g/kg ash
Na	-1.13 (retained)	-1.04 (retained)	-1.04 (retained)	g/kg ash
Ca	-3.12 (retained)	1.97 (leached)	2.61 (leached)	g/kg ash

The chemistry, which explains the removal of Ca from the water in the presence of CO_2, can be found in section 2.3.1. The relevant reactions are 2-7, 2-8 and 2-9.

The liberation of CO_2

The results from these experiments further confirmed that the Ca in the ash system is converted to calcite during the weathering process. These results are presented in table 4.46.

Table 4.46: Carbon Dioxide Liberation

Ash Sample	CO_2 liberated (Ncm^3/g ash)
Fresh fine ash	None
Fine ash after column experiment with CO_2	4.8
Fine ash after column experiment with air	1.5
Fine ash after column experiment with N_2	None

From the XRD results of the fine ash analysis (section 4.3.3.2), one would not expect CO_2 to be liberated since the Ca is in the form of lime (CaO) in the ash, and there is no calcite ($CaCO_3$) present. The fact that CO_2 is liberated for the ash exposed to both air and CO_2 confirms that Ca is present in the ash in the form of calcite. It is evident that more CO_2 is liberated from the ash exposed to CO_2 than from the ash exposed to air. This suggests that the addition of CO_2 to the ash water system enhances the calcium carbonate chemistry, with the result being that more Ca is removed from the water and retained as a precipitate in the ash.

Remobilisation of retained salts by rainwater

The result of adding rainwater to the columns after each experiment was that all the major salts initially retained in the ash were flushed out to some extent. Table 4.47 compares the results obtained by Pretorius (2002) and the results obtained from the flushing experiments discussed in section 4.2.4. It is important to note that the two experimental procedures were slightly different, and obviously the amount of each component flushed from the ash will depend, to a large extent, on the amount of water used. The differences in the two experimental procedures are that in this investigation,

the flushing tests were performed using distilled water, whereas Pretorius (2002) used rainwater. The amount of water used was also different. For the flushing tests in this study, about five litres per kg of ash (5*l*/kg ash) was used, whereas Pretorius (2002) used the amount of rainwater equivalent of a 40mm storm event.

Table 4.47: Comparison of Flushing Tests

	Average Remobilisation (mass of component leached as a % of the mass initially retained in the ash)	
Component	**Koch (2002)**	**Pretorius (2002)**
SO_4	5.6%	39%
Na	68%	86%
Cl	84%	70%

What is evident from the results in table 4.47 is that the amount of SO_4 flushed from the ash is the least for both types of flushing experiments examined. A reason why the value for the flushing experiments using rainwater (Pretorius, 2002) is higher than that for distilled water could be due to the fact that the rainwater contains some SO_4.

Overall

In summary one can conclude that the results obtained by Pretorius (202) correlate well with the results obtained during this investigation. The column experiments performed under different atmospheres, as well as the CO_2 liberation tests provided further confirmation of the calcium carbonate chemistry discussed in section 2.3.1.

4.3 Results and discussion: the solid phase

4.3.1 Major Element Analysis

4.3.1.1 Overview

Mass balances were performed for the solid phase (ash) of the column experiments. The data used for these mass balances was attained by means of XRF analysis of the ash samples. The samples that were analysed were the fresh fine ash, the ash from the slurry samples (after 5 minutes of mixing and after 2½ hours of mixing), and the ash left in the column after the experiment was completed. XRF analyses were only performed on the complete set of ash samples from certain experiments, thus only the results from these experiments can be discussed in terms of solid phase mass balances. The overall mass balance results for the major elements are presented in figure 4.26. In keeping with the presentation of the results for the liquid phase, a positive value indicates that the component is leached from the ash into the liquid phase, and a negative value indicates that the component is retained in the ash (removed from the liquid phase). In all these experiments ash effluent was used as the liquid phase.

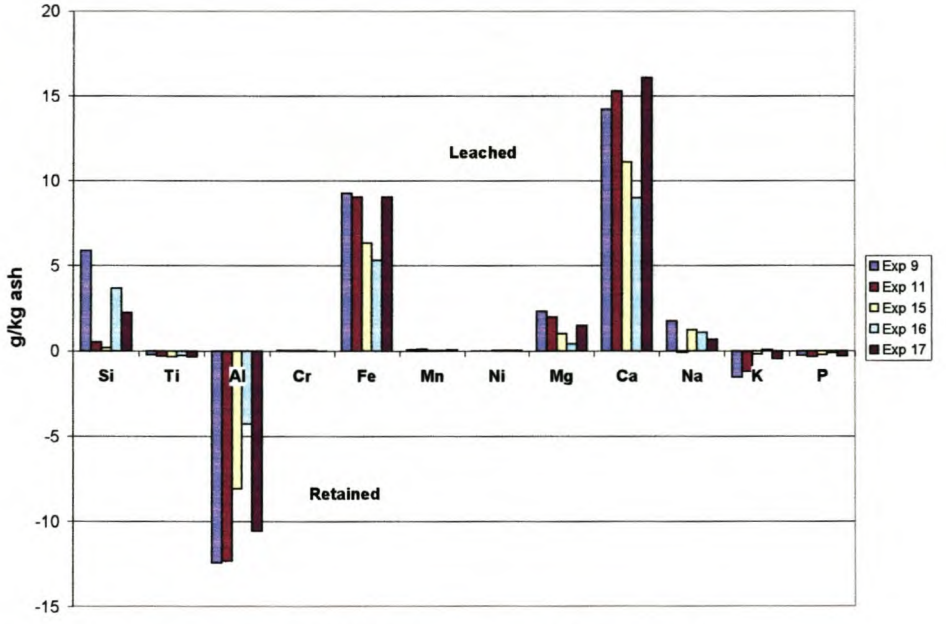

Figure 4.26: Comparison of Solid Phase Mass Balance Results

From these results it is evident that there is an overall leaching of Si, Fe, Mg, Ca and Na from the ash into the water. There also appears to be an overall increase of Al in the ash (i.e. removal of Al from the ash effluent).

The mass balance results, for the experiments in which distilled water was used as the liquid phase, are shown in figure 4.27. These results reveal which components of the ash leach from the ash when the ash is in contact with distilled water.

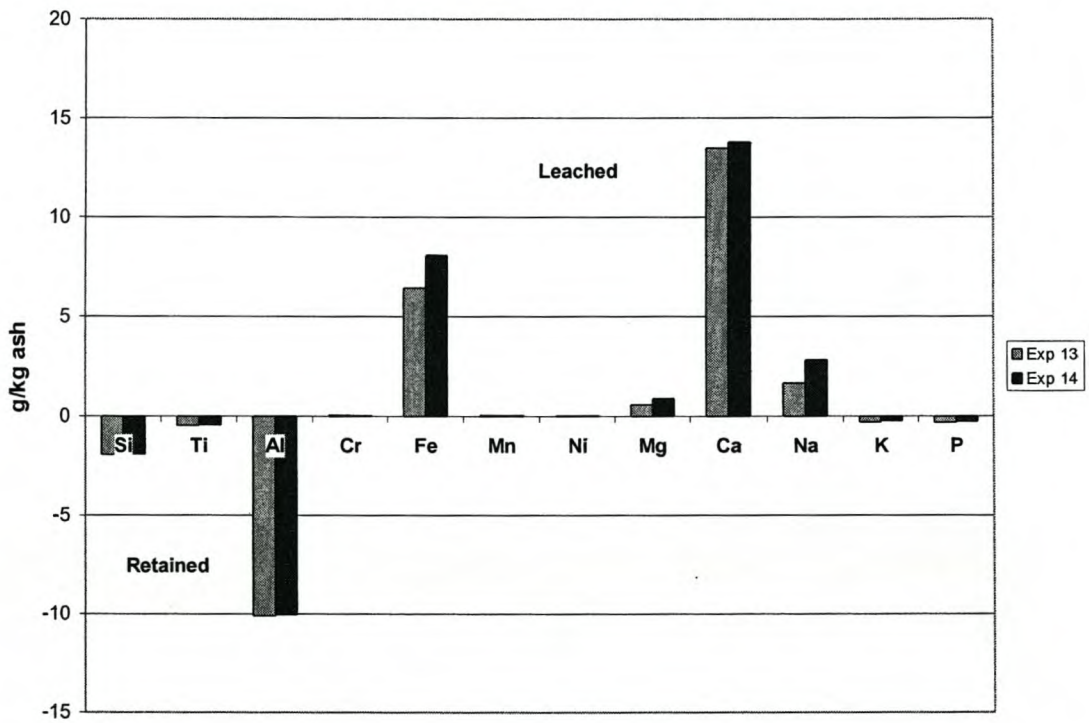

Figure 4.27: Overall mass balance results for distilled water column experiments

These results are very similar to the results from the column experiments using ash effluent as the liquid phase; Fe, Mg, Ca and Na all appear to be leached from the ash. The retention of the Al and Si in the ash reveals that it is not easy to leach these two components from the ash, and reinforces what was noted from previous research, that the solubilities of the Al and Si containing phases are very low (sections 2.3.5 and 2.3.6). It was also noted that more Al and Si are leached from weathered ash as opposed to fresh

ash (Bezuidenhout, 1995). This suggests that the processes involved in the release of Al and Si from the ash are slow, and would not be applicable to these column experiments where fresh ash was used and the entire experiment only lasted for one week. The low values of Al and Si measured in the leachate further support this notion that in the laboratory column experiments performed in this investigation, the Al and Si chemistry does not simulate the chemistry that occurs in the actual ash disposal system.

The effect of flushing the ash in the column with distilled water can be seen in figure 4.28. The values displayed in figure represent (on a g/kg ash basis) the quantity of each component in the ash before and after it was flushed with distilled water.

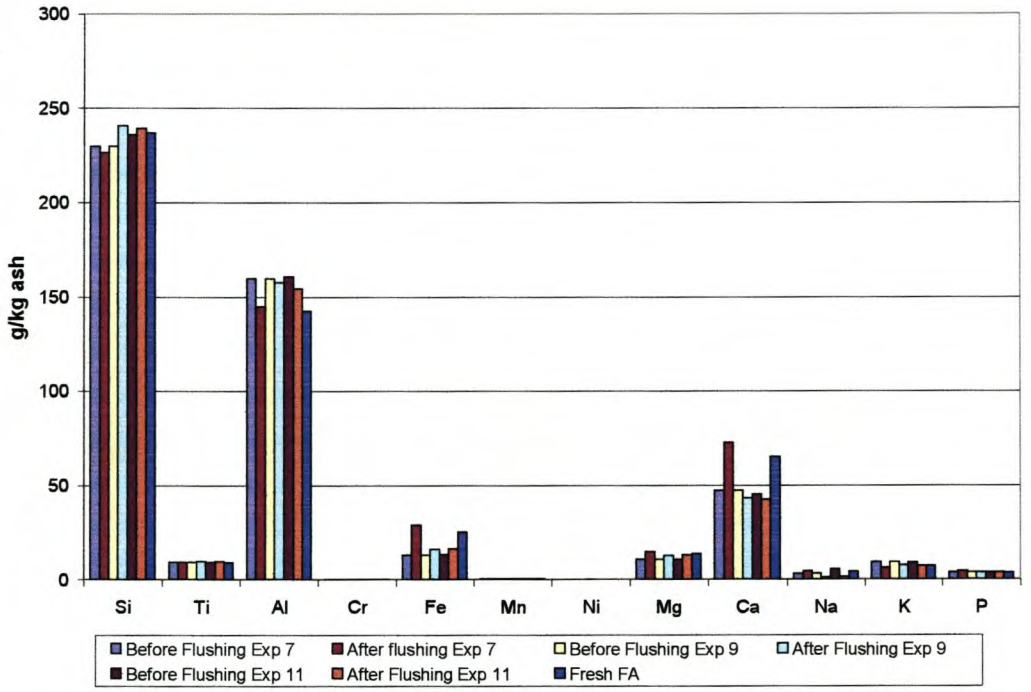

Figure 4.28: Comparison of ash composition before and after flushing with distilled water

If one examines figure 4.28 it is evident that there is not much difference in the composition of the ash before and after flushing, which suggests that by the time the

flushing occurred (one week after start of experiment), the majority of the leachable components had already been leached from the ash. The majority of the elements that are flushed from the ash column (section 4.2.4) are those that are retained by means of hydraulic retention.

4.3.1.2 Phase 1 and Phase 2

The overall mass balance results have already been presented in section 4.3.1.1. This section serves to compare the changes in the ash composition during phase 1 (mixing stage) and phase 2 (the ash/water contact in the column). The results will be presented per element, and only the elements of primary concern will be discussed.

Calcium

The solid phase mass balance results for Ca during phase 1 and phase 2 are presented in table 4.48.

Table 4.48: Solid Phase Mass Balance Results for Ca during Phase 1 and Phase 2

Experiment	Phase 1 (2½ hours of mixing)	Phase 2	Units
Exp 9	2.9	15.0	g/kg ash
Exp 11	5.9	13.9	g/kg ash
Exp 15	1.8	13.7	g/kg ash
Exp 16	3.1	8.9	g/kg ash
Exp 17	8.5	11.3	g/kg ash

The results in table 4.48 show that the majority of the leaching of the Ca from the ash occurs during phase 2, i.e. the time that the ash and water are in contact in the column. The fact that the values for phase 2 are slightly higher for Exp 9 and Exp 11 could be attributed to the fact that the final ash sample for these two experiments was taken after a week, whereas the final ash sample for Exp 15, Exp 16 and Exp 17 was taken after only a day. Thus, the ash and water had a longer contact time during which leaching could occur for Exp 9 and Exp 11. The reason the difference is not that great is because the majority of the water had leached from the ash in the column after a period of 24 hours.

Table 4.49 shows the mass balance results for Ca during the two stages of phase 1, i.e. the change in the Ca content of the ash during the first five minutes as opposed to after 2½ hours of mixing. Due to the fact that Exp 15, Exp 16 and Exp 17 were identical, it is the results from these three experiments that are compared in table 4.49.

Table 4.49: Solid Phase Mass Balances Results for Ca During Phase 1

Experiment	After 5 minutes of mixing	After 2½ hours of mixing	Units
Exp 15	1.9	-0.1	g/kg ash
Exp 16	-0.3	3.4	g/kg ash
Exp 17	5.0	0.5	g/kg ash

The difference in the Ca content of the ash during the first five minutes of mixing compared to the full 2½ hours is not as evident from the solid phase mass balance results as it is from the liquid phase mass balance results (section 4.2.5.1). There is an overall leaching of the Ca from the ash during the mixing stage, however, this leaching does not appear to occur preferentially in the first five minutes of ash/water contact as was evident from the liquid phase mass balance results (table 4.13).

Sodium

The solid phase mass balance results for Na during phase 1 and phase 2 are presented in table 4.50. Only the results from Exp 15, Exp 16 and Exp 17 could be used since the XRF analyses for Na for Exp 9 and Exp 11 were not reliable.

Table 4.50: Solid Phase Mass Balance Results for Na during Phase 1 and Phase 2

Experiment	Phase 1 (2½ hours of mixing)	Phase 2	Units
Exp 15	1.8	-1.0	g/kg ash
Exp 16	2.3	-1.7	g/kg ash
Exp 17	2.3	-2.1	g/kg ash

It is clear that although there is an overall leaching of Na from the ash (figure 4.26), this leaching occurs during the mixing stage, and after that there is actually a retention of Na in the ash (removal from the ash water).

Table 4.51 displays the mass balance results for Na during the two stages of phase 1. These results show an overall leaching of the Na during phase 1 as presented in table 4.50. As was the case with the liquid phase mass balance results (table 4.23), there doesn't appear to be more leaching of the Na from the ash during the first five minutes of ash/water contact as opposed to after 2½ hours.

Table 4.51: Solid Phase Mass Balances Results for Na During Phase 1

Experiment	After 5 minutes of mixing	After 2½ hours of mixing	Units
Exp 15	2.14	-0.47	g/kg ash
Exp 16	1.49	0.81	g/kg ash
Exp 17	1.14	1.19	g/kg ash

Potassium

The solid phase mass balance results for K during phase 1 and phase 2 are presented in table 4.53. From these results it is apparent that there is a leaching of the K from the ash into the liquid phase during the mixing stage, however, during the contact time of the ash and water in the column, the K is retained in the ash (removed from the water). The result of this is the overall retention of K in the ash as seen in figure 4.26. As was the case with Ca, there is a greater retention of K in the ash for Exp 9 and Exp 11. A possible reason for this could be the longer ash/water contact time for Exp 9 and Exp 11 (one week) compared to Exp 15, Exp 16 and Exp 17 (24 hours). For Exp 9 and Exp 11 the ash was removed from the column a week after the experiment was started, whereas for Exp 15, Exp 16 and Exp 17, the ash was removed from the column after 24 hours. The reason for this was that the majority of the water had leached from the ash in the column after a period of 24 hours, and the column was needed for the next experiment.

Table 4.52: Solid Phase Mass Balance Results for K during Phase 1 and Phase 2

Experiment	Phase 1 (2½ hours of mixing)	Phase 2	Units
Exp 9	0.2	-2.3	g/kg ash
Exp 11	0.1	-2.0	g/kg ash
Exp 15	0.3	-0.7	g/kg ash
Exp 16	0.3	-0.3	g/kg ash
Exp 17	0.2	-0.9	g/kg ash

Table 4.53 shows the mass balance results for K during the two stages of phase 1. Due to the fact that Exp 15, Exp 16 and Exp 17 were identical, it is the results from these three experiments that are compared in table 4.53.

Table 4.53: Solid Phase Mass Balances Results for K During Phase 1

Experiment	After 5 minutes of mixing	After 2½ hours of mixing	Units
Exp 15	0.27	-0.04	g/kg ash
Exp 16	0.33	-0.03	g/kg ash
Exp 17	0.22	-0.07	g/kg ash

These results show that the leaching of the K from the ash occurs during the first five minutes of ash/water contact. After that there is actually a retention of the K in the ash (removal from the liquid phase).

Iron

Although Fe could not be detected in the ash water in significant quantities to be classified as a major element, in the ash it is one of the main components. It was also evident from the overall mass balance results (figure 4.26) that there was a significant change in the Fe content of the ash during the experiments. Therefore, these changes in the Fe content of the ash were explored further. The solid phase mass balance results for Fe during phase 1 and phase 2 are presented in table 4.54. These results show that there is a leaching of the Fe from the ash during both phase 1 and phase 2, however, the majority of the leaching occurs during phase 2. The fact that the leaching of Fe during phase 2 for Exp 9 and Exp 11 is greater than the leaching for Exp 15, Exp 16 and Exp 17, can be

attributed to the longer ash/water contact time in the column for Exp 9 and Exp 11 (as described in section 4.2.2.1).

Table 4.54: Solid Phase Mass Balance Results for Fe during Phase 1 and Phase 2

Experiment	Phase 1 (2½ hours of mixing)	Phase 2	Units
Exp 9	0.1	12.1	g/kg ash
Exp 11	2.6	9.3	g/kg ash
Exp 15	1.7	7.0	g/kg ash
Exp 16	1.7	5.5	g/kg ash
Exp 17	5.5	5.3	g/kg ash

The mass balance results during the two stages of phase 1 are presented in table 4.55. These results once again show that Fe is leached from the ash during the mixing stage (phase 1). Leaching of the Fe occurs during the first five minutes as well as during the full 2½ hours, with no discernable pattern evident as to when the majority of the leaching occurs.

Table 4.55: Solid Phase Mass Balances Results for Fe during Phase 1

Experiment	After 5 minutes of mixing	After 2½ hours of mixing	Units
Exp 15	0.5	1.2	g/kg ash
Exp 16	0.9	2.6	g/kg ash
Exp 17	3.4	2.1	g/kg ash

Magnesium

It was difficult to assess the changes in magnesium during the column experiments from a liquid phase viewpoint, since the concentrations of Mg in the ash water were too low. Therefore, the changes in the Mg content of the ash were considered, base on solid phase mass balances. The solid phase mass balance results for Mg during phase 1 and phase 2 are presented in table 4.56.

The results of the mass balances for the two different phases, namely, phase 1 and phase 2, reveal that the majority of the leaching of the Mg from the ash occurs during phase 2.

During the mixing stage there is very little change in the Mg content of the ash. There is also a noticeable difference between the amount of Mg leached from the ash for Exp 9 and Exp 11 compared to the amount leached during Exp 15, Exp 16 and Exp 17. The increased leaching observed for Exp 9 and Exp 11, during phase 2, can be attributed to the longer ash/water contact time for these two experiments. A detailed explanation of the difference in the contact time in the column for the experiments is given in section 4.2.2.1.

Table 4.56: Solid Phase Mass Balance Results for Mg during Phase 1 and Phase 2

Experiment	Phase 1 (2½ hours of mixing)	Phase 2	Units
Exp 9	-0.4	3.6	g/kg ash
Exp 11	-0.1	3.1	g/kg ash
Exp 15	0.0	1.6	g/kg ash
Exp 16	-0.3	1.2	g/kg ash
Exp 17	0.2	1.9	g/kg ash

Table 4.57 presents the mass balance results for Mg during the first five minutes of mixing and after 2½ hours of mixing.

Table 4.57: Solid Phase Mass Balances Results for Mg during Phase 1

Experiment	After 5 minutes of mixing	After 2½ hours of mixing	Units
Exp 15	-0.5	0.5	g/kg ash
Exp 16	-0.8	0.5	g/kg ash
Exp 17	-0.2	0.4	g/kg ash

The results in table 4.57 reveal that there appears to be an initial increase in the Mg content of the ash (during the first five minutes of mixing), after which time there is a decrease. This suggests that the leaching of the Mg from the ash is not as rapid as for an element such as Ca.

4.3.1.3 Consolidation of the solid phase results for the major elements

- There appears to be an overall leaching of Si, Fe, Mg, Ca and Na from the ash into the liquid phase, and an overall retention of Al in the ash (removal from the ash water).
- Flushing of the ash column after an experiment does not seem to alter the chemical composition of the ash greatly, i.e. the majority of the leachable components are leached from the ash during the duration of the experiment.
- During phase 1 there is an overall leaching of Ca, Na, K, and Fe from the ash into the water. For K, this leaching occurs during the first five minutes after which time the K appears to be retained in the ash (removed from the water). There isn't any drastic change in the Mg content of the ash during the mixing stage.
- During phase 2, Ca, Fe and Mg are leached from the ash. The amount of Ca leached from the ash during phase 2 is significantly more than during phase 1. Na and K are both retained in the ash during phase 2, i.e. they are removed from the water in contact with the ash in the column.
- The amount of Ca, Fe and Mg leached from the ash, and the K retained in the ash, during phase 2, is much greater for Exp 9 and Exp 11 compared to Exp 15, Exp 16 and Exp 17. A reasonable explanation for this is that for Exp 9 and Exp 11, the ash was left in the column for a week before the final ash sample was taken, whereas for Exp 15, Exp 16 and Exp 17, the ash was only left in the column for a period of 24 hours. This longer ash/water contact time appears to affect the chemical processes occurring in the column. It should, however, be noted that the majority of the water passes through the ash column in the first 24 hours; after 24 hours there is no visible sign of leachate passing from the column into the collecting dish. Thus, the water retained in the ash by means of hydraulic retention, continues to react with the ash causing a change in the composition of the ash.

4.3.2 Trace element analysis

Mass balances were performed for the solid phase (ash) of the column experiments. The data used for these mass balances was attained by means of XRF analysis of the ash samples. The samples that were analysed were the fresh fine ash, the ash from the slurry samples (after 5 minutes of mixing and after 2½ hours of mixing), and the ash left in the column after the experiment was completed. XRF analyses were only performed on the complete set of ash samples from certain experiments, thus only the results from these experiments can be discussed in terms of solid phase mass balances. The overall mass balance results for the trace elements are presented in figure 4.29. In all these experiments ash effluent was used as the liquid phase.

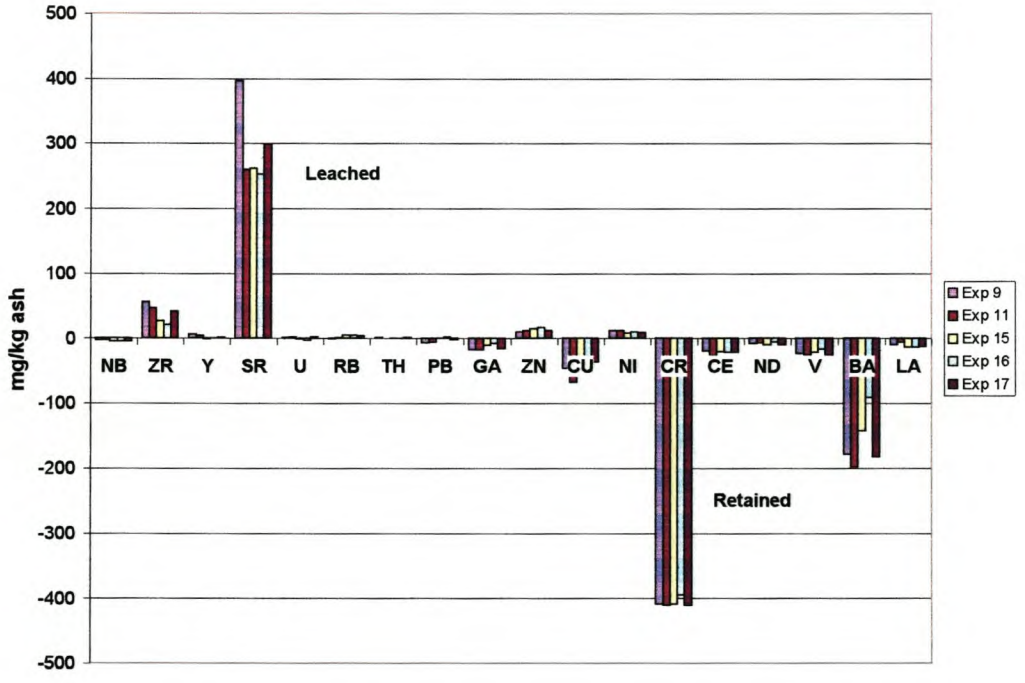

Figure 4.29: Comparison of solid phase mass balance results (trace elements)

The results displayed in figure 4.29 reveal that there is an overall leaching of Sr and Zr from the ash into the liquid phase. Ba, Cu and Cr on the other hand appear to be removed

from the liquid phase and retained in the ash. The change in composition of the other trace elements in the ash, during the column experiments, is minimal.

It is interesting to compare the mass balance results for the trace elements to the relative quantities of the trace elements in the fresh fine ash before it was mixed with ash effluent. Figure 4.30 displays the distribution of the trace elements in the fresh fine ash.

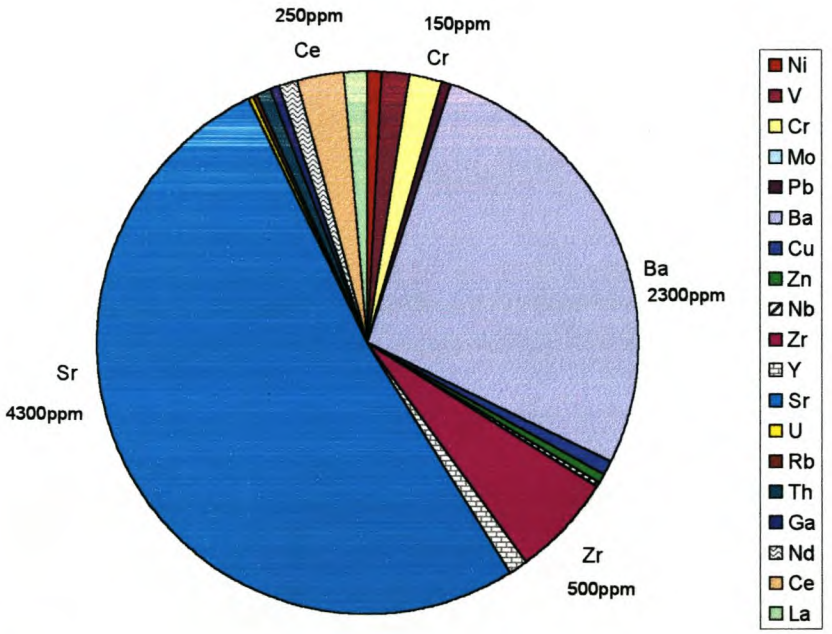

Figure 4.30: Distribution of trace elements in fresh fine ash

From figure 4.30 it is evident that Ba is present in the ash at fairly high concentrations, however, the mass balance results in figure 4.29 show that Ba is not leached from the ash during the column experiments. The same can be said for Cr and Ce even though they are present in the ash at lower concentrations than Ba. Sr on the other hand is present in the ash at high concentrations, but is leached from the ash into the water. Zr is also leached from the ash into the water in small quantities.

4.3.3 Mineral phases

4.3.3.1 Overview

When the bulk ash was removed after an experiment for XRD and XRF analyses, there was still pore water present in the ash. The samples were, therefore left to dry in the air before being analysed. However, during this time it is possible that reactions could still occur and thus, alter the analyses. Hassett et al. (1985) investigated this possibility with their weathered ash samples. Some of the samples they ground in a large excess of ethanol prior to analysis, and others they left to air-dry over a period of a couple of days. The only difference that they found in the XRD analyses of the samples was that there was more calcite present in the samples that were left to air-dry (CO_2 present). This can be explained by the following reactions 2-7, 2-8, and 2-9, given in section 2.3.1.

Hassett et al. (1985) also found that the diffractograms of the fresh ash did not differ much from the diffractograms of the ash after the leaching experiments. The only difference that they found was that the peak heights of calcite, periclase and melilite increased relative to the other phases. Overall, they found that the amount of crystalline phases was greater in the leached samples. A possible explanation for this could be the preferential dissolution of the glass phase(s) in the ash compared to the more resistant crystalline phases. They identified melilite, quartz and ferrite spinel to be the main phases present after the leaching experiments, and therefore, concluded that phases most resistant to leaching are melilite, quartz, hematite and ferrite spinel.

The secondary mineral phases which have been identified in fly ash include ettringite [$Ca_6Al_2(SO_4)_3(OH)_{12}.26H_2O$], calcium aluminates and silicates, calcite and amorphous ferric hydroxide. The important role of these secondary mineral phases is in controlling the dissolution of the trace elements.

Rousseau (1997) found the following minerals and relative proportions in the two different fly ashes studied (see table 4.58):

Table 4.58: Mineral Phases Present in Fly Ash

	Hendrina	Kriel
Mullite	48.6	35.4
Alpha quartz	29.2	20.5
Lime	0.5	3.7
Anhydrite	<0.1	0.3
Calcite	<0.1	<0.1
Hematite	1	<0.1
Magnetite	2.7	2.1
Glass	18	38
TOTAL	100	100

4.3.3.2 Column experiments

Pretorius (2001) found the relative percentages of the main crystalline in the fresh fine ash at Secunda to be:

Mullite: 67%

Quartz: 26%

Lime: 7%

Calcite: 0%

The fresh fine ash used in the column experiments was analysed by means of XRD. The main mineral phases present in the fresh fine ash were found to be mullite, quartz and lime (also identified by Pretorius, 2001), as well as hematite. The diffractogram of the fresh fine ash is given in section 5.2.6 (figure 5.35). Campbell (1999) also found mullite and quartz, to be present in unweathered fly ash, as well as lesser amounts of lime and hematite. No calcite was detected in the fresh fine ash analysed in this investigation, or in the fresh fine ash (produced at Secunda) analysed by Pretorius (2001). Table 4.59 presents the results of the XRD analyses performed on the ash after the column experiments (the diffractograms for all these ash samples can be found in Appendix C3).

From the results displayed in table 4.59 it is evident that there is not much difference in the mineralogical composition of the ash before and after the column experiments, however, there is a significant difference in the Ca-containing minerals.

Table 4.59: Mineral Phases Present in Ash After Column Experiments

Experiment	Sample Name	$Al_6Si_2O_{13}$ mullite	SiO_2 quartz	$CaCO_3$ calcite	Al_2SiO_5 sillimanite	$CaSiO_3$ calcium silicate	$FeO(OH)$ goethite	Fe_2O_3 hematite	MgO periclase	CaO Lime
	Fresh FA	mullite	quartz					henatite		lime
After Exp 7	FA-8	mullite	quartz	calcite	sillimanite	calcium silicate				
After flushing Exp 7 ash	FA-9	mullite	quartz		sillimanite	calcium silicate				
After Exp 9	FA-10	mullite	quartz	calcite	sillimanite	calcium silicate				
After flushing Exp 9 ash	FA-11	mullite	quartz	calcite	sillimanite					
After Exp 11	FA-12	mullite	quartz	calcite	sillimanite					
After flushing Exp 11 ash	FA-13	mullite	quartz		sillimanite					
After Exp 13 (Dist. Water)	FA-14	mullite	quartz	calcite	sillimanite		goethite			
After Exp 14 (Dist. Water)	FA-15	mullite	quartz	calcite	sillimanite			hematite		
After Exp 15	FA-16	mullite	quartz	calcite	sillimanite					
After Exp 16	FA-17	mullite	quartz	calcite	sillimanite				periclase	
After Exp 17	FA-18	mullite	quartz	calcite	sillimanite			hematite		

In the fresh fine ash, the dominant Ca-containing mineral is lime and no calcite was detected. In the ash samples taken from the column after the respective experiments, Ca is present predominantly as calcite. Some of the ash samples also show that Ca is present as calcium silicate. In two of the ash samples (FA-9 and FA-13), no Ca-bearing mineral phase was detected by means of XRD. However, both these ash samples were taken after the ash column was flushed with distilled water, and prior to the flushing of the column calcite was detected in the ash (FA-8 and FA-12 respectively).

It is also interesting to note that Fe-containing minerals were detected in both the ash samples after distilled water was used as the liquid phase in the column experiment. In most of the other samples, no Fe-containing phases were detected. The mineral periclase (MgO) was found to be present in the ash after experiment 16, which is not surprising since according to Bezuidenhout (1995), Swaine (1995) and Jones (1995), the dominant crystalline compound of Mg is periclase. The fact that no periclase was detected in the other ash samples can be attributed to the low concentrations of Mg in both the ash and the effluent to begin with.

4.3.4 Consolidation of the solid phase results

The results obtained from the column experiments, from a solid phase viewpoint, can be summarised as follows:

- There appears to be an overall leaching of Si, Fe, Mg, Ca and Na from the ash into the liquid phase, and an overall retention of Al in the ash (removal from the ash water).
- Flushing of the ash column after an experiment does not seem to alter the chemical composition of the ash greatly.
- During phase 1 there is an overall leaching of Ca, Na, K, and Fe from the ash into the water. For K, this leaching occurs during the first five minutes after which time the K appears to be retained in the ash (removed from the water). There isn't any drastic change in the Mg content of the ash during the mixing stage.

- During phase 2, Ca, Fe and Mg are leached from the ash. Na and K are both retained in the ash during phase 2. Therefore, the water, retained in the ash by means of hydraulic retention, continues to react with the ash causing a change in the composition of the ash. The length of the ash/water contact time in the column appears to affect the degree of leaching or retention of the various elements.
- There appears to be an overall leaching of Sr and Zr from the ash into the liquid phase. Ba, Cu and Cr on the other hand appear to be removed from the liquid phase and retained in the ash. The change in composition of the other trace elements in the ash, during the column experiments, is minimal.
- The main mineral phases present in the ash after the column experiments were found to be mullite, quartz, calcite, sillimanite, and to a lesser extent, Fe-containing minerals such as hematite. The most significant change in the mineralogical composition of the ash during the column experiments is the conversion of lime (CaO) to calcite ($CaCO_3$).

4.4 Comparison of liquid and solid phase experimental results

4.4.1 Overall

After a period of a week, the liquid phase mass balance results show that there is an overall leaching of Ca from the ash into the water (±2.8g/kg ash), and an overall retention of Na, Cl and SO_4 in the ash. The solid phase mass balance results also show that there is an overall leaching of the Ca from the ash (±13.0g/kg ash). The difference in the leaching of the Ca, from the ash, for the liquid and solid phases can be accounted for by the removal of Ca from the liquid phase due to the precipitation of calcite.

The solid phase mass balance results show that there is an overall leaching of Na from the ash. However, if one examines the mass balances per phase, it is evident that this leaching only occurs during phase 1 (the mixing stage). During phase 2, Na is actually

retained in the ash (removed from the ash water). A further explanation for the retention of Na, as seen from a liquid mass balance viewpoint, is the Na retained in the ash column by means of hydraulic retention.

The solid phase mass balance results show further that there is a leaching of Mg, Fe and Si from the ash, and a retention of Al. These results cannot be compared to results from liquid phase mass balances since their concentrations in the liquid phase were too low. As mentioned above, one can compare the liquid and solid phase mass balance results for Ca and Na, since both were tested for in the liquid phase and in the solid phase.

4.4.2 Calcium

Phase 1

Both the liquid and solid phase mass balance results reveal a leaching of Ca during the mixing stage of the column experiments. A comparison of these results is given in table 4.60.

Table 4.60: Comparison of Liquid and Solid Phase Mass Balance Results for Ca

Experiment	Liquid	Solid	Units	
Exp 9	3.55	2.9	g/kg ash	leached
Exp 11	5.93	5.9	g/kg ash	leached
Exp 15	3.45	1.8	g/kg ash	leached
Exp 16	2.93	3.1	g/kg ash	leached
Exp 17	1.97	8.5	g/kg ash	leached

It is evident from these results that although both the liquid and solid phase mass balance results reveal that Ca is leached from the ash into the water, the values are not exactly the same (except for Exp 11). A possible explanation for the differences in these values is that the calcite precipitates during phase 1. In other words, all the Ca that is leached from the ash will not necessarily be evident as an increase in the liquid phase; some of it will be removed from the liquid phase as calcite precipitate. This notion is reinforced by the results from the liquid phase that show that the majority of the Ca is leached during the first five minutes of ash/water contact (table 4.33). If one compares these values to the

values for the leaching after 2½ hours, it is clear that there is not a large increase in the Ca content of the water during the full 2½ hours of mixing. However, the solid phase mass balance results reveal that there is still leaching of Ca from the ash during the entire mixing period. Therefore, if Ca is leached from the ash, but not reflected as an increase in Ca ions in solution, then this suggests the formation of a Ca based precipitate.

Phase 2

During phase 2, the liquid phase mass balance results show that on average there is a 4.15g/ kg ash increase of Ca in the water. The solid phase mass balance results reveal a leaching of 13.0g/kg ash of Ca from the ash into the water. Since there is only a 4.15g/kg ash increase in the Ca ions in solution, the rest of the Ca that is leached from the ash must be accounted for by the formation of a Ca based precipitate.

4.4.3 Sodium

Phase 1

During the mixing stage of the experiments, both the liquid phase and solid phase mass balance results reflect that Na is leached from the ash into the water. Neither set of results reveal a preferential leaching of the Na during the first five minutes of ash/water contact.

Phase 2

During phase 2, both the liquid phase and solid phase mass balance results show that there is a retention of Na in the ash, i.e. a removal of the Na ions from solution. The average retention from a liquid mass balance viewpoint is 1.7g Na per kg ash, whereas the average retention of Na in the ash from a solid phase mass balance viewpoint is only 0.9g Na per kg ash. An explanation for the difference in these two values is that not all the Na retained is bound to the ash; some of it is retained in the ash column by means of hydraulic retention.

4.4.4 Strontium

There is a good correlation between the liquid phase and solid phase mass balance results for Sr: they both reveal that Sr is leached from the ash into the water.

4.5 Summary

Precaution should be taken when attempting to use the results obtained from laboratory scale batch experiments in the actual ash disposal system. These laboratory tests, in isolation, do not provide sufficient information regarding thermodynamic and kinetic properties of the primary geochemical processes occurring in the actual ash disposal system. However, these results do provide some insight into the changes, which occur when fine ash is contacted with an effluent, and combined with the actual plant data, should provide one with a more comprehensive understanding of the working of a wet ash disposal system.

4.5.1 The liquid phase

From the results obtained for the column experiments, as seen from a change in the composition of the liquid phase, the following conclusions can be drawn:

- The main elements to consider when looking at the change in composition of the effluent are: Ca, Na, Cl, and SO_4.
- Na, Cl and SO_4 are retained in the ash, i.e. these components are removed from the liquid phase. However, during the mixing stage (phase 1), an overall increase in the Na and Cl ions in solution was evident i.e. they are initially leached from the ash.
- The SO_4 that was removed from the water and retained in the ash, appears to be retained in a stable form within the ash and cannot be easily flushed out. This suggests that the ash system could act as a possible salt sink for SO_4.
- Some of the Na that is retained in the ash was flushed out when distilled water was added to the ash column, however, there is still an overall retention of Na within the ash column.

- Most of the Cl retained in the ash can be flushed out with distilled water; suggesting that it is either retained by means of hydraulic retention, or else by means of adsorption.
- Ca is initially leached from the ash, but is further removed from the liquid phase by means of calcite precipitation, which occurs during phase 3 of the entire disposal process.
- The formation of calcite during phase 3 was confirmed due to the fact that both the Ca and the CO_3^{2-} were removed from the leachate during the five weeks that the leachate was allowed to stand in the collecting dish (Exp 15, Exp 16, and Exp 17). Furthermore, the XRD analysis of the calcite precipitate collected from the surface of the leachate in the collecting dish showed that the dominant mineral phase present in the precipitate was calcite.
- The majority of the Ca is leached from the ash during the first five minutes of ash/water contact.
- In general, the pH remains fairly constant throughout the experiments (at a value of approximately 12). However, there is an initial increase in the pH during the mixing stage; then a fairly constant pH for the time the water spends percolating through the ash column and for the first 24 hours that the leachate spends in the collecting dish; and finally after a week there is a reduction in the pH of the leachate. This variation in pH can be attributed to the various chemical reactions that occur during the different phases of the disposal process.
- When a concentrated NaCl stream is added to the initial ash effluent, Na and Cl are still retained in the ash, however, when the ash is flushed with distilled water after the experiments, all the Cl that was retained appears to be flushed from the ash.
- When distilled water is used as the liquid phase instead of effluent, Ca, Na, Cl, and SO_4 are leached from the ash into the water.
- An overall leaching of Sr from the ash into the liquid phase was observed.

4.5.2 The solid phase

From the results obtained for the column experiments, as seen from a change in the composition of the ash, the following conclusions can be made:

- Overall, Si, Fe, Mg, Ca and Na all appear to be leached from the ash into the liquid phase, and Al appears to be retained in the ash (removal from the ash water).
- Flushing of the ash column after an experiment does not seem to alter the chemical composition of the ash greatly.
- During phase 1 Ca, Na, K, and Fe are leached from the ash into the water. For K, this leaching occurs during the first five minutes after which time the K appears to be retained in the ash (removed from the water). There isn't any drastic change in the Mg content of the ash during the mixing stage.
- During phase 2, Ca, Fe and Mg are leached from the ash. Na and K are both retained in the ash during phase 2. Therefore, the water, retained in the ash by means of hydraulic retention, continues to react with the ash causing a change in the composition of the ash. The length of the ash/water contact time in the column appears to affect the degree of leaching or retention of the various elements.
- There appears to be an overall leaching of Sr and Zr from the ash into the liquid phase. Ba, Cu and Cr on the other hand appear to be removed from the liquid phase and retained in the ash. The change in composition of the other trace elements in the ash, during the column experiments, is minimal.
- The main mineral phases present in the ash after the column experiments were mullite, quartz, calcite, sillimanite, and to a lesser extent, Fe-containing minerals such as hematite. The most significant change in the mineralogical composition of the ash during the column experiments is the conversion of lime (CaO) to calcite ($CaCO_3$).

4.5.3 Overall

If one examines both the liquid and the solid phase results, it is evident that there are some discrepancies with respect to certain elements. For example, solid phase mass balances show that Ca is leached from the ash, whereas if one examines the change in the

Ca content of the liquid phase, Ca is actually removed from the effluent. This observation highlights the fact that it is not merely the contact of the ash with the water that plays a role in the chemical changes that occur in the disposal system, but also the retention time of the effluent in the evaporation and CAE dams (phase 3). It is during phase 3 that many important chemical reactions occur, such as the precipitation of calcite, which result in an improved ash water quality. If these salts were not removed during phase 3 they would build up in the effluent that is recycled to the factory and in turn the entire operation of the ash disposal would be affected.

Both the liquid phase and solid phase mass balance results divulge that during phase one, the initial contact of the ash with the water, a lot of chemical reaction occur which alter both the ash water quality and the composition of the ash.

4.6 Recommendations

From the results obtained from the laboratory column experiments, the following recommendations can be made:

- In order to assess the extent to which SO_4 is retained in the ash, it is suggested that further column experiments be performed. These column experiments should incorporate the addition of a concentrated SO_4 stream to the effluent during the mixing stage. Since K does not appear to play a major role in the ash disposal system, it is recommended that the form in which SO_4 be added to the effluent is as dissolved K_2SO_4. One cannot add SO_4 in the form of H_2SO_4 since this would lower the pH of the system, and as the results of this investigation have shown, the chemical reactions that occur are extremely sensitive to pH.
- The addition of CO_2 to the system should be investigated. The calcium carbonate chemistry, which occurs prominently in the ash water system, could be enhanced by the addition of CO_2. Column experiments could be used to determine during which phase the addition of the CO_2 is the most effective. However, one needs to bear in

mind that if CO_2 is added during phase 1, the precipitation of calcite in the pipelines at Inside Ash could cause scaling problems.

- The retention time for phase 3 could be explored further. As was evident from the results of this investigation, when the retention time was extended from one week to three weeks, the quality of the ash water changed dramatically (especially with respect to Ca). It is suggested that both the leachate as well as the precipitate be examined at regular time intervals. XRF as well as XRD analyses should be performed on the precipitate, which forms on the surface of the leachate, in order to understand both the chemical and mineralogical variations of the precipitate with time.
- Further investigations should be carried out on the chemistry which occurs during the initial ash water contact (phase 1). The results from this chapter reveal that this initial contact period is important and may be the most effective point of addition of concentrated salt streams to the system.

Chapter 5

Core Drilling into an Active and Inactive Ash Dam

The change in the chemical composition of the ash effluent throughout the ash disposal system is well documented, and is discussed in chapter 3. However, in order to obtain a more comprehensive understanding of the salt holding capacity and efficiency of the ash dams, it is necessary to look more closely at the ash itself under field conditions. For this reason, boreholes were drilled into some of the ash dams at Sasol, Secunda.

McKnight Geotechnical Consulting (Pty) Ltd (MGC) was appointed to perform the drilling procedure, which incorporated the drilling of three vertical boreholes: one in the centre of an inactive ash dam, and two in an active ash dam; one near the edge and one near the centre. Each of the boreholes was through the ash dam and approximately 5m into the underlying material in order to provide information concerning the nature of both the ash and the underling material. Standard Penetration Testing (SPT) was carried out in each borehole at approximately 2.5m depth centres in order to provide a profile of the variation in the density of the ash with depth. Shelby samples were taken at 5m depth centres where possible so as to provide undisturbed sample material for test purposes. The rest of the core material, retrieved from the aluminium split-tube core barrel, was packaged, labelled and stored for test procedures that did not require undisturbed samples.

The aim of this investigation was to obtain samples for analysis so as to provide data concerning: texture, void ratio, density, specific gravity, Atterberg Limits, natural moisture content, permeability, and chemical and mineralogical composition. The results

of these analyses were used in conjunction with the previously available plant data (chapter 3) and the laboratory column experiments (chapter 4) to attain a more thorough understanding of the working of the ash disposal system utilised by Sasol 2 and Sasol 3 in Secunda.

5.1 Materials and methods

5.1.1 The drilling site

The drilling of the core sections through the ash dams used by Sasol II and Sasol III, in Secunda, was based on the following criteria:

- The site had to be accessible by a 7-ton drill rig/truck.
- At least one core section needed to be located close to the deepest part of the ash dam in order to assess the ash that had been in the dam for the longest period of time.
- At least one core section had to be located on an active ash dam, and one on an inactive ash dam.
- If possible, one core section should be drilled near the centre of an ash dam, and one near the edge, in order to ascertain the water table profile in the dams.

5.1.1.1 Geology of the site

McKnight Geotechnical Consulting (Pty) Ltd (MGC) assessed the geology of the site beneath the ash dams in Secunda. They found it to consist of horizontal layers of sedimentary rocks of the Vryheid Formation of the Karoo Supergroup. According to MGC, Jurassic aged dolerite dykes and sills infringe on this planar bedded rock mass. Typically, layers of highly weathered, weak rock mudstone, siltstone, and harder sandstone can be found underlying the plant area in Secunda. MGC report further that a thick layer of fine-grained clayey soil that constitutes both ancient alluvium and *in situ* residual soil mantles the weathered bedrock. It is known that remnants of calcrete can be present in the area incorporating the ash dams.

5.1.1.2 Geomorphology and drainage

The ash disposal site in Secunda lies within the confines of a broad concave slope near the base level of the late Neogene-aged Post African Landsurface I. MGC identified that the fine ash dams lie on a broad, shallow interfluve between two streams, one to the north and one to the south of the dams, which both flow in a westerly direction. A third smaller stream passes close to the east and northeast of the inactive ash dams (fine ash dam 1 and 2). Therefore, surface drainage is generally in a north-westerly and north-easterly direction. They further identified that a perched water table could exist at a shallow depth just below the landsurface. A simplified schematic diagram of the drainage system is given in figure 5.1.

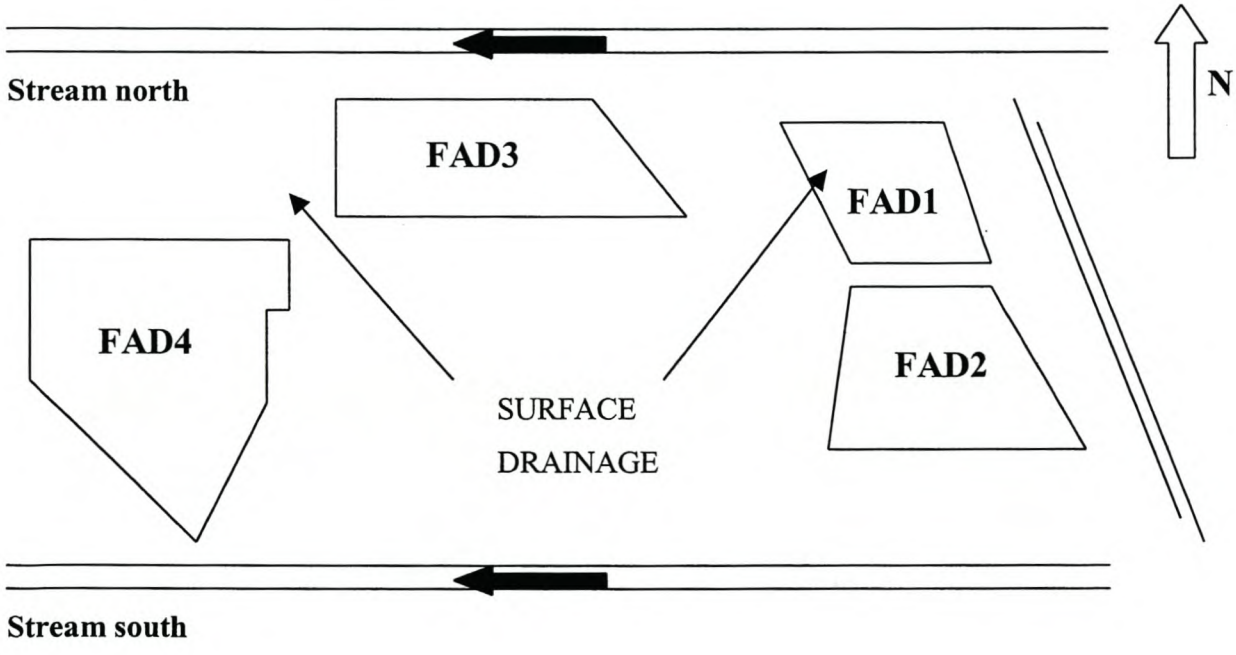

Figure 5.1: Drainage system around the ash dams

5.1.2 The drilling of the boreholes

Three boreholes were drilled at the following positions (in accordance with the criteria given in section 5.1.1):

- FAD2A – near the centre of Fine Ash Dam 2 (inactive dam).
- FAD4A – on the northern edge of Fine Ash Dam 4 (active dam).
- FAD4B – near the centre of Fine Ash Dam 4 (active dam).

Figure 5.2 shows the set-up of the drill rig in the centre of fine ash dam 2 (FAD2A)

Figure 5.2: Drill rig in position for the drilling of borehole FAD2A

The drilling was conducted by geomechanics under the supervision of MGC, and lasted for a period of three weeks – approximately one week was spent on the drilling of each core. The boreholes were drilled using both soil auger and then Nx rotary core drilling methods (which used an aluminium split-tube NWD4 core barrel). These two types of drilling methods used are shown in figures 5.3 and 5.4, respectively.

Figure 5.3: The auger drill

Figure 5.4: Aluminium split-tube NWD4 core barrel

The three boreholes were drilled approximately 5m into the material underlying the ash dams, and a temporary casing was installed to a certain depth in each borehole. The depths of the boreholes and the casing are given in table 5.1.

Table 5.1: Borehole and Casing Depths

Borehole	Depth	Depth of Casing
FAD2A	36.73m	33.0m
FAD4A	31.50m	27.0m
FAD4B	27.20m	24.0m

In each of the boreholes, two 25mm slotted PVC standpipe piezometers were inserted to allow for the levels of the water systems both within the underlying material and the ash to be measured and monitored, and for the permeabilities of the materials to be tested separately. One piezometer was inserted to a depth within the underlying material, and one below the phreatic surface of the material in the ash dam itself. Figure 5.5 illustrates the configuration of the piezometers and table 5.2 displays the installation depths of the different piezometers for the different boreholes.

Table 5.2: Relative Piezometer Depths in Boreholes

Borehole	Borehole Depth	Lower Margin of Ash Dam	Piezometer 1	Piezometer 2	Units
FAD2A	36.73	31.70	32.70	15.78	m
FAD4A	31.50	24.45	25.62	17.61	m
FAD4B	27.20	21.50	24.64	16.70	m

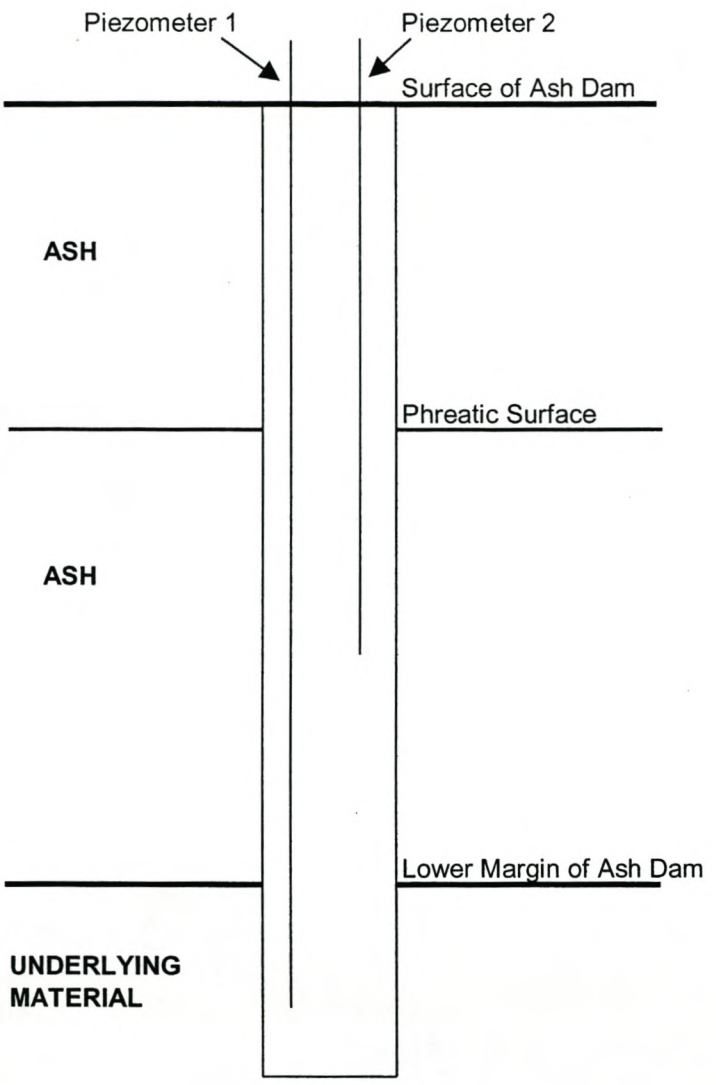

Figure 5.5: Schematic representation of piezometer set-up

5.1.3 Field tests

5.1.3.1 Sampling of the core material

Samples of the core material were taken at regular intervals for a variety of tests. For the determination of the particle size distribution, Atterberg Limits, specific gravity, chemical composition (XRF analyses) and the mineralogy (XRD analyses), undisturbed samples were not required. Even though it was not necessary to obtain undisturbed

samples for determining the Natural Moisture Content (NMC), the contamination of the sample by water used in the drilling process should be avoided. For this reason SPT samples were utilised in the determination of the NMC. In order to determine the bulk density and void ratio of the samples, undisturbed samples were required. Therefore, at regular intervals, samples were taken by means of Shelby Tubes. This involved the insertion of a 63mm diameter steel tube (with bevelled front edges narrowed by 2% of the tube diameter) into the ash/soil at the bottom of the hole at specific depths. Once this tube, containing the core sample, was brought to the surface, it was sealed on site by means of a wax plug (figure 5.6).

Figure 5.6: Sealing of a Shelby Tube with wax

A summary of the different samples obtained from each borehole is given in table 5.3. These samples were utilised for the necessary test procedures as described above.

Table 5.3: Summary of the Number and Type of Samples Retrieved from Borehole

Borehole	No. of SPT Samples Obtained	No. of Shelby Samples Attempted	No. of undisturbed (Shelby) Samples Obtained	No. of Core Samples Taken for Permeability Testing
FAD2A	14	10	4	1
FAD4A	12	5	5	1
FAD4B	8	8	7	1

5.1.3.2 Standard penetration tests

The Standard Penetration Tests (SPT) were performed approximately every 2.5m in each of the boreholes. These tests involved the driving of a 450mm split tube sampler (Raymond Spoon) into the ash/soil at the bottom of the hole. A 63.5kg weight was used with a drop height of 760mm. The number of blows were recorded per 150mm increment that the sampler penetrated the ash/soil. The number of blows for three 150mm increments was recorded, with the first 150mm penetration consisting of the seating drive, and the summation of the last two 150mm increment representing the N-value. A description of the consistency of the material related to the N-value is given in table 5.4.

Table 5.4: Description of Material Consistency Based on SPT N-Values

SPT N-value	Description
Sandy Materials	
<5	Very loose
5 – 10	Loose
10 – 30	Medium Dense
30 – 50	Dense
>50	Very Dense
Clayey Materials	
<2	Very Soft
2 – 4	Soft
4 – 8	Firm
8 – 15	Stiff
15 - 30	Very Stiff

These measured SPT values are shown on the borehole profiles in section 5.2.1. The description of the material consistency related to the SPT N-values at various depths is also given on these profiles.

5.1.3.3 Field permeability tests

After the completion of the drilling exercise, field permeability tests were performed on each borehole. Both rising head and falling head permeability tests were performed in each piezometer, which ensured verification of the results obtained. The permeability tests performed in piezometer 1 of each hole represent the permeability of the underlying material, and the tests performed in piezometer 2 of each hole represent the permeability of the ash fill material (at the local depth of the tip of the piezometer tube). Prior to both the rising head and falling head permeability tests, the level of the phreatic surface (groundwater level) within the piezometer was measured (using a dipmeter).

Rising head permeability test

For this type of permeability test, all the water within the piezometer was removed by means of pressurised oxygen, and then the water level in the piezometer was allowed to recharge. The rate at which the water level rose in the piezometer tube was calculated by measuring the water level in the piezometer tube at various time intervals. Obviously as the water level in the tube rises, the difference in the piezometric head becomes smaller and therefore the time for a given increment of recharge becomes longer.

Falling head permeability test

For this type of permeability test, the piezometer tube was completely filled with water, and then the water level was allowed to return to its natural level (as noted prior to the experiment) under the head difference of the water in the tube and the water in the material being tested. The rate at which the water level dropped was calculated in the same manner as with the rising head permeability tests, and once again, as the water level falls, the difference in head becomes smaller and the time for the water to drop a given increment becomes longer.

5.1.4 Laboratory tests

5.1.4.1 Laboratory tests performed by MGC

The laboratory tests performed by MGC on the core samples were:

- Particle size distribution.
- Atterberg Limits.
- Natural Moisture Content.
- Void ratio (which included specific gravity and dry density).
- Falling head permeability tests.

The laboratories on site at Secunda also performed moisture content tests. The purpose of these tests was to test the samples as soon as they were retrieved from the core to ensure no loss of moisture occurred. The samples used for these tests were taken from the tip of the SPT sampler and can therefore, be classified as undisturbed.

5.1.4.2 Chemical characterisation of the ash

In order to determine the variation in the chemical composition of the ash with depth in the dam, core samples were collected and analysed by mean of X-ray Fluorescence Spectrometry (XRF). The samples used for these analyses were disturbed samples, but as mentioned in section 5.1.3.1, this does not influence the results obtained. Both the major and trace elements were analysed for in all the core samples selected.

5.1.4.3 Mineralogical investigation

XRD analyses were conducted for specific core samples from each borehole. The motivation behind this investigation was to establish whether or not the mineralogy of the ash changed with depth in the dam.

5.2 Results and discussion

5.2.1 Description of the boreholes

Table 5.5 presents a summary of the three borehole profiles as logged by MGC.

Table 5.5: A Summary of the Borehole Profiles

Material	FAD2A		FAD4A		FAD4B	
	Depth to Surface (m)	Thickness (m)	Depth to Surface (m)	Thickness (m)	Depth to Surface (m)	Thickness (m)
Ash surface layer	0.00	1.96	0.00	1.10	Not well defined	21.50
Bulk of ash fill	1.96	29.49	1.10	23.20		
Lower margin of ash fill	31.45	0.25	24.30	0.15		
Upper vertisol (dark brown clayey sandy silt)	31.70	0.13	24.45	0.55	21.50	2.05
Lower vertisol Grey, clayey sandy silt with decomposing calcrete)	-	-	25.00	>6.50	23.55	>3.65
Residual/highly weathered Dolerite	31.83	>4.9	-	-	-	-

It should be noted that below Fine Ash Dam 2 (inactive dam), highly weathered, very weak rock dolerite was detected. However, rock was not detected below Fine Ash Dam 4, neither beneath FAD4A nor FAD4B. Figure 5.7 shows the core samples as obtained from the split-tube NWD4 core barrel.

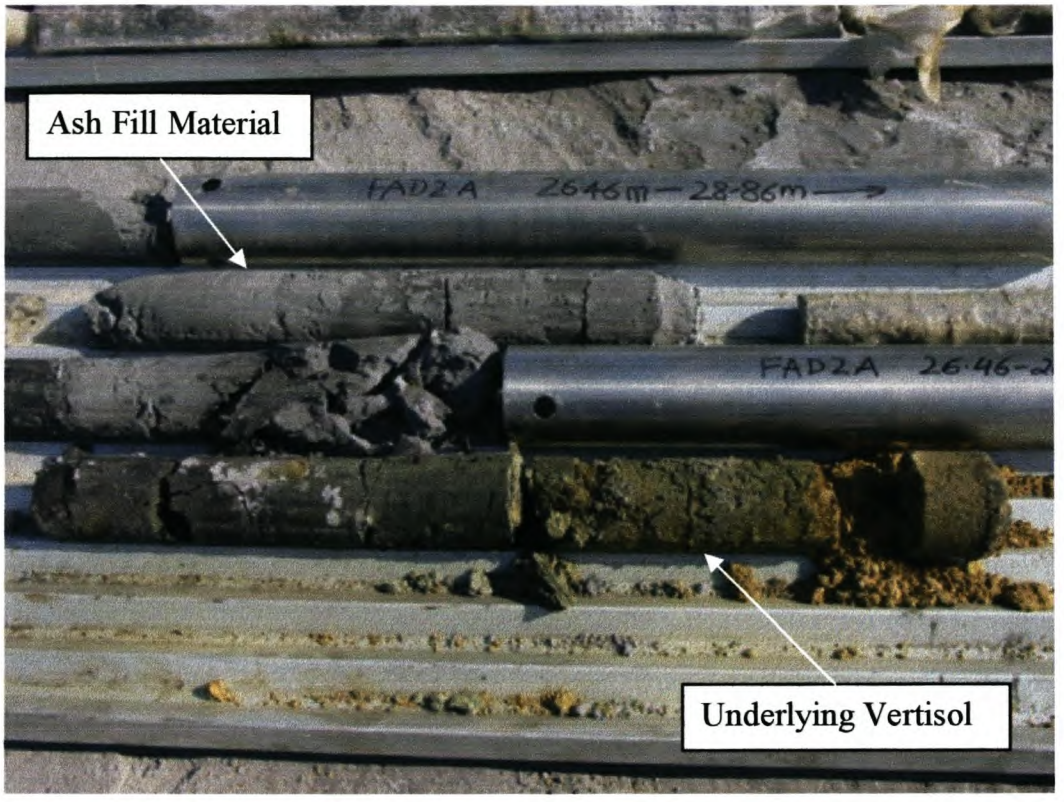

Figure 5.7: Core samples obtained

The general characteristics of the boreholes can be summarised as follows:

- There is a dense surface layer of between 1m and 2m thick, which contains course grains of calcareous (calcium-rich) material. This surface layer is not as well defined for FAD4B (located at the centre of Fine Ash Dam 4).
- The majority of the ash fill material consists of alternating light and dark grey layers of fine to medium grained ash. This ash shows a variable consistency, with the subordinate layers containing courser calcareous material.
- There is a thin (± 0.2m) layer at the base of each of the fine ash dams. It is composed of medium grained ash that may contain course calcareous material, and it is dark grey in colour. Once again this layer is less obvious in borehole FAD4B.
- Below each ash dam there is a thin layer of dark brown, clayey, sandy silt.

- Below the layer of dark brown material is a layer of grey, clayey, sandy silt, in which the formation of a calcrete layer has occurred. The calcrete layer, however, appears to be decomposing.

  Note: Calcrete is a hard crust of calcium carbonate material, which is largely impermeable to water movement. All calcretes are formed by the concentration of lime resulting from evaporation.
- Below Fine Ash Dam 2 a dolerite intrusion is present. This sandy residual dolerite, grading into highly weathered very weak rock dolerite, was found locally at the bottom of borehole FAD2A, therefore, one cannot predict to what extent this dolerite underlies Fine Ash Dam 2.

Detailed borehole profiles are given in figure 5.8, 5.9 and 5.10.

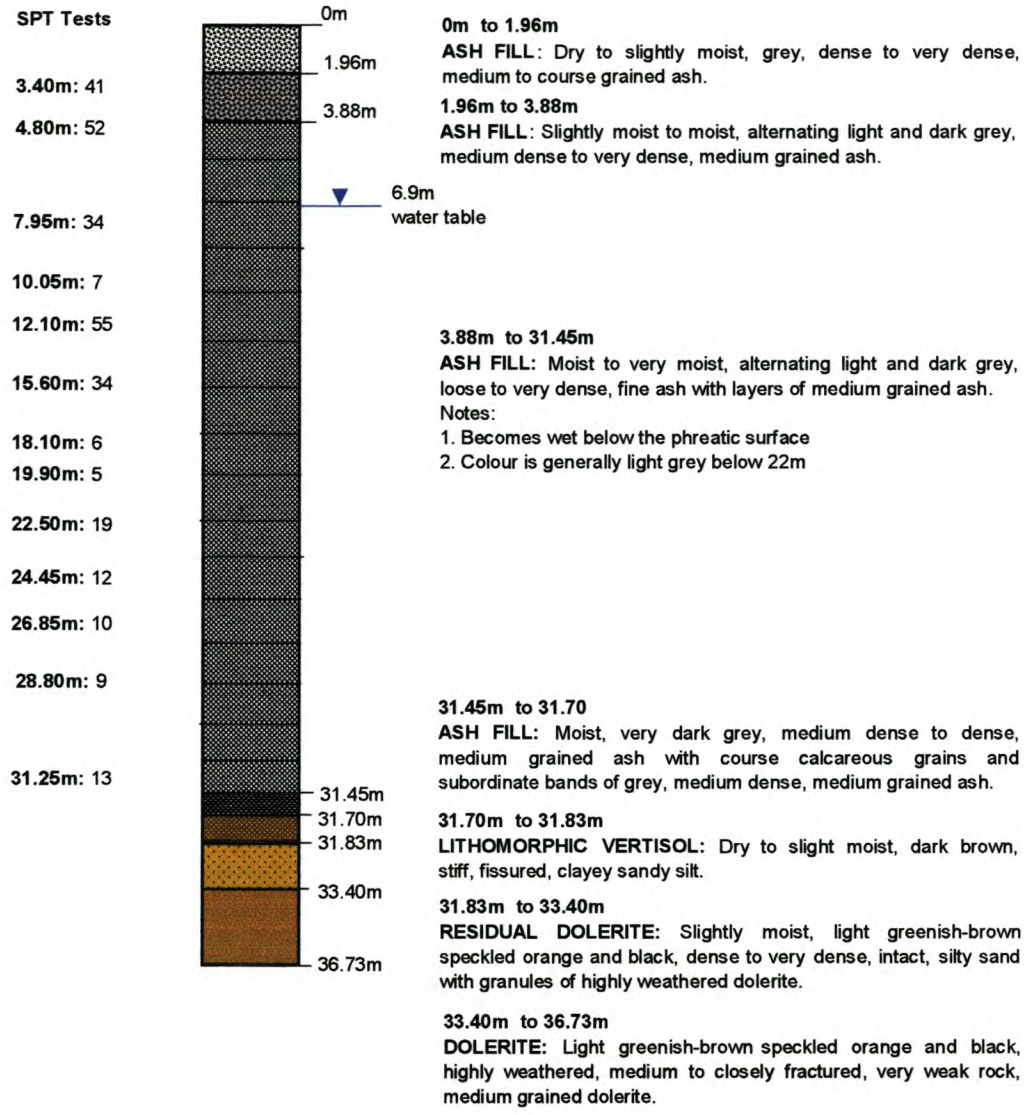

Figure 5.8: Borehole profile for FAD2A

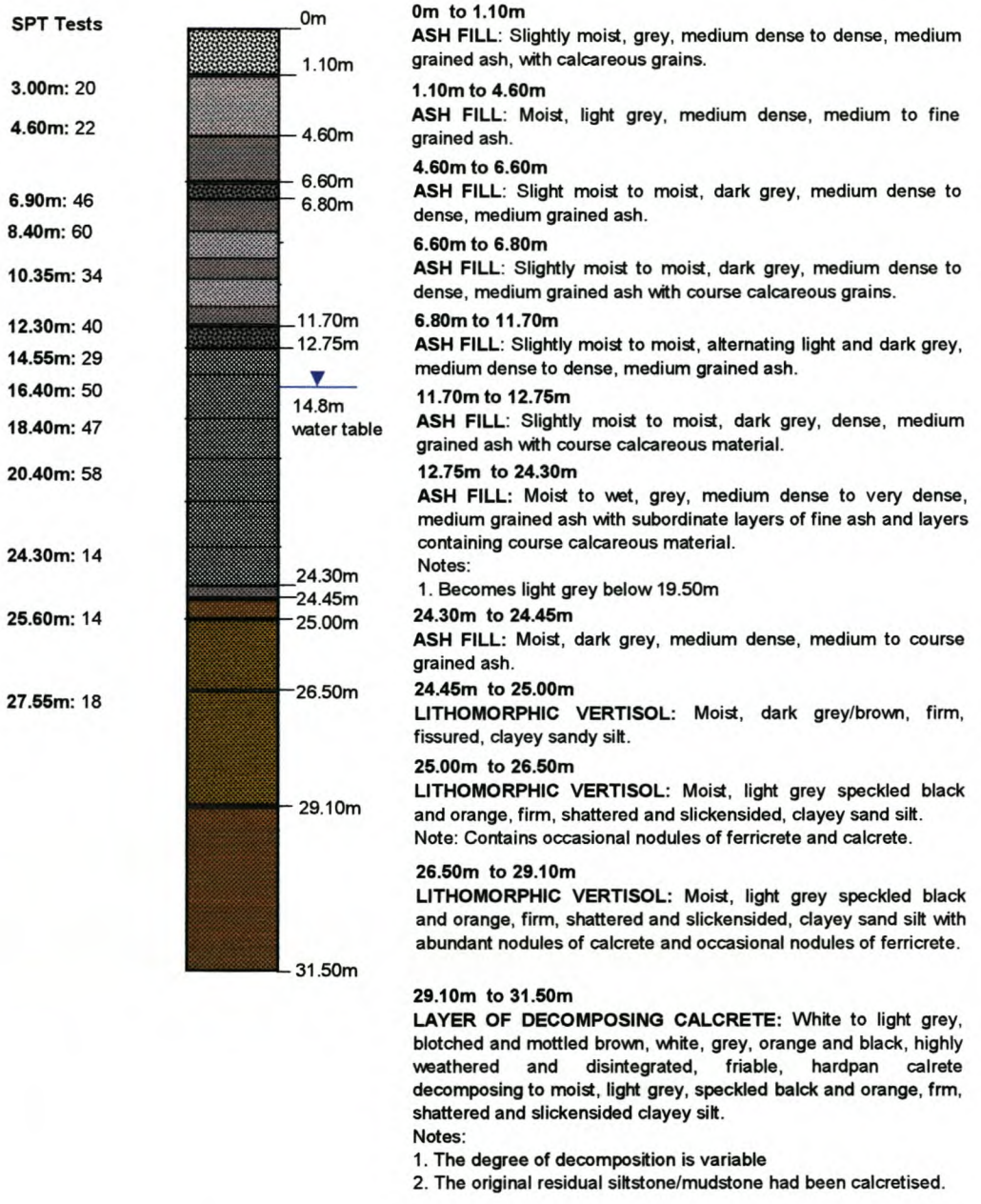

Figure 5.9: Borehole profile for FAD4A

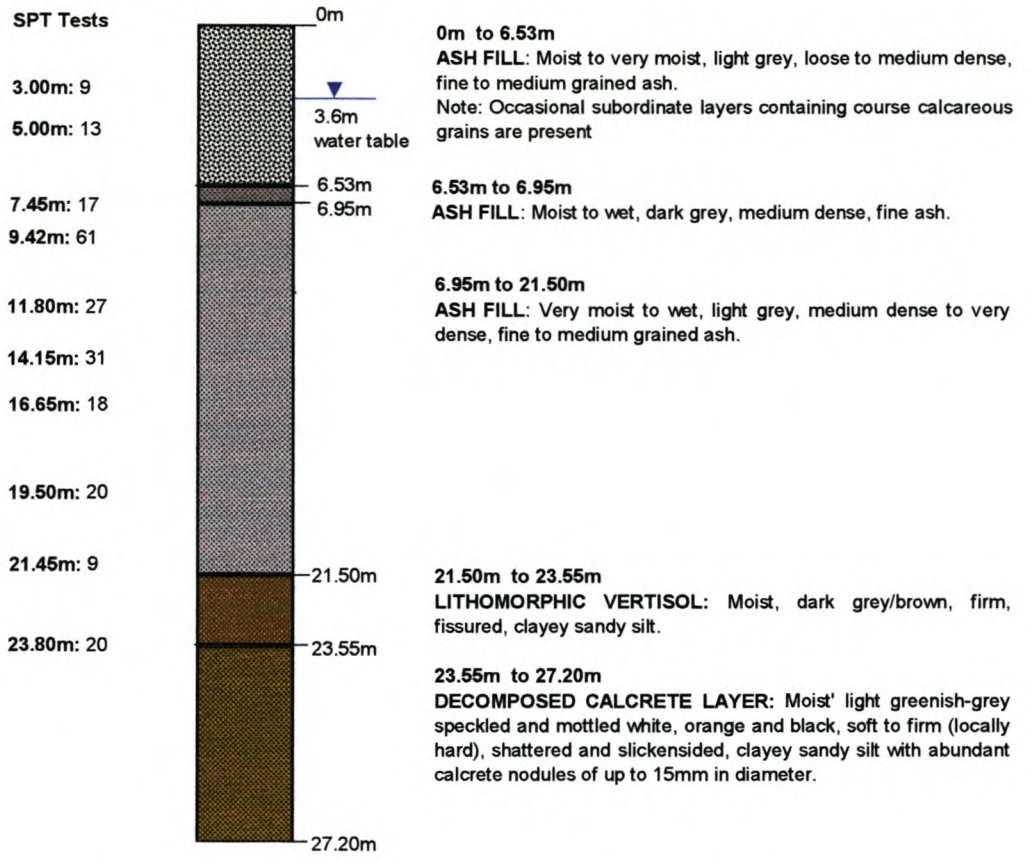

Figure 5.10: Borehole profile for FAD4B

5.2.2 Laboratory test results

5.2.2.1 Particle size distribution

The relative proportions of gravel, sand, silt and clay (or clay sized particles) was determined by means of grading tests. The results of these tests, for a selection of samples from each borehole, are presented in table 5.6. Figure 5.11 displays the relative percentages of gravel, sand, silt and clay in the samples from the ash fill section of the dams as listed in table 5.6.

Table 5.6: Grading Properties of Borehole Samples

Borehole	Sample Depth (m)	Gravel (%)	Sand (%)	Silt (%)	Clay-size particles (%)	Material Type
Ash Fill Material						
FAD2A	9.60	0.3	15.2	68.6	15.9	Ash
	15.20	0.0	18.4	61.3	20.3	Ash
	22.10	0.0	25.1	57.8	17.1	Ash
	26.46	0.0	6.6	77.1	16.3	Ash
FAD4A	4.45	0.0	38.8	56.1	5.1	Ash
	6.70	1.2	60.5	32.6	5.7	Ash
	18.35	2.6	44.0	47.7	5.7	Ash
FAD4B	4.50	0.7	9.8	69.4	20.2	Ash
	6.95	0.1	37.2	50.4	12.3	Ash
	11.40	0.0	8.7	71.0	20.3	Ash
	13.75	1.5	21.6	59.4	17.5	Ash
	16.15	0.2	8.9	74.9	15.9	Ash
Underlying Material (Lithomorphic Vertisol)						
FAD4A	26.50	0.2	40.0	35.9	23.9	Clayey sandy silt
	29.60	2.2	38.6	33.3	25.9	Clayey sandy silt with calcrete
FAD4B	23.40	1.6	38.7	42.9	16.8	Clayey sandy silt
	26.80	2.3	29.9	45.1	22.7	Clayey sandy silt with calcrete

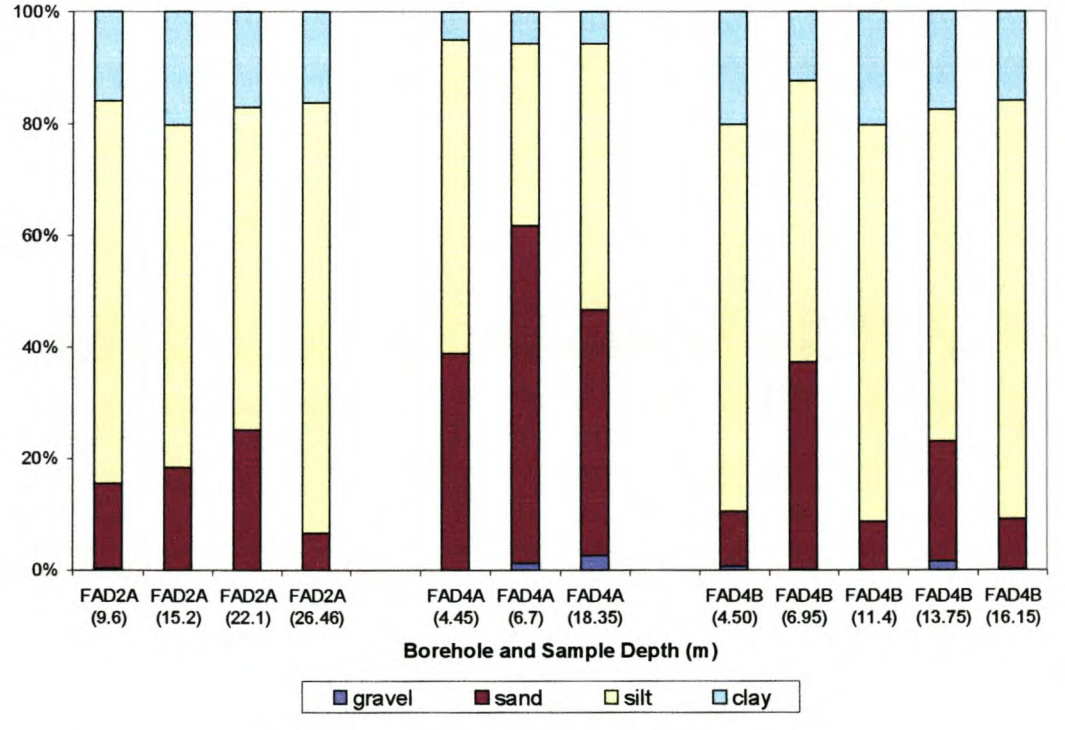

Figure 5.11: Relative proportions of gravel, sand, silt and clay in ash fill material

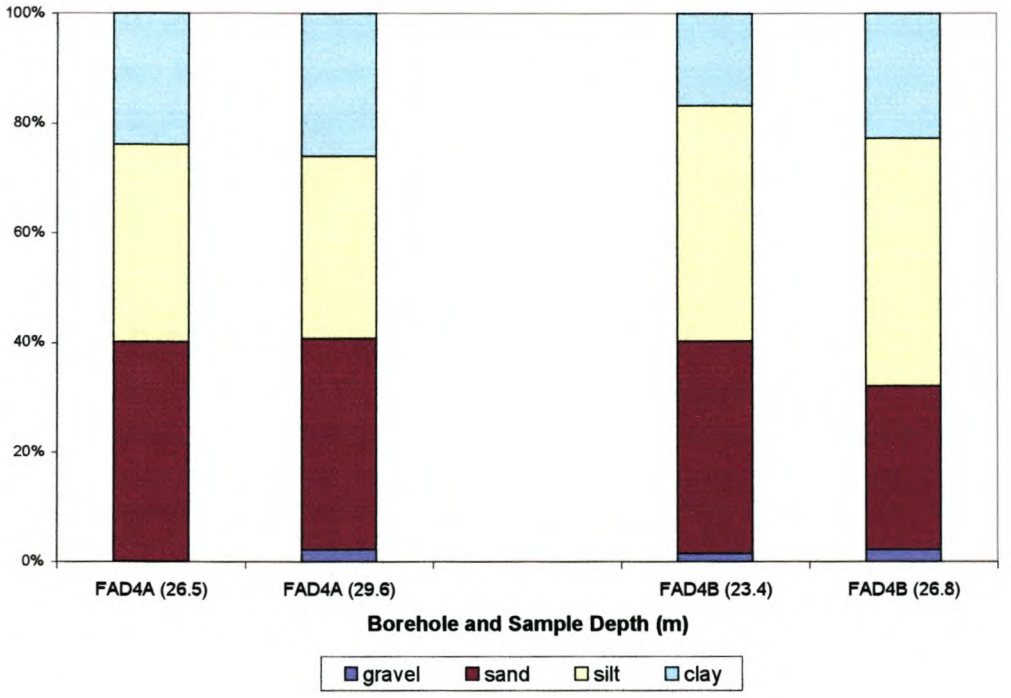

Figure 5.12: Relative proportions of gravel, sand, silt and clay in underlying material

The data in table 5.6 and figures 5.11 and 5.12 reveal that there is variability in the proportions of sand, silt and clay (or clay-sized particles) within both the ash fill material and the underlying lithomorphic vertisol material. This variability is seen both laterally (FAD4A vs. FAD4B) and with depth. In general, the ash fill material would best be described as clayey (occasionally sandy) silt. Although there are clay-sized particles present, they do not exhibit the properties of clay material. It is also evident from figure 5.6 that the materials sampled within borehole FAD4A (on the edge of active Fine Ash Dam 4) have a much higher percentage of courser sand-sized particles and lower percentage of clay-sized particles, than the boreholes drilled near the centre of the dams. The underlying material can best be described as clayey sandy silt.

5.2.2.2 Atterberg Limits

Atterberg limits are a set of index tests performed on fine-grained silt/clay soils to determine the relative activity of the soils and their relationship to moisture content. The objective of the Atterberg limit tests is to obtain information about the soil that can be used to estimate strength and settlement characteristics. It is the primary form of classification for cohesive soils. The liquid limit and plastic limit define the water content boundaries between non-plastic, plastic and viscous fluid states. The liquid limit (LL) defines the boundary between plastic and viscous fluid states, and the plastic limit (PL) defines the boundary between non-plastic and plastic states. The plasticity index (PI) defines the complete range of plastic state. Figure 5.13 illustrates these Atterberg limits.

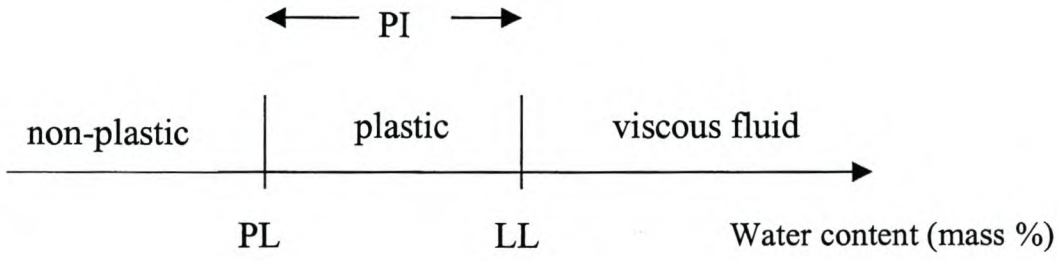

Figure 5.13: Illustration of Atterberg Limits

Table 5.7 summarises the Atterberg limits for the material obtained from the three boreholes. The natural moisture content (NMC) of the samples is also given in this table.

The plasticity of the ash fill material, as indicted by the plasticity index (PI) in table 5.7, is very low. On the other hand, the plasticity of the underlying lithomorphic material is very high.

Table 5.7: Summary of Atterberg Limits and Natural Moisture Content

Borehole	Sample Depth (m)	LL (%)	PL (%)	PI (%)	NMC (%)	Material Type
Ash Fill Material						
FAD2A	9.60	82.3	81.2	1.1	76.0	Ash
	15.20	72.3	71.7	0.6	92.0	Ash
	22.10	54.5	53.4	1.1	55.9	Ash
	26.46	66.5	66.4	1.1	62.8	Ash
FAD4A	4.45	61.7	60.5	1.1	47.4	Ash
	6.70	55.4	54.3	1.0	40.2	Ash
	18.35	56.4	55.4	1.0	57.0	Ash
FAD4B	4.50	53.3	43.5	9.5	65.0	Ash
	6.95	53.5	52.8	0.7	44.4	Ash
	11.40	64.6	55.6	9.0	63.6	Ash
	13.75	55.5	54.6	0.9	62.8	Ash
	16.15	56.8	54.5	1.3	75.7	Ash
Underlying Material (Lithomorphic Vertisol)						
FAD4A	26.50	65.8	37.7	26.1	60.7	Clayey sandy silt
	29.60	79.3	45.4	31.2	43.9	Clayey sandy silt with calcrete
FAD4B	23.40	63.2	37.2	23.8	53.6	Clayey sandy silt
	26.80	72.5	39.5	30.7	47.8	Clayey sandy silt with calcrete

5.2.2.3 Natural moisture content, void ratio and density

The results of the natural moisture content, void ratio and density calculations for the core samples are given in table 5.8. The porosity (n) shown in table 5.8 was calculated from the void ratio (e) in the following manner:

$$n = \frac{e}{(1+e)} \qquad (5\text{-}1)$$

The bulk density (ρ) was calculated from the dry density (ρ_d) using the following equation:

$$\rho = \rho_d(1+w) \qquad (5\text{-}2)$$

where w is the moisture content

Table 5.8: Summary of NMC, Void Ratio and Density Results

Borehole	Sample Depth (m)	Void Ratio (e)	Porosity (n)	Specific Gravity	Dry Density (kg/m^3)	Bulk Density (kg/m^3)	NMC (%)	Material Type
Ash Fill Material								
FAD2A	9.60	2.39	0.705	2.49	733	1290	76.0	Ash
	15.20	1.30	0.566	2.06	894	1716	92.0	Ash
	22.10	1.59	0.614	2.25	869	1355	55.9	Ash
	26.46	1.62	0.619	2.11	808	1315	62.8	Ash
FAD4A	4.45	1.18	0.541	2.21	1016	1498	47.4	Ash
	6.70	1.06	0.514	2.14	1038	1455	40.2	Ash
	18.35	1.26	0.558	2.36	1043	1638	57.0	Ash
FAD4B	4.50	1.43	0.589	2.17	893	1473	65.0	Ash
	6.95	0.941	0.485	2.18	1125	1625	44.4	Ash
	11.40	1.50	0.600	2.34	937	1533	63.6	Ash
	13.75	1.22	0.550	2.17	979	1594	62.8	Ash
	16.15	1.62	0.619	2.31	881	1548	75.7	Ash
Underlying Material (Lithomorphic Vertisol)								
FAD4A	26.50	1.13	0.531	2.60	1219	1959	60.7	Clayey sandy silt
	29.60	0.960	0.490	2.65	1353	1947	43.9	Clayey sandy silt with calcrete
FAD4B	23.40	1.21	0.546	2.46	1117	1716	53.6	Clayey sandy silt
	26.80	1.03	0.508	2.12	1043	1542	47.8	Clayey sandy silt with calcrete

Figure 5.14 displays the difference in porosity and specific gravity for the ash fill material and underlying lithomorphic vertisol.

It is evident from the data presented in table 5.8 and figure 5.14 that the void ratio, and therefore porosity, varies slightly in the ash fill material. Moreover, it appears as if the porosity is somewhat higher in the ash fill material than in the underlying lithomorphic vertisol (figure 5.14). There also appears to be a difference in the specific gravity of the ash fill material and underlying vertisol; the specific gravity of the material underneath the ash dams is generally higher than the specific gravity of the ash fill material (figure 5.14). The combined effect of the lower porosity and higher specific gravity of the underlying material results in a greater *in situ* density of the material beneath the ash dams. Furthermore, this also results in the NMC (expressed as a mass %) of the saturated underlying material, to be lower than that of the saturated ash fill material.

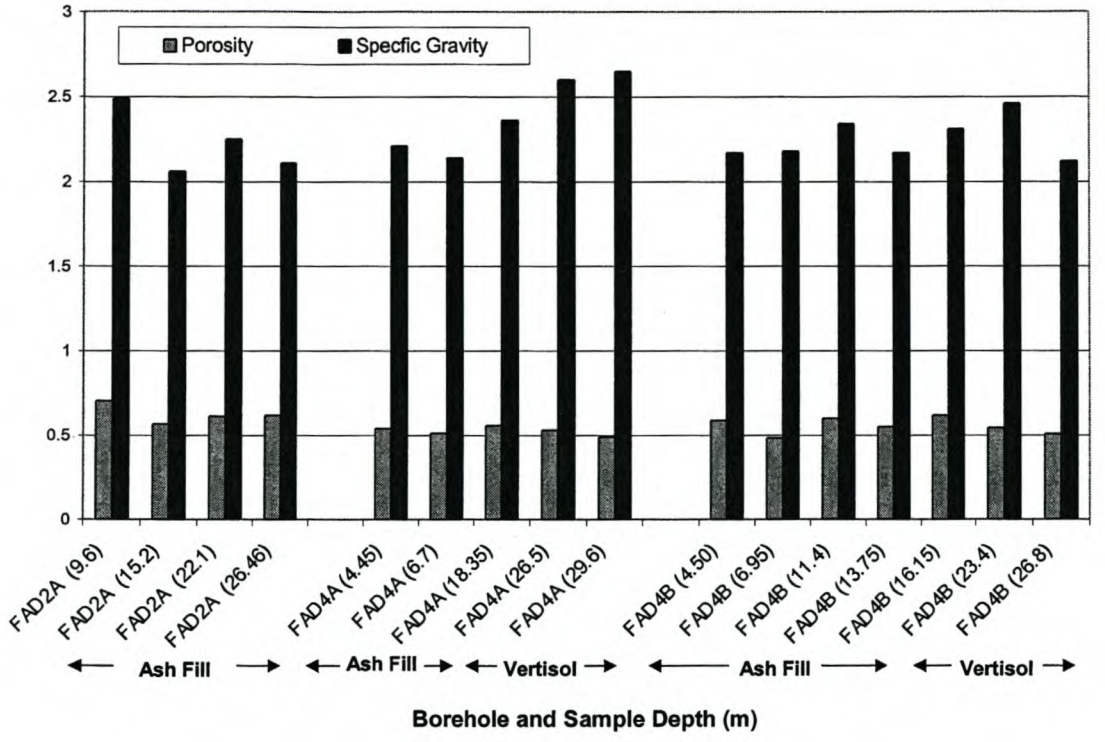

Figure 5.14: Comparison of porosity and specific gravity in ash fill and underlying material

5.2.2.4 Permeability

The results of the laboratory permeability tests are summarised in table 5.9.

Table 5.9: Laboratory Falling Head Permeability Results

Borehole	Sample Depth (m)	Permeability (m/s)	Material Description
FAD2A	31.8 – 32.0	Residual/weathered fractured rock ∴ test could not be performed	Residual Dolerite
FAD4A	25.0 – 25.2	1.9×10^{-5}	Clayey sandy silt with calcrete
FAD4B	22.3 – 22.5	8.6×10^{-6}	Clayey sandy silt with calcrete

The results of these permeability tests are discussed further in section 5.2.4 combined with the results obtained from the field permeability tests.

5.2.3 Moisture content profiles

The moisture content of the core samples was determined by means of calculating the difference between a wet core sample and a dry core sample. The amount of water present in the samples is therefore reported as a mass percentage. The complete moisture content results for all three boreholes are presented in table 5.10 and figure 5.15. From the data displayed graphically in figure 5.15 it is evident that the moisture content varies with depth in the boreholes. Some trends, which can be noted, are:

- The NMC of the ash fill near the surface of borehole FAD2A and FAD4A is much lower than the NMC near the surface of borehole FAD4B. One would expect such results since FAD4B is located near the centre of active Fine Ash Dam 4 where the slurry would have had less time exposed to the effect of evaporation.
- Below the phreatic surface of each borehole the ash material is saturated with water, therefore, one would expect the percentage moisture present to be similar to the porosity at that depth. The average porosity of the ash fill material is approximately 0.6 (60%) and is shown on figure 5.15. Although the NMC below the phreatic surface in each borehole varies around the value of 60%, the average moisture content of the ash fill material below the phreatic surface in each borehole is close to 60%:
  FAD2A: 62%
  FAD4A: 46%
  FAD4B: 63%
- As one would expect, the average moisture content of the ash fill material (from the surface to the just above the underlying material) in the centre of the ash dams (FAD2A and FAD4B) is greater than near the edge (FAD4A). These average values are:
  FAD2A: 61% (centre)
  FAD4B: 62% (centre)
  FAD4A: 42% (edge)
  What is also reflected in these average values is that the moisture content in the centre of an active dam is slightly higher than in the centre of an inactive ash dam. This was expected, although one might have expected to see a larger difference in the two values.

Table 5.10: Natural Moisture Content Results

FAD2A		FAD4A		FAD4B	
depth (m)	NMC (%)	depth (m)	NMC (%)	depth (m)	NMC (%)
1.3	32.9	3	39	3.2	68.7
4.8	68.3	4.45	47.4	4.5	65
7.95	50.9	5.05	35.8	5.2	62.5
9.6	76	6.7	40.2	6.95	44.4
10.55	66.3	7.3	40.5	7.6	55.8
12.5	65.3	8.5	42.9	9.6	42.1
15.2	92	10.4	34.9	11.4	63.6
16.2	82	12.3	38.1	12	58.2
18.05	69.8	14.5	40.2	13.75	62.8
22.1	55.9	16.4	53.4	16.15	75.7
22.5	44	18.35	57	17.3	73.1
24.85	57.8	18.85	40	19.8	66.4
26.46	62.8	20.35	39.1	21.6	83.9
26.86	45.6	24.3	39.3	23.4	53.6
28.8	62.7	26.05	31.7	26.8	47.8
31.25	42.8	26.5	60.7		
33.2	58.7	29.6	43.9		

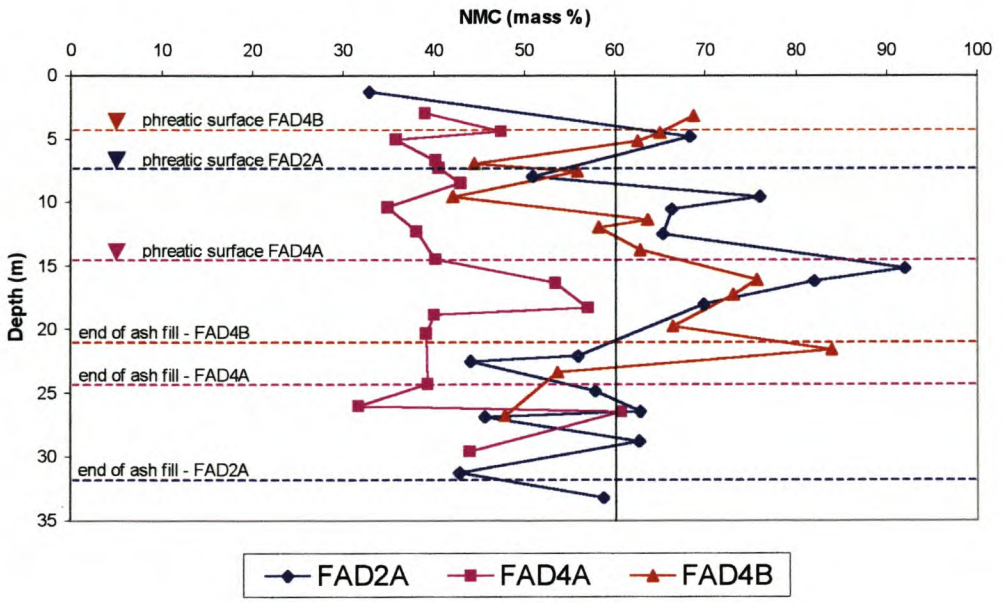

Figure 5.15: Moisture content profile in each of the boreholes

The identification of the phreatic surfaces in each of the boreholes assisted in the understanding of the water table profile in the ash dams. From the available data, the water table profile in an active and an inactive dam can be illustrated as shown in figure 5.16.

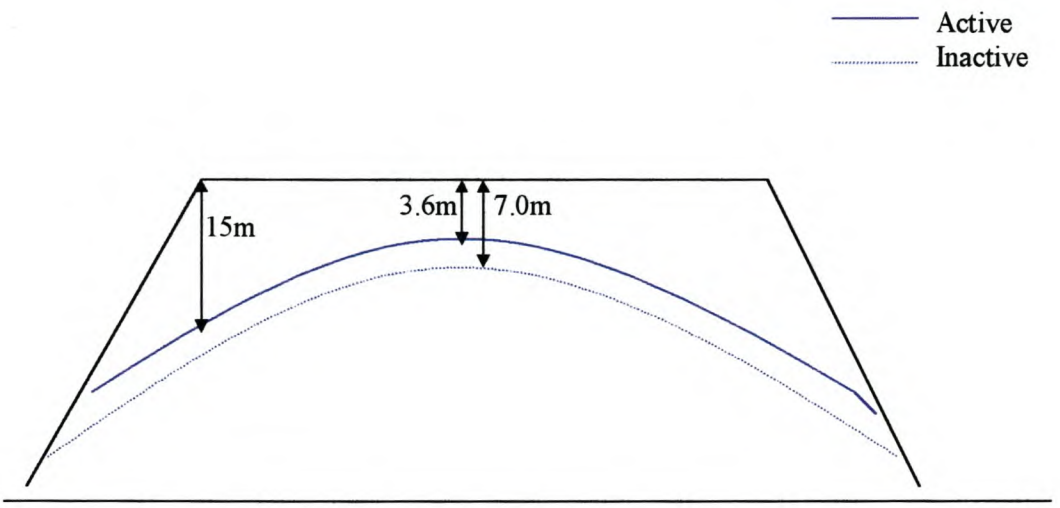

Figure 5.16: Water table profile in an active and inactive ash dam

5.2.4 Permeability tests

The results from the laboratory permeability tests have already been presented in section 5.2.2.4 (table 5.9). In brief these results are:

- No permeability tests could be performed on the sample material from FAD2A
- The permeability of the material from FAD4A (25.0m – 25.2m) was 1.9 x 10^{-5}m/s
- The permeability of the material from FAD4B (22.3m – 22.5m) was 8.6 x 10^{-6}m/s

For the field permeability tests, both the rising head and falling head methods were used. The results of the field permeability tests are given in table 5.11. These results represent the overall permeabilities calculated in each piezometer, since there was some variability

in the permeabilities calculated for the different time intervals during the rising head and falling head tests.

Table 5.11: Summary of the Results from the Field Permeability Tests

Borehole	Piezometer	Rising Head Permeability (m/s)	Falling Head Permeability (m/s)	Average (m/s)
FAD2A	Piez. 1	1.00×10^{-5}	9.37×10^{-5}	5.19×10^{-5}
	Piez. 2	No test possible	1.34×10^{-5}	1.34×10^{-5}
FAD4A	Piez. 1	5.21×10^{-6}	2.06×10^{-5}	1.29×10^{-5}
	Piez. 2	5.97×10^{-5}	5.25×10^{-5}	2.92×10^{-5}
FAD4B	Piez. 1	3.72×10^{-5}	3.22×10^{-5}	3.47×10^{-5}
	Piez. 2	1.34×10^{-4}	1.17×10^{-4}	1.26×10^{-4}

The positioning of the piezometers in the boreholes is given in figure 5.5. Piezometer 1 is inserted in the underlying material, and piezometer 2 is inserted in the ash fill material below the phreatic surface. The field permeability tests do have greater restrictions, however, they do also provide a more realistic indication of the actual permeability of the dams on a large scale. Some observations that can be made concerning the results of both the field and the laboratory permeability tests are:

- For boreholes FAD2A and FAD4A there is very little difference in the permeability of the ash fill and the underlying material. The permeability of both materials at the location of these two boreholes falls in the range of 1×10^{-5} to 5×10^{-5}m/s.
- The highest permeability value is found for piezometer 1 in borehole FAD2A. This piezometer lies at a depth of 32.79m within silty sand and residual dolerite. Even though this material is very dense, one could expect it to display a higher permeability than the vertisol material into which piezometer 1 of FAD4A is installed.
- There appears to be a significant difference in the permeabilities recorded for piezometer 1 and piezometer 2 installed in borehole FAD4B. The permeability of the underlying vertisol material is calculated to be 3.47×10^{-5}m/s, whereas a permeability of 1.25×10^{-4}m/s is recorded for the ash material. The value obtained for the material beneath the ash fill in this borehole is similar to the permeabilities for the ash fill material in FAD2A and FAD4A. Therefore, the ash fill material in the centre of an

active ash dam appears to be more permeable (better drainage) than the ash fill material towards the edge of an active dam, or in the centre of an inactive ash dam.

- If one compares the permeability results for the laboratory and the field permeability tests it is evident the permeability of 1.9 x 10^{-5}m/s obtained from the laboratory tests on the vertisol material retrieved from borehole FAD4A, correlates well to the permeability obtained in piezometer 1 during the field tests (1.29 x 10^{-5}m/s).

5.2.5 Variation in the chemical composition of the core samples

The core samples from each of the three boreholes were analysed by means of X-ray Fluorescence (XRF). The results for the major elements are discussed in section 5.2.5.1, and the results for the variation in the trace elements are discussed in section 5.2.5.2.

5.2.5.1 Major element analyses

Samples at selected intervals were analysed for the presence of the following major elements: Si, Al, Fe, Ca, Na, K, Mg, Cr, Mn, Ti, Ni, and P, as well as the loss on ignition (LOI). The data is reported as a mass percent of the relative oxide of each element.

Silicon

Figure 5.17 displays the variation in the mass percentage of Si with depth in each of the three boreholes. From the results displayed in figure 5.17, the following observations can be made:

- The Si content is practically the same in each of the three boreholes and for all three there is a slight decrease in Si content with increasing depth.
- In all three boreholes it is evident that there is a sharp increase in the Si content at the ash fill/underlying vertisol interface. This same trend was seen for the core drilled into an ash dam at the Kriel Power Station in South Africa (Bezuidenhout, 1995). A possible explanation for this could be related to the mixing of the ash with the topsoil containing quartz. However, both FAD4A and FAD4B show that after the increase in Si content at the interface, there is a decrease in the Si content in the underlying material. Therefore the effect that the soil has on the Si content at the ash/soil

interface cannot be the only explanation for this observation. Another possibility is the effect that the lining of the dams has the chemical composition of the samples taken at the ash/soil interface. If a soil layer with a high Si content was placed at the base of the ash dam on top of the lining then this could explain the observed increase in the Si content.

- For boreholes FAD2A and FAD4A, the mass % of Si in the first sample (i.e. near the surface of the ash dam), is less than that of the fresh fine ash.

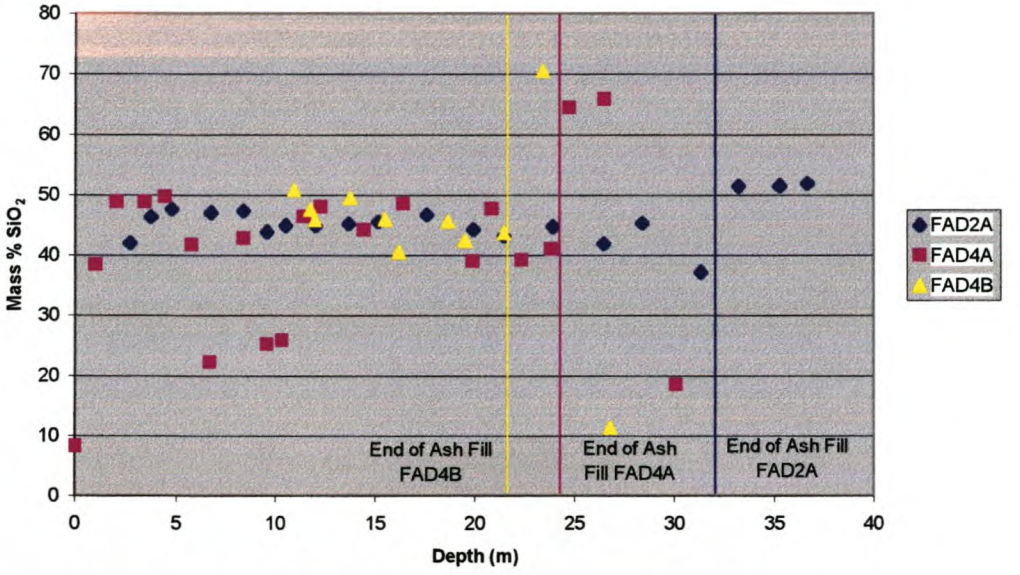

Figure 5.17: Variation of Si in the three boreholes

Aluminium

The variation in the mass percentage of Al with depth in the boreholes is shown in figure 5.18. From the results displayed in figure 5.18, the following observations can be made:

- The Al content of the ash fill material in borehole FAD4A is very erratic with depth. Overall there is less Al found in the sample from borehole FAD4A than in FAD4B or FAD2A.
- From a depth of approximately 12m into each of the dams, at the locations of the boreholes drilled, there appears to be a decrease in the Al content with depth until the

ash/soil interface is reached. This decrease is more pronounced for boreholes FAD2A and FAD4B than for FAD4A. A decrease in the Al_2O_3 concentration with depth was also apparent in the core drilled into an ash dam at the Kriel Power Station in South Africa (Bezuidenhout, 1995).

- In all three boreholes, it is evident that at the ash/soil interface there is a sudden decrease in the Al content of the core samples. After this initial decrease the amount of Al in the sample remains low – for FAD4A and FAD4B the Al content below the ash fill material is very low.
- For boreholes FAD2A and FAD4A, the mass % of Al in the first sample (i.e. near the surface of the ash dam), is less than that of the fresh fine ash.

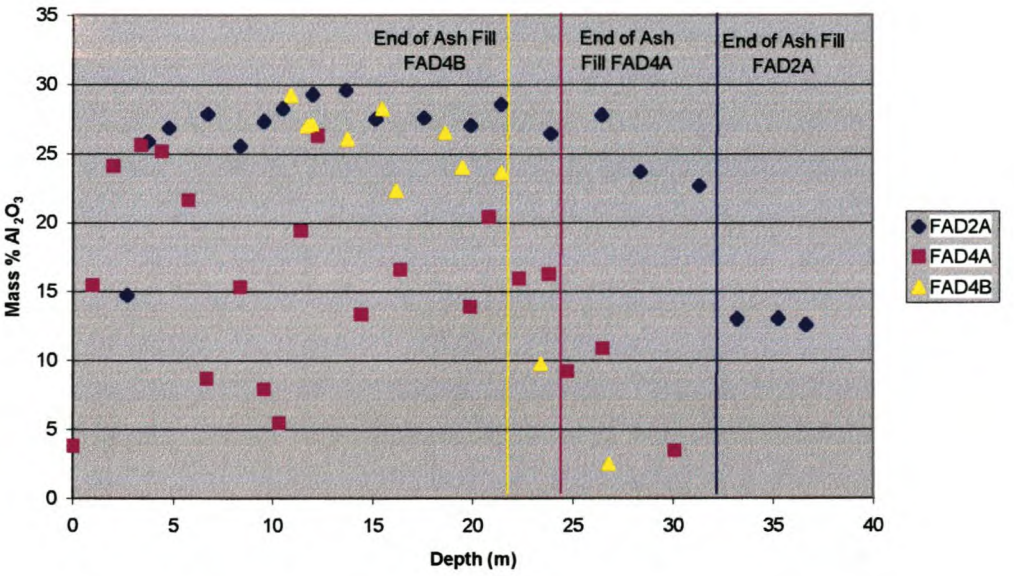

Figure 5.18: Variation of Al in the three boreholes

Iron

Figure 5.19 displays the variation in the mass percentage of Fe with depth in each of the three boreholes.

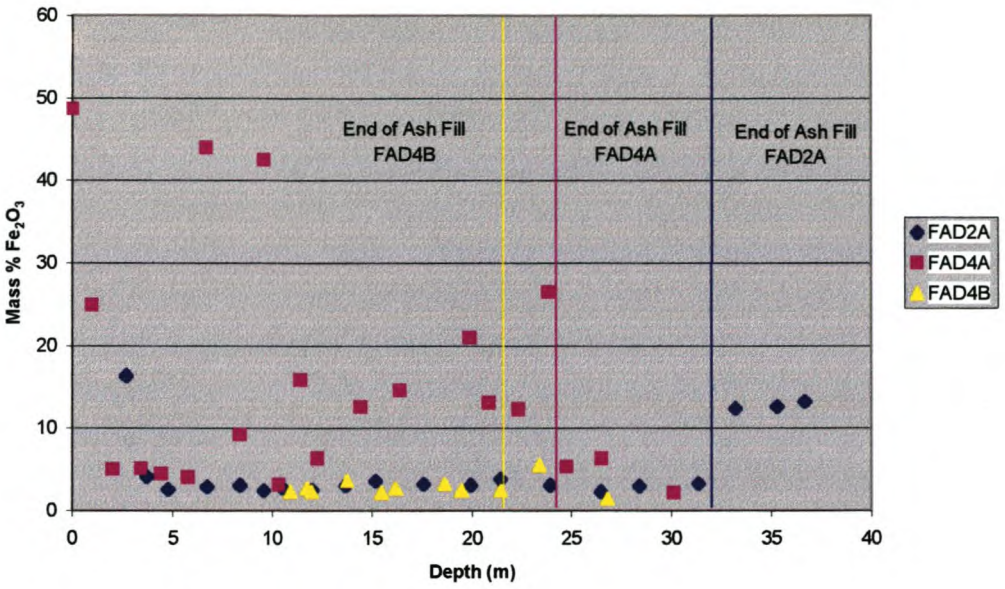

Figure 5.19: Variation of Fe in the three boreholes

The results displayed in figure 5.19 reveal that:

- The variation in the Fe content with depth in borehole FAD4A is very erratic, and in general, the Fe content of the core samples from FAD4A is much higher than for boreholes FAD2A and FAD4B.
- There is not much variation in the Fe content of the core samples from boreholes FAD2A and FAD4B – the iron content is low for both boreholes throughout the ash fill material.
- In borehole FAD2A there is much more iron present in the core samples taken from the underlying vertisol than in the samples taken from the ash fill material. In boreholes FAD4A and FAD4B there is less iron present in the samples in the samples taken from the underlying vertisol material.
- For boreholes FAD2A and FAD4A, the mass % of Fe in the first sample (i.e. near the surface of the ash dam), is more than that of the fresh fine ash.

Calcium

The variation in the mass percentage of Ca in each of the three boreholes is displayed in figure 5.20. If one examines these results shown in figure 5.20, it is evident that:

- The Ca content of the core samples from the ash fill material in all three boreholes varies between about 5 mass% and 10 mass%. There doesn't appear to be any trend in the Ca content with depth in the ash dam.
- In all three boreholes it is evident that there is a decrease in the Ca content just beneath the ash fill material. This decrease is more pronounced in boreholes FAD4A and FAD4B.
- The Ca content of the deepest samples taken from boreholes FAD4A and FAD4B is very high. This trend is not apparent in FAD2A – here the Ca content remains fairly constant in the underlying vertisol material.
- At a depth of 10.35m in borehole FAD4A there is a lot of Ca present. This particular sample is discussed further in section 5.2.7.2.

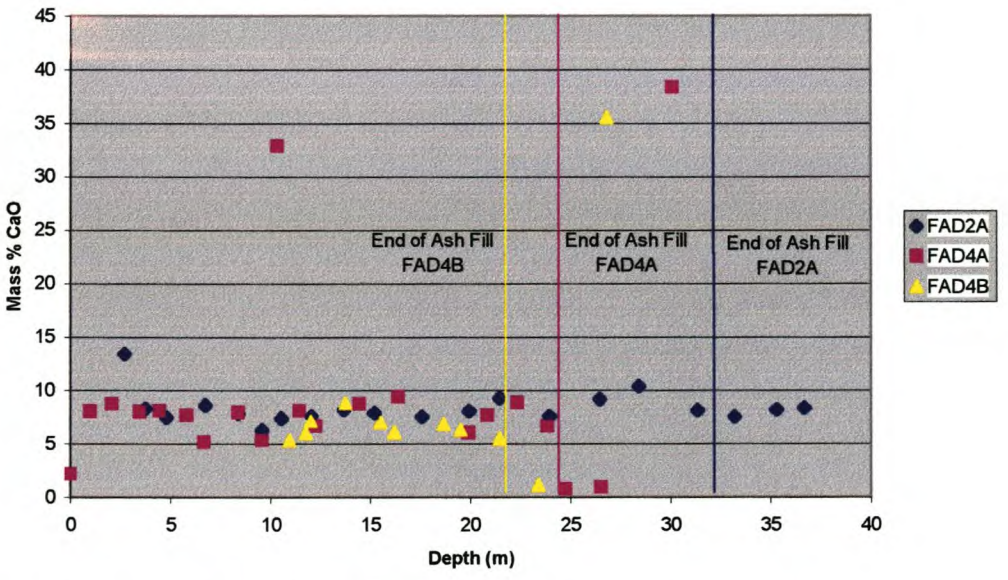

Figure 5.20: Variation of Ca in the three boreholes

Sodium

Figure 5.21 displays the variation in the mass percentage of Na with depth in each of the three boreholes.

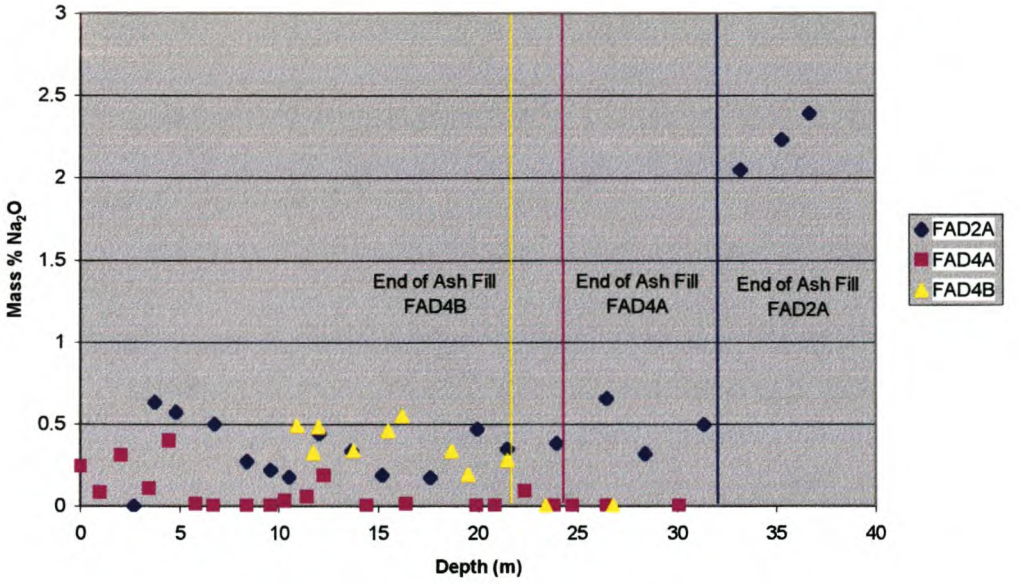

Figure 5.21: Variation of Na in the three boreholes

From the results displayed in figure 5.21, the following observations can be made:

- There doesn't appear to be any trend in the Na content with depth in borehole FAD2A. The Na content varies erratically with depth.
- In boreholes FAD4A and FAD4B there appears to be an overall decrease in the Na content of the core samples with increasing depth in the ash fill material.
- In borehole FAD2A there is significantly more Na present in the underlying vertisol material than in the ash fill material. At the location of boreholes FAD4A and FAD4B it is apparent that there is no Na present in the underlying vertisol material.
- For boreholes FAD2A and FAD4A, the mass % of Na in the first sample (i.e. near the surface of the ash dam), is less than that of the fresh fine ash.

Potassium

The variation in the K content of the core material from the three boreholes is given in figure 5.22. From this figure it is apparent that:

- There doesn't appear to be any trend in the K content with depth in any of the boreholes. The K content varies erratically with depth.
- In borehole FAD2A there is more K present in the core samples taken from the underlying vertisol material than in the core samples taken from the ash fill material.
- In boreholes FAD4A and FAD4B there is much less K present in the underlying vertisol material.

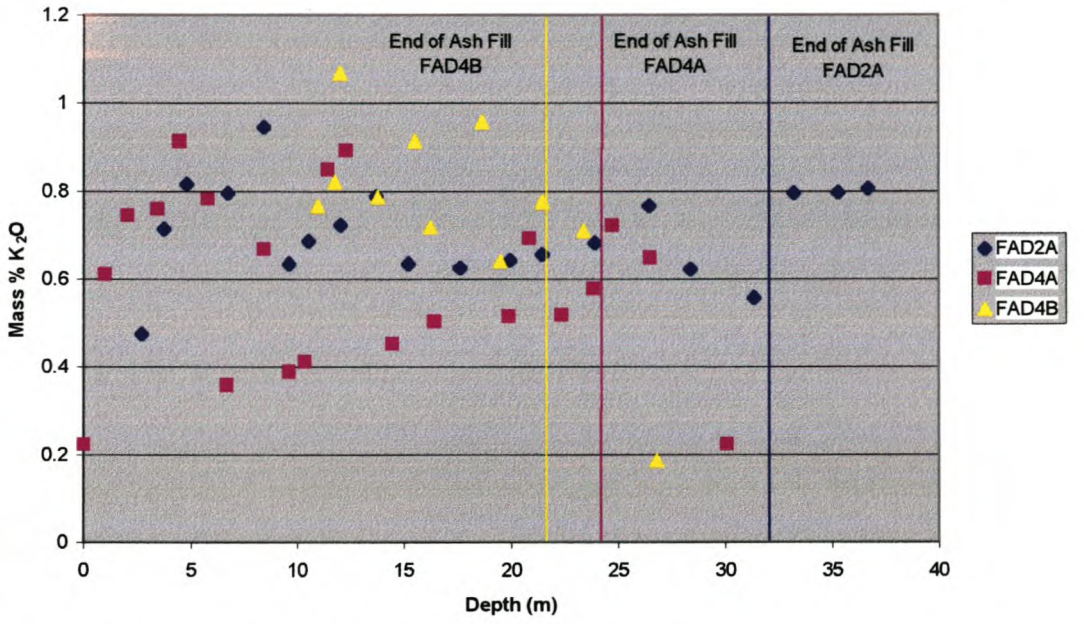

Figure 5.22: Variation of K in the three boreholes

Magnesium

Figure 5.23 shows the variation in the mass percentage of Mg with depth in each of the three boreholes.

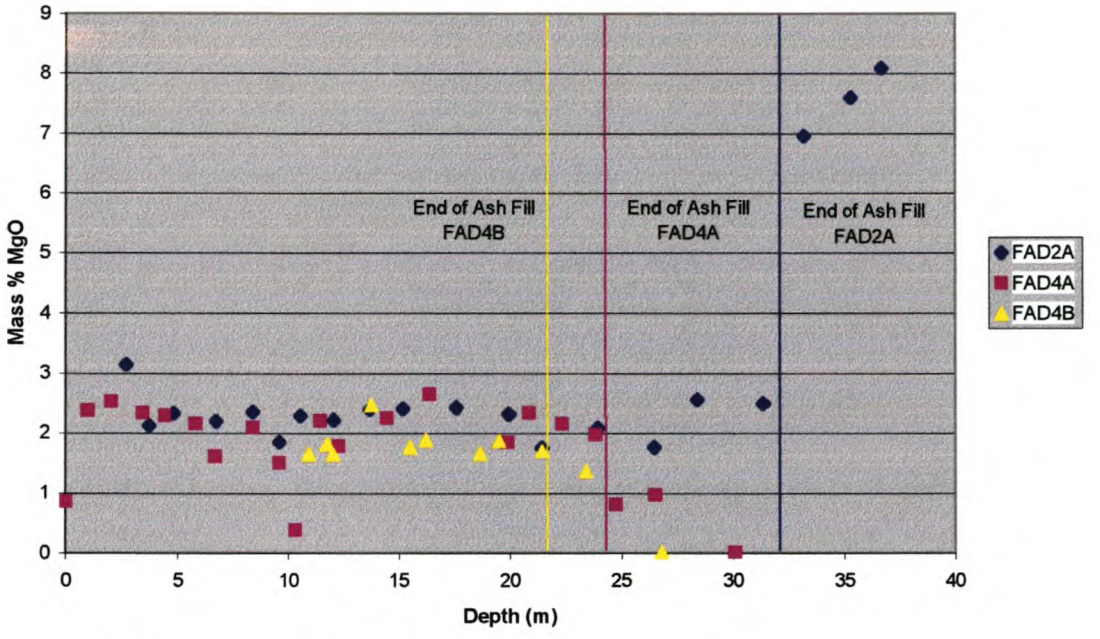

Figure 5.23: Variation of Mg in the three boreholes

From the results displayed in figure 5.23, the following remarks can be made:

- The magnesium concentration appears to remain fairly constant through out the ahs fill material in all three boreholes, although there does seem to be slightly less Mg towards the bottom of the ash fill material.
- At the ash/soil interface there is a sharp decrease in the Mg concentration in boreholes FAD4A and FAD4B, and no Mg present in the underlying vertisol material.
- In borehole FAD2A there is an increase in the Mg concentration in the underlying material.

Chromium

The variation in the mass percentage of Cr with depth in the three boreholes can be seen in figure 5.24. From the results displayed in figure 5.24, the following observations can be made:

- Although the variation in the Cr content of the core samples from borehole FAD4A is very erratic, there does appear to be an overall decrease in the Cr content of the ash

fill material with increasing depth. There is also an overall decrease in the Cr content evident in borehole FAD4B.

- In borehole FAD2A there is an initial increase in the Cr content of the ash fill material to a depth of about 27m, and then there is a decrease in the Cr content until the ash/soil interface.
- In boreholes FAD4A and FAD4B there is less Cr in the underlying material compared to in the ash fill material, whereas in FAD2A there is much more Cr present in the underlying material.

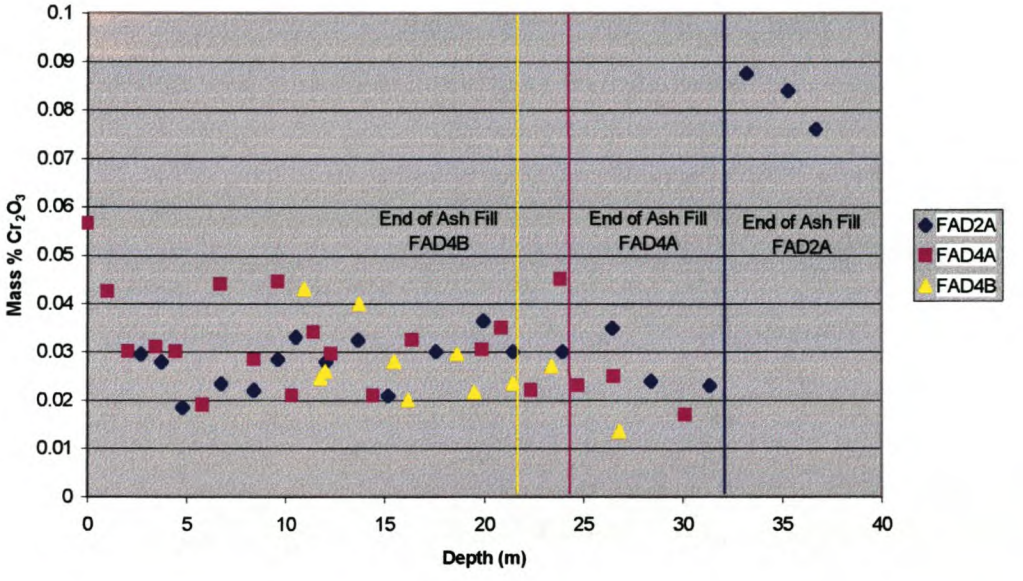

Figure 5.24: Variation of Cr in the three boreholes

Manganese

Figure 5.25 displays the variation in the mass percentage of Mn with depth in each of the three boreholes.

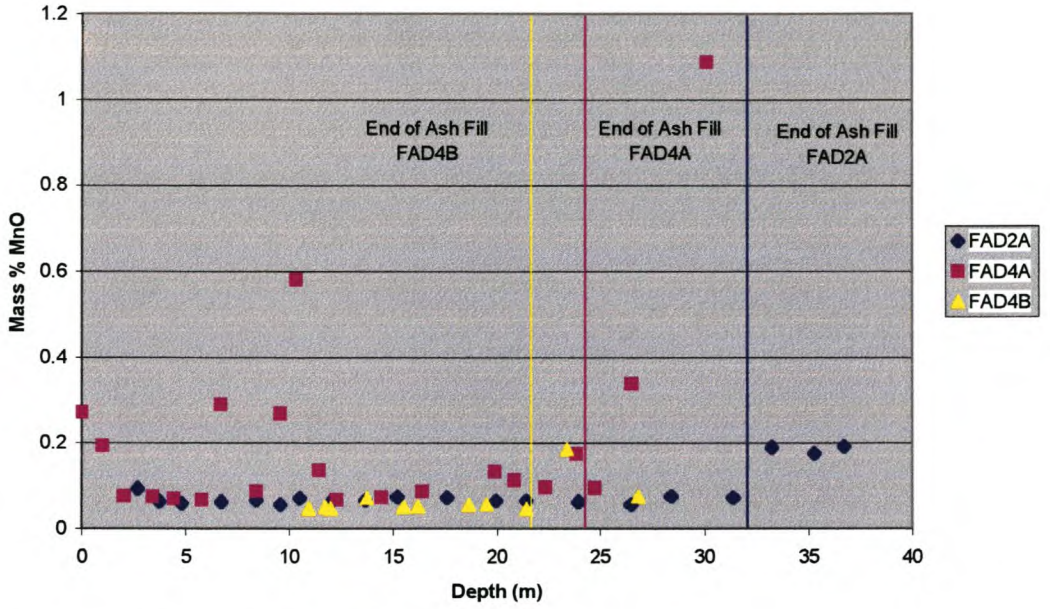

Figure 5.25: Variation of Mn in the three boreholes

The results displayed in figure 5.25 reveal that:

- The Mn content of the ash fill material in boreholes FAD2A and FAD4B remains fairly constant with depth. The Mn content in borehole FAD4A shows some variation.
- In all three boreholes there appears to be more Mn in the underlying material compared to the ash fill material.

Phosphorous

The results for the variations in P with depth in the boreholes are given in figure 5.26. From the results displayed in this figure, the following remarks can be made:

- In borehole FAD2A there is an increase in the P content of the core samples to a depth of 13m. From 13m to the ash/soil interface there is a decrease in the P content of the ash fill material.
- In borehole FAD4A there is an overall decrease in the P content of the ash fill material with depth.

- In borehole FAD4B there is a decrease in the P content of the ash fill material from a depth of about 15m to the ash/soil interface.
- There appears to be no P in the material underlying the ash fill in borehole FAD4A and FAD4B.
- In borehole FAD2A there is some P present in the underlying material, however, the mass percentage in the underlying material is less than that in the ash fill material.

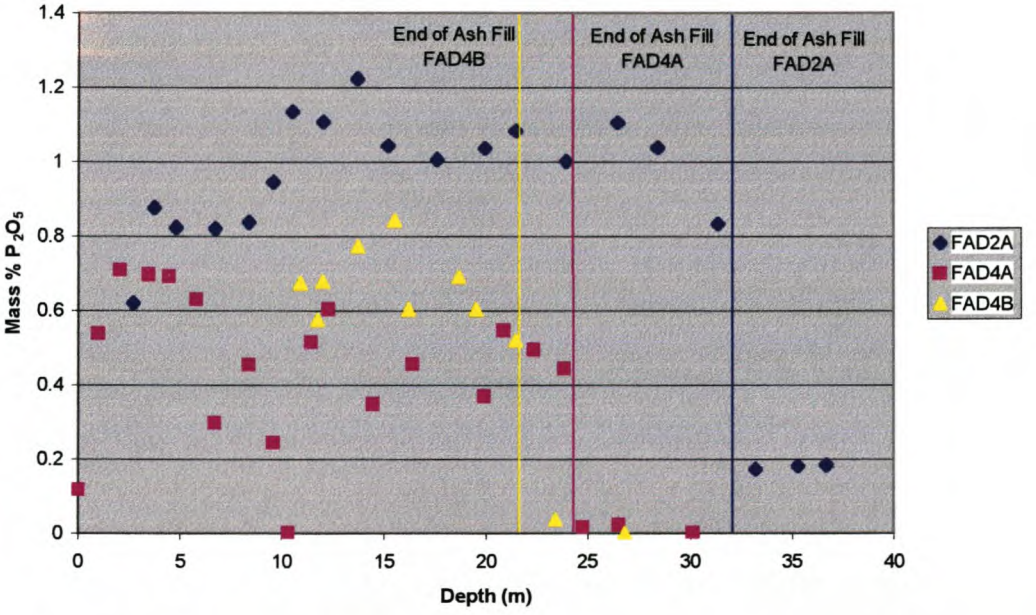

Figure 5.26: Variation of P in the three boreholes

Titanium

The variation in the mass percentage of Ti in the boreholes is presented in figure 5.27. From the results displayed in figure 5.27, the following observations can be made:

- The variation in Ti content in the core samples from FAD4A is very erratic, although there appears to be a slight overall decrease in the Ti content with depth in the ash fill material.
- It is evident that there is a decrease in the Ti content of the core samples from borehole FAD4B. This decrease is seen from about 10m to the ash/soil interface.

- In borehole FAD2A there is an increase in Ti with depth until a depth of about 27m. From 27m to the ash/soil interface a decrease is evident.
- In the material underlying FAD2A there appears to be a slight increase in the Ti concentration, whereas in boreholes FAD4A and FAD4B there is significantly less Ti in the underlying material.

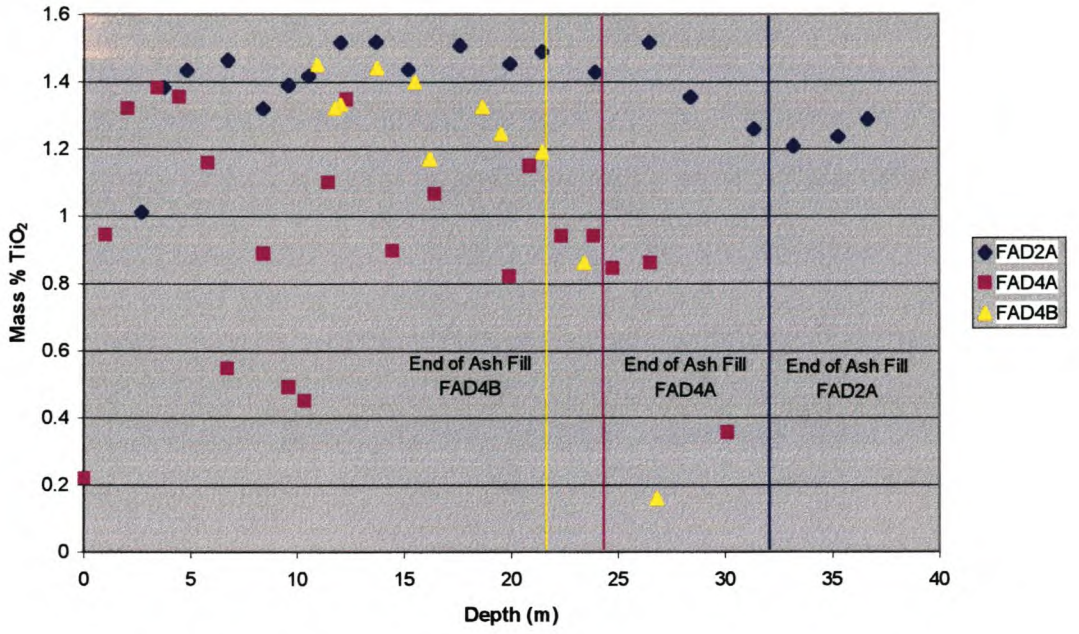

Figure 5.27: Variation of Ti in the three boreholes

Loss on ignition (LOI)

Figure 5.28 displays the variation in the mass percentage of LOI with depth in each of the three boreholes. The LOI represents the amount of volatile substances, such as SO_4, present in the samples. If one examines the results presented in figure 5.28 it is evident that:

- In all three boreholes there doesn't seem to be any trend in the variation of the LOI with depth in the boreholes.

- There appears to be slightly more volatile substances present in the centre of the ash dams than near the edge (mass % LOI in FAD2A and FAD4B higher than FAD4A).
- In boreholes FAD4A and FAD4B the amount of volatile substances in the sample taken at the deepest point is much higher than in the ash fill material.
- In borehole FAD2A the amount of volatile substances in the underlying material is less than in the ash fill material.
- In all the boreholes, at different depths, there are some very high peaks in the mass percentage LOI. In particular, in borehole FAD4A at a depth of 10.35m the mass percentage of volatile substances is very high. In this particular sample it was also noted that the mass percentage of Ca was also extremely high. As mentioned previously, the chemical and mineralogical composition of this particular sample are discussed in more detail in section 5.2.7.2.
- For boreholes FAD2A and FAD4A, the mass % LOI in the first sample (i.e. near the surface of the ash dam), is more than that of the fresh fine ash.

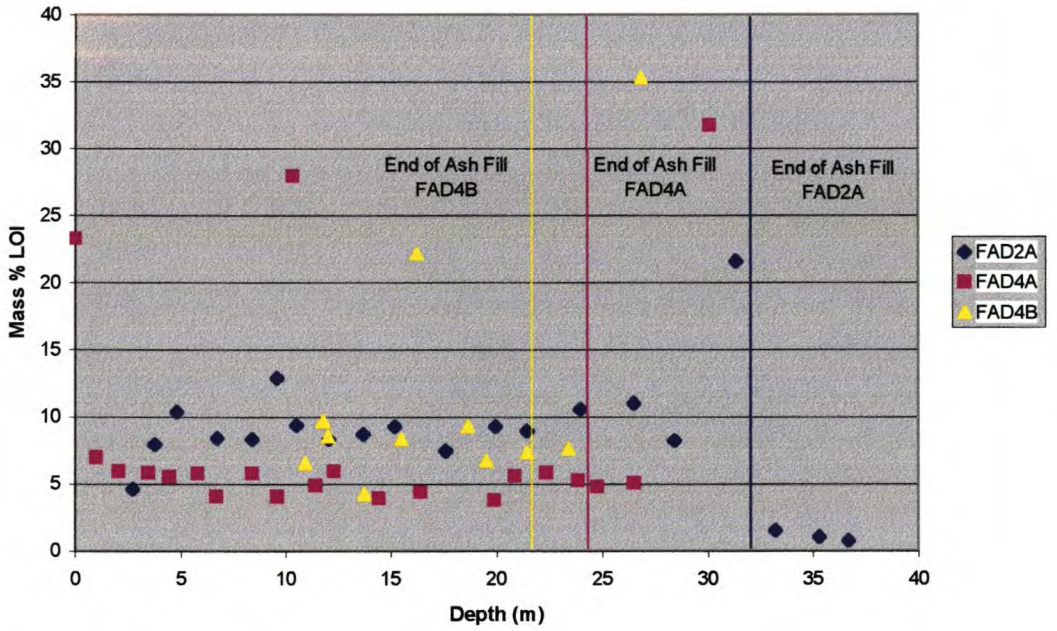

Figure 5.28: Variation of LOI in the three boreholes

5.2.5.2 Review of variations in the major elements

From the results discussed in section 5.2.5.1, the following conclusions, pertaining to the variation in the major elements, can be made:

- In general, the variation in the major elemental composition of the ash fill in borehole FAD4A was found to be much more erratic than in boreholes FAD2A and FAD4B. This could be attributed to the fact that both FAD2A and FAD4B were drilled near the centre of the respective dams, whereas FAD4A was drilled near the edge of fine ash dam 4.
- The mass percentages of Al, Fe, Na, K, Mg, Cr, P and Ti are all higher in the underlying material of borehole FAD2A (inactive dam) than in the underlying material of boreholes FAD4A and FAD4B (active dam). This could be due to the fact that fine ash dam 2 is much older as well as being inactive, whereas fine ash dam 4 is still in use. Moreover, it should be noted that currently course ash is being dumped on top of fine ash dam 2, which could be the cause of the seepage of some of the water, that was initially retained in the ash fill material, into the underlying material. If the water was forced out of the ash fill material into the underlying material, obviously some of the elements that were retained by means of hydraulic retention, would also pass into the underlying material. A further explanation for the higher concentrations of the elements mentioned above, beneath the ash fill of fine ash dam 2, could be the quality of the lining use at the bottom of the ash dam. Since fine ash dam 2 was one of the first ash dams constructed for the use in the ash disposal process, the lining may not be as effective as the lining used at the bottom of fine ash dam 4.
- There appears to be a relationship between the amount of Ca in the ash fill material and the amount of volatile substances (LOI). In borehole FAD4A, at a depth of 10.35m, there is a drastic increase in the amount of Ca (33%) as well as the volatile substances (LOI = 30%) in the ash fill material. Also in borehole FAD4A at a depth of 30.10m, and in borehole FAD4B at a depth of 26.80m there is a sharp increase in both the amount of Ca and volatile substances in the underlying material (38% Ca, 32% LOI in FAD4A and 36% Ca, 35% LOI in FAD4B). Furthermore, in the

underlying material in borehole FAD2A there is both a reduction in the percentage of Ca and a reduction in the percentage LOI.

- If one compares the major element distribution in the fresh fine ash and in the core sample closest to the surface of the ash dam, it is evident that there is less Si, Al, and Na in the core sample then in the fresh fine ash; and more Fe and volatile substances (LOI). These results hold true for both boreholes FAD2A (depth 2.70m) and FAD4A (depth 0.0m). No samples close to the surface of borehole FAD4B were obtained. A reduction in the percentages of Si, Al and Na suggests that these elements are leached from the ash during the transport of the slurry to the dams, and further due to initial weathering of the ash on the dam. The fact that the mass percentages of Fe and LOI are higher in the surface core sample than in the fresh fine ash suggests that there is a retention of Fe and some volatile substances during the transport of the slurry as well as due to initial weathering of the ash. These observations are based on the assumption that the composition of the fresh fine ash does not vary significantly.
- The overall decrease in Al content with depth, observed in boreholes FAD2A, FAD4A and FAD4B was also evident in the core drilled into the ash dam at the Kriel Power Station. Furthermore, the sharp increase in the mass percent Si observed at the ash/soil interface in boreholes FAD2A, FAD4A and FAD4B, was also detected at the ash/soil interface of the Kriel Power Station Ash Dam (Bezuidenhout, 1995).

5.2.5.3 Trace element analyses

The trace elements analysed for by means of XRF were Nb, Zr, Y, Sr, U, Rb, Th, Pb, Ga, Zn, Cu, Ni, Cr, Ce, Nd, V, Ba, and La. The results of all these analyses are given in Appendix D1. The results for the elements present in the largest quantities, or those that showed the greatest variation in the core material are discussed further in this section.

The variation in the Sr content of the ash and the ash effluent has already been discussed, with respect to the column experiments, in chapter 4. Thus it is interesting to examine the variation in the Sr content of the ash fill material in the ash dams. Figure 5.29 displays the variation in Sr concentration with depth in each of the three boreholes.

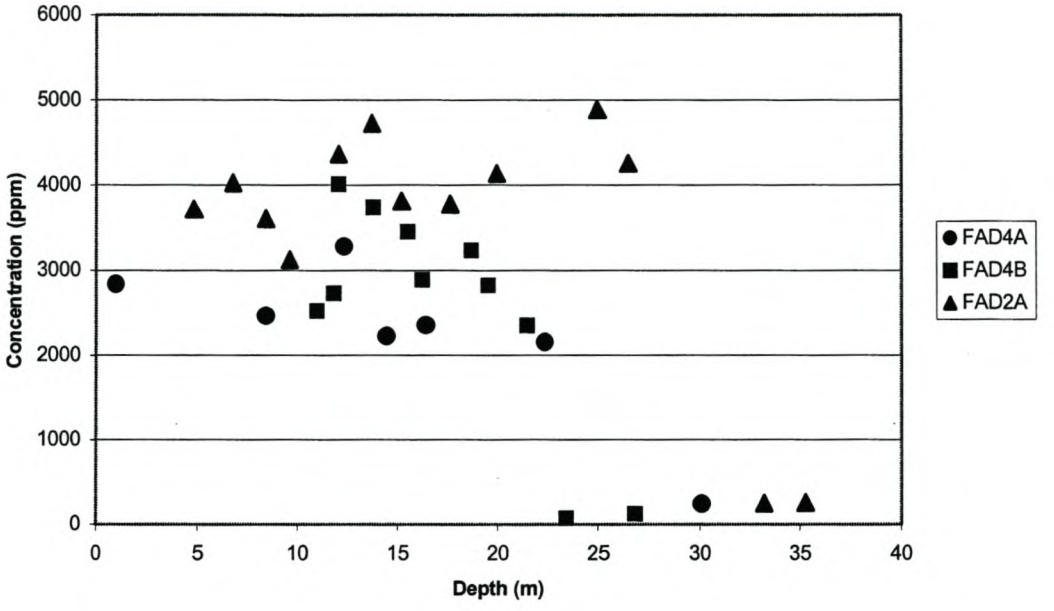

Figure 5.29: Variation in Sr concentration with depth in the boreholes

In all three boreholes it is evident that there is less Sr in the underlying material than in the ash fill material, which implies that even though Sr is leached from the ash, it does not contaminate the underlying soil.

Figures 5.30 and 5.31 represent the variation in Zr and Ce with depth in the ash dams. From figures 5.30 and 5.31 it is evident that there is less Zr and Ce in the underlying material than in the ash fill material. This is the same trend that was observed with respect to Sr. If one examines figure 5.30, it is evident that Zr is actually leached from the ash, however, as was the case with Sr, even though it is leached from the ash, it does not percolate into the underlying material.

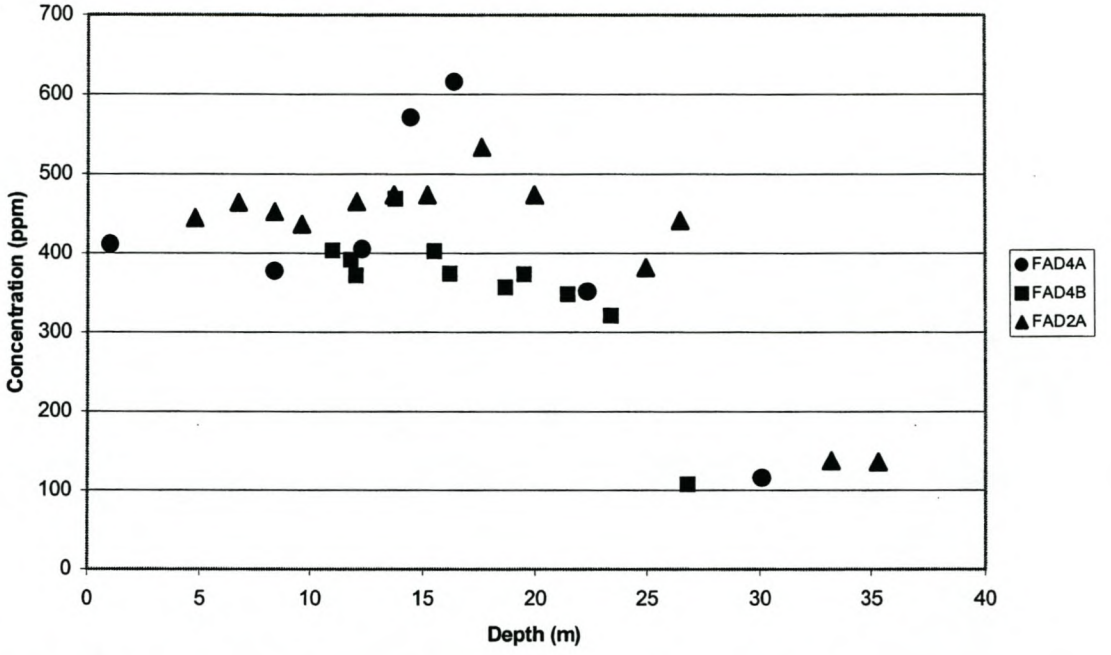

Figure 5.30: Variation in Zr concentration with depth in the boreholes

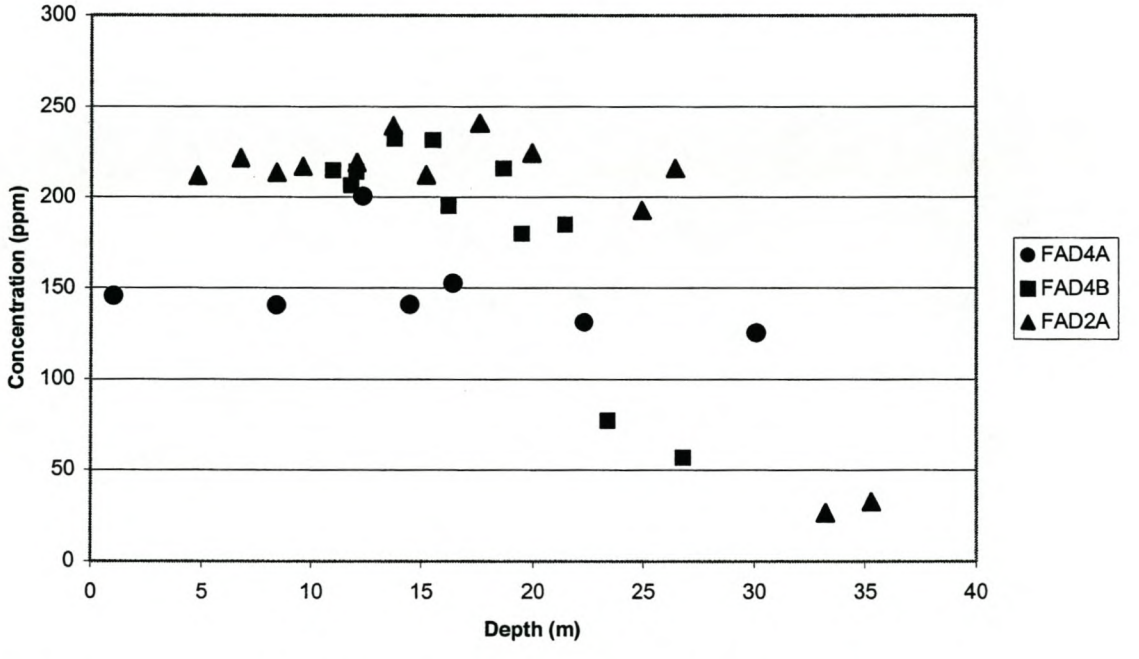

Figure 5.31: Variation in Ce concentration with depth in the boreholes

Figures 5.32, 5.33 and 5.34 represent the variation in V, Cr and Ba, respectively, with depth in the ash dams. It is apparent from figures 5.32, 5.33 and 5.34 that in borehole FAD2A that there is more V and Cr in the underlying material than in the ash fill material, and in borehole FAD4A there is more Ba in the underlying material compared to in the ash fill material. In order to asses whether these trace elements have been leached from the ash into the underlying material, one would need to conduct a survey of the composition of the soil in the vicinity of the ash dams. If these specific trace elements have leached from the ash into the underlying soil, it reinforces the trends seen for the major elements: that seepage of certain elements from the ash dams into the underlying material is more apparent in inactive fine ash dam 2.

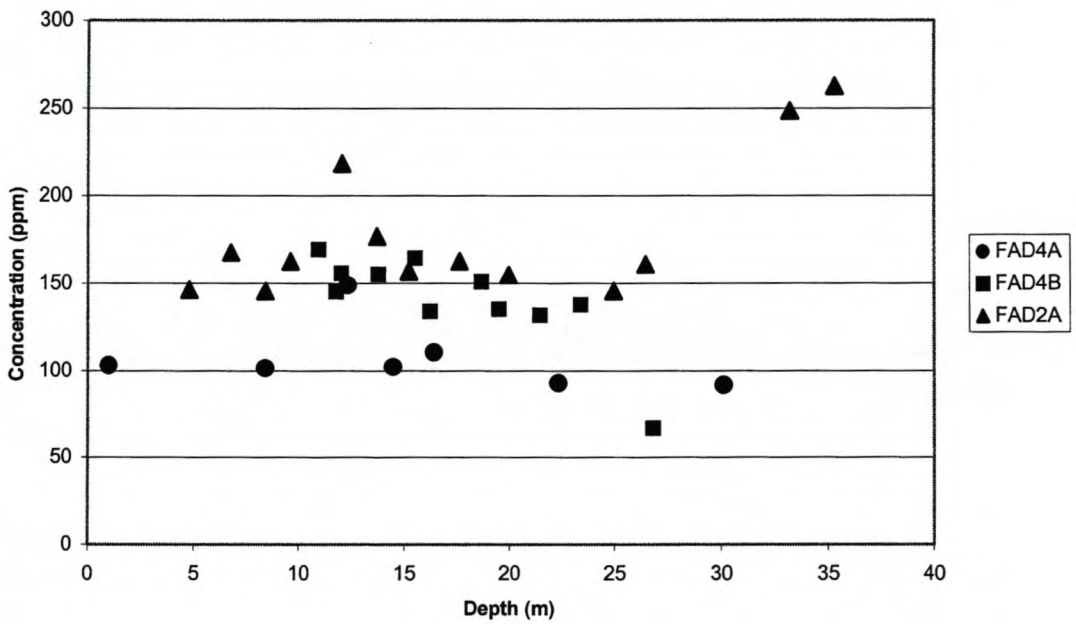

Figure 5.32: Variation in V concentration with depth in the boreholes

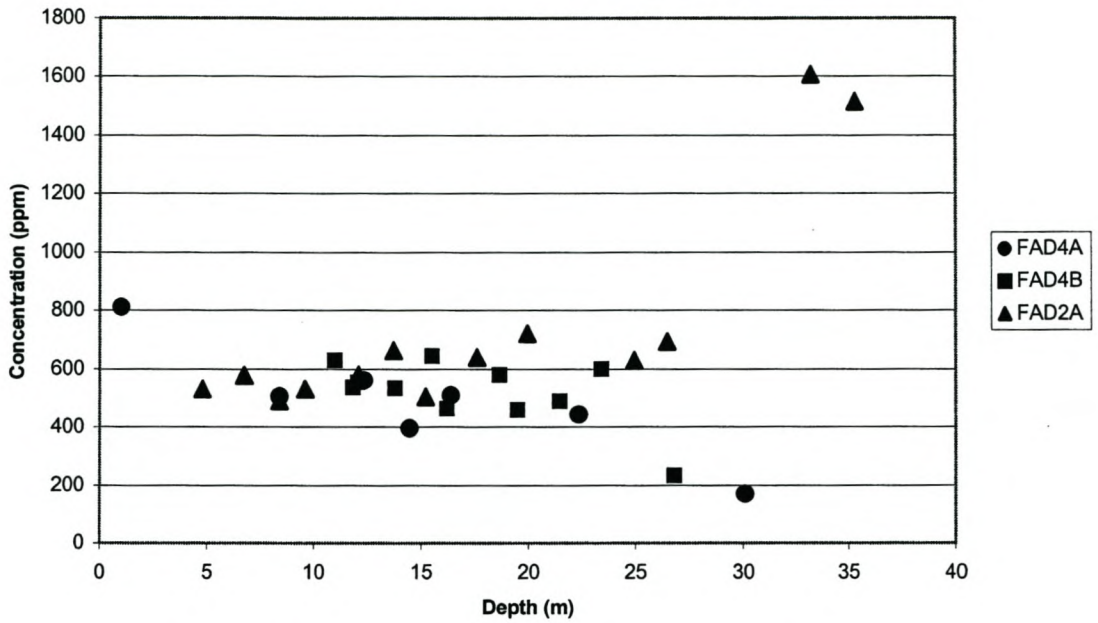

Figure 5.33: Variation in Cr concentration with depth in the boreholes

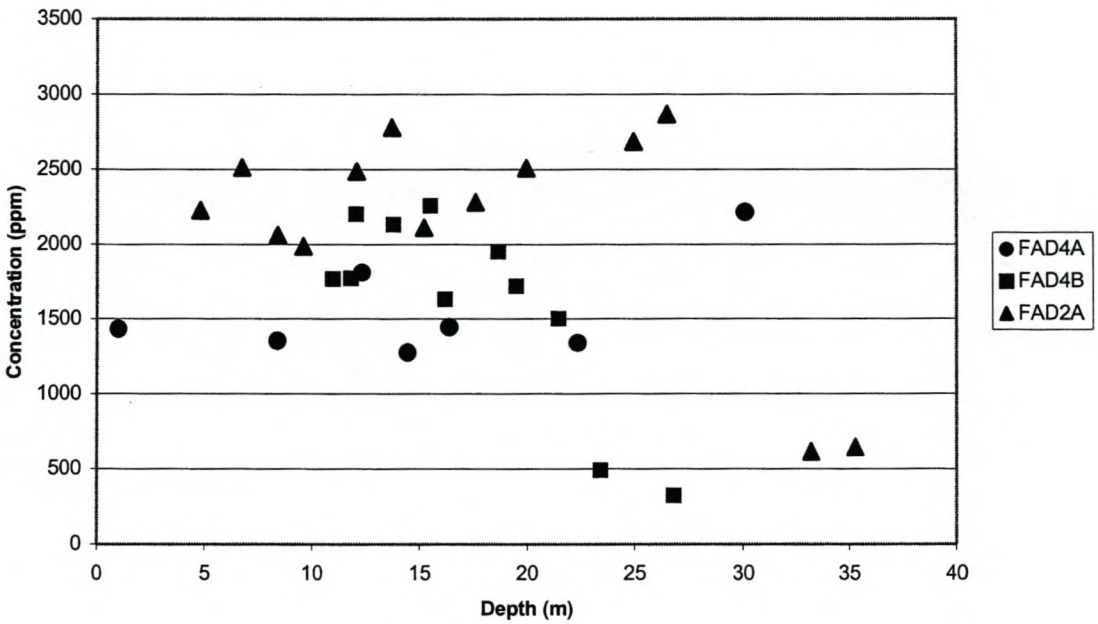

Figure 5.34: Variation in Ba concentration with depth in the boreholes

5.2.6 Mineralogy of the core samples

Apart from analysing the core samples for the variation in the chemical composition with depth, the variation of the main mineral phases with depth was also investigated. The results of the XRD analyses for the inactive dam, fine ash dam 2, are discussed in section 5.2.6.1, and the XRD results for the active dam, fine ash dam 4, are discussed in section 5.2.6.2. It is, however, also important to understand the mineral phases present in the fresh fine ash. Pretorius (2001) found the relative percentages of the main crystalline in the fresh fine ash at Secunda to be:

Mullite: 67%

Quartz: 26%

Lime: 7%

Calcite: 0%

Figure 5.35 displays the diffractogram for the fresh fine ash used in this study.

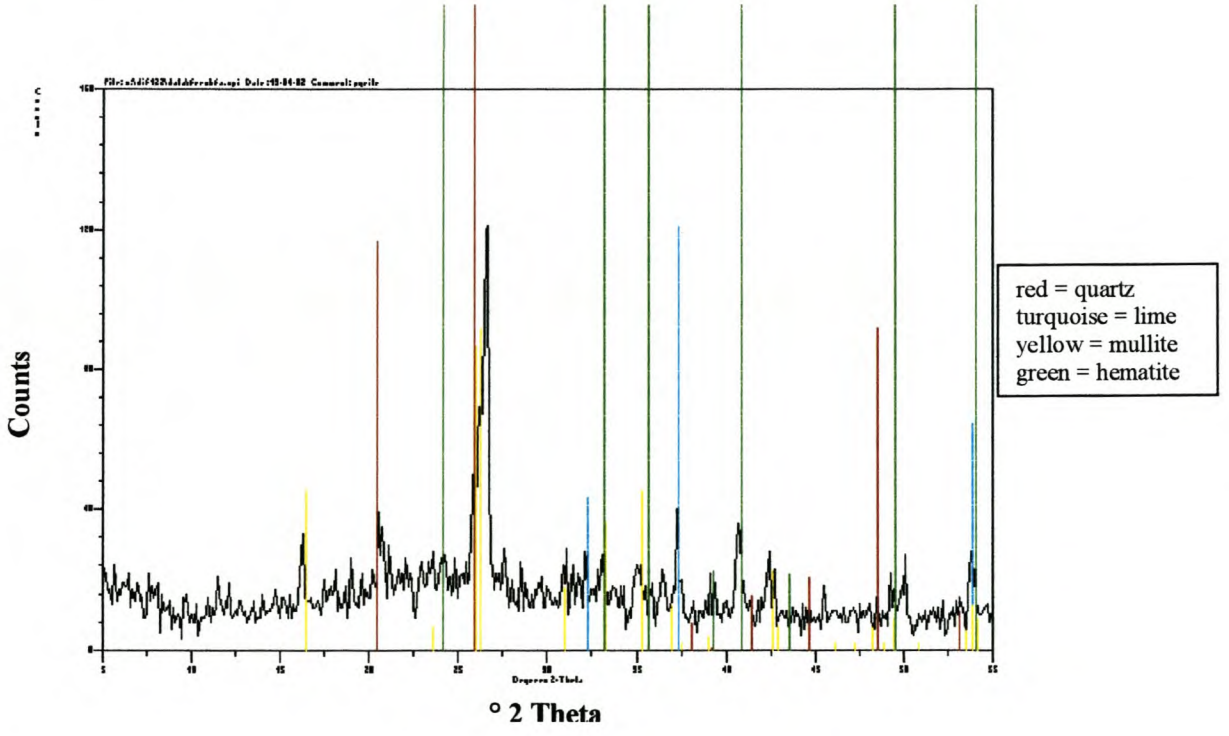

Figure 5.35: Diffractogram of fresh fine ash

It is evident from the diffractogram in figure 5.35 that the main mineral phases present in the fresh fine ash are mullite, quartz and lime (also identified by Pretorius, 2001), as well as hematite. Campbell (1999) also found mullite and quartz, to be present in unweathered fly ash, as well as lesser amounts of lime and hematite. No calcite was detected in the fresh fine ash analysed in this investigation, or in the fresh fine ash (produced at Secunda) analysed by Pretorius (2001).

5.2.6.1 An inactive ash dam

Figure 5.36 shows the 3-dimensional diffractograms for the core samples from borehole FAD2A. Eight core samples at different depths were analysed, however, the first sample (at a depth of 2.70m) proved to be difficult to analyses by means of XRD, thus only seven samples are represented in figure 5.36.

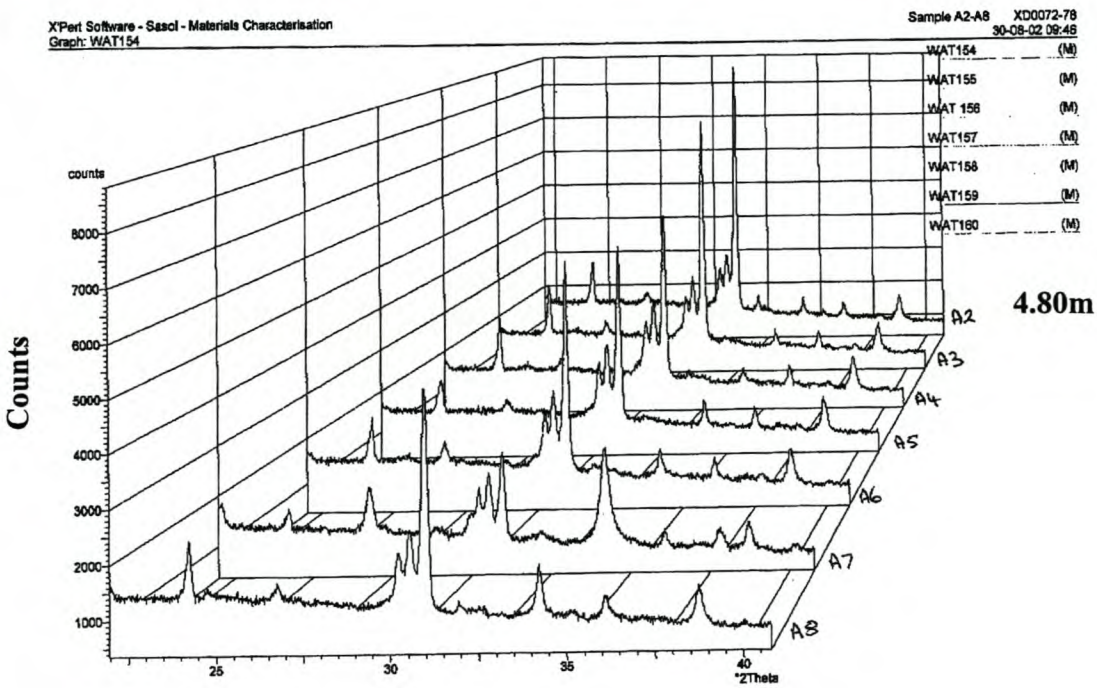

Figure 5.36: 3-Dimensional diffractograms for borehole FAD2A

The diffractograms shown in figure 5.36 reveal that there is not much variation in the mineral phases with depth. The only sample, which appears to be slightly different to the

others, is A7, at a depth of 24.45m. The peak at about 34° 2 Theta is much higher for sample A 7 than for the others. Also the sharp peak at 31° 2 Theta seen in all the other samples, it not as prominent for sample A7. The actual mineral phases identified in each sample are given in table 5.12.

Table 5.12: Mineral Phases Identified in Borehole FAD2A

Sample number	Depth (m)	$Al_6Si_2O_{13}$	SiO_2	$Ca_6Al_2(SO_4)_3(OH)_{12}.26H_2O$	$CaCO_3$	Fe_3O_4	Fe_2O_3
A1	2.70	mullite	quartz	ettringite	calcite		
A2	4.80	mullite	quartz	ettringite	calcite	magnetite	hematite
A3	8.40	mullite	quartz	ettringite	calcite	magnetite	
A4	10.55	mullite	quartz	ettringite	calcite		hematite
A5	13.70	mullite	quartz	ettringite	calcite	magnetite	
A6	19.95	mullite	quartz	ettringite	calcite	magnetite	
A7	24.45	mullite	quartz	ettringite	calcite	magnetite	
A8	28.40	mullite	quartz	ettringite	calcite	magnetite	hematite

From the results displayed in table 5.12 it is evident that mullite, quartz, ettringite and calcite are present throughout the ash fill material. It is only the form of the Fe that varies with depth. The Fe was identified it exist as magnetite, hematite, or both. Since both mullite and quartz are present in fresh fine ash, it is not surprising that they are present in the weathered fine ash. The presence of calcite was also anticipated due to the formation of calcite as a secondary mineral phase (from the CaO present in the fresh fine ash). It is the presence of ettringite throughout that ash fill material that proved to be an interesting discovery. Therefore, the presence of ettringite was investigated further.

Ettringite

According to literature, ettringite forms as a precipitate from hydrothermal solutions. It consists mainly if water (four out of every five atoms in ettringite is either a part of a water molecule or a hydroxide.) Both calcite and zeolites are minerals, which have been identified to be associated with ettringite. Ettringite consists of 19.16% Ca (26.81% CaO), 4.30% Al (8.12% Al_2O_3), 5.14% H (45.93% H_2O), 7.66% S (19.14% SO_3), and 63.74% O.

Tishmack (1999) performed detailed mineralogical characterisations on six calcium rich fly ashes. Pastes were made from fly ash and water and the hydration products were investigated. Ettringite was one of the principal phases produced at room temperature. Bezuidenhout (1995) found the main sulphate-containing phase, in the core samples from the Kriel Ash Dam, to be gypsum. However, no gypsum as found in the core samples from borehole FAD2A. O'Brien (2000) suggests that ettringite exists at a pH above 10, and below this pH it dissolves incongruently to gypsum and Al hydroxides. Since the pH in the ash dams should be above 10 (based on the pH data from the ash water), one would expect to find ettringite and not gypsum in the core samples. Campbell (1999) investigated weathered fly ash samples from Kriel and Matla Power Stations, as well as from Sasol. He found ettringite to be present in the samples from Kriel and Matla, and he also found no gypsum in any of the weathered fly ash samples. In saturated paste and dilute aqueous extract experiments conducted by Campbell (1999), he found that Na and Cl co-precipitated with Ca and SO_4 (removal from the liquid phase), which indicated the formation of a secondary phase more complex than gypsum. He suggests that the removal of Na, Cl, Ca and SO_4 could be attributed to the formation of ettringite since it is a more complex mineral phase than gypsum, is stable at a high pH, and is structurally more amenable to accommodating impurities. Thus, in hindsight, the presence of ettringite in the core samples from borehole FAD2A should not be unexpected.

Table 5.13 displays an indication of the relative amounts (calculated as integrated areas) of ettringite present in each of the samples analysed.

Table 5.13: Relative Proportions of Ettringite in Borehole FAD2A

Sample number	Depth (m)	Integrated area (degree counts)
A2	4.80	290
A3	8.40	326
A4	10.55	280
A5	13.70	258
A6	19.95	360
A7	24.45	744
A8	28.40	123

The results in table 5.13 show that at a depth of 24.45m there is a lot more ettringite present compared to the rest of the ash fill material. Precipitates such as ettringite ($Ca_6Al_2(SO_4)_3(OH)_{12}.26H_2O$) and $CaCO_3$ have the tendency to cement the ash particles together and thus reduce the permeability of the ash.

Magnetite and hematite

It is clear from the results presented in table 5.12 that Fe is present throughout the entire depth of the ash fill material; it is just the form of the Fe that varies. From figure 5.35 one can see that in the fresh fine ash Fe is present as hematite, whereas in the weathered ash, the form of Fe varies between magnetite and hematite. Therefore, the differences in these two minerals were examined further.

Magnetite (Fe_3O_4) consists of 72.36% Fe and 27.64% O. The Fe is present in both the +2 and +3 oxidation states. For every mol of magnetite, there is one mol of Fe^{2+} and two moles of Fe^{3+}. In other words, the Fe in the magnetite exists as 31.03% FeO and 68.97% Fe_2O_3 (hematite). Magnetite is a mineral that exhibits strong magnetism whereas hematite displays only weak magnetic behaviour. Magnetite, in the presence of oxygen, will be converted to hematite by the following reaction:

$$4Fe_3O_4\ (magnetite) + O_2 \leftrightarrow 6Fe_2O_3\ (hematite) \qquad (5\text{-}3)$$

Hematite is comprised of 69.94% Fe and 30.06% O, and the Fe exists as 100% Fe_2O_3. Therefore all the Fe in hematite exists in the +3 oxidation state. Thus it appears as if the from of the Fe in the ash material is dependent on the availability of oxygen. One would therefore expect the samples deeper in the ash dam to contain less hematite than those near the surface due to the lack of oxygen within the ash dam. If one examines the data presented in table 5.12 it is evident that although some hematite does exist towards the bottom of the ash dam, there is definitely more magnetite: below a depth of 11m, 4/4 samples contain magnetite, and only 1/4 contain hematite.

5.2.6.2 An active ash dam

XRD analyses were performed on both boreholes drilled into the active fine ash dam 4. FAD4A represents the variation in the mineral phases near the edge of an active dam, whereas FAD4B represents the mineral phases present near the centre of an active fine ash dam. Table 5.14 displays the identified mineral phases in a variety of samples from both FAD4A and FAD4B. The diffractograms for all these samples can be found in Appendix D2. The data highlighted in red in table 5.14 is the core sample from FAD4A at a depth of 10.35m that was noted to have a very different chemical composition to the other samples (section 5.2.5.1). The data highlighted in blue represents the samples that lie beneath the ash fill material, i.e. in the underlying vertisol material.

From the data presented in table 5.14 it is evident that there is a lot more variation in the mineral phases near the edge of the active ash dam then near the centre. This is probably due to the fact that the water table near the centre of the fine ash dam 4 is at a depth of 3.6m into the ash fill material, whereas near the edge it is at a depth of 14.8m.

In borehole FAD4B the main mineral phases throughout the ash fill material are mullite, quartz, calcite and sillimanite. These results are similar to those for borehole FAD2A, except in FAD2A ettringite was also present throughout the ash fill material, as well as magnetite and/or hematite. Sillimanite on the other hand was only found in borehole FAD4B and not in FAD2A. Both these boreholes are near the centre of the respective ash dams, however, the difference in the mineral phases present is probably due to the fact that fine ash dam 2 is much older than fine ash dam 4, and is also inactive (with the result being a lower water table). In borehole FAD4B, only quartz and calcite were found to be present in the underlying material.

Table 5.14: Mineral Phases Identified in Boreholes FAD4A and FAD4B

Depth	$Al_6Si_2O_{13}$	SiO_2	$CaCO_3$	Fe_3O_4	Fe_2O_3	Fe_2O_3	Fe_7S_8	Al_2SiO_5	$Ca_2Al_2O_5.6H_2O$	$CaSO_4.2H_2O$	$K(Li, Al)_3(Si,Al)_4O_{10}(F,OH)_2$
(m)	mullite	quartz	calcite	magnetite	hematite	maghemite	pyrrhotite	sillimanite	CaAlO hydrate	gypsum	lepidolite
Borehole FAD4A											
0		quartz		magnetite		maghemite	pyrrhotite				
2.05	mullite	quartz	calcite					sillimanite			
4.45	mullite	quartz	calcite					sillimanite			
6.7	mullite	quartz	calcite					sillimanite			
9.6		quartz	calcite	magnetite							
10.35		quartz	calcite		hematite	maghemite			CaAlO hydrate		
11.45	mullite	quartz	calcite			maghemite					
14.45	mullite	quartz									
19.9	mullite	quartz	calcite	magnetite							
22.35	mullite	quartz	calcite	magnetite						gypsum	
24.75		quartz									lepidolite
26.5		quartz									lepidolite
30.1		quartz	calcite								
Borehole FAD4B											
10.5-11.4	mullite	quartz	calcite								
11.8-12.25	mullite	quartz	calcite					sillimanite			
14.5-16.5	mullite	quartz	calcite					sillimanite			
17.9-19.4	mullite	quartz	calcite					sillimanite			
21.45	mullite	quartz	calcite					sillimanite			
26.8		quartz	calcite								

From the mineral phases shown in table 5.14 it is obvious that there is considerable variation in the mineral phases with depth in the borehole. Quartz is present in all the samples, both in the ash fill material and in the underlying material, however, mullite is not present at all in the underlying material. There is also a lack of mullite in the underlying material in borehole FAD4B. No major Fe containing phase was identified in the underlying material in either borehole FAD4A or FAD4B. In borehole FAD4A, most of the core samples taken within the ash fill material contain Fe in one from or another; however, in the ash fill material of borehole FAD4B, no Fe containing phases were identified by means of XRD.

It is evident that some of the core samples in boreholes FAD4A and FAD4B contain both mullite ($Al_6Si_2O_{13}$) and sillimanite (Al_2SiO_5). The difference between these two aluminium silicon oxide minerals is that mullite contains more Al than sillimanite, and sillimanite contains more Si than mullite. Therefore mullite has a larger percentage of Al_2O_3 than sillimanite, and less SiO_2. The relative percentages of these elements and their oxides, in mullite and sillimanite, are given in table 5.15.

Table 5.15: Elemental Distribution in Mullite and Sillimanite

	Mullite		Sillimanite	
Aluminium	38.00% Al	71.79% Al_2O_3	33.30% Al	62.92% Al_2O_3
Silicon	13.18% Si	28.21% SiO_2	17.33% Si	37.08% SiO_2
Oxygen	48.82% O		49.37% O	

Calcite was detected for all the samples in borehole FAD4B (from a depth of 10.5m), as well as in most of the core samples from borehole FAD4A. However, no calcite was detected in the sample on the surface of fine ash dam 4 at the location of borehole FAD4A, and also at a depth of 14.45m into the ash fill material. The lack of calcite on the surface of the dam is interesting since one would expect it to be found concentrated on the surface of the dam due to the availability of CO_2. One should bear in mind that this result is for only one point on the entire ash dam surface and is not necessarily a true reflection of what could be found on the surface of the dam. Moreover, Pretorius (2000),

found calcite to be present on the surface of a weathered fine ash dam, as was expected (section 3.9.3, table 3.15). The lack of calcite at a depth of 14.45m could be related to the fact that the water table starts at a depth of 14.8m in borehole FAD4A. A further explanation for the lack of calcite present in the sample at a depth of 14.45m could be due to an error during the sampling procedure or during the analysis of the sample.

It is interesting to note that S-containing mineral phases were not detected in most of the core samples from borehole FAD4A, and no S-containing mineral phases were found in the core samples from borehole FAD4B. In borehole FAD4A, at a depth of 0m, pyrrhotite (Fe_7S_8) was found, and at a depth of 22.35m, just before the ash/soil interface, gypsum ($CaSO_4.2H_2O$) was found. It is possible that some S-containing phases do exist in the other samples, but, either due to low concentrations, or obstruction of these peaks in the diffractogram by other more dominant minerals, they were not detected by means of XRD.

In borehole FAD4A there is a distinct change in the mineral phases present in the ash fill material and in the underlying vertisol material. The end of the ash fill material in this borehole is at a depth of 24.45m. The very next sample after this point, at a depth of 24.75m, contains only quartz and lepidolite. Further into the underlying material, at a depth of 26.50m, still only quartz and lepidolite are present, and at a depth of 30.10m, quartz and calcite that are the main mineral phases present. These variations in the mineral phases are addressed again in conjunction with the variations in the chemical composition of the different samples (section 5.2.7.1). The presence of lepidolite just beneath the ash fill material is an interesting finding and will therefore be discussed further.

Lepidolite is a potassium lithium aluminium silicate hydroxide fluoride. Its chemical formula is K(Li,Al)3(Si, Al)4O10(F,OH)2, its empirical formula is $KLi_2AlSi_4O_{10}(OH)F$. The relative percentages of each of the elements present in lepidolite are given in table 5.16.

Table 5.16: Elemental Distribution in Lepidolite

Potassium	10.07% K	12.13% K_2O
Lithium	3.58% Li	7.70% Li_2O
Aluminium	6.95% Al	13.13% Al_2O_3
Silicon	28.93% Si	61.89% SiO_2
Hydrogen	0.26% H	2.32% H_2O
Oxygen	45.32% O	
Fluorine	4.89% F	4.89% F

From the data presented in table 5.16 it is apparent that lepidolite consists mainly of Si and O in the form of SiO_2. One of the minerals reported in literature to be associated with lepidolite is quartz. This is apparent in the core samples from FAD4A at 24.75m and 26.50m, where quartz and lepidolite are the main mineral phases present.

5.2.7 Correlation between chemical and mineralogical analyses

The variation in the chemical composition of the core material with depth was discussed in section 5.2.5, and the change in mineralogical composition of the core samples was discussed in section 5.2.6. In this section the correlation between the chemical and mineralogical composition of the samples is addressed.

5.2.7.1 In general

Silicon

XRF results show the Si is present in all core samples for all three boreholes. The XRD results also show that Si is present in one form or another in all the core samples analysed, both in the ash fill material and in the material underlying the ash dams. Quartz was found to be present in all the core samples, and other Si-containing minerals phases detected were mullite, sillimanite and lepidolite.

Aluminium

XRD analyses of the core samples show that the main Al-containing mineral phase in all three boreholes is mullite. Mullite was found throughout the ash fill material of boreholes FAD2A as well as FAD4B, as well as in most of the samples in borehole FAD4A.

Another Al-containing mineral phase found in some of the core samples from the ash fill material in boreholes FAD4A and FAD4B, was sillimanite. In borehole FAD2A ettringite was another Al-containing mineral phase that was detected in all the samples. The XRF results also show Al to be present throughout the ash fill material. In the underlying material of borehole FAD4A, no mullite was detected, however, lepidolite was found just below the ash/soil interface. In the deepest sample taken in both boreholes FAD4A and FAD4B, no Al-containing mineral phases were detected. This correlates well with the XRF results, which reveal that the mass percentage of Al in the deepest samples of boreholes FAD4A and FAD4B is very low. The XRF results also show that the mass percentage of Al in the sample taken at 0m in borehole FAD4A is very low, which is probably why no Al-containing phase was detected by means of XRD analysis.

Iron

In borehole FAD2A, the XRD analyses of the core samples show that Fe is present throughout the ash fill material either as magnetite or hematite. The XRF analysis results reveal that the mass percentage of Fe in the core samples remains approximately the same right through the ash fill material. Therefore, even though the XRD results only give a qualitative and not a quantitative indication of the Fe in the samples, the fact that Fe-containing minerals are detected throughout the ash fill material correlates with the results of the XRF analyses.

In borehole FAD4B, no Fe-containing minerals were detected using XRD even though the XRF reveal that there is Fe present in all the core samples. In borehole FAD4A however, the results from the XRD analyses reveal Fe-containing minerals in some of the core samples. The XRF results also show that Fe is present throughout borehole FAD4A. The mass percentage of Fe present in borehole FAD4A is greater than in borehole FAD4B, which is a possible explanation as to why Fe-containing minerals are detected in some samples from borehole FAD4A and not in any sample from FAD4B.

Calcium

Almost all of the ash fill material samples analysed by means of XRD contained calcite, which correlates well to the XRF analyses that show Ca to be present throughout the ash fill material. XRF results reveal that in the deepest sample taken of the underlying material in boreholes FAD4A and FAD4B, the mass percentage of Ca is very high; therefore one would expect to find a Ca-containing mineral phase in these samples. XRD analyses of these samples show that at ±30m in borehole FAD4A and at ±26m in borehole FAD4B, calcite is present. A further correlation between the XRF and XRD results for Ca is that in borehole FAD4A, at a depth of ±25m and at ±26m (both in the underlying vertisol material), practically no Ca was detected by means of XRF, and also no Ca-containing mineral phases were found to be present.

5.2.7.2 Sample FAD4A at a depth of 10.35m

As mentioned previously, the core sample of ash fill material taken at a depth of 10.35m in borehole FAD4A showed interesting XRD and XRF results, and is thus discussed in more detail in this section. Figure 5.37 displays the diffractogram of this particular sample. The mineral phases present in this sample are:

Quartz (SiO_2)

Hematite (Fe_2O_3)

Calcium aluminium oxide hydrate ($Ca_2Al_2O_5.6H_2O$)

Maghemite (Fe_2O_3)

Calcite ($CaCO_3$)

If one compares these mineral phases to the phases found in the other samples it is evident that the composition of this particular sample is very different from the ash fill material in general. In most of the other samples, the dominant Al-containing mineral phase is mullite, whereas in this sample it is calcium aluminium oxide hydrate. Also this is the only sample out of all three boreholes in which calcium aluminium oxide hydrate was detected.

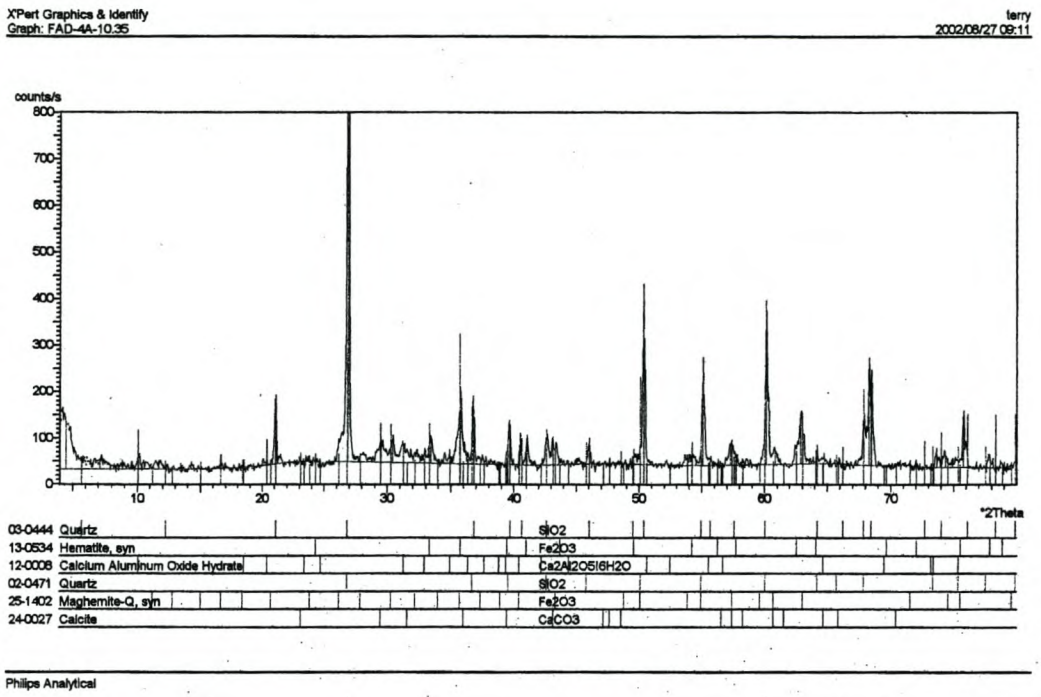

Figure 5.37: Diffractogram of core sample from FAD4A at a depth of 10.35m

If one examines figure 5.37 it is apparent that in the sample taken at 10.35m in borehole FAD4A the mass percentage of Ca as well as the percentage of volatile substances is much higher than in the other core samples. This correlates well with the XRD results, which, as discussed, reveal that not only calcite but also calcium aluminium oxide hydrate is present in this sample. In the preparation of the samples for XRD and XRF analyses, it was also noted that this particular was much harder than the other samples (was very hard to crush it) and it was also a very dark blackish colour (most of the ash fill material samples were a grey colour).

5.3 Summary

Three boreholes were drilled into the Sasol ash dams in Secunda; one was drilled into the centre of inactive fine ash dam 2 (FAD2A), and two were drilled into active ash dam 4 – one in the centre (FAD4B) and one near the edge (FAD4A). Each borehole was drilled to a depth of approximately 5m below the ash dam into the underlying soil, and a temporary casing was installed in each borehole. In each of the boreholes, two 25mm slotted PVC standpipe piezometers were inserted to allow for the levels of the water systems both within the underlying material and the ash to be measured and monitored, and for the permeabilities of the materials to be tested separately. Core material was retrieved from each borehole at a variety of depths for analysis purposes. The different analyses performed on the core material were: permeability tests (field and laboratory), standard penetration tests, determination of the particle size distribution, Atterberg Limits, natural moisture content and the void ratio.

The basic profile in the three boreholes consisted of a dense surface layer of between 1m and 2m thick, which contained course grains of calcareous (calcium-rich) material underlain by ash fill material, the majority of which consisted of alternating light and dark grey layers of fine to medium grained ash. A thin (± 0.2m) layer was found at the base of each of the fine ash dams. It was composed of dark grey, medium grained ash with varying amounts of course calcareous material. A thin layer of dark brown, clayey, sandy silt existed below each ash dam. Below the layer of dark brown material a layer of grey, clayey, sandy silt was found, in which a decomposing calcrete layer was evident. Below Fine Ash Dam 2 (inactive dam), highly weathered, very weak rock dolerite was detected. However, rock was not detected below Fine Ash Dam 4, neither beneath FAD4A nor FAD4B.

The particle size distribution tests revealed that there is variability in the proportions of sand, silt and clay (or clay-sized particles) within both the ash fill material and the underlying lithomorphic vertisol material. In general, the ash fill material can be described as clayey (occasionally sandy) silt; although clay-sized particles were found to

be present in the ash fill material, they did not exhibit the properties of clay material. The underlying material can best be described as clayey sandy silt.

The plasticity (determined by means of the Attenberg Limits) of the ash fill material was found to be very low. On the other hand, the plasticity of the underlying lithomorphic material was found to be very high. The void ratio, and therefore porosity, was found to vary with depth in the ash fill material. Moreover, it was apparent that the porosity was higher in the ash fill material than in the underlying lithomorphic vertisol. Furthermore, the specific gravity of the material underneath the ash dams was found, in general, to be higher than the specific gravity of the ash fill material. The combined effect of the lower porosity and higher specific gravity of the underlying material results in a greater *in situ* density of the material beneath the ash dams.

The identification of the phreatic surfaces in each of the boreholes assisted in the understanding of the water table profile in the ash dams. The natural moisture content (NMC) was found to vary with depth in the boreholes. Below the phreatic surface in each borehole, the NMC of the ash fill material was approximately the same as the porosity – about 60%. As was anticipated, the average moisture content of the ash fill material (from the surface to the just above the underlying material) in the centre of the ash dams (FAD2A and FAD4B) is greater than near the edge (FAD4A).

Although the field permeability tests that were performed have greater restrictions, they provided a more realistic indication of the actual permeability of the dams on a large scale. The permeability tests performed revealed that for boreholes FAD2A and FAD4A there was very little difference in the permeability of the ash fill and the underlying material. The permeability of both materials at the location of these two boreholes fell within the range of 1×10^{-5} to 5×10^{-5}m/s. Furthermore, the ash fill material in the centre of an active ash dam appears to be more permeable (better drainage) than the ash fill material towards the edge of an active dam, or in the centre of an inactive ash dam.

The chemical analysis, by mean of XRF, of selected core samples from each of the three boreholes revealed that:

- In general, the variation in the major elemental composition of the ash fill material near the edge of an active ash dam appears to be more erratic than the variation in the centre of both an active and an inactive dam.
- The mass percentages of Al, Fe, Na, K, Mg, Cr, P and Ti were all found to be higher in the underlying material of borehole FAD2A (inactive dam) than in the underlying material of boreholes FAD4A and FAD4B (active dam). This can be attributed to either the age difference between the dams, that fact that course ash is currently being stacked on top of ash dam 2, or the difference in the lining of the two dams. However, what can be concluded from this finding is that fine ash dam 4 appears to retain salts more efficiently than fine ash dam 2.
- There appears to be a relationship between the amount of Ca and the amount of volatile substances in the ash fill material.
- The trace element analyses reveal that even though Sr and Zr are leached from the ash (section 4.3.2, figure 4.29), less Sr and Zr are present in the underlying material compared to in the ash fill material. Therefore, even though they are leached from the ash, they do not percolate through the ash fill material into the underlying soil. There is also less Ce in the underlying material compared to the ash fill material.
- In borehole FAD2A, trace element analyses divulged that there is more V and Cr in the underlying material, and in borehole FAD4A, more Ba was found in the underlying soil compared to the ash fill material. It is interesting to note that both the major element analyses and trace elements analyses showed more Cr to be present in the underlying material of borehole FAD2A.
- There is some similarity between the findings of this core drilling exercise, and the one performed by Bezuidenhout (1995) on an ash dam at the Kriel Power Station: The overall decrease in Al content with depth, observed in boreholes FAD2A, FAD4A and FAD4B was also evident in the core drilled into the ash dam at the Kriel Power Station. Furthermore, the sharp increase in the mass percent Si observed at the ash/soil interface in boreholes FAD2A, FAD4A and FAD4B, was also detected at the ash/soil interface of the Kriel Power Station Ash Dam (Bezuidenhout, 1995).

The general mineralogy of core samples, taken from the ash fill material, consisted of quartz, mullite and calcite and lesser amount of Fe-containing minerals such as magnetite and hematite. Sillimanite was also found to be present in many of the core samples from boreholes FAD4A and FAD4B, and ettringite was a prominent mineral found throughout the ash fill material of the borehole drilled into the centre of the inactive fine ash dam 2 (FAD2A). No S-containing minerals were detected by means of XRD in either borehole FAD4A or FAD4B, except for the identification of gypsum near the ash/soil interface in borehole FAD4A. No mullite was found in the core samples taken from the underlying material in boreholes FAD4A and FAD4B, however, the Al and Si-containing mineral, lepidolite, was found in the region just below the ash/soil interface. Furthermore, no major Fe containing phase was identified in the underlying material in either borehole FAD4A or FAD4B. The deepest sample taken from both boreholes FAD4A and FAD4B consisted of only quartz and calcite, with the mass percentage of Ca in these samples being extremely high. A lot more variation in the mineralogical composition of the ash fill material was found in borehole FAD4A. The mineralogical composition of the ash fill samples from boreholes FAD2A and FAD4B was very consistent with depth in the respective ash dams. This finding, combined with the fact that the chemical composition of the core samples varied more significantly in borehole FAD4A, suggests that the lateral position of the ash in the ash dam influences the chemical reactions that occur. Overall, a good correlation was found between the XRF and XRD analyses of the core samples.

5.4 Recommendations

From the insight gained through this core drilling exercise the following recommendations can be made:

- Core material from the three boreholes is still available, and could be used for further chemical and mineralogical analyses. Although XRD analysis techniques are generally used as a qualitative indication of the mineral present in a particular sample, it would be interesting if one could use this analysis technique in order to attain a quantitative indication of the different mineral present in the ash dams.

- In order to achieve a better understanding of the variation in the ash fill material as well as the underlying material, it is proposed that more boreholes be drilled into the ash dams – both active and inactive dams. This will also assist one in obtaining a more comprehensive understanding of the water table profile in an active and an inactive ash dam.
- The chemical and mineralogical composition of the material beneath the ash dams should be compared to soil samples taken from the area surrounding the ash dams in order to assess the seepage of certain elements from the ash into the underlying soil.

Chapter 6

Conclusions and Recommendations

The four different aspects of this project are presented in chapters 2 to 5. In each chapter conclusions were made pertaining to the specific scope of work covered in the chapter. It is, however, important that the results from the literature survey, plant data, laboratory column experiments, and core drilling are combined, in order to attain a thorough understanding of chemistry involved in the mixing of an industrial effluent with fine ash; specifically the chemistry which occurs throughout the wet ash disposal system employed by Sasol 2 and Sasol 3 in Secunda, South Africa.

The purpose of this chapter is to present the most significant conclusions drawn from the investigation as a whole. Based on these conclusions, recommendations will be made with regard to future research.

6.1 Summary of the Methodology

6.1.1 Literature survey

In summary, the literature review provided one with an overview of fly ash: how it is produced, how it is disposed of, and the general chemical and mineralogical composition of fly ash. The chemistry of specific components, related to a wet ash disposal system, was discussed in detail, and in particular, the chemistry involving calcium. The calcium carbonate chemistry is well documented in the literature, and is a component of particular importance in the Secunda ash water system; therefore it was examined in more detail. It is imperative that before undertaking an investigation of a specific ash disposal system,

one understands the basic composition of fly ash, the related chemistry, as well as previous studies carried out on similar systems.

6.1.2 The actual ash disposal system

The complexity of the actual disposal system is the greatest hindrance in understanding the changes that occur during the transportation and disposal of the fine ash. The lack of flow data prevented the calculation of mass balances over some parts of the system; therefore, the most comprehensive results were based on the variations in concentration of the different constituents of the ash water. Three different phases of the disposal of the ash were identified:

- Phase 1: the initial contact of the ash and the effluent.
- Phase 2: the time the ash spends in contact with the effluent.
- Phase 3: the retention of the effluent in the holding dams[1] before being recycled.

Sufficient data, in the form of chemical analyses of the ash water streams, was available for phase 3; less data was available for phase 2; and very little data existed for phase 1.

6.1.3 Laboratory column experiments

The laboratory column experiments carried out were evaluated in terms of mass balances on the liquid phase, as well as on the solid phase (ash). If one examines both the liquid and the solid phase results, it is evident that there are some discrepancies with respect to certain elements. For example, solid phase mass balances show that Ca is leached from the ash, whereas if one examines the change in the Ca content of the liquid phase, Ca is actually removed from the effluent. This observation highlights the fact that it is not merely the contact of the ash with the water that plays a role in the chemical changes that occur in the disposal system, but also the retention time of the effluent in the evaporation and CAE dams (phase 3). It is during phase 3 that many important chemical reactions

[1] The evaporation and clear ash effluent dams

occur, such as the precipitation of calcite, which result in an improved ash water quality. If these salts were not removed during phase 3 they would build up in the effluent that is recycled to the factory and in turn the entire operation of the ash disposal would be affected.

Both the liquid phase and solid phase mass balance results divulged that during phase one, the initial contact of the ash with the water, a lot of chemical reaction occur which alter both the ash water quality and the composition of the ash.

6.1.4 Core drilling

Three boreholes were drilled into the Sasol ash dams in Secunda; one was drilled into the centre of inactive fine ash dam 2 (FAD2A), and two were drilled into active ash dam 4 – one in the centre (FAD4B) and one near the edge (FAD4A). Core material was retrieved from each borehole at a variety of depths (in the ash fill material and in the underlying vertisol material) for analysis purposes. The results of these analyses served to provide one with an enhanced understanding of the working of the ash dams.

6.2 Overall Conclusions

It is essential that the conclusions of the four different aspects of this project be combined in order to achieve a comprehensive understanding of the chemistry involved in the Secunda ash water system. Therefore, from this investigation one can conclude that salts are retained in the ash dams. Based on the results obtained from the laboratory column experiments (section 4.2.2.1, table 4.11) and the production rate of the fine ash from Sasol 2 and Sasol 3 (section 3.2, figure 3.3), the potential amount of salts that can be removed from the system (either due to precipitation or retention in the ash dams) is approximately 95 tons/day. The salts most pertinent to the wet ash disposal system utilised by Sasol 2 and 3 are Ca, SO_4, Na, and Cl. Of these, Ca, SO_4 and Na were identified in literature to be the components most commonly associated with fly ash leachate. Calcium, initially present in the fresh fine ash as lime, is leached from the ash into the effluent, where it reacts with carbon dioxide in the atmosphere. The Ca is

therefore removed from the system due to the precipitation of calcite. Sodium, SO_4, and Cl are retained in the ash dams; the SO_4 appears to be retained in a stable form within the ash, not merely due to hydraulic retention, which suggests that the ash system has the potential to act as a salt sink for SO_4.

The salts that are retained in the ash dams are predominantly retained by means of hydraulic retention, and therefore have the potential to be flushed out of the ash dams into the underlying soil material. However, results from the core drilling exercise revealed that there doesn't appear to be a significant seepage of elements from the ash fill material into the underlying vertisol material. Some components (Al, Fe, Na, K, Mg, Cr, P, Ti and V) from the older, and inactive ash dam, fine ash dam 2, do appear to have percolated into the underlying material, however, a significant amount of water, and therefore salts, are still retained in the dam.

In terms of the mineralogical composition of the ash dams, there is a significant difference between the mineral phases present in the ash fill material of an active and an inactive ash dam. The identification of a mineral phase such as ettringite throughout borehole FAD2A suggests that this mineral is formed in the dam over a long time period. The minerals quartz and mullite were found in the fresh fine ash as well as in most of the core material obtained from the drilling exercise. The mineralogical composition of the ash fill samples, from boreholes FAD2A and FAD4B, was very consistent with depth in the respective ash dams. This finding, combined with the fact that the chemical composition of the core samples varied more significantly in borehole FAD4A, suggests that the lateral position of the ash in the ash dam influences the chemical reactions that occur. Overall, a good correlation was found between the XRF and XRD analyses of the core samples.

From these conclusions it is evident that although the chemistry, involved in the mixing of an industrial effluent with fine ash, is extremely complex and site-specific, it is possible to determine the most pertinent changes which occur within a wet ash disposal system. Besides providing one with a better understanding of the working of the Secunda

ash disposal system, the results of this investigation have also provided the framework for future research on this topic and related issues. Recommendations pertaining to further research are discussed in section 6.3.

6.3 Recommendations

From the results of this investigation it was evident that the scope, for further research on this topic and related issues is vast. Some recommendations and suggestions for future research are:

- The necessity for a pilot plant to be constructed. It was apparent from this investigation that due to the complexity and scale of the Secunda ash disposal system, it is impossible to understand completely the changes that occur under field conditions. A pilot scale ash dam would allow one to examine and evaluate the changes, which occur in the full-scale ash dams, more effectively.
- In terms of plant data, the identified sample points around phase 1 and 2 need to be monitored on a more regular basis, which should incorporate both chemical analyses and the measurement of flow rates. In order to be able to perform mass balance calculations over phase 3, accurate flow rate data is essential, including the flow from the toe drains.
- The "foreign" inlet streams to the system (at Inside Ash) need to be constantly monitored in order to assess the influence that these streams have on the operation of the entire ash disposal process. The salts, added to the system via these streams, need to be controlled, especially the Na and the salts from the demineralisation regeneration waters.
- The data that has been generated during this investigation could be analysed further to determine the correlation between the various chemical species in the effluent. During this study the variation in the species over the different phases was considered separately, however, it is imperative that the influence that one element has on another be investigated.
- The column experiments, performed in this study, could be modified to further investigate the retention of SO_4 in the ash. It is suggested that the concentration of SO_4 ions in the effluent be increased by the addition of dissolved K_2SO_4 (from the

experiments performed in this investigation it was evident that K does not play a major role in the chemical reactions that occur). Sulphuric acid (H_2SO_4) cannot be used since this would alter the pH of the system, and as the results of this investigation have shown, the chemical reactions that occur are extremely sensitive to pH.

- The reactions, which occur during phase 3, could be investigated further using column experiments such as those described in section 4.2.2. It is proposed that the retention time of the leachate in the collecting dish be assessed, as well as the chemical and mineralogical composition, and the quantity of precipitate formed during this stage.
- The combined influence of various factors on the results from the column experiments should be investigated further. The main purpose of the column experiments performed in this investigation was to be able to quantify the chemical changes in terms of mass balances. Some factors were varied during the experiments to determine their influence, if any, on the mass balance results, however, the interaction between the various factors was not investigated.
- The addition of CO_2 to the system should be investigated. The calcium carbonate chemistry and therefore precipitation of Ca, which occurs prominently in the ash water system, could be enhanced by the addition of CO_2. The exact point of the CO_2 addition to the system, for optimum removal of the Ca, needs to be determined.
- The core drilling exercise provided one with more insight into the effectiveness of the ash dams in retaining salts, however, it is suggested that additional boreholes be drilled into the dams to reinforce these findings. Furthermore, the core material that is still available from boreholes FAD2A, FAD4A, and FAD4B, could be used for additional chemical and mineralogical analyses.
- The chemical and mineralogical composition of the material beneath the fine ash dams should be compared to the composition of the soil in the vicinity of the ash dams. This would provide one with an indication of the influence, if any, that the ash dams have had on their surrounding environment.

Thus, it is evident that the results obtained from this investigation have unveiled a multitude of possibilities for future research related to operation and efficiency of the wet ash disposal system employed by Sasol 2 and Sasol 3.

References

Alberts, C.J., 1996, The Immobilisation of Inorganic Pollutants in Fly-Ash and Other Waste Components, MSc Thesis, University of Stellenbosch, South Africa, pp 27-28.

Benefield, L.D., Judkins, J.F., Weand, B.L., 1982, Process Chemistry for Water and Wastewater Tretament, Prentice-Hall, U.S.A, pp 242-248.

Bezuidenhout, N., 1995, Chemical and mineralogical changes associated with leachate production at Kriel power station ash dams, MSc Thesis, University of Cape Town, South Africa, pp 25-90.

Billik, K., and Mashike, J., 1991, Ash water system of the Secunda plants (Sasol II and III), Sastech R&D Internal Report (no. 91/WATER/02).

Bosch, G.L., 1990, The mineralogy and chemistry of pulverised fuel ash produced by three South African coal-burning power stations, MSc Thesis, University of Cape Town, South Africa, pp. 54-56, 91-103, 107-120, 155-159.

Campbell, A., 1999, Chemical, physical and mineralogical properties associated with the hardening of some of South African fly ashes, MSc Thesis, University of Cape Town, South Africa.

Combustion Products Management Inc., 2000, [online]:
http://www.cpmash.com/ash/flyash.html

Dhanpat, R., Eary, L.E., Mattigold, S.V., Ainsworth, C.C., and Zachara, J.M., 1986, Leaching Behavior of Fossil Fuel Wastes: Mineralogy and Geochemistry of Calcium. In: McCarthy, G.J., Glasser, F.P., Roy, D.M., and Diamond, S., (Eds.) Fly Ash and Coal

Conversion By-products: Characterization, Utilisation and Disposal III, Materials Research Society Symposia Proceedings, Boston, vol. 86, pp 3-12.

Ginster, M., 1997, A study to assess the long term changes in water quality of the Secunda ash water system, Sastech R&D Internal Report.

Godbeer, W.C., and Swaine, D.J., 1995, The deposition of trace elements in the environs of a power station. In: Swaine, J. and Goodarzi, F. (Eds.) Environmental Aspects of Trace Elements in Coal, Kluwer Academic Publishers, pp 178-203.

Groenewald, G.H., Hassett, D.J., Koor, R.D., and Manz, O.E., 1984, Disposal of Western Fly Ash in the Northern Great Plains. In: McCarthy, G.J., and Lauf, R.J., (Eds.) Fly Ash and Coal Conversion By-products: Characterization, Utilisation and Disposal I, Materials Research Society Symposia Proceedings, Boston, vol. 43, pp 213-226.

Hassett, D.J., Henke, K.R., McCarthy, G.J., 1985, Leaching Behavior of Fixed-Bed Gasification Ash Derived from North Dakota Lignite. In: McCarthy, G.J., Glasser, F.P., and Roy, D.M., (Eds.) Fly Ash and Coal Conversion By-products: Characterization, Utilisation and Disposal II, Materials Research Society Symposia Proceedings, Boston, vol. 65, pp 285-299.

Hassett, D.J., Henke, K.R., McCarthy, G.J., and Korynta, E.D., 1984, Characterization of a lignite ash from the METC gasifier III. Correlation of leaching behavior and mineralogy. In: McCarthy, G.J., and Lauf, R.J., (Eds.) Fly Ash and Coal Conversion By-products: Characterization, Utilisation and Disposal I, Materials Research Society Symposia Proceedings, Boston, vol. 43, pp 187-194.

Jones, D.R., 1995, The Leaching of Major and Trace Elements from Coal Ash. In: Swaine, J. and Goodarzi, F. (Eds.) Environmental Aspects of Trace Elements in Coal, Kluwer Academic Publishers, pp 221-262.

Kemp, P. H., 1971, Chemistry of Natural Waters – I, Water Research, vol. 5, pp 267.

Lee, S., Hahn, J., 1997, Geochemistry of leachate from fly ash disposal mound. In: Journal of Environmental Science and Health, Part A: Environmental Science and Engineering & Toxic and Hazardous Substance Control, vol. 32, issue 3, pp 649-669.

Loewenthal, R.E., Marais, G.v.R., 1976, Carbonate Chemistry of Aquatic Systems: Theory and Application, Ann Arbour Science Publishers, Michigan, pp 127-137.

Mackechnie, J.R., 1989, The Durability of Fly Ash Concrete in Marine and Soft water Environments, MSc Thesis, University of Cape Town, South Africa, pp. 5-6.

Marais, E., 2002, Mass Balances on the Secunda Ash Water System, Sastech R&D, Water and Environmental Technology Research, Internal Report.

O'Brien, R.D., 2000, The Neutralisation of Acid Mine Drainage by Fly Ash, MSc Thesis, University of Cape Town, South Africa, pp 2.1 – 2.2 and pp 4.1

Parkhurst, D.L., and Appelo, C.A.J., 1999, User's guide to PHREEQC (version 2) – a computer program for speciation, batch-reaction, one-dimensional transport, and inverse geochemical calculations, U.S. Geology Survey Water-Resources Investigations Report, pp 99-4259.

Petersen, J., 1998, Assessment and Modelling of Chromium Release in Minerals Processing Waste Deposits, PhD Thesis, University of Cape Town, South Africa, pp. 92,93

Pourbaix, M.,1966, Atlas of Electrochemical Equilibria in Aqueous Solutions, Pergamon Press, London, pp 122-131, 139-154, 579-603, 307-313.

Pretorius, P.C., and Nieuwenhuis, J.G., 2002, An investigation into the salt holding capacity of the Secunda ash system, Sastech R&D, Water and Environmental Technology Research, Internal Report.

Ritter, B., 1991, Production of Low Cost Building Materials by the Sintering of Fly Ash, MSc Thesis, University of Stellenbosch, South Africa, pp 5-10, 91-93.

Rousseau, P.D.S., 1997, Analysis of single fly ash particles for application to environmental geochemistry, MSc Thesis, University of Stellenbosch, South Africa, pp 2.7-2.34, 4.68 – 4.74, 4.88-5.113

Shen-Yu, F., and Zwane, S.T., 2001, Relationship between salinity and metal availability in solid waste leachates, Internal Report, University of Cape Town, South Africa, pp 1-44.

Smit, J.G.S., 1999, Calibration of models used for predicting process water and ash water dams levels, JGS Smit Design Services, pp 1-39.

Smit, J.G.S., February 2000, SSF Water Balances: Actual vs. Predicted Dam Level Trends (August 1999 to January 2000), JGS Smit Design Services, pp 1-27.

Smit, J.G.S., June 2000, SSF Water Balances: Actual vs. Predicted Dam Level Trends (November 1999 to June 2000), JGS Smit Design Services, pp 1-28.

Smit, J.G.S., January 2001, SSF Water Balances: Actual vs. Predicted Dam Level Trends (November 1999 to November 2000), JGS Smit Design Services, pp 1-29.

Smit, J.G.S., May 2001, SSF Water Balances: Actual vs. Predicted Dam Level Trends (December 2000 to April 2001), JGS Smit Design Services, pp 1-25.

Swaine, D.J., 1995, The Formation, Composition and Utilisation of Flyash. In: Swaine, J. and Goodarzi, F. (Eds.) Environmental Aspects of Trace Elements in Coal, Kluwer Academic Publishers, Netherlands, pp 204-220.

Tishmack, J.K., Olek, J., and Diamond, S., 1999, Characterization of high-calcium fly ashes and their potential influence on ettringite formation in cementitious systems, Cement, Concrete and Aggregates, vol. 21, pp 82-92.

Villaume, J.F., Bell, J.W., and Labuz, L.L., 1987, Evaluation of Leachate generation at the Montour, Pennsylvania Fly Ash Test Cell. In: McCarthy, G.J., Glasser, F.P., Roy, D.M., and Hemmings, R.T., (Eds.) Fly Ash and Coal Conversion By-products: Characterization, Utilisation and Disposal IV, Materials Research Society Symposia Proceedings, Boston, vol. 113, pp 325-332.

Vining, G., 1998, Statistical Methods for Engineers, Duxbury Press, pp 42-51.

Willis, J.P., 1987, Variations in the composition of South African fly ash, Ash – a valuable resource, CSIR, vol. 3.

Appendix A

General Information

A1: Abbreviations and definitions

A1.1 Abbreviations

CAE: clear ash effluent, a general name given to the water that is recycled and used to transport the ash from where it is produced, into the ash water system.

FAM: CAE combined with some 'foreign' process streams, i.e. the exact composition of the effluent that is mixed with the ash. The composition of the CAE and FAM are very similar since the majority of the FAM is made up of CAE.

New FAM: A different sample of the FAM used in some of the column experiments.

FAD: Fine Ash Dam

TRO: Tubular reverse osmosis desalination plant.

MAlk: M alkalinity is a measure of the total alkalinity of a solution.

PAlk: Empirically P alkalinity represents all of the hydroxide ions present plus one half of all the carbonate ions.

COD: Chemical Oxygen Demand.

TDS: Total Dissolved Solids.

SS: Suspended Solids.

LI: Langelier Saturation Index.

MGC: McKnight Geotechnical Consulting (Pty) Ltd

SPT: Standard Penetration Test

NMC: Natural Moisture Content (mass %)

CSIR: The Council of Scientific and Industrial Research

A1.2 Definitions

Chemical Oxygen Demand (COD): The chemical oxygen demand (COD) test is widely used as a means of measuring the pollutional strength of domestic and industrial wastes. This test allows measurement of a waste in terms of the total quantity of oxygen required for oxidation to carbon dioxide and water.

Conductivity: The conductivity of a solution is a measure of its ability to carry an electrical current, and varies both with the number and type of ions the solutions contains. (Sawyer, 1978). According to Hassett (1985), the electrical conductivity (EC) of a solution is an indicator of the total dissolved ionic species.

Oxyanions: Oxyanions are poly-atomic ions (usually anions) containing oxygen plus another non-metal (other than H). Some elements are able to form more than one oxyanion, each containing a different number of oxygen atoms. For example, chlorine can combine with oxygen in four ways to form four different oxyanions: ClO_4^-, ClO_3^-, ClO_2^-, and ClO^-. (Note that in a family of oxyanions, the charge remains the same; only the number of oxygen atoms varies).

Pozzolanic: A pozzolanic material is one which possesses hydraulic cementing properties when mixed with water in the presence of $Ca(OH)_2$.

Zeolites: Zeolites are microporous crystalline solids with well-defined structures. Generally they contain silicon, aluminium and oxygen in their framework and cations, water and/or other molecules within their pores. Many occur naturally as minerals, and are extensively mined in many parts of the world. Others are synthetic, and are made commercially for specific uses, or produced by research scientists trying to understand more about their chemistry.

A2: Mineral names

Table A1: Mineral Names and Formulae

Mineral	Formula
Anhydrite	$CaSO_4$
Aragonite	$CaCO_3$
Calcite	$CaCO_3$
Carnegieite	$NaAlSiO_4$
Chalcedony	SiO_2
Dolomite	$CaMg(CO_3)_2$
Ettringite	$Ca_6Al_2(SO_4)_3(OH)_{12}.26H_2O$
Fluorite	CaF_2
Goethite	$FeO(OH)$
Gypsum	$CaSO_4.2H_2O$
Hematite	Fe_2O_3
Jarosite-K	$KFe_3(SO_4)_2(OH)_6$
Lime	CaO
Maghemite	Fe_2O_3
Magnetite	Fe_3O_4
Melanterite	$FeSO_4:7H_2O$
Melilite	$(Ca,Na)_2(Al,Mg,Fe^{2+})(Si,Al)_2O_7$
Merwinite	$Ca_3Mg(SiO_4)_2$
Mullite	$Al_6Si_2O_{13}$
Nepheline	$(Na,K)AlSiO_4$
Periclase	MgO
Portlandite	$Ca(OH)_2$
Pyrite	FeS_2
Quartz	SiO_2
Sepiolite	$Mg_2Si_3O_7.5OH:3H_2O$
Sepiolite(d)	$Mg_2Si_3O_7.5OH:3H_2O$
Siderite	$FeCO_3$
Sodalite	$Na_8Al_6Si_6O_{24}Cl_2$
Spinel	$MgAl_2O_4$
Talc	$Mg_3Si_4O_{10}(OH)_2$
Wollastonite	$CaSiO_3$

Appendix B

Actual Plant Data

B1: Diagrams of the ash disposal system

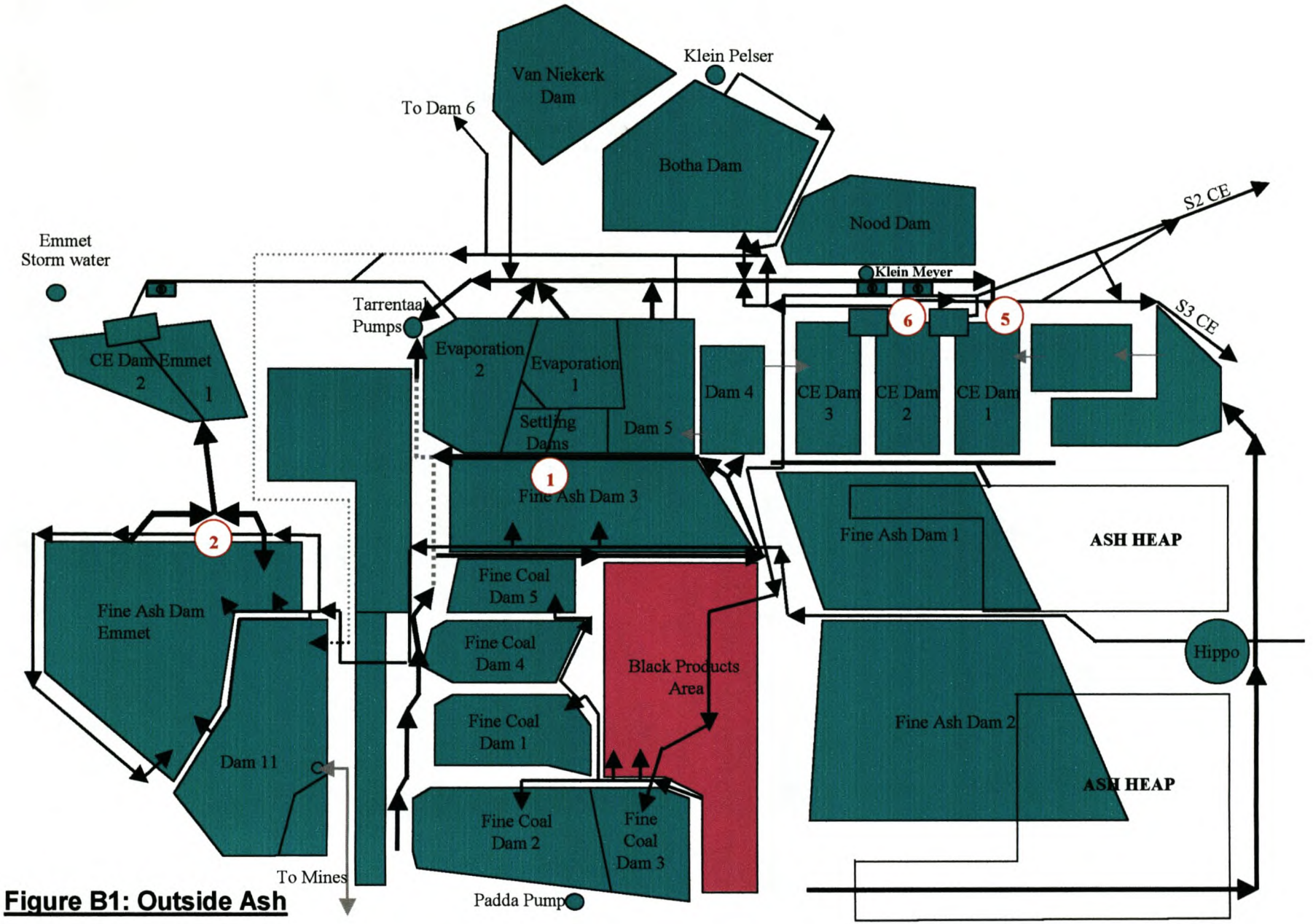

Figure B1: Outside Ash

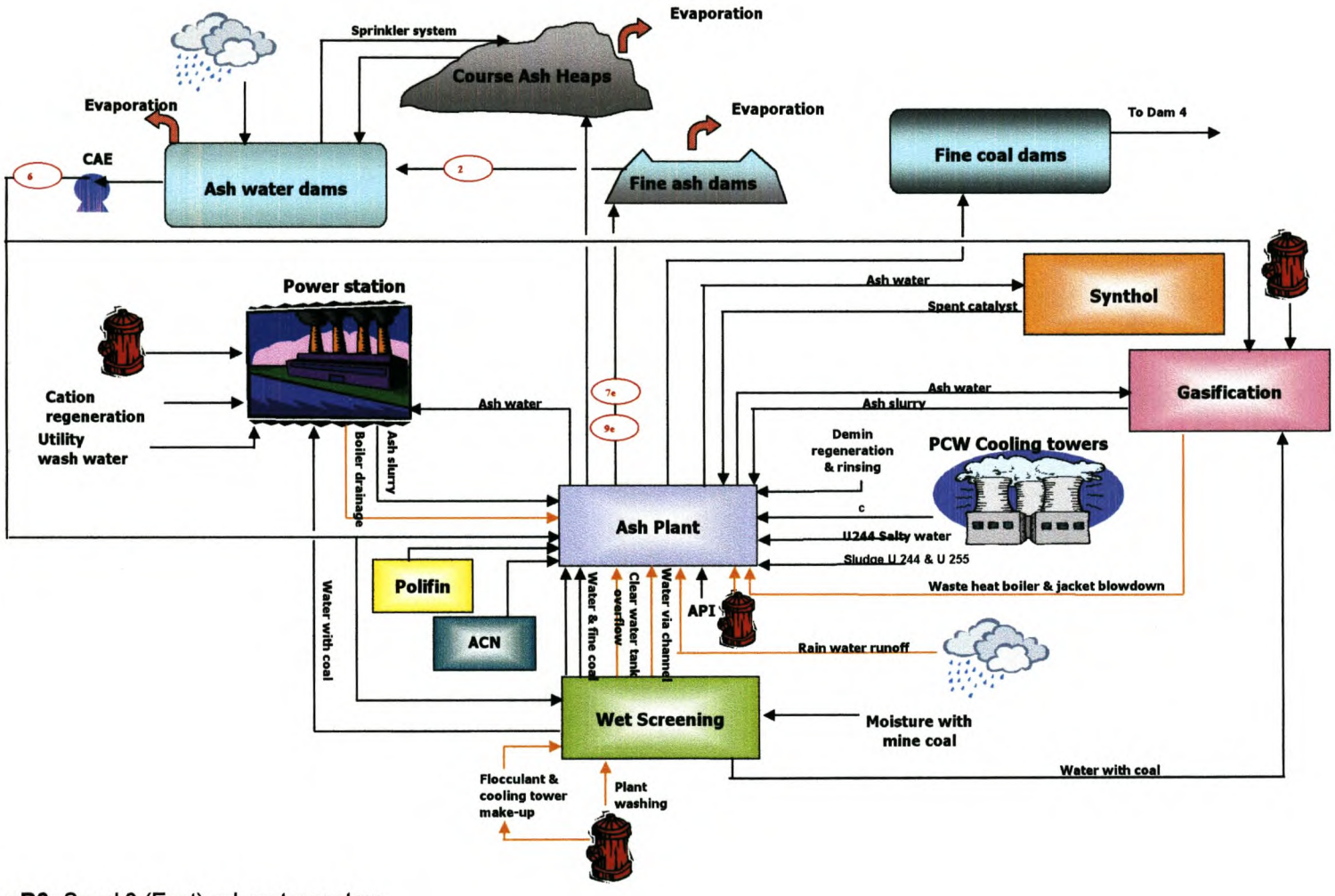

Figure B2: Sasol 3 (East) ash water system

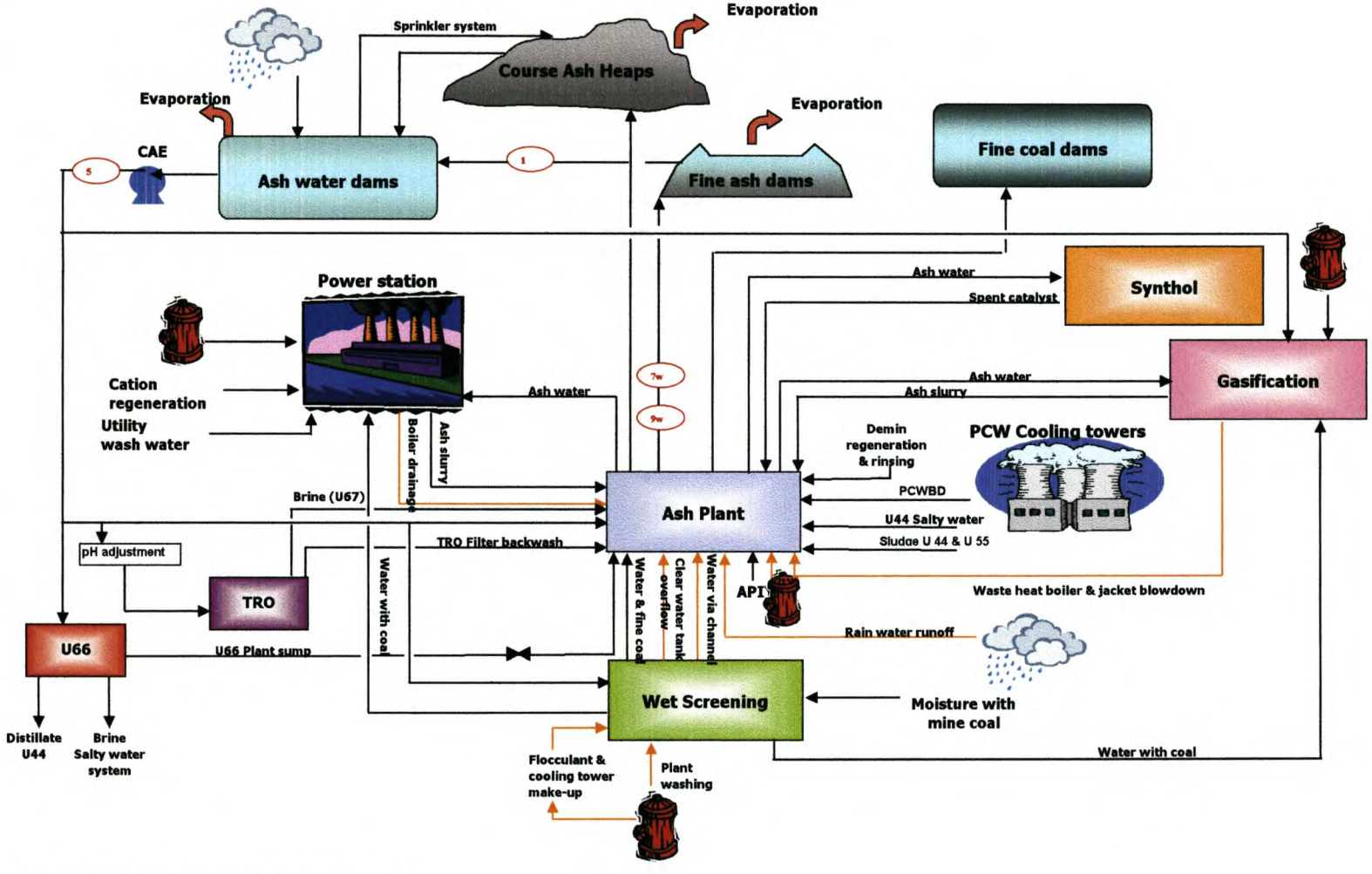

Figure B3: Sasol 2 (West) ash water system

Compact Disc

Contains the following appendices in electronic format:

APPENDIX B

ACTUAL PLANT DATA

APPENDIX C

COLUMN EXPERIMENTS

APPENDIX D

CORE DRILLING DATA

APPENDIX E

PRINCIPAL COMPONENT ANALYSIS